

FUNCTIONAL MORPHOLOGY, VARIATION, AND
NICHE SEPARATION IN THE LARGE-BODIED FOSSIL COLOBINES

by

MONYA ANDERSON

A DISSERTATION

Presented to the Department of Anthropology
and the Graduate School of the University of Oregon
in partial fulfillment of the requirements
for the degree of
Doctor of Philosophy

June 2019

DISSERTATION APPROVAL PAGE

Student: Monya Anderson

Title: Functional Morphology, Variation, and Niche Separation in the Large-Bodied Fossil Colobines

This dissertation has been accepted and approved in partial fulfillment of the requirements for the Doctor of Philosophy degree in the Department of Anthropology by:

Stephen Frost	Chairperson
Frances White	Core Member
Nelson Ting	Core Member
Samantha Hopkins	Institutional Representative

and

Janet Woodruff-Borden	Vice Provost and Dean of the Graduate School
-----------------------	--

Original approval signatures are on file with the University of Oregon Graduate School.

Degree awarded June 2019

© 2019 Monya Anderson

DISSERTATION ABSTRACT

Monya Anderson

Doctor of Philosophy

Department of Anthropology

June 2019

Title: Functional Morphology, Variation, and Niche Separation in the Large-Bodied Fossil Colobines

Colobines are ecological referents that can be used to assess and reconstruct paleoenvironmental conditions. Colobine taxa discussed here include *Paracolobus mutiwa*, *P. Cercopithecoides williamsi*, *C. kimeui*, and *Rhinocolobus turkanensis*. All of these taxa except for *R. turkanensis* display postcranial adaptations consistent with terrestrial locomotion in contrast to their exclusively arboreal African counterparts. At sites like these of the Upper Burgi Member of Koobi Fora, these four large colobines, up to four species of hominins, and three large-bodied cercopithecine taxa are known. This level of sympatry in primate communities is unmatched in modern habitats emphasizing the importance of niche separation for understanding diversity in the fossil record.

The descriptions of two previously undescribed specimens: *P. mutiwa* specimen KNM-WT 16827 and the informally designated *P. mutiwa* specimen L895-1 are presented here with detailed qualitative and quantitative postcranial analyses. Postcranial measurements from fossil colobines, fossil cercopithecines, and a large extant sample for comparative purposes. Measurements include 112 linear metrics and 54 functional indices. Body mass estimates for the fossil descriptions were calculated based on published equations for postcranial estimation. Dietary proxies for the fossil taxa are based on dental

morphology and taken from the literature. Substrate preference is estimated using qualitative description of skeletal elements, quantitative comparison to extant taxa, and observational data of substrate use of extant species.

Paracolobus mutiwa specimen KNM-WT 16827 shows postcranial morphologies consistent with terrestriality distinct from *Cercopithecoides* and *Theropithecus* and is distinct from *P. chemeroni* to a degree warranting generic reassessment of the species. Specimen L895-1 shows postcranial morphology consistent with terrestriality, is distinct from other contemporaneous cercopithecids, and is most similar in size and morphology to *P. mutiwa*. The niche separation analyses show *C. williamsi* to be the most terrestrial of the large colobines with the largest consumption of leaves. *P. mutiwa* overlaps with *C. williamsi* in size, but is less terrestrial and *R. turkanensis* is the least. There is also clear separation among the large colobines and *Theropithecus* in diet and substrate use. The sympatry and diversity of these large-bodied colobines suggests a much more diverse and dynamic primate environment than seen in East Africa today.

CURRICULUM VITAE

NAME OF AUTHOR: Monya Anderson

GRADUATE AND UNDERGRADUATE SCHOOLS ATTENDED:

University of Oregon, Eugene, OR
Purdue University, West Lafayette, IN

DEGREES AWARDED:

Doctor of Philosophy, Biological Anthropology, 2019, University of Oregon
Master of Science, Biological Anthropology, 2012, University of Oregon
Bachelor of Arts, Anthropology, 2010, Purdue University

AREAS OF SPECIAL INTEREST:

Biological anthropology, non-human and human primate fossil record,
paleoanthropology, functional morphology, paleoenvironmental reconstruction,
vertebrate paleontology

PROFESSIONAL EXPERIENCE:

Graduate Employee, Department of Anthropology, University of Oregon,
2010-2019

Instructor of Record, Department of Anthropology, University of Oregon,
2017-2019

GRANTS, AWARDS, AND HONORS:

Graduate Teaching Fellowship, Department of Anthropology, University of
Oregon, 2010-2019

Johnston Scholarship Graduate Research Fellowship, Department of
Anthropology, University of Oregon, 2018

Departmental Nominee for Dissertation Research Fellowship, Department of
Anthropology, University of Oregon, 2018

Doctoral Dissertation Improvement Grant, National Science Foundation, 2017

Graduate School Research Award, University of Oregon, 2013

Johnston Scholarship Graduate Research Fellowship, Department of Anthropology, University of Oregon, 2013

Departmental Travel Award, Department of Anthropology, University of Oregon, 2012

Departmental Travel Award, Department of Anthropology, University of Oregon, 2011

Outstanding Senior in Anthropology, Department of Anthropology, Purdue University, 2010

O. Michael Watson Anthropology Senior Capstone Award, Department of Anthropology, Purdue University, 2010

Dean's List, Purdue University, 2006-2010

University Honors, Purdue University, 2006-2010

College of Liberal Arts Honors, Purdue University, 2006-2010

College of Liberal Arts Dean's Scholar, Purdue University, 2006

National Honor Society, Terre Haute South Vigo High School, Terre Haute, IN, 2006

PUBLICATIONS:

Anderson, M., 2019. An assessment of the postcranial skeleton of the *Paracolobus mutiwa* (Primates: Colobinae) specimen KNM-WT 16827 from Lomekwi, West Turkana, Kenya. *Journal of Human Evolution* (In Review)

Anderson, M., Frost, S.R., 2016. Pedal Functional Morphology of *Paracolobus chemeroni*. *American Journal of Physical Anthropology* 159(S62), 80.

Anderson, M., Frost, S.R., 2015. A Reassessment of the Phylogeography of Sulawesi macaques based on 3D geometric morphometrics, *American Journal of Primatology* 77, 49-50.

Anderson, M., Frost, S.R., Gilbert, C.C., Delson, E., 2014. A reassessment of dental variation in the genus *Cercopithecoides* and its implications for species diversity. *American Journal of Physical Anthropology*. 153, 67.

Anderson, M., Frost, S.R., Gilbert, C.C., Delson, E., 2013. Morphological diversity and species recognition in South African *Cercopithecoides williamsi*. *American Journal of Physical Anthropology*. 150, 68.

Anderson, M., Frost, S.R., Gilbert, C.C., Delson, E., 2015. Cranial shape and intrageneric diversity in the genus *Cercopithecoides*. 156(S60), 69.

Arenson, J.L., Anderson, M., Eller, A.R., Simons, E.A., White, F.J., Frost, S.R., 2015. Bergmann's rule in skull size of wild vs. captive fascicularis group macaques. American Journal of Physical Anthropology. 156 (S60), 71.

Arenson, J.L., Anderson, M., White, F.J., Frost, S.R., 2016. Morphological assessment of a putative hybrid species, *Trachypithecus pileatus*, based on a 3D geometric morphometric analysis of cranial morphology. American Journal of Physical Anthropology 159(S62), 82.

Clarke, K.S., Anderson, M., Eller, A.R., Simons, E., White, F.J., Frost, S.F., 2015. Morphological signals of stress and socioendocrinology: Comparing measures of cranial fluctuating asymmetry and second to fourth digit ratio in cercopithecids. American Journal of Physical Anthropology 156, 106.

Clarke, K.S., McNulty, K.P., Eller, A.R., Arenson, J.L., Anderson, M., Simons, E.A., White, F.J., Frost, S.R., 2015. Morphological signals and mating systems: Comparing measures of cranial fluctuating asymmetry and second-to-fourth digit ratio in anthropoid primates. American Journal Primatology. 77(S1), 56.

Gilbert, C.C., Pugh, K., Anderson, M., Frost, S.R., Delson, E., 2018. Evolution of the modern baboon (*Papio hamadryas*): A reassessment of the African Plio-Pleistocene record. Journal of Human Evolution 122, 38-69.

Glenzer, R.R., Clarke, K.S., Anderson, M., Eller, A.R., White, F.J., Frost, S.R., 2015. Comparing morphometric methods in *Macaca mulatta* crania. American Journal of Physical Anthropology. 156(S60), 146.

Reda, H., Frost, S.R., Simons, E., Anderson, M., Haile-Selassie, Y., Preliminary Study of the Cercopithecidae from Leado Didoa locality, Woranso-Mille (central Afar), Ethiopia. American Journal of Physical Anthropology 162(S64), 328-329.

ACKNOWLEDGMENTS

This dissertation is the result of many years of patience, support, and collaborative effort. I have been very fortunate over the years to have had the encouragement of dozens of teachers, colleagues, friends, and family. I would first like to thank my amazing advisor Stephen Frost for his intellectual guidance, fieldwork opportunities, and availability over the past nine years. Thank you for introducing me the amazing world of monkeys; I have enjoyed giving them their due and look forward to discovering more! A special thanks also to all the member of my committee: Frances White, Nelson Ting, and Samantha for your feedback, suggestions, and support over the years. Thank you.

This project could not have been done without extensive fieldwork for which I would like to thank the curators, staff, and researcher as the Kenya National Museum (Emma Mbua, Frederick Manthi, Mzalendo Kibunjia, Rose Nyaboke, & Cecilia Kanyua), National Museum of Ethiopia (ARCCH, Getachew Senishaw, Tomas Getachew, Yohannes Haile-Selassie, Jean-Renaud Boisserie, William Kimbel, Kaye Reed, & Sahle Melaku), the Anthropological Institute and Museum in Zurich (Mark Scherrer), the Muséum National D'histoire Naturelle (Christine Argot & Antoine Suoron), the Natural History Museum in London (Louise Tomsett), the Smithsonian National Museum of Natural History (Darrin Lunde), and the Harvard Museum of Comparative Zoology (Mark Omura & Judy Chupasko). Thank you for allowing me access to the collections in your care and providing me with research space during my trips. Thank also to the National Science Foundation (DDRIG No. 1650923) and the UO Department of Anthropology for the funding support that made this project possible. Special thanks to all faculty and staff in the Department of UO Anthropology for your help, guidance, and patience over the years!

Special thanks also to all members of the Gona Palaeoanthropological Research Project for giving me the opportunity to work at such an amazing site and to Chris Gilbert for letting me be a part of your project in South Africa. Thank you to Eric Delson; I would not be where I am were it not for your research and years of student support in paleoprimatology. Thank you also to Emily Guthrie for sharing your comparative measurements without which my analyses would have been so much less interesting!

In addition to professional support, this dissertation would not have been possible without the support of all of my friends both within and outside of the UO; I wish I had space to thank you all in the ways you deserves! An extra special thanks goes out to my trivia team Trivial Science The Science of Trivia in all its iterations for providing comfort, friendship, and much-needed solace during grad school. Thank you to the Frost Lab: Evan Simons, Aileen Fernandez, and Hailay Reda for your field stories. An extra special thanks goes out to Theresa Gildner for being such an incredible friend and roommate and an extra thank you also to the entire Gildner family for being my PNW family. To James Herron for your support, patience, and encouragement during my writing days. Whatever happens you have been an incredible partner and have helped me through this stressful time more than I can express. Thank you also to my best friend of nearly 25 years Lauren Stuart for being there for me during so many important moments from 1st grade through college graduation. To my sister Karis Anderson for your passion and conversation; whatever you end up doing you will smash it! To my father Eric Anderson for the nature walks, museum trips, science fair projects, and introducing me to the wonderful field of anthropology and my mother Dr. Veanne Anderson for being such an amazing academic and personal role model, I love you all very much!

To all of my family and friends.

TABLE OF CONTENTS

Chapter	Page
I. BACKGROUND	1
II. MATERIALS AND METHODS: POSTCRANIAL FUNCTIONAL MORPHOLOGY	
.....	8
Materials	8
Comparative Fossil Sample	8
Comparative Extant Sample	8
Linear Metrics	9
Description of Measurements	9
Description of Indices	9
Qualitative Descriptions of Functional Morphology	20
Body Mass Estimates	20
III. AN ASSESSMENT OF THE POSTCRANIAL SKELETON OF THE	
<i>PARACOLOBUS MUTIWA</i> (PRIMATES: COLOBINAE) SPECIMEN KNM-WT 16827	
FROM LOMECKWI, WEST TURKANA, KENYA.....	23
Introduction.....	23
Results.....	29
Scapula.....	31
Preservation.....	32
Description.....	33
Humerus.....	35
Preservation.....	36

Chapter	Page
Description.....	37
Ulna	43
Preservation.....	43
Description.....	45
Radius	47
Preservation.....	47
Description.....	48
Os Coxae.....	49
Preservation.....	50
Description.....	51
Femur	55
Preservation.....	55
Description.....	56
Astragalus	63
Preservation.....	63
Description.....	63
Calcaneus	66
Preservation.....	66
Description.....	67
Discussion.....	70

Chapter	Page
<p>IV. AN ASSESSMENT OF THE POSTCRANIAL SKELETON OF THE LARGE- BODIED COLOBINE SPECIMEN L895-1 FROM SHUNGURA, OMO VALLEY, ETHIOPIA</p>	
	76
Background.....	75
Results.....	82
Humerus.....	83
Preservation.....	83
Description.....	84
Ulna.....	90
Preservation.....	90
Description.....	92
Radius	96
Preservation.....	96
Description.....	97
Femur	100
Preservation.....	101
Description.....	102
Tibia	108
Preservation.....	108
Description.....	109
Astragalus	113
Preservation.....	113

Chapter	Page
Description	114
Calcaneus	115
Preservation.....	115
Description	116
Cuboid.....	119
Preservation.....	119
Description	121
Navicular.....	122
Preservation.....	122
Description	122
Middle Cuneiform.....	123
Preservation.....	123
Description	123
MT I	124
Preservation.....	124
Description	124
Body Mass Estimates	125
Humerus	127
Femur	127
Tibia	128
Discussion.....	128
Sex Estimation	128

Chapter	Page
Functional Morphology	129
Body Mass Estimates	134
Taxonomic Status.....	135
V. NICHE SEPARATION AMONG THE LARGE-BODIED COLOBINAE OF THE	
TURKANA BASIN	137
Background.....	137
Materials and Methods.....	140
Estimates of Terrestriality for Extant Cercopithecidae.....	140
Estimates of Terrestriality for Fossil Cercopithecidae.....	142
Dietary Estimates	143
Results.....	144
Estimates of Terrestriality for Extant Cercopithecidae.....	144
Estimates of Terrestriality for Fossil Cercopithecidae.....	148
Niche Separation: Body mass and substrate use.....	149
Niche Separation: Body mass and diet	152
Niche Separation: Substrate use and diet	153
Discussion.....	154
VI. CONCLUSIONS	158
APPENDICES	162
A. CATALOGUE OF EXTANT COMPARATIVE SAMPLE	162
A.1: Extant colobine specimens.....	162
A.2: Extant cercopithecine specimens	167

Chapter	Page
B. FOSSIL CERCOPITHECIDAE INDICES	170
B.1: Humeral indices	170
B.2: Radial indices	173
B.3: Ulnar indices	174
B.4: Os coxae indices.....	176
B.5: Femoral indices	177
B.6: Tibial indices	178
B.7: Astragalus and Calcaneus indices	179
REFERENCES CITED.....	180

LIST OF FIGURES

Figure	Page
2.1 Illustration of postcranial metrics	13
2.1A. Scapula	13
2.1B. Humerus	14
2.1C. Radius and Ulna	15
2.1D. Os Coxae	16
2.1E. Femur	17
2.1F. Tibia	18
2.1G. Astragalus and Calcaneus	13
3.1 Stratigraphic map of KNM-WT 16872's locality	26
3.2 Elements included in the functional description of ♂ <i>Paracolobus mutiwa</i> specimen KNM-WT 16827	27
3.3 Scapula of <i>Paracolobus mutiwa</i> specimen KNM-WT 16827O.	32
3.4 Lateral view of the scapulae	33
3.5 Ventral view of <i>Paracolobus mutiwa</i> right humerus	36
3.6 Ventral view comparing humeri	37
3.7 Proximal humerus in ventral view	39
3.8 Ventral view of distal humeri	40
3.9 Dorsal view of distal humeri	40
3.10 Inferior view of the distal humeral articular surface	42
3.11 Box plots showing ranges of humeral indices.	43
3.12 Right ulna fragment of <i>Paracolobus mutiwa</i> specimen WT 16827L.	44

Figure	Page
3.13 Ventral view comparing ulnae.....	46
3.14 Ventral view of right radius fragment of specimen WT 16827AD	47
3.15 Ventral view of proximal radii.....	48
3.16 <i>Paracolobus mutiwa</i> right os coxae.....	50
3.17 Lateral comparative innominates.....	51
3.18 Ventral (L) and dorsal (R) view of <i>Paracolobus mutiwa</i> specimen WT 16827I.	56
3.19 Comparative ventral view of femora.	57
3.20 Scatter plot of femoral head width and lower iliac height by genus.....	61
3.21 Scatter plot of femoral head width and greater trochanter height by genus	62
3.22 Box plot showing index of relative greater trochanter height.....	63
3.23 Superior view of left and right astragali	64
3.24 Superior view comparing left astragali	65
3.25 Box plots of astragalus indices associated with locomotor mode.....	66
3.26 Superior (L) and plantar (R) view of left side calcaneus	67
3.27 Superior view comparing left calcanei	68
3.28 Box plot showing calcaneal indices	69
4.1 Stratigraphic map of L895-1's locality within the Shungura Formation	77
4.2 All postcranial elements associated with specimen L895-1	78
4.3 Left humerus L895-1i.	83
4.4 Ventral view comparing humeri	85
4.5 Ventral view comparing distal humeri.....	86

Figure	Page
4.6 Inferior view comparing the distal humeral articular surface	88
4.7 Box plots showing ranges of humeral indices	89
4.8 Ventral view of right (L895-1f) and left (L895-1e) ulnae	91
4.9 Ventral view comparing ulnae	94
4.10 Ventral view comparing proximal right ulnae	95
4.11 Medial view comparing right ulnae	95
4.12 Ventral view of left radius fragment L895-1g	96
4.13 Ventral view comparing radii	98
4.14 Box plots showing radial indices	99
4.15 Femora associated with L895-1	100
4.16 Ventral comparing femora	102
4.17 Box plots showing femoral indices	104
4.18 Ventral view of tibiae associated with L895-1	108
4.19 Ventral view comparing tibiae	110
4.20 Box plots showing tibial indices	111
4.21 Inferior view comparing the talar surface of the left distal tibia	112
4.22 Superior view of right astragalar fragments from L895-1	113
4.23 Superior view comparing astragali	114
4.24 Superior view of right calcaneus from L895-1m	115
4.25 Superior and plantar view comparing	116
4.26 Box plots showing calcaneal indices	119
4.27 Scatter plot of relative posterior calcaneal facet length (IC2) and body mass	120

Figure	Page
4.28 Superior and distal view of the left cuboid of L895-1n	121
4.29 Navicular bones L895-1o (Rt. side) and L895-1p (Lt. side).....	122
4.30 Middle cuneiforms of L895-1	124
4.31 Left side MT1 of L895-1t	124
5.1 Regression plots of relevant functional indices from the forelimb and observed time spent on the ground in extant Cercopithecidae	145
5.2 Regression plots of functional indices from the hindlimb and observed time spent on the ground in extant Cercopithecidae	146
5.3 Plot showing the range overlap in male body mass and relative terrestriality.....	151
5.4 Plot showing the range in overlap in male body mass and diet	153
5.5 Plot showing the range in overlap in relative terrestriality and diet	154

LIST OF TABLES

Table	Page
2.1 Fossil colobine specimens included in the comparative postcranial dataset	9
2.2 Linear metrics collected on postcranial specimens.....	10
2.3 Indices taken on all specimens with relevant preserved linear metrics	21
3.1 All identified postcranial elements associated with specimen KNM-WT 16827..	28
3.2 Linear metrics from all postcranial elements associated with KNM-WT 16827 ..	30
4.1 All identifiable elements associated with L895-1.....	81
4.2 Body mass estimates of comparative extant and fossil specimens.....	126
5.1 Data on observed terrestriality of extant Cercopithecidae.....	142
5.2 Male body mass range estimates used in the niche separation plots	143
5.3 Minimum, maximum, and range midpoints for leaf consumption	144
5.4 Results of the regression of functional indices on observed terrestriality for the extant Cercopithecidae.....	147
5.5 Results of the terrestriality estimate regressions on the extant taxa	147
5.6 Estimates of terrestriality for the fossil taxa	149

CHAPTER I

BACKGROUND

The Colobinae are a geographically widespread subfamily of the Cercopithecidae with extant forms present in Africa and Asia and a diversity of fossil taxa known from sites in Africa, Europe, and Asia. The living forms occupy a wide range of climates and environments suggesting an adaptive evolutionary history marked by multiple radiations (Delson, 1994; Wang et al., 2013). Molecular analyses have estimated that the group diverged from the cercopithecines between 14.4 and 17.9Ma (Raum et al., 2005; Ting, 2008; Steiper and Seiffert, 2012) first appearing in the fossil record by at least 12.5Ma (Rossie et al., 2013). Unfortunately, the fossil record is scarce during this formative period with many of the fossil forms absent until the Plio-Pleistocene and many of the living forms not visible until the late Pleistocene (Jablonski, 2002; Ting, 2008).

The two major colobine radiations are found in Eurasia and Africa. There are no extant colobines endemic to Europe, but the extant Asian colobines are more taxonomically diverse than their African counterparts although their fossil record is relatively sparse (Bennett and Davies, 1994; Delson, 1994). This radiation is hypothesized to have arisen by the Late Miocene when *Mesopithecus*, the earliest known Eurasian colobine, appears in the fossil record with a diversification of forms occurring during the Pliocene (Delson, 1994; Takai et al., 2008). The relatively terrestrial *Dolichopithecus* is found throughout southern Europe during the Pliocene and shares some aspects of cranial morphology with earlier *Libypithecus* and *Mesopithecus* (Szalay & Delson, 1979; Strasser & Delson, 1987; Jablonski & Frost, 2010; Nishimura et al., 2010). By the late Pliocene in Asia at least two taxa known only from the fossil record

are present. The first of these is *Parapresbytis* (Jablonski, 2002; Takai et al., 2008), which is sometimes argued to be a junior synonym of *Dolichopithecus* (Delson, 1994). This genus is morphologically similar to some extant Asian colobines with some more arboreal postcrania than its European contemporaries (Maschenko, 2005) although others characterize the group as terrestrial (Delson, 1994). The other fossil Asian taxon from the Pliocene of Japan is the recently described *Kanagawapithecus* which has no obvious relationship with any living Asian groups (Nishimura et al., 2012).

In Africa the earliest identifiable taxon is *Microcolobus* which has been dated to about 10 Ma in Kenya (Benefit and Pickford, 1986; Gilbert et al., 2010; Nakatsukasa et al., 2010). Other African genera known exclusively from the fossil record include *Rhinocolobus*, *Cercopithecoides*, *Kuseracolobus*, and *Paracolobus* many of which are represented by both craniodental and postcranial remains (Leakey, 1969; Birchette, 1982; Leakey, 1982; Harris et al., 1988; Frost, 2001; Jablonski, 2002; Frost et al., 2003; Hlusko, 2006, 2007). These taxa are distinct from extant taxa by being relatively large-bodied and disappear from the fossil record after about 1.5Ma (Jablonski, 2002; Frost and Alemseged, 2007; Jablonski and Frost, 2010). Extant colobinans by contrast are notably less diverse with three recognized genera: *Colobus*, *Procolobus*, and *Piliocolobus* none of which are present in the fossil record until the Plio-Pleistocene (Harrison and Harris, 1996; Jablonski, 2002; Grubb et al., 2003; Ting, 2008).

In addition to being primarily arboreal quadrupeds, the most distinctive feature of the living colobines is their complex digestive tract which is an adaptation to a largely folivorous diet (Szalay and Delson, 1979). Many of the living colobines are characterized by having relatively slender bodies and relatively elongate hind limbs, which is

characteristic of both arboreal and terrestrial quadrupeds (Szalay and Delson, 1979; Fleagle, 2013). All of the extant African colobines are arboreal quadrupeds so a brief discussion of how this locomotor pattern affects the morphology of the skeleton is necessary to contextualize the fossil record. Many of the features used to distinguish colobines from cercopithecines are soft tissue or craniodental. The latter are related to dietary differences and often diagnostic even when fragmentary. Postcranial anatomy can be just as important for evaluating evolutionary history in the context of locomotor behavior and substrate preference but is more difficult to assign taxonomically in the absence of associated craniodental remains (Strasser and Delson, 1987; Strasser, 1988; Frost et al., 2015). It is therefore important to consider variation in extant and fossil samples when assessing the functional and taxonomic significance of undescribed specimens.

Many early colobines possess morphology consistent with arboreality, but some fossil taxa, including Eurasian *Mesopithecus* and *Dolichopithecus*, and African *Cercopithecoides* and *Paracolobus*, appear to have been at least partially terrestrial (Birchette, 1982; Leakey, 1982; Frost and Delson, 2002; Pan et al., 2004; Jablonski et al., 2008). Interestingly, other fossil taxa, some of which are contemporary with the more terrestrial forms, display postcranial morphology more consistent with arboreality. These include the earliest known colobine species *Microcolobus tugenensis* and the Plio-Pleistocene *Kuseracolobus aramisi*, *K. hafu*, and *Rhinocolobus turkanaensis* (Delson, 1994; Benefit 1999; Hlusko 2006, 2007; Jablonski et al., 2008; Frost et al., 2009; Jablonski and Frost, 2010; Nakatsukasa et al., 2010; Harrison, 2011).

Many of the arboreal adaptations and morphologies present in extant African

colobines are also seen in some fossil taxa. *Rhinocolobus* displays many of the forelimb, hind limb, phalangeal, and trunk morphologies consistent with arboreality in extant colobines and has been described as the most arboreal of all the Pliocene colobines (Leakey, 1982; Elton, 2000; Frost and Delson, 2002; Jablonski, 2002). Another arboreal colobine from East Africa is *Kuseracolobus* known from late Miocene-early Pliocene deposits in Ethiopia (Frost, 2001; Hlusko, 2006). This taxon ranges in size from similar to extant *Nasalis* up to approximately the size of *Rhinocolobus* and *Cercopithecoides williamsi* (Delson et al., 2000; Frost and Delson, 2002; Hlusko, 2006). *Paracolobus* possesses an intriguing mix of terrestrial and arboreal postcranial morphology. This taxon is known from the Plio-Pleistocene of the Tugen Hills, Koobi Fora and West Turkana, Kenya, and the Omo Valley, Ethiopia (Jablonski, 2002). Its large size and forelimb robusticity are similar to what is seen in large terrestrial colobines, but many argue that this is the result of allometry rather than substrate preference (Birchette, 1982). This genus is most often described as primarily an arboreal quadruped with intermediate morphologies consistent with some terrestrial behavior (Birchette, 1982; Delson, 1994; Anderson and Frost, 2016).

Three fossil colobine taxa appear to have at least some postcranial adaptations for terrestriality: *Mesopithecus*, *Dolichopithecus*, and *Cercopithecoides*. *Mesopithecus* is the earliest definite Eurasian colobine and was originally thought to be extremely terrestrial in its long bone robusticity and forelimb morphology (Simons, 1970; Delson, 1973; Jablonski, 2002; Koufos et al., 2003), although some cite this robusticity as evidence for semi-terrestriality (de Bonis et al., 1990; Delson, 1994). The genus has been described as postcranially similar to extant Asian colobines suggesting a closer relationship to this

clade than to African taxa (Delson, 1973; Pan et al., 2004; Nakatsukasa et al., 2010; Frost et al., 2015). *Dolichopithecus* is another at least semi-terrestrial colobine and is characterized by robust long bones, a long humerus, and a shallow radial notch on the ulna (Szalay and Delson, 1979; Strasser and Delson, 1987; Gosselin-Ildari, 2013). *Cercopithecoides* is perhaps the most terrestrially adapted of the fossil colobines, with at least *C. williamsi* and *C. kimeui* being large-bodied (Leakey, 1982; Delson et al., 2000; Frost et al., 2003; McKee et al., 2011) although this terrestriality may be secondarily derived as it retains a relatively reduced pollex which is more associated with arboreal colobines (Frost et al., 2015).

Sympatry of multiple large-bodied primates, including hominins, in the fossil record suggests that niche-partitioning has played an important role in both cercopithecoid and human evolution (Elton, 2006). This idea is used to explain the shared occupation of similar ecological zones by multiple, sometimes closely related, taxa that exploit different food sources and/or substrates. The more closely-related these sympatric species, the more competition for resources predicted. In many sympatric primates, niches can overlap not only among species, but also among subfamilies like colobinae and cercopithecinae (Reed and Bidner, 2004). However, resource overlap alone is not necessarily evidence for competition and richer habitats, like the tropical forests inhabited by many colobines and other primates, have more ecological niches and therefore increased species diversity (Ganzhorn, 1989; Fleagle and Reed, 1996; Reed and Bidner, 2004). This idea has also been applied to examine the incongruity between fossil and extant forms (Cerling et al., 2015). One example of this approach in extant Platyrrhines hypothesized that changes to the rainforest micro-habitats and river courses over time led

to much of the extant species differentiation (Rosenberger, 1992). An example of this in extant colobines is seen with *Piliocolobus* and *Colobus* which overlap in their ecological zones with multiple mammalian and avian predators including humans (Reed and Bidner, 2004). Niche-partitioning has also driven the evolution of interspecific variation particularly in body size among guenons (Cardini and Elton, 2008). It is also important to consider competitive pressures of other mammalian species and how they may be affecting the exploitation of certain environments by primates. Many terrestrial habitats may have previously been exploited by large-bodied colobines become dominated by large mammals like alcelaphine bovids. Some hypothesize that colobines were limited in range expansion by their morphology leading to the extinction of terrestrial colobines in Africa seen today (Jablonski and Leakey, 2008).

The chapters are as follows: Chapter II provides a background into the materials and methods that will be used to assess the functional morphology of the fossil colobines. Chapter III provides a detailed functional postcranial description of *P. mutiwa* specimen KNM-WT 16827 and compares it to both *P. chemeroni* and other contemporaneous large-bodied cercopithecids. Chapter IV provides a detailed functional analysis and description of the unpublished specimen L895-1 from the Shungura Formation to assess its locomotor mode and similarities with other contemporaneous colobines. Chapter V incorporates the functional analyses and conclusions from Chapters III and IV to understand broad patterns of niche separation among these large-bodied cercopithecoid taxa. It combines body mass estimates, observed locomotor modes in extant taxa, and dietary proxies to better understand in what ways these primates may have overlapped. This dissertation highlights the importance of postcranial analyses for understanding how

niche separation affects these large primate taxa and may help to clarify the forces that lead to shifts in species diversity and the pressures that shaped human evolution.

CHAPTER II

POSTCRANIAL FUNCTIONAL MORPHOLOGY MATERIALS AND METHODS

Materials

Comparative Fossil Sample

In addition to the colobine specimens listed in Table 2.1, also included in the comparative fossil dataset are 110 cercopithecine specimens of which 78 were measured by E. Guthrie and used with permission (see Appendix B).

Comparative Extant Sample

A total of 488 individual specimens with associated postcrania were chosen to represent as diverse a range of locomotor modes, size, and taxa possible. This comparative dataset includes 309 colobine specimens representing 46 sub/species with 148 females, 136 males, and 18 unknown sex individuals; and 180 cercopithecine specimens representing 18 sub/species with 65 females, 107 males, and 8 unknown sex individuals from 11 domestic and international museums. Of the 488 extant cercopithecoid specimens, 25 colobine and 152 cercopithecines were measured by E. Guthrie and used with permission in the analyses presented here (see Appendix A).

Linear Metrics

Description of Measurements

Functional morphology analysis of specimens KNM-WT 16827 (Chapter III) and L895-1 (Chapter IV) were described qualitatively and quantitatively with a comparative set of both fossil and extant cercopithecoid postcranial specimens (Appendix A and B). In addition to Plio-Pleistocene taxa, extant cercopithecine and colobine taxa are included in

Table 2.1 Fossil colobine specimens included in the comparative postcranial dataset. All colobine specimens were measured by M. Anderson.

<i>Cercopithecoides kimeui</i>	<i>Rhinocolobus turkanensis</i>
KNM-ER 176	KNM-ER 16
<i>Cercopithecoides meaveae</i>	KNM-ER 1542
NME AL2	KNM-ER 5488
<i>Cercopithecoides williamsi</i>	KNM-ER 40076
KNM-ER 4420	KNM-ER 45611
<i>Cercopithecoides cf. williamsi</i>	<i>cf. Rhinocolobus sp. indet.</i>
KNM-ER 974	KNM-ER 12
<i>cf. Cercopithecoides</i>	KNM-ER 551
KNM-ER 30320	KNM-ER 40078
KNM-ER 37117	KNM-ER 40081
KNM-ER 39355	<i>Rhinocolobus cf. turkanensis</i>
<i>Paracolobus chemeroni</i>	KNM-ER 5481
KNM-BC 3	KNM-ER 40058
<i>Paracolobus mutiwa</i>	NME AL300-1
KNM-WT 16827	

the comparative sample to represent a wide a range of locomotor behaviors and body mass. The qualitative descriptions included state of preservation, taphonomic effects, and discussion of functionally relevant features and included 112 linear taken from right side elements in the comparative sample unless preservation or pathology prevented. All quantitative measurements and indices are either standard for postcranial description or have been modified from previous studies deeming them potentially functionally relevant (Birchette, 1982; Harrison, 1989; Strasser, 1989; Ting, 2001; Frost and Delson, 2002; Guthrie, 2011).

Description of Indices

Linear metrics were transformed into 54 ratios to more easily assess proportions of bones and features, relative sizes of functionally important regions, and reduce the effects of individual and species. All indices are standard postcranial ratios adapted from

Table 2.2 Linear metrics collected on postcranial specimens.

Metric Code	Scapula (Figure 2.1A)
S1	bottom of glenoid fossa to vertebral border of the spine
S2	maximum distance from superior to inferior angle
S3	superior to inferior edge
S4	lateral to medial along inferior portion
S5	superior surface of spine to superior angle
S6	spine to inferior angle
Humerus (Figure 2.1B)	
H1	greater tuberosity to distal capitulum
H2	head to distal capitulum
H3	most proximal point of head to most distal point of trochlea
H4	maximum medio-lateral (ML) diameter of proximal end
H5	maximum antero-posterior (AP) diameter of proximal end
H6	most anterior edge of head to most posterior edge of head
H7	most medial edge of head to most lateral edge head
H8	most distal edge of deltoid tuberosity to head
H9	maximum ML width of deltoid plane
H10	maximum AP diameter of midshaft
H11	maximum ML diameter of midshaft
H12	maximum AP dimension of shaft at extent of PBF
H13	maximum ML dimension of shaft at extent of PBF
H14	PBF to most distal extent of capitulum
H15	most medial medial epicondyle to most lateral lateral epicondyle
H16	medial trochlea to lateral capitulum
H17	lateral epicondyle to medial trochlea
H18	proximal trochlea edge to most distal edge
H1	diameter of most anterior to most posterior point of capitulum
H20	maximum AP length of olecranon fossa
H21	maximum ML width of olecranon fossa
Ulna (Figure 2.1C)	
U1	proximal olecranon process to most distal styloid process
U2	proximal olecranon process to most distal end excluding styloid process
U3	AP length of olecranon process
U4	proximo-distal (PD) height of olecranon process
U5	coronoid process to beak
U6	widest ML width of trochlear notch
U7	lateral radial notch to medial humeral facet
U8	maximum AP ulnar head breadth
U9	maximum ML ulnar head breadth
Radius (Figure 2.1C)	
R1	maximum length excluding styloid process
R2	maximum length with styloid process
R3	most distal radial head to most proximal radial tuberosity
R4	mid radial tuberosity to most proximal radial head

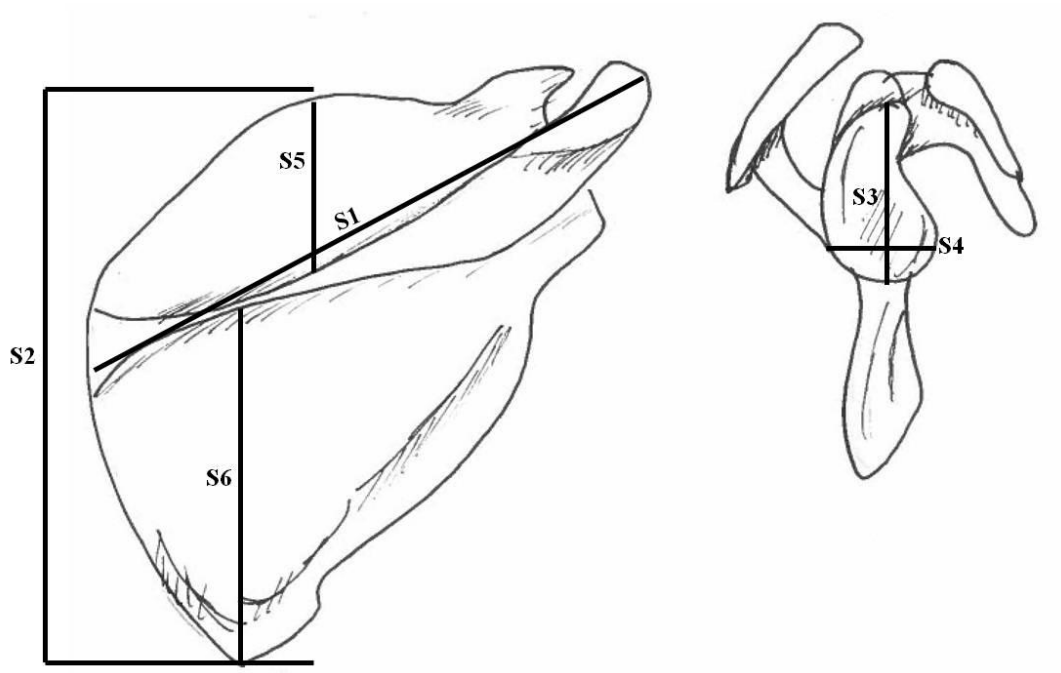
Table 2.2 continued

Metric Code	
R5	AP diameter of radial head
R6	ML diameter of radial head
R7	ML diameter of distal end
R8	AP diameter of distal end
<hr/> Innominate (Figure 2.1D) <hr/>	
IL1	iliac blade width
IL2	ventral iliac width
IL3	maximum width of the sacral face
IL4	length 1
IL5	length 2
IL6	iliac neck width
IL7	lower iliac height (LIH)
IL8	sacral face length
IL	AP auricular surface length
IL10	PD auricular surface length
IL11	maximum auricular surface height
PB1	maximum length of superior ramus
PB2	minimum width superior ramus
PB3	inferior ramus length
PB4	maximum inferior ramus width
PB5	minimum inferior ramus width
IS1	maximum greater sciatic notch width
IS2	maximum ischial tuberosity width
IS3	maximum ischial tuberosity length
AC1	PD acetabular fossa diameter
AC2	maximum AP acetabulum diameter
<hr/> Femur (Figure 2.1E) <hr/>	
F1	greater trochanter to most distal lateral condyle
F2	most proximal head to most distal medial condyle
F3	most medial head to most lateral greater trochanter
F4	fovea to midpoint of lesser trochanter
F5	maximum height of greater trochanter above neck
F6	maximum extension of lesser trochanter
F7	most proximal head to most distal edge
F8	most medial head to most lateral head edge
F9	anterior edge of head to posterior edge
F10	AP diameter of midshaft
F11	ML diameter of midshaft
F12	most distal medial condyle edge to most proximal edge of groove
F13	medial to distal patellar ridge (anterior view)
F14	medial edge of medial condyle to lateral edge of lateral condyle
F16	most posterior medial condyle to most anterior medial patellar ridge
F17	most posterior to most anterior edge of condyle in distal view

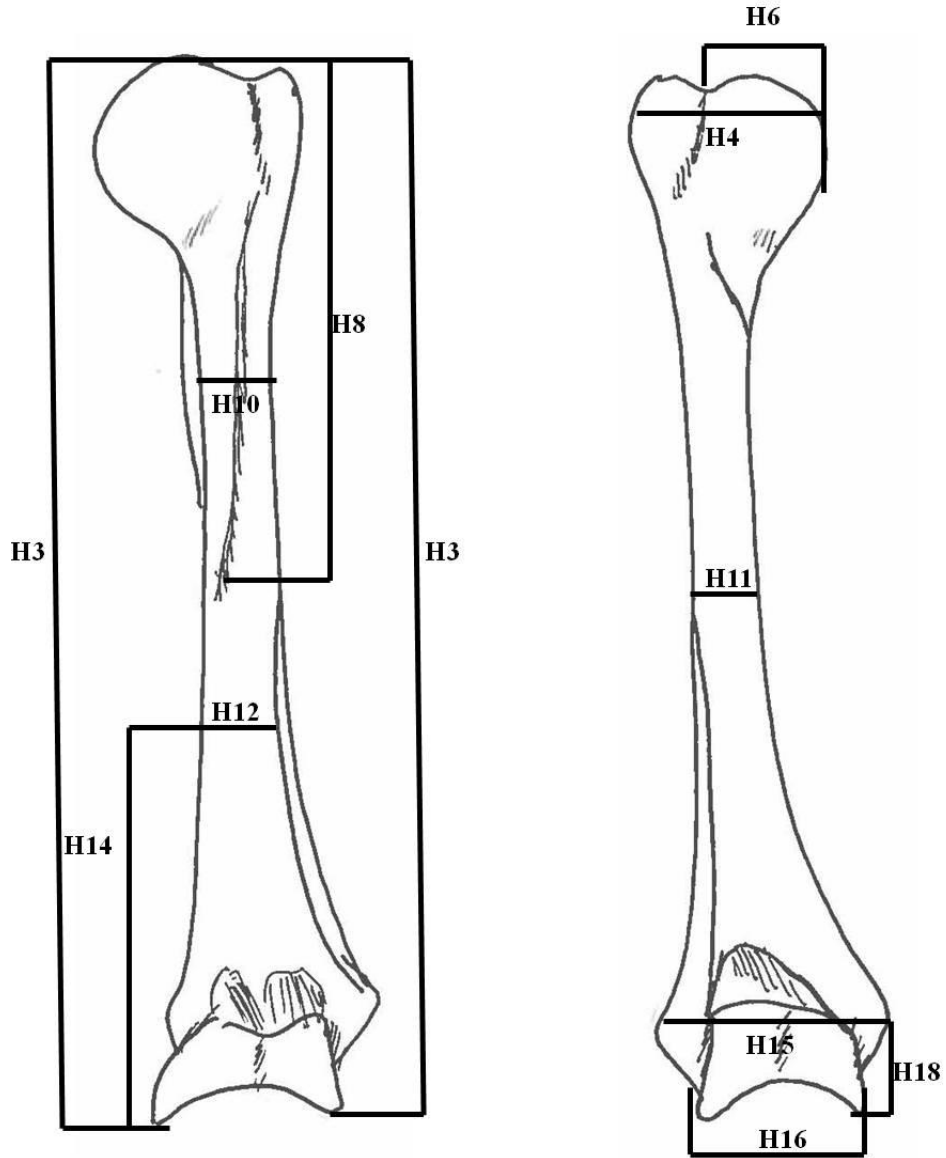
Table 2.2 continued	
Metric Code	
F18	most medial to most lateral edge in posterior view
F1	most medial edge to most lateral edge in posterior view
F20	most proximal to most distal edge in posterior view
F21	most proximal to most distal edge in posterior view
F22	deepest portion on intercondylar groove to deepest portion of patellar surface
Tibia (Figure 2.1F)	
T1	maximum length including medial malleolus
T2	maximum length excluding medial malleolus
T3	maximum ML length of proximal end
T4	maximum AP length of proximal end
T5	maximum AP length of lateral condyle
T6	maximum AP length of medial condyle
T7	maximum ML width of lateral condyle
T8	maximum ML width of medial condyle
T9	maximum ML width of distal end
T10	maximum ML width of malleolus in distal view
T11	most lateral medial malleolus edge to most lateral talar surface
T12	maximum AP length of talar surface
Astragalus (Figure 2.1G)	
TL1	maximum PD length
TL2	maximum PD length of lateral margin
TL3	maximum breadth
TL4	maximum breadth excluding malleolar facet
TL5	maximum height in lateral view of lateral keel
TL6	maximum ML breadth of trochlear surface at distal end
TL7	maximum ML breadth of trochlear surface at proximal end
Calcaneus (Figure 2.1G)	
C1	maximum PD length
C2	PD anterior length
C3	PD length of anterior segment to posterior articulation
C4	PD posterior facet length
C5	PD anterior articular facet length
C6	ML breadth

Figure 2.1 Illustrations of postcranial metrics used in this study (Table 2.2).

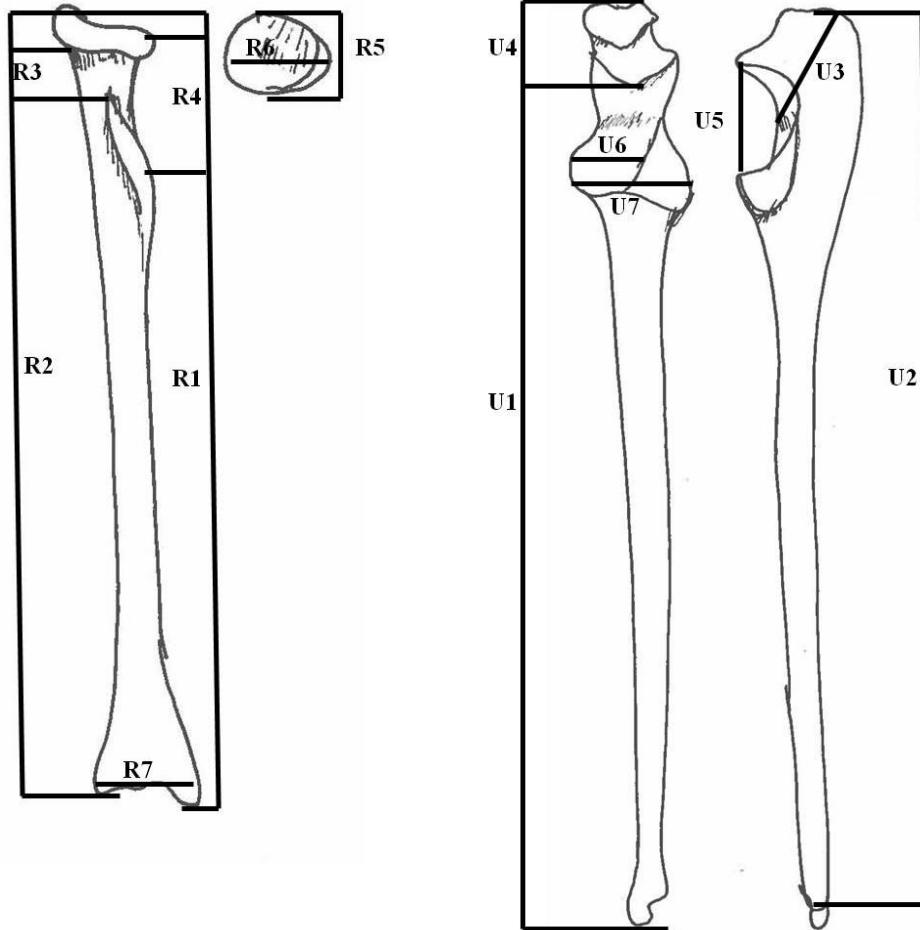
A. Scapula



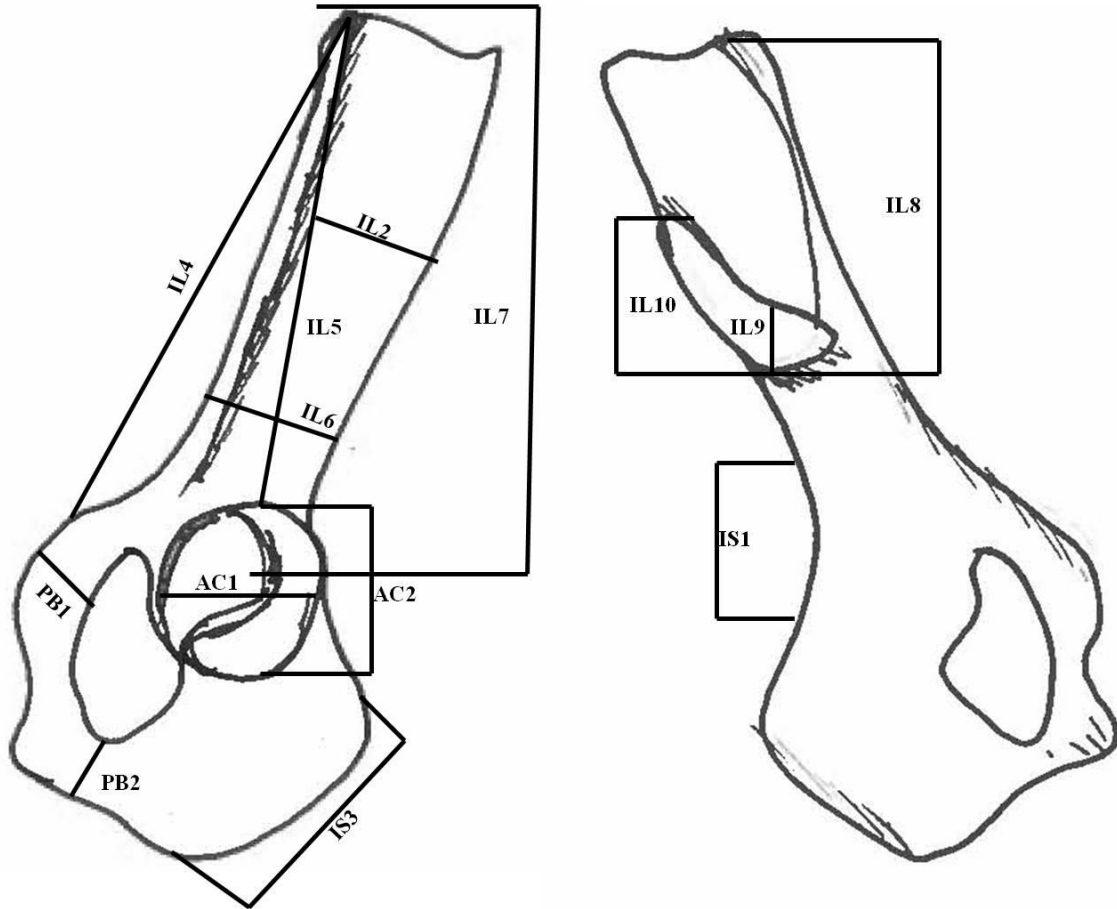
B. Humerus



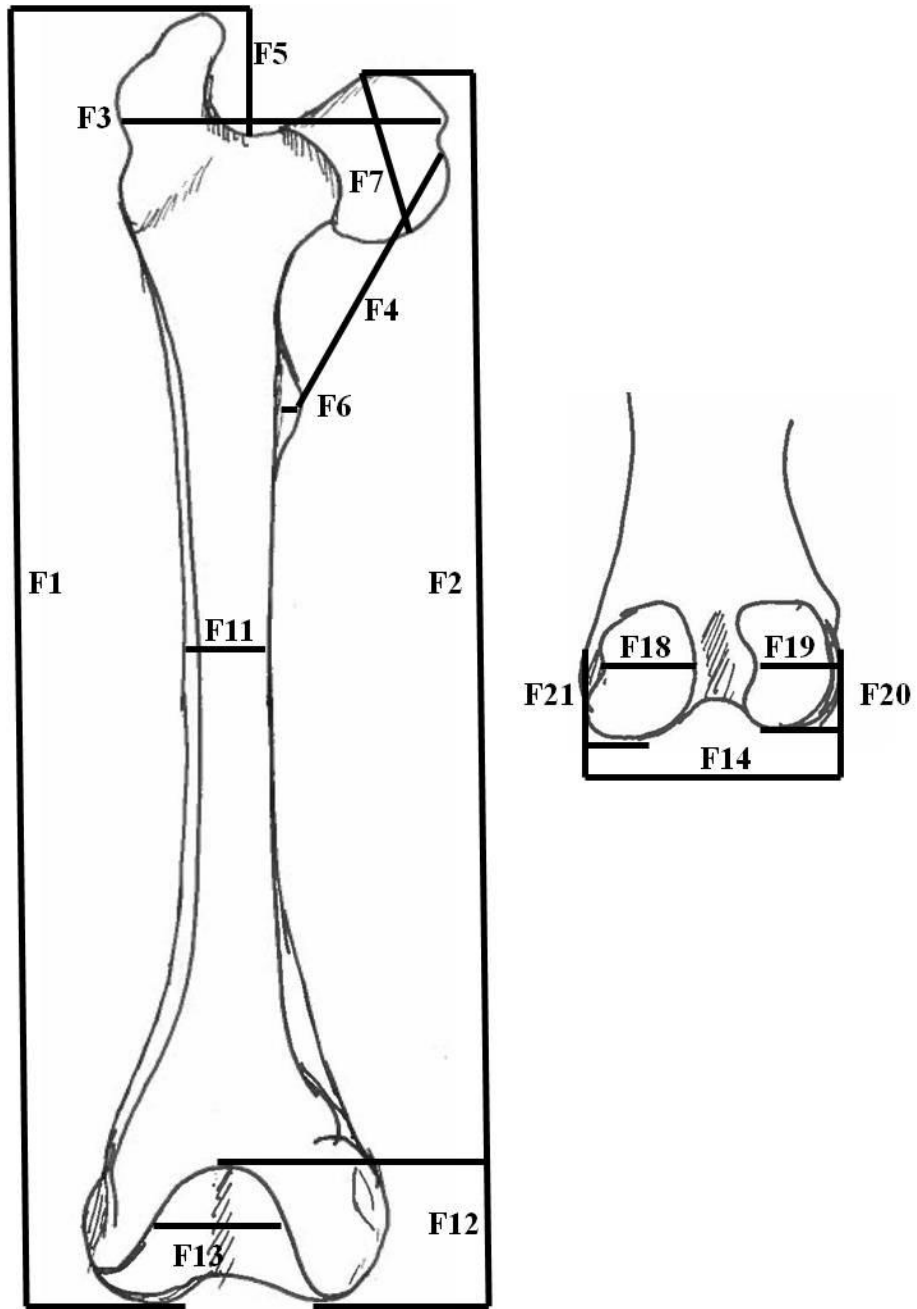
C. Radius and Ulna



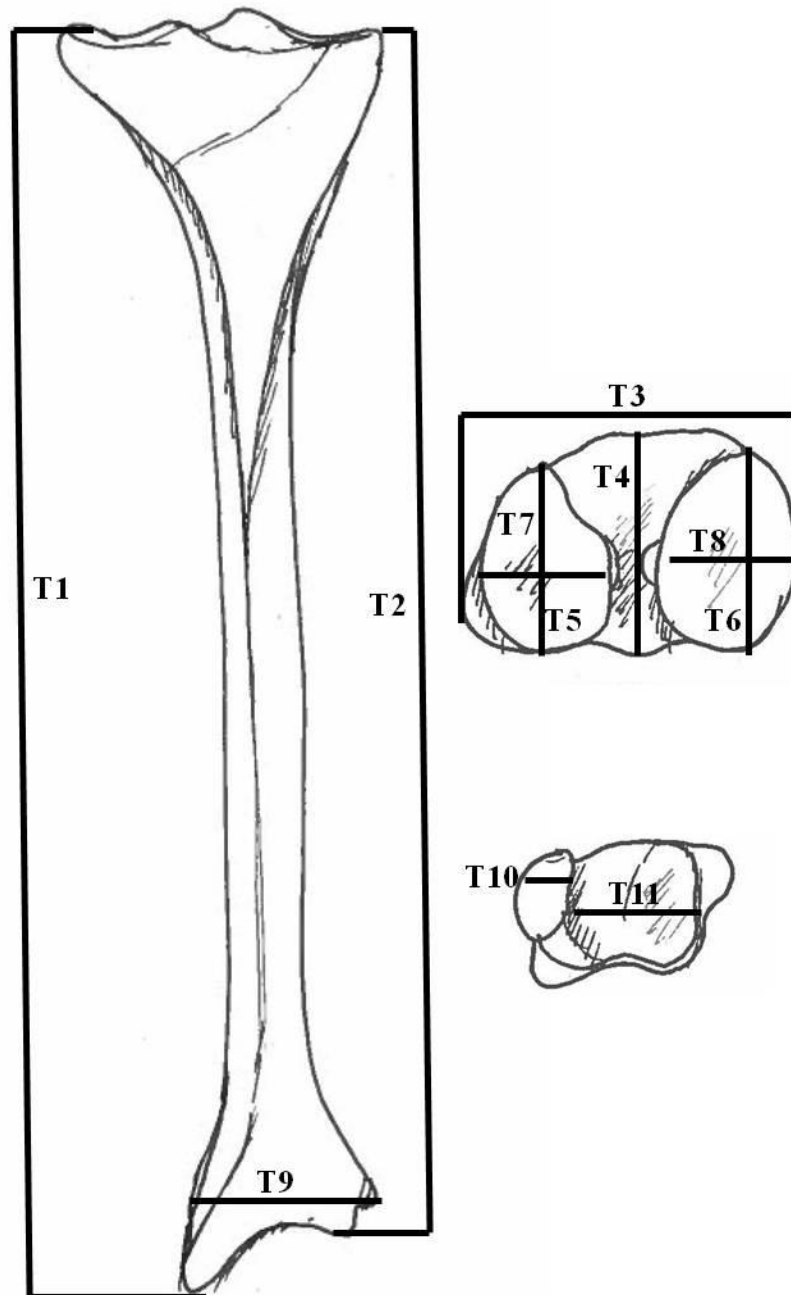
D. Os Coxae



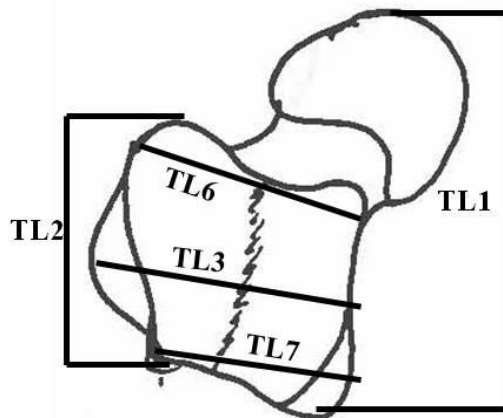
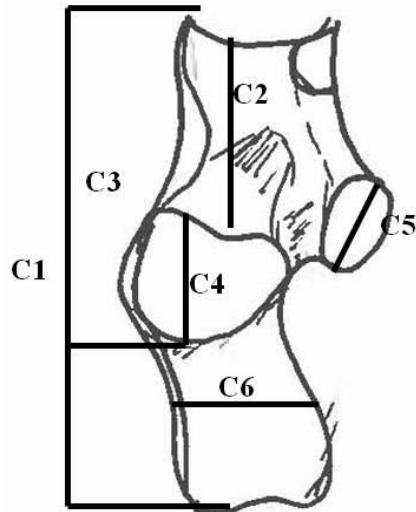
E. Femur



F. Tibia



G. Astragalus and Calcaneus



previous studies that are thought to have functional relevance (Table 2.3; Birchette, 1982; Harrison, 1989, 1990; Ting, 2001; Frost and Delson, 2002; Guthrie, 2011). Indices were calculated using the collected linear metrics given in Table 2.2. Given the variability in available elements and preservation of the comparative datasets, not all indices were able to be calculated on all taxa. For a full list of all indices collected on the fossil taxa see Appendix B.

Qualitative Descriptions of Functional Morphology

Qualitative descriptions included state of preservation, taphonomic effects, and assessment of features that have been deemed functionally relevant in previous studies (Birchette, 1982; Harrison, 1989; Strasser, 1989; Ting, 2001; Frost and Delson, 2002; Guthrie, 2011). Comparisons within the element descriptions highlight comparisons with large extant taxa such as *Nasalis*, *Semnopithecus*, and *Trachypithecus*, as well as *Colobus* for an example of a contemporary African group as well as with other known large-bodied taxa with associated postcranial elements including *P. chemeroni*, *C. meaveae*, *C. kimeui*, *C. williamsi*, *R. turkanensis*, *T. oswaldi*, and *T. brumpti*.

Body Mass Estimates

Body masses were estimated using the mean of 7 postcranial metrics deemed appropriate for fossil cercopithecids, including two from the humerus, three from the femur, and three from the tibia (Table 2.2; Delson et al., 2000; Ruff et al., 2002, 2003). These included the length of the humerus (H2), medial-lateral of the humerus at midshaft (H11), femoral length (F2), anterior-posterior width of the femur at midshaft, medial-lateral width of the femur at midshaft (F11), the medial-lateral width of the proximal tibia (T3), and the talar facet area (T11 x T12). Body mass estimates for the fossil and extant

Table 2.3 Indices taken on all specimens with relevant preserved linear metrics. Indices in bold are included in the functional estimations in Chapter V.

Index Code	Scapula	Description
IS1	shape	(S2/S1) x 100
IS2	glenoid fossa shape	(S4/S3) x 100
IS3	supraspinatus fossa	(S5/S1) x 100
IS4	infraspinatus fossa	(S6/S1) x 100
Humerus		
IH1	relative head height	(H1/H2) x 100
IH2	humeral head shape 1	(H4/H5) x 100
IH3	humeral head 2	(H7/H2) x 100
IH4	medial epicondyle breadth	[(H17-H15) x 100]/H17
IH5	relative trochlea length	(H18 x 100)/H16
IH6	relative capitulum depth	(H19/H15) x 100
IH7	distal width index	(H15/H2) x 100
IH8	Harrison's breadth	(H17/H15) x 100
IH9	olecranon fossa index	(H20/H21) x 100
Ulna		
IU1	olecranon process length index	(U3/U5) x 100
IU2	olecranon process shape	(U3/U4) x 100
IU3	trochlear notch 1	(U5/U6) x 100
IU4	trochlear notch 2	(U5/U7) x 100
IU5	trochlear notch 3	(U7/U6) x 100
Radius		
IR1	head shape	(R5/R6) x 100
IR2	neck length	(R3/R6) x 100
Hip1	femoral head relative to LIH	ln(F9)/ln(IL7)
Hip2	greater trochanter relative to femoral head	ln(F9)/ln(F5)
Femur		
IF1	femoral shape	(F8/F1) x 100
IF2	relative breadth	(F3/F1) x 100
IF3	greater trochanter length	(F5/F1) x 100
IF4	lesser trochanter length	(F6/F1) x 100
IF5	relative trochanter height	(F5 x 100)/F9
IF6	distal shape	(F14/F15) x 100
IF7	femoral groove	(F22/F1) x 100
IF8	patellar groove shape	(F13/F12) x 100
IF9	condyle depth	(F17/F16) x 100
IF10	condyle length	(F21/F20) x 100
IF11	condyle width	(F19/F18) x 100
Tibia		
IT1	proximal end shape	(T4/T3) x 100
IT2	condyle width	(T7/T8) x 100
IT3	condyle length	(T5/T6) x 100

Table 2.3 continued

Index Code	Tibia	
IT4	medial malleolus length	$(T1-T2)/T1 \times 100$
IT5	medial malleolus width	$(T10/T1) \times 100$
TTSA	distal articular surface shape	$(T12/T11) \times 100$
Astragalus		
ITL1	trochlear shape	$(TL6/TL7) \times 100$
ITL2	trochlea width proportion	$(TL4/TL3) \times 100$
ITL3	trochlear height	$(TL5/TL4) \times 100$
Calcaneus		
IC1	anterior index	$(C2/C1) \times 100$
IC2	posterior facet	$(C4/C1) \times 100$
IC3	anterior facet	$(C5/C1) \times 100$
IC4	calcaneal tuberosity length	$[(C1 - C3)/C1] \times 100$

comparative samples are based on taxon means presented in Delson et al. (2000) or based on body masses reported for individual specimens as reported in their respective collections database. For all analyses including body mass as a variable, the taxon means calculated from dental and postcranial estimates are used except for L895-1 for which only postcranial estimates are known (Table 4.5; Delson et al., 2000).

CHAPTER III

AN ASSESSMENT OF THE POSTCRANIAL SKELETON OF *PARACOLOBUS MUTIWA* (PRIMATES: COLOBINAE) SPECIMEN KNM-WT 16827 FROM LOMECKWI, WEST TURKANA KENYA

Introduction

The Colobinae are a geographically widespread subfamily of the Cercopithecidae with extant forms present in Africa and Asia and a diversity of fossil taxa known from sites in Africa and Europe, and Asia with living forms occupying a wide range of climates and environments suggesting an evolutionary history marked by multiple radiations (Delson, 1994; Wang et al., 2013). Molecular analyses have estimated a divergence from cercopithecines by 14.4-17.9 Ma (Raaum et al., 2005; Steiper and Seiffert, 2012), but the fossil record is not abundant until the Plio-Pleistocene and many of living forms do not appear until much later (Delson, 1975, 1994; Szalay and Delson, 1979; Leakey, 1982, 1987; Strasser and Delson, 1987; Ting, 2008; Jablonski et al., 2002, 2008; Wang et al., 2013). KNM-WT 16827 is an associated partial skeleton of a large colobine monkey from the upper part of the Lomekwi Member of the Nachukui Formation at West Turkana dated to 2.58-2.53 Ma and is classified as a male *Paracolobus mutiwa* based on its cranial similarities to specimens known from the Omo Valley and Koobi Fora. (Harris et al., 1988; Feibel et al., 1989; McDougall, 2012). It is currently the only specimen attributed to this taxon with associated postcranial elements making it invaluable for understanding both the diversity of functional adaptations in fossil colobines and for what these adaptations may say about the paleoecological conditions under which this such a diversity of cercopithecidae were able to thrive (Leakey, 1982, 1985, 1987; Harris et al, 1988).

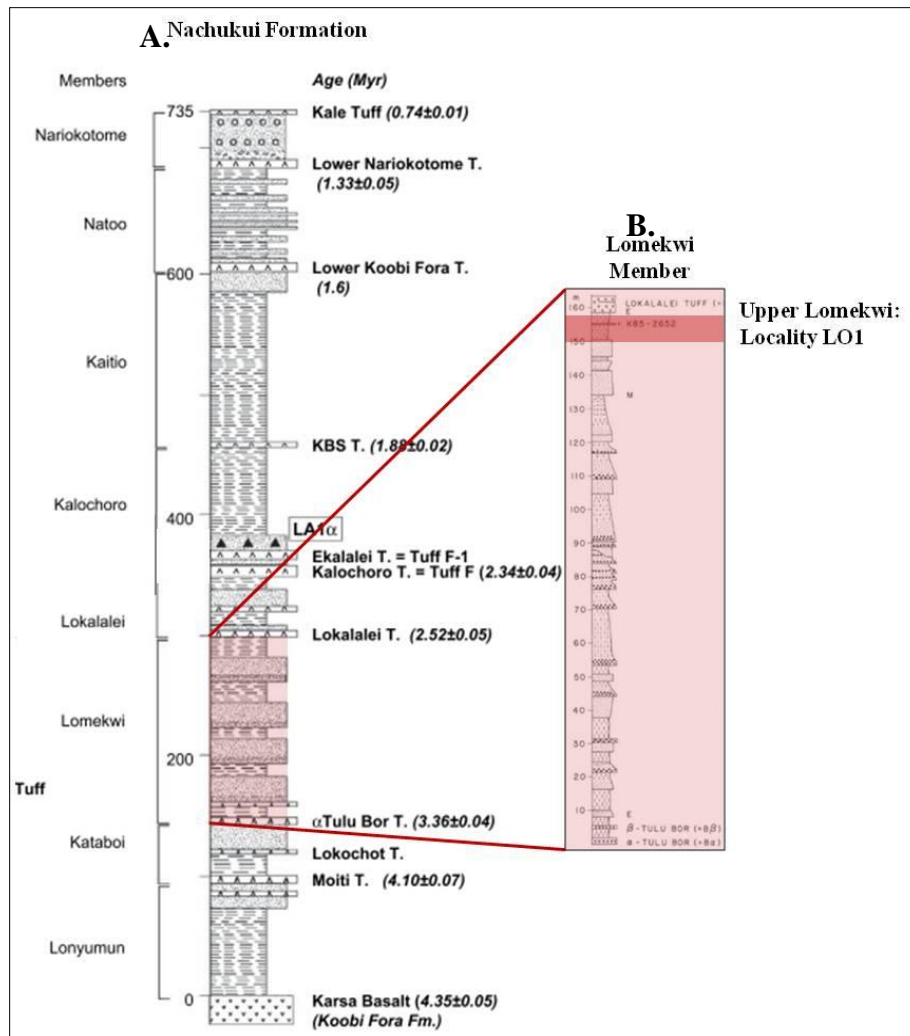
In addition to *Paracolobus*, several African genera are known exclusively from the fossil record including *Rhinocolobus*, *Cercopithecoides*, and *Kuseracolobus*; many of which are represented by both craniodental and postcranial remains (Leakey, 1982; Delson, 1994; Elton, 2000; Frost and Delson, 2002; Hlusko, 2006; Jablonski et al., 2008; Frost et al., 2009). These taxa are all larger than and morphologically distinct from extant colobinans and disappear from the fossil record after 1.5 Ma (Jablonski, 2002; Jablonski and Frost, 2010). Although the relationships between fossil and extant colobinans are unclear, there are many hypotheses that try to link the fossil taxa to extant forms with some suggesting that all of the Plio-Pleistocene taxa are stem African colobinans (Delson, 1975, 1994; Szalay and Delson, 1979; Strasser and Delson, 1987). Earlier Eurasian taxa such as *Mesopithecus* and *Dolichopithecus* show adaptations for terrestriality that may have evolved secondarily in Plio-Pleistocene taxa such as *C. williamsi*, *P. chemeroni*, and *P. mutiwa* (Leakey, 1982; Jablonski et al., 2008; Frost et al., 2015). Frost et al. (2015), however, showed that *C. williamsi* possesses the reduced pollex of extant colobinans. Additionally, a close relationship between *Rhinocolobus* and extant *Nasalis* has also been proposed (Leakey, 1982; Jablonski et al., 2008). Extant colobinans are notably less diverse than their fossil counterparts in being almost exclusively arboreal with only three recognized genera: *Colobus*, *Procolobus*, and *Piliocolobus*, none of which are prevalent in the fossil record until the late Pleistocene (Delson, 1994; Harrison and Harris, 1996; Jablonski, 2002; Grubb et al., 2003; Ting et al., 2008).

There are three recognized species within *Paracolobus*: *P. enkorikae* (Hlusko, 2007), *P. chemeroni* (Leakey, 1969), and *P. mutiwa* (Leakey, 1982) as well as specimens

attributed to *Paracolobus sp.* found at Laetoli (Leakey, 1982; Leakey and Delson, 1987) that were later reassigned to *Rhinocolobus sp.* (Harrison, 2011). *P. chemeroni* and *P. mutiwa* are currently the only two species represented by specimens with associated postcranial elements. *P. chemeroni* is known definitively from the well-preserved male specimen KNM-BC 3 from the Baringo Basin, Kenya dated to 3.2 Ma and a tentatively assigned mandible from the Middle Awash (Leakey, 1969; Kalb, 1982; Leakey, 1982; Frost, 2001; Deino et al., 2002). *Paracolobus mutiwa* is known only from the Turkana Basin with a holotype female maxilla (KNM-ER 3843), and mandible of unknown sex (KNM-ER 125) from the Upper Burgi Member of Koobi Fora, Kenya dated between 1.95 and 1.87 Ma (Leakey, 1982; Jablonski et al., 2008; MacDougall et al., 2012;). Several maxillary and mandibular fragments from Members C6-9 to G1-5 of the Shungura Formation, Ethiopia expand this range from 2.6 to 2.2 Ma while isolated teeth from Members A1 through G27-29 and the Usno Formation also in Shungura may further extend the species' range from 3.6 to 1.9 Ma (Leakey, 1982; 1987; MacDougall et al., 2012; Kidane et al., 2014). KNM-WT 16827 was collected from locality Lomekwi 1 making it from the upper part of the Lomekwi Member just below the Lokalalei Tuff (=D) and above the Emekwi Tuff (=C9) dating it to between 2.58 and 2.53 Ma (Figure 3.1; Harris et al., 1988; MacDougall et al., 2012).

Like many extant cercopithecids, *P. mutiwa* displays significant sexual dimorphism with body masses from dentition estimated at 27 and 52 kg for females and males respectively (Leakey, 1982; 1987; Harris et al., 1988; Delson et al., 2000; MacDougall et al., 2012). A lower male estimate of 35 kg for male body mass based on the postcrania of KNM-WT 16827 has also been proposed (Ting, 2001). In addition to *P.*

Figure 3.1. Stratigraphic map of KNM-WT 16872's locality within the Nachukui Formation. A. Modified from Prat et al., 2005, Figure 3.1, pg. 232. B. Modified from Harris et al., 1988, Figure 3.7, pg. 14.



chemeroni and *P. mutiwa* share several cranio-dental features including a wide muzzle, broad interorbital region, deep and robust mandibular corpus, well-developed P³ protocone, and M₃ with a distal lophid that is narrower than the mesial (Leakey, 1982, 1987; Harris et al., 1988; Frost, 2001; Jablonski et al., 2008). *P. mutiwa* is cranially distinguished from *P. chemeroni* by a longer and taller rostrum, maxillary ridges and postcanine fossa, less sharply converging temporal lines, deeper mandibular corpus,

expanded gonial angle in males, and relatively larger dentition (Leakey, 1982, 1987; Harris et al., 1988; Frost, 2001a,b; Jablonski et al., 2008).

Paracolobus mutiwa specimen KNM-WT 16827 includes partial maxillae and mandible with nearly complete dentition, as well as numerous postcranial elements (Figure 3.2; Table 3.1). Although several have been reconstructed, the preserved long bones are largely undistorted with well-preserved articular surfaces and relevant

Figure 3.2 Elements included in the functional description of ♂ *Paracolobus mutiwa* specimen KNM-WT 16827. See Table 1 for full list of associated elements.



Table 3.1 All identified postcranial elements associated with specimen KNM-WT 16827. Elements in bold were complete enough to be included in this description and functional analysis.

Catalog Number	Side	Element	Description
WT 16827AD	R	radius	proximal to midshaft fragment
WT 16827AE	R	radius	distal shaft fragment
WT 16827AF	L	radius	proximal shaft fragment
WT 16827AG	L	ulna	shaft fragment
WT 16827AH		radius?	shaft fragment
WT 16827AI	L	tibia	shaft fragment
WT 16827G	L	innominate	ilium, acetabulum, & ischium fragment
WT 16827H	R	innominate	ilium, acetabulum, & ischium fragment
WT 16827I	R	femur	proximal & shaft fragment
WT 16827J	L	humerus	distal & shaft fragment
WT 16827K+M+V	R	humerus	
WT 16827L	R	ulna	proximal & shaft fragment
WT 16827N	L	MT I	proximal fragment
WT 16827O	R	scapula	glenoid, coracoid, & acromion fragment
WT 16827P	L	calcaneus	
WT 16827Q	L	talus	
WT 16827R	R	talus	
WT 16827S	L	navicular	
WT 16827T			long bone fragment
WT 16827U			long fragment
WT 16827W		P2	
WT 16827X			long bone fragment
WT 16827Y	R	MT II	
WT 16827Z	R	MT III	

functional features. Associated elements include a left scapula fragment, a nearly complete left humerus, distal right humerus, right radius, right ulna, left and right innominates, right femur, right and left astragali, and left calcaneus. KNM-WT 16827 also preserves fragments of the vertebrae, left tibia, right metatarsals I-III, right navicular, and phalanges which are not described here. It shows postcranial morphologies distinct from *P. chemeroni* including having shorter and more robust long bones relative to the size of the crania. Postcranial comparisons of these two taxa have brought the generic status of *P. mutiwa* into question and although the postcrania of KNM-WT 16827 is

largely undescribed, analyses of the scapula, humerus, pelvis, femur, and tarsals as have been proposed as being more terrestrial than *P. chemeroni* (Leakey, 1969; Harris et al., 1988; Ting, 2001; Hammond, 2013). The specimen is also distinct from contemporary large-bodied colobines in the Turkana Basin such as *Rhinocolobus turkanensis*, *Cercopithecoides williamsi*, and *Cercopithecoides kimeui*. Of these, *R. turkanensis* is the most arboreal and although much larger, possesses forelimb and hindlimb adaptations similar to extant colobines (Leakey, 1982; Delson, 1994; Elton, 2000; Frost and Delson, 2002; Jablonski et al., 2008). All *Cercopithecoides* species with associated postcrania, including the slightly smaller *C. meaveae* from the earlier Pliocene, show limb morphology consistent with more terrestrial locomotion, and with *C. williamsi* showing extreme terrestrial adaptations compared to other colobines (Leakey, 1982; Delson, 1994; Delson et al., 2000; Frost and Delson, 2002; Frost et al., 2003; Jablonski et al., 2008; Frost et al., 2015). The description presented here includes most of the postcranial skeleton associated with KNM-WT 16827 to provide a detailed functional and comparative analysis of this specimen relative to *P. chemeroni* specimen KNM-BC 3 and other identified Plio-Pleistocene colobine, cercopithecine, and extant taxa.

Results

The linear metrics collected on KNM-WT 16827 are listed in Table 3.2. These measurements were used to calculate all functionally relevant indices for both the qualitative and quantitative comparisons for each element.

Scapula (KNM-WT 16827O)

Very little of the scapular blade is present making overall shape impossible to estimate, but the preserved portion is large and robust relative to those of extant colobines

Table 3.2 Linear metrics from all postcranial elements associated with KNM-WT 16827.
See Table 2.1 for full descriptions.

Postcranial Metric	Value (mm.)
Scapula	
S3 superior to inferior edge of glenoid fossa	35.64
S4 lateral to medial width of inferior glenoid fossa	21.66
Humerus	
H2 proximal humeral head to distal capitulum	241
H3 proximal humeral head to most distal point of trochlea	241
H4 anterior edge of head to most posterior edge	29.82
H5 medial edge of head to most lateral edge	29.56
H8 distal edge of deltoid tuberosity to most proximal head	119.8
Table 3.2 continued	
Postcranial Metric	Value (mm.)
H9 maximum medio-lateral (ML) width of deltoid plane	20.62
H10 maximum anterior-posterior (AP) diameter of midshaft	19.14
H11 maximum ML diameter of midshaft	17.67
H12 maximum AP width of shaft at proximal brachioradialis flange (PBF)	16.31
H13 maximum ML width of shaft at extent of PBF	20.16
H14 PBF to most distal extent of capitulum	87.48
H15 most medial medial epicondyle to most lateral lateral epicondyle	48.96
H16 most medial trochlea to most lateral capitulum	39.88
H17 lateral epicondyle to medial trochlea (Harrison's breadth)	43.37
H18 proximal trochlea edge to most distal edge	18.38
H19 maximum AP diameter of capitulum	25.61
H20 maximum AP length of olecranon fossa	16.73
H21 maximum ML width of olecranon fossa	21.42
Ulna	
U3 AP length of olecranon process	16.02
U4 proximo-distal (PD) length of olecranon process	18.15
U5 coronoid process to beak	19.91
U6 maximum ML width of trochlear notch	12.99
U7 lateral radial notch to medial humeral facet	22.84
Radius	
R3 most distal radial head to most proximal radial tuberosity	*8.19
Os coxae	
IL1 maximum iliac blade width	*55.39
IL2 maximum width of ventral iliac face	31.99
IL3 maximum width of sacral iliac face	33.08
IL4 most proximal iliac blade to most distal acetabulum border	133.12
IL5 iliac neck width	28.61
IL6 most proximal Iliac crest to most distal auricular surface	*74.84
IL7 middle of acetabulum to distal auricular surface (lower iliac height)	67.34

Table 3.2 continued

Postcranial Metric	Value (mm.)
IL8 AP length of auricular surface	16.37
IL9 maximum cranio-caudal length of auricular surface	11.93
IL10 most PD height of auricular surface	25.87
IL11 maximum greater sciatic notch width	12.7
IS2 maximum width of ischial tuberosity	33.98
IS3 maximum length of ischial tuberosity	53.12
AC1 maximum PD acetabular fossa diameter	40.21
AC2 maximum A-P acetabulum diameter	29.37
Femur	
F3 most medial head to most lateral greater trochanter	56.93
F4 fovea to midpoint of lesser trochanter	43.09
F5 maximum height of greater trochanter above neck	14.46
F6 maximum extension of lesser trochanter from shaft	11.37
F7 most proximal head to most distal edge	28.19
F8 most medial head to most lateral head	26.64
F10 AP length of head	29.55
F11 AP diameter of midshaft	20.04
F12 ML diameter of midshaft	18.66

Table 3.2 continued

Astragalus	
Postcranial Metric	Value (mm.)
TL1 maximum PD length	38.25
TL2 maximum PD length of lateral margin	22.04
TL3 maximum M-L breadth	28.25
TL4 maximum M-L breadth excluding malleolar facet	26.18
TL5 maximum height in lateral view of lateral keel	19.37
TL6 maximum M-L breadth of trochlear surface at distal end	15.61
TL7 anterior trochlear surface breadth	19.81
Calcaneus	
C1 maximum PD length	52.86
C2 anterior edge of posterior talar facet to cuboid facet	16.09
C3 PD length of anterior segment to posterior articulation	33.71
C4 maximum PD length of posterior facet	17.6
C5 maximum PD length	12.84
C6 maximum M-L breadth	15

and *C. williamsi* but similar in size to *P. chemeroni* and *R. turkanensis*. The scapula is incomplete with only the glenoid fossa, coracoid process, and parts of the acromion

process and spine, but most of the blade is broken off. It is also highly fragmented, although minimally distorted with strong and prominent muscle attachments on its preserved surfaces (Figure 3.3).

Figure 3.3 Ventral (Lt.) and lateral (Rt.) view of Rt. scapula of *Paracolobus mutiwa* specimen KNM-WT 168270.



Preservation

The glenoid fossa is well-preserved except for some mild weathering and the coracoid process is similarly complete except for a small piece that is missing from its ventro-inferior aspect. The supraspinous fossa is broken just medial to the coracoid process and this break extends supero-laterally to infero-medially where it meets the scapular spine. The acromion process lacks its lateral extensions and the scapulo-clavicular articular surface is also broken off. The medial portion of acromion process neck is also broken and is missing a small portion from the most medial aspect, but enough of the dorsal projection is present to estimate prominence of the scapular spine.

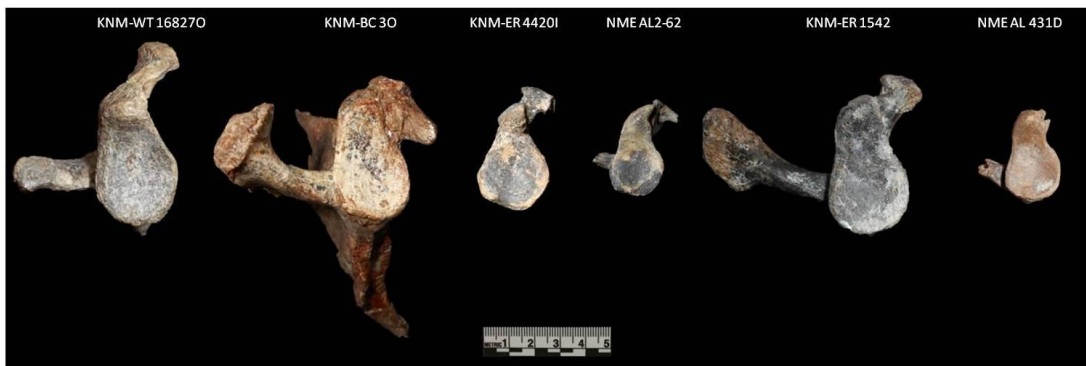
About 25 mm of the spine is preserved and although the apex is weathered, the original height of this feature does not appear to be distorted. More of the infraspinous fossa is preserved than the supraspinous fossa, but the blade and vertebral border

immediately inferior and medial to the spine is missing. The preserved portion of the costal margin is in good condition except for a small part missing immediately inferior to the base of the acromion process. The total length of the preserved costal margin is approximately 7 cm measured from the inferior portion of the glenoid fossa to the most medial extension. As many of the functionally relevant features of the scapula scale relative to body size, all comparisons to extant taxa are with identified male specimens.

Description

The articular surface of the glenoid fossa is piriform in outline and concave. Its superior margin projects slightly more laterally than does the inferior. The glenoid fossa is comparable in size to that seen in the other large fossil colobines, but not as round as that of *R. turkanensis* or *C. williamsi* (Figure 3.4). Compared to *P. chemeroni*, KNM-WT

Figure 3.4 Lateral view of the scapulae of (L-R) KNM-WT 16827, ♂ *Paracolobus chemeroni*, ♂ *C. williamsi*, ♂ *Cercopithecoides meaveae*, ♂ *Rhinocolobus turkanensis*, and *Theropithecus oswaldi*. Specimens KNM-ER 4420I and NME AL2-62 have been flipped vertically for ease of comparison.



16827 has a supero-inferiorly taller glenoid with more lateral projection of its superior edge and both have a low-level of concavity to their articular surfaces suggesting an emphasis on flexibility at the scapulo-humeral joint (Roberts, 1974; Larson, 1993; Dunham et al. 2015; Bailey et al., 2017). In inferior view, the blunt and thick glenoid

fossa borders give the articular surface a “golf tee” shape with a small indentation just medial to the base where the neck of the acromion process begins.

Both KNM-WT 16827 and *P. chemeroni* have a sharper glenoid lip than *R. turkanensis* and *C. williamsi*, but the weathered nature of this feature in KNM-WT 16827 may exaggerate the bluntness. The supraglenoid tubercle is smooth with a small eminence and round indentation on its ventral face immediately before grading into the coracoid process. The tubercle is smaller than in *R. turkanensis* and more closely resembles *C. williamsi* in prominence suggesting a similarly well-developed long head of *m. biceps brachii* and a stronger emphasis on stability during elbow flexion and forearm supination (Ashton and Oxnard, 1964; Rose, 1988; Jablonski and Leakey, 2008). The coracoid process is broken so comparison of all *m. biceps brachii* attachments is impossible but, what is preserved of the base is not as robust as *P. chemeroni* and *R. turkanensis* (Figure 3.4) or extant arboreal colobines such as *Nasalis*, *Colobus* and *Trachypithecus*.

The acromion process of KNM-WT 16827 is less robust than that of *P. chemeroni* but the apex cannot be compared due to damage. The articular surface for the clavicle is not preserved, but the base of the acromion process as it extends dorsally away from the scapular spine is narrow and triangular in cross-section. The most lateral portion is not preserved but appears to have been relatively supero-inferiorly shallow with some incline as it projected away from the body of the scapula. It is more inferiorly positioned than it is in *P. chemeroni*, and it lacks the small crest running medially from the superior border of the acromion process's most lateral projection present in *P. chemeroni*. Instead KNM-WT 16927 has a slight keel and is missing the subtle bulge on the lateral margin of the

inferior surface of the acromion process that is present in *P. chemeroni*. The attachment site of *m. deltoideus* is a small rough area partially preserved on the lateral-most aspect of the acromion process and is similar in rugosity to that of *P. chemeroni*.

About 2.5 cm of the scapular spine is preserved and is straight as it extends medially beginning at the base of the acromion process. Only a small portion of the supraspinous fossa is present and does not include the *m. supraspinatus* facet. The costal margin is the best-preserved portion of the infraspinous fossa and slopes steeply medio-laterally beginning immediately inferior to the glenoid fossa. The lateral margin is thickened with marked concavity on the dorsal surface inferior to the scapular spine for the attachment of *m. teres major*. Unfortunately, not enough of the scapular blade is preserved for functional analysis.

Humerus: KNM-WT 16827K+M+V (Rt.) & KNM-WT 16827J (Lt.)

Both the right and left humerus are present at varying degrees of preservation. The right side is more complete with a head, diaphysis, and the distal articular surface all preserved allowing for functional analyses involving length (Figure 3.5). The left side is missing the proximal end but retains part of the diaphysis and the whole distal articular surface. The humerus is robust and short relative to *P. chemeroni* with a well-developed brachioradialis flange and strong distal muscle attachments for well-developed flexors and wrist extensors consistent with terrestrial locomotion although not to the extreme seen in *Theropithecus* (Jolly, 1967, 1972; Harrison, 1989; Schmitt, 1998; Gilbert et al., 2010). The humerus is distinct from arboreal taxa such as *R. turkanensis* and more closely resembles the terrestrial *P. chemeroni* and *C. williamsi* particularly in its robust proportions and the morphology of the distal articular surface (Figure 6-9).

Preservation

The right side preserves more than the left side allowing for length estimates and has been reconstructed from three large pieces: KNM-WT 16827K+M+V (Figure 3.5).

Figure 3.5 L-R: Ventral view of *Paracolobus mutiwa* right humerus KNM-WT 16827K+M+V, ventral view left humerus specimen WT 16827J, dorsal view of right humerus, and dorsal view of left humerus.



The proximal end is missing the greater tubercle and is weathered around the humeral head with a few small pieces also broken off from the surgical neck and lateral aspect. The diaphysis is well-preserved and undistorted with minor damage in the form of small pieces missing from the proximo-lateral aspect, the dorsal aspect immediately proximal to the brachioradialis flange, proximal to the lateral epicondyle, and the deepest point of the olecranon fossa. The left side preserves a more complete distal articular surface but is missing all of the proximal ends and about half of the diaphysis. About 8 cm of the most

proximal portion of the mid-shaft are preserved only on the medial aspect. It has also been reconstructed and is undistorted.

Description

The humeral head is spherical and displays the medio-lateral compression seen in more arboreal extant colobines such as *Trachypithecus*, *Nasalis*, and *Colobus*, but is similar in shape to *P. chemeroni* and not as compressed as extant cercopithecines. Although the greater tubercle is not preserved, the base is large, but its size relative to the head cannot be securely determined (Figures 3.6, 3.7). The distal extension of the greater

Figure 3.6 Ventral view comparing humeri of (L-R) ♂ *Paracolobus mutiwa*, ♂ *Paracolobus chemeroni*, ♂ *Cercopithecoides williamsi*, ♂ *Cercopithecoides meaveae*, ♂ *Rhinocolobus turkanensis*, and ?*Theropithecus oswaldi*. KNM-ER 4420C, AL2-63/64, KNM-ER 1542, and NMT O67/5600 have been flipped vertically for ease of comparison.



tubercle is greater in KNM-WT 16827 than *P. chemeroni* and merges distally with a more rugose, blunted deltoid crest. The lesser tubercle is ovoid in shape and its most

proximal point is below the most proximal extension of the humeral head similar to *P. chemeroni* (Figure 3.7). The lesser tubercle is long and merges with the crest for the *m. teres major* at its distal extension on the medial aspect of the proximal diaphysis. There is a small and rounded articular surface on the superior aspect for the insertion of the *m. subscapularis* which is longer ventro-dorsally in KNM-WT 16827 than *P. chemeroni* where the facet is mostly convex. The inter-tubercular groove tapers quickly as it extends distally and is wider than *P. chemeroni* but slightly narrower than *C. williamsi* and *C. meaveae* (Figure 3.7). The medial lip continues to blend with the deltoid crest with a deeper distal extension than in *P. chemeroni*, but not as extreme as *C. williamsi*, but relative depth is difficult to assess because the greater tubercle is not preserved. The preserved portion of the humeral head is wider than *P. chemeroni* with an articular surface that projects further ventrally on its lateral surface and is proportionally more robust relative to the total length of the element compared to *P. chemeroni* and extant colobines. These proportions are also seen in more terrestrial taxa such as *C. williamsi*, *Theropithecus*, and *Papio* (Figure 3.11A).

The proximal portion of the deltoid tuberosity is formed as a distal extension of the medial lip of the greater tubercle (Figure 3.7). The deltoid crest is rugose and thicker than in *P. chemeroni*, but blunt suggesting a stronger pectoral aponeuroses. The lateral border more prominent and thicker than *P. chemeroni* and extant colobines such as *Nasalis* and *Colobus*, but not as broad or prominent as in *C. williamsi* and *T. oswaldi* (Figure 3.6). This combined with the relatively small crest for the *m. latissimus dorsi* insertion and the moderate deltoid crest that extends just past mid-shaft, suggests developed *m. triceps brachii* and *m. subscapularis* for strong adduction, rotation, and

Figure 3.7 Proximal humerus in ventral view of (L-R) ♂ *Paracolobus mutiwa*, ♂ *Paracolobus chemeroni*, ♂ *Cercopithecoides williamsi*, ♂ *Cercopithecoides meaveae*, ♂ *Rhinocolobus turkanensis*, and ?*Theropithecus oswaldi*. Specimens KNM-ER 4420C, AL2-63, KNM-ER 1542, and NME AL693-1A have been flipped vertically for ease of comparison.



flexion at the shoulder joint (Ashton and Oxnard, 1964; Larson, 1993; Gebo and Sargis, 1994; Jablonski et al., 2008). The diaphysis is straight with a slight ventral curvature in lateral view caused by the prominence of the deltoid tuberosity that is more pronounced than *P. chemeroni*, but not as extreme as *C. williamsi*. The anterior crest extending from the distal deltoid tuberosity to the trochlea is blunter than in *P. chemeroni*. The distal diaphysis immediately proximal to the articular surface is antero-posteriorly compressed as in extant colobines, *P. chemeroni*, *C. williamsi*, *C. meaveae*, and *R. turkanensis*.

The brachioradialis flange is sharper than *P. chemeroni* and *R. turkanensis* and extends about a 1/3 of the way up the diaphysis (Figure 3.8). The prominence of this feature shows well-developed *m. brachioradialis*, *brachialis*, and *extensor carpi radialis longus* similar to what is seen in terrestrial cercopithecids (Figure 3.12; Jolly, 1972; Conroy, 1976; Harrison, 1989; Fleagle and McGraw, 2002; Gilbert et al., 2010). The flange merges distally into a small, round tubercle just above the lateral epicondyle for the *m. extensor carpi radialis longus* attachment that is more prominent than *R. turkanensis*, but similar in size to *P. chemeroni*. This may suggest an emphasis on wrist

Figure 3.8 From L-R: Ventral view of distal humeri of ♂ *Paracolobus mutiwa*, ♂ *Paracolobus chemeroni*, ♂ *Cercopithecoides williamsi*, ♂ *Cercopithecoides meaveae*, *Rhinocolobus turkanensis*, and ?*Theropithecus darti*. Specimens KNM-ER 4420C, AL2-63, KNM-ER 1542, and NMT O67/5600 have been flipped vertically for ease of

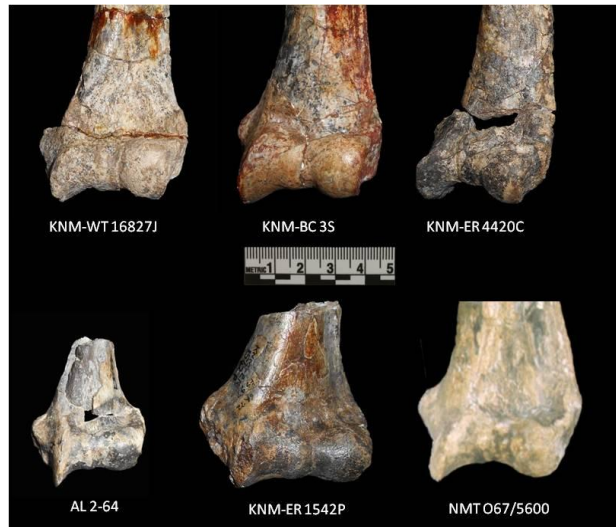
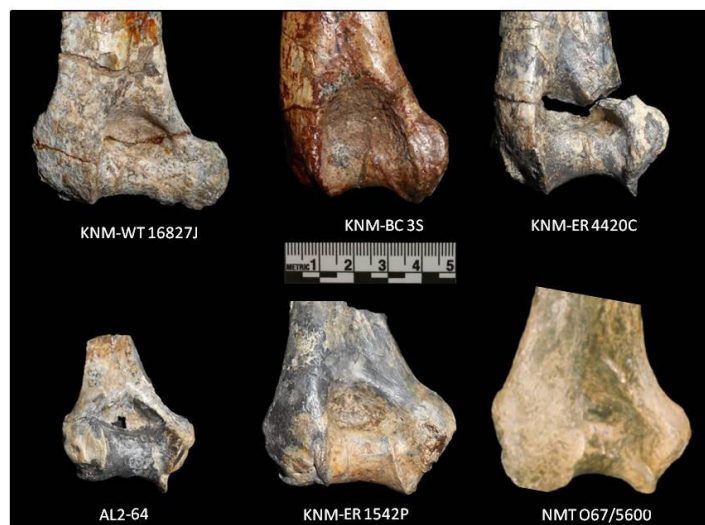


Figure 3.9 From L-R: Dorsal view of distal humeri of ♂ *Paracolobus mutiwa*, ♂ *Paracolobus chemeroni*, ♂ *Cercopithecoides williamsi*, ♂ *Cercopithecoides meaveae*, ♂ *Rhinocolobus turkanensis*, and ?*Theropithecus darti*. Specimens KNM-ER 4420C, AL2-63, KNM-ER 1542, and NMT O67/5600 have been flipped vertically for ease of comparison.



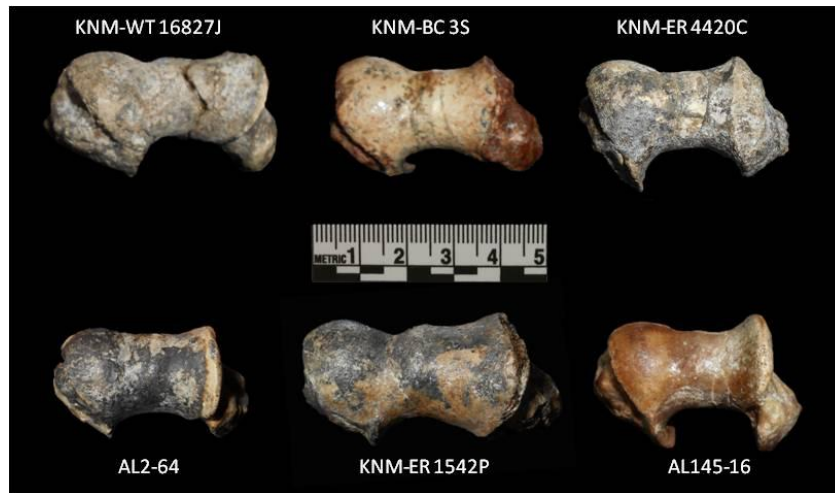
abduction and hand extension which could be useful in palmigrade terrestrial locomotion although the lack of distal forearm bones prevents detailed analysis of the wrist (Jablonski et al., 2008; Patel, 2010).

In lateral view, the distal end is antero-posteriorly deep compared to *R. turkanensis*, *Nasalis*, and *Colobus*, but not as much as *C. williamsi*. The supra-radial and ulnar fossae are shallow, with a markedly larger radial fossa (Figure 3.9). As is typical for colobines, the lateral pillar of the olecranon fossa is wider and taller than the medial pillar with a well-defined border that extends medially into the fossa. This morphology is also seen, although to a lesser degree, in *C. williamsi*, *R. turkanensis*, and *P. chemeroni* and provides stability in the humero-ulnar joint during elbow extension and pronation (Delson, 1973; Birchette, 1982; Rose, 1988; Harrison, 1989). The olecranon fossa is oval-shaped and deep and more compressed proximo-distally than *P. chemeroni* and in this metric both more resemble the colobine shape than *Theropithecus*; although the depth of the fossa combined with the prominent lateral margin is more associated with terrestrial locomotion (Figure 3.9; Jolly, 1972; Rose, 1988; Harrison, 1989; Guthrie, 2011; Rector and Vergamini, 2018).

The lateral epicondyle has a pit of moderate depth on its anterior aspect for attachment of the radial collateral ligaments. There is some weathering on this portion of the humerus so the full size of this feature is difficult to determine. The medial epicondyle is directed posteriorly at an angle of 48° to the distal articular surface axis of the humerus. This angle is within the range of terrestrial and semi-terrestrial cercopithecines, not as high as more extreme terrestrial taxa such as *C. williamsi* and *T. oswaldi*, and slightly lower than *P. chemeroni* (Figure 3.10; Harrison, 1989; Frost and Delson, 2002). This retroflexion is associated with increased weight bearing on the medial portion of the olecranon fossa consistent with stronger pronation and flexion of

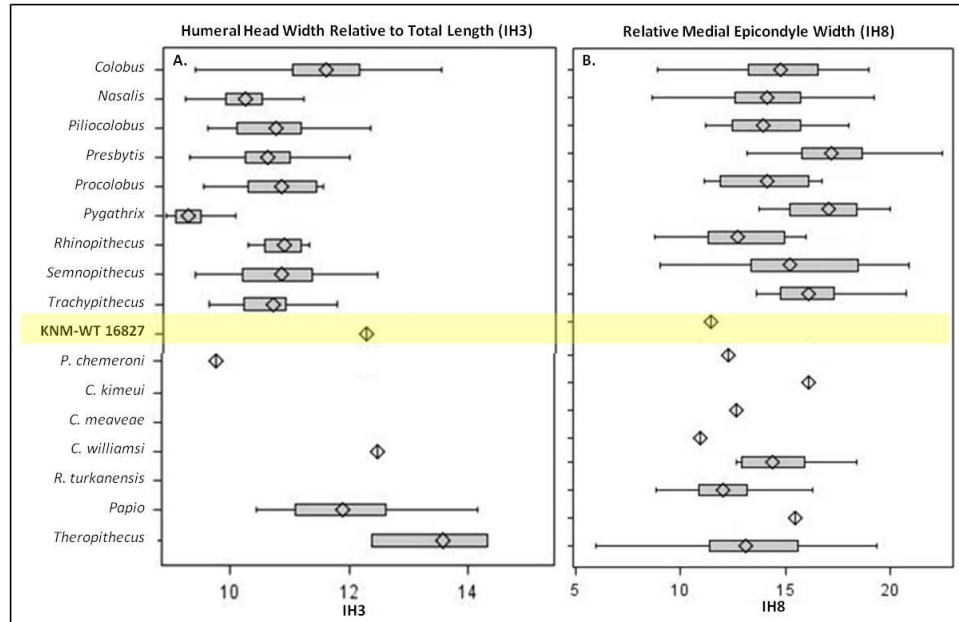
the elbow seen terrestrial cercopithecids (Jolly, 1967, 1972; Fleagle and Simons, 1982; Harrison, 1989; Schmitt, 1998; Benefit et al., 2008).

Figure 3.10 Top (L-R): Inferior view of the distal humeral articular surface of ♂ *Paracolobus mutiwa*, ♂ *Paracolobus chemeroni*, ♂ *Cercopithecoides williamsi*. Bottom (L-R): ♂ *Cercopithecoides meaveae*, ♂ *Rhinocolobus turkanensis*, and *Theropithecus oswaldi*. Specimens KNM-ER 4420C, AL2-63, and KNM-ER 1542 have been flipped vertically for ease of comparison.



The breadth of the medial epicondyle gives the distal end a flared appearance not seen in *P. chemeroni* and with its wide articular surface more resembles terrestrial taxa like *C. williamsi*, *C. meaveae*, and *Theropithecus* than extant colobines (Figure 3.8, 3.11). The trochlear flange is moderately crested and extends slightly distally past the capitulum similar to *P. chemeroni* and *C. williamsi*, but it is not as prominent as *Theropithecus* and also consistent with a more terrestrial locomotor function (Figure 3.8; Jolly, 1967; Delson, 1973; Frost and Delson, 2002). The flange does not meet the medial epicondyle but extends distally where it wraps around onto the dorsal surface to merge with the inferior margin of the olecranon fossa. The capitulum is broad, about half of the total articular surface, and has a faint zona conoidea which is seen in extant colobines as well

Figure 3.11 A. humeral head to total length and **B.** distal articular surface relative to the medial epicondyle ("Harrison's Breadth") indices organized by genus for comparative sample. *P. chemeroni* is represented by KNM-BC-3. For a full list of extant taxa included in the sample and metric descriptions see Tables 2 and 4.



as *P. chemeroni*, *C. williamsi*, *C. meaveae*, and *R. turkanensis* (Delson, 1973; Frost and Delson, 2002).

Ulna (KNM-WT 16827L + AR Rt.; AG L side)

The olecranon process and distal diaphysis. Preserved portions are in good condition and undistorted save for minor weathering. A fragment of the left ulnar diaphysis is also preserved but does not preserve any functionally relevant features (Figure 3.12). The proximal end and diaphysis are robust compared to *P. chemeroni* despite the latter having a longer and more gracile diaphysis (Figure 3.13).

Preservation

The proximal fragment (L) and diaphysis fragment (AR) fit together but are missing too much intervening matrix to be fully reconstructed. The proximal fragment is

Figure 3.12 Right ulna fragment of *Paracolobus mutiwa* specimen WT 16827L.



missing the olecranon process but is otherwise in good condition. A small section of diaphysis is also broken off immediately distal to the base of the olecranon process on the dorsal surface. The radial notch, lunate fossa, coronoid process, and most of the trochlear notch are in good condition except for a small portion missing from the most medial lip of the trochlear notch. About 2 cm of the proximal diaphysis is still attached while another 3 cm has been reattached (Figure 3.12).

Specimen KNM-WT 16827AR is a diaphysis fragment about 8 cm. in length. The proximal end is broken obliquely latero-medially and fits onto KNM-WT 16827L at its most proximo-medial portion. The specimen was originally in two pieces and the reattached portion is visible about 6 cm. from the proximal end. KNM-WT 16827AG is a left ulnar mid-shaft fragment just under 10 cm. in length preserving part of the interosseous crest, but no other functionally relevant features are present.

Description

The olecranon process is damaged making its height impossible to estimate or compare to other specimens. In ventral view, the anconeal process is symmetrical and aligned with the coronoid process. The anconeal process does not have the sharp lateral incline towards the olecranon process seen in *P. chemeroni* and the coronoid process projects slightly more ventrally suggesting a more restricted flexibility at the elbow joint consistent with more terrestrial locomotion (Conroy, 1976; Larson, 1993; Schmitt, 1998; Jablonski et al., 2008). The articular surface of the trochlear notch is relatively wide in KNM-WT 16827 and very similar in shape to *P. chemeroni*. In both specimens, the medial portion of the articular surface bulges out terminating in a sharply defined border. Both *P. chemeroni* and KNM-WT 16827 have more convex trochlear notch than *C. williamsi* or *C. meaveae* and possess more lateral extension than *R. turkanensis* (Figure 3.13). KNM-WT 16827 has an overall deeper trochlear notch than *Theropithecus* which would provide stability in prolonged flexion of the elbow. (Jolly, 1967, 1972; Conroy, 1976; Schmitt, 1988).

The radial notch is round and relatively small with an articular surface than is a continuation of the trochlear notch with only a small groove separating them at their most medial aspect. It appears to be similar in shape to *P. chemeroni*, but the latter specimen is pathological making it difficult to compare original morphologies (Birchette, 1982). The radial notch is larger and more excavated than *C. meaveae*, *R. turkanensis*, or *Theropithecus* (Figure 3.13). Immediately distal to the olecranon process on the medial surface is an elliptical and moderately excavated groove for the origin of the *m. flexor digitorum profundus*. Moving obliquely immediately inferior to the medial lip of the

Figure 3.13 From L-R: Ventral view comparing ulnae of ♂ *Paracolobus mutiwa*, ♂ *Paracolobus chemeroni*, ♂ *Cercopithecoides williamsi*, ♂ *Cercopithecoides meaveae*, ♂ *R. turkanensis*, and *Theropithecus oswaldi*. Specimens NME AL2-65 and KNM-ER 1542T have been flipped vertically for ease of comparison. Lengths for NME AL2-65 and KNM-ER 1542T are estimates.



trochlear notch is a small ridge for the insertion of the *m. brachialis*. This insertion is more prominent than in *P. chemeroni* where it fades parallel to the edges of the diaphysis rather than merging with the posterior aspect. This relatively weak *m. brachialis* indicates less of an emphasis on the flexibility in elbow flexion seen in arboreal taxa such as *R. turkanensis* and extant colobines (Fleagle, 1978; Morbeck, 1979; Rose, 1988; Schmitt, 1998). The preserved portion of the interosseous crest is sharp, but not prominent, and

extends distally to the radial notch before quickly tapering and fading in definition at the mid-shaft (Figure 3.5).

Radius (KNM-WT 16827AD + AE Rt.)

Approximately 10 cm of the radial diaphysis is preserved in two pieces: a proximal diaphysis fragment (AD) with part of the radial tuberosity and a reattached diaphysis fragment (AE) broken just below mid-shaft. The preserved portions of the radius are robust and comparable in size and thickness to *P. chemeroni* (Figure 3.14).

Figure 3.14 Ventral view of right radius fragment of *Paracolobus mutiwa* specimen WT 16827AD.



Preservation

Approximately 10 cm. of the radial diaphysis is preserved in two pieces: a proximal diaphysis fragment (AD) broken immediately distal to radial preserving about $\frac{3}{4}$ of the radial tuberosity and a reattached diaphysis fragment (AE) which is broken just below mid-shaft (Figure 3.6). The radial head is missing with none of the proximal

articular surface remaining, but the radial tuberosity is in good condition except for a fragment of cortical bone missing from the distal lateral aspect (Figure 3.14).

Description

The shape of the proximal articular surface cannot be estimated due to damage, but the neck appears to have been relatively short with more marked anterior-posterior compression than *P. chemeroni* but not as pronounced as in *C. williamsi* or *C. meaveae* (Figures 3.15). The proximal diaphysis is notably more robust than *C. meaveae* even

Figure 3.15 From L-R: Ventral view of proximal radii from ♂ *Paracolobus mutiwa*, ♂ *Paracolobus chemeroni*, ♂ *Cercopithecoides williamsi*, ♂ *Cercopithecoides meaveae*, *Theropithecus oswaldi*. Specimens KNM-ER 4420Q and NME AL 2-66 have been flipped vertically for ease of comparison.



when considering the difference in body mass between the taxa. Unfortunately there are no radii associated with *R. turkanensis* for a contemporary arboreal comparison, but what is preserved of the neck is more similar in relative thickness to more terrestrially reconstructed taxa such as *P. chemeroni*, *C. williamsi*, and *T. oswaldi* (Figure 3.15) than extant arboreal colobines such as *Nasalis*, *Colobus*, and *Trachypithecus*. The proximal portion of the radial tuberosity arises smoothly from the diaphysis in contrast with *P. chemeroni* which has a small depression created by the prominent medial lip. The tuberosity in KNM-WT 16827 also extends more distally than in *P. chemeroni* and has a

small crest extending obliquely to merge with the preserved portion of the lateral diaphysis border. The tuberosity is long and well-defined with a weak medial lip compared to *P. chemeroni* and *C. williamsi*, but a prominent and thick lateral border. There is marked longitudinal rugosity indicating moderate *m. biceps brachii* attachment but the lack of a strong medial lip and groove as is seen in more terrestrially adapted colobines such as *C. williamsi*, *C. meaveae*, *Theropithecus*, and extant cercopithecines (Figure 3.15; Conroy, 1974; Schmitt, 1988; Harrison, 1989; Ciochan, 1993; Jablonski et al., 2002, 2008). This suggests less emphasis on the shoulder flexion and stability characteristic of extreme terrestriality in *Theropithecus* and *C. williamsi*, but more than in arboreal taxa such as *R. turkanensis*, *Semnopithecus*, *Nasalis*, and *Colobus*.

The preserved diaphysis is straight and triangular in cross-section at its proximal end with an interosseous crest that begins about 1 cm. below the medial lip of the radial tuberosity. This feature is more prominent and blunter than in *P. chemeroni* suggesting a well-developed *m. flexor pollicis longus* and a small fossa immediately distal to the radial tuberosity is the attachment for the *m. flexor digitorum superficialis*. Unfortunately, the distal diaphysis is not preserved making the full length and distal articular surface impossible to analyze.

Os Coxae (KNM-WT 16827H Rt. & KNM-WT 16827G Lt.)

The right (H) and left (G) os coxae are both present although incomplete with the left side preserving more functionally relevant features although both preserve the acetabulum and parts of the ilium (Figure 3.16). Each has been reconstructed from multiple fragments although on the left most of the damage was restricted to the ilium while the acetabulum and ischium are intact. The relative rarity of os coxae in the fossil

record makes the comparative sample available for this relatively specimen small. Unless otherwise noted, the functional descriptions will focus on the left side (KNM-WT 16827G) as it is in better condition.

Preservation

The left os coxae is incomplete but minimally distorted preserving most of the iliac blade although the iliac crest is missing. The auricular surface is preserved although there is a fragment missing from its posterior aspect. The neck and acetabulum are both preserved and in good conditions except for some weathering of the acetabular border. The ischial tuberosity shows evidence of damage to the cortical bone prior to fossilization. Although the articular surface cannot be analyzed, general dimensions of the ischial tuberosity

Figure 3.16 R-L: *Paracolobus mutiwa* right os coxae specimen WT 16827H and left innominate specimen WT 16827G.



have been estimated based on what is preserved. The pubic bone is missing and only the most lateral border of the obturator foramen is still present. The right side preserves about 2/3 of the iliac blade and most of the articular surface although both are significantly

more weathered than on the left side. The neck is mostly complete with extensive reconstruction. The acetabulum is well-preserved, but a portion of the lunate surface on the superior aspect is missing. The ischium and ischial tuberosity are badly damaged and retain only the most posterior aspect. As with the left side, the pubic bone is not preserved

Description

The iliac margins and crest are too damaged on KNM-WT 16827 to fully assess its shape or height, but what is preserved of the blade is relatively tall as is also seen in *P. chemeroni* (Figure 3.17). Relatively tall ilia are associated with more terrestrial

Figure 3.17 From L-R: Lateral comparative innominates from (L-R) ♂ *Paracolobus mutiwa*, ♂ *Paracolobus chemeroni*, and *Theropithecus oswaldi*. Specimen NME AL431-E/M has been flipped vertically for ease of comparison.



locomotion in extant cercopithecines, while having shorter ilia relative to the size of the os coxae is seen in extant colobines with leaping locomotor function (Fleagle, 1978; Morbeck, 1979; Steudal, 1981; Ting, 2001). The functional significance of the lower iliac

height (Table 3) relative to the greater trochanter and femoral head breadth is correlated with function and is discussed in more detail in the femur description (Figure 19, 20). The gluteal plane on both KNM-WT 16827 and *P. chemeroni* is concave and similar in depth to extant colobines such as *Nasalis* and the Asian langurs. The inferior-most aspect of the dorsal surface partially encircles the acetabulum and is flat in both specimens. The rugosities for the *m. rectus femoris* attachments noted in *P. chemeroni* (Birchette, 1982) are not present in KNM-WT 16827 due to damage on both the left and right os coxae. Approximately 2/3 of the sacral face is preserved in KNM-WT 16827G. Like *P. chemeroni*, it is trapezoidal in outline, but its full outline cannot be determined due to damage. The auricular surface is wider than *P. chemeroni*, particularly in its infero-dorsal portion, which projects to form a more prominent posterior inferior iliac spine. The articular surface is heavily weathered but is similar in shape to that of *P. chemeroni* and extant colobines with a slightly sharper border at its most superior-dorsal aspect. Superior to the auricular surface is a moderately ridged and rugose region with none of the visible striations Birchette (1982) noted in *P. chemeroni* and are likely obscured by weathering.

Immediately inferior to the auricular surface, the iliac neck is curving medially below the ilio-pectineal line and continuing caudally to blend into the lateral wall of the pelvic inlet. The iliopectineal line is blunter than in *P. chemeroni* where it is almost a crest. The acetabular border is more rounded in KNM-WT 16827, although this could be due to wear, and is weakly concave in lateral view. At the level of the neck, the border is thickened for the attachment of *m. rectus femoris* although it is too damaged for comparison.

The ventral border is better preserved on the right side in KNM-WT 16827 and is

similar in shape to that of *P. chemeroni*. The crest separating it from the auricular surface is sharply crested in both. The tubercle for the attachment of *m. iliacus* is not preserved in KNM-WT 16827. Inferior to the posterior inferior iliac spine are several small rugosities for attachments of the sacro-iliac ligament. This region is wider in KNM-WT 16827, but it extends further down into the greater sciatic notch in *P. chemeroni*. Although many functionally features are too damaged for confident comparison, KNM-WT 16827, has an ilium more similar in shape to large-bodied colobines such as *Nasalis* and the langurs than extant cercopithecines. However, when compared proportionally to the morphology of the proximal femur, it more closely resembles terrestrial taxa such as *P. chemeroni*, *Theropithecus*, *Mandrillus*, and *Papio* than arboreal taxa such as *Colobus* and *Procolobus* (Figure 19-20).

The acetabulum is elliptical in outline and longer cranio-caudally than *P. chemeroni* (Figure 3.17). Both have a small groove between the margin and the tubercle for the ilio-femoral ligament attachment. Birchette (1982) mentions this feature could be a result of erosion, but its presence in KNM-WT 16827 suggests otherwise as there are no obvious signs of degradation and is bilaterally present. The lunate surface is smooth and raised above the surface of the acetabular fossa with a dorsal portion that is larger than the ventral surface which is typical of quadrupedal cercopithecids (MacLatchy, 1998; Gebo, 2014).

Both KNM-WT 16827 and *P. chemeroni* have guttering beneath the border of the inferior horn where it meets the acetabular fossa. The acetabular fossa in both is well-excavated, but smaller in proportion to the total lunate surface than *P. chemeroni*. The fossa in KNM-WT 16827 is mildly compressed cranio-caudally although the acetabulum

is about the same size as *P. chemeroni* matching the relatively large femoral head and proximal articular surface for rotational flexibility at the hip joint (McCrossin and Benefit, 1992; McCrossin et al., 1998; Harrison and Harris, 1996; Hammond, 2013). The surface where the ilium merges with the superior ramus of the pubis is significantly thicker antero-posteriorly in KNM-WT 16827 than *P. chemeroni*. The inferior ramus is not preserved so cannot be compared. The lateral margin of the obturator foramen is present in the left os coxae of KNM-WT 16827. It appears to have been longer cranio-caudally than *P. chemeroni*, but the entire pubic symphysis and attached rami are not present.

The pelvic face is cranio-caudally shorter and narrower than *P. chemeroni* and what is preserved of the pelvic face is curved slightly cranially in both (Figure 3.17). Both also have a marked keel descending distally from the inferior border of the acetabulum to merge with the ventro-lateral edge of the ischial tuberosity. This keel shorter and blunter in KNM-WT 16827 than *P. chemeroni*. The ventro-lateral surface is wide and smooth in both, but markedly shorter cranio-caudally and wider M-L in KNM-WT 16827. The lesser sciatic notch is significantly more compressed and defined in KNM-WT 16827 than in *P. chemeroni*. In the latter, the ischial spine is prominent and wide and the notch extends in a gentle curve before merging with the border of the ischial border. The spine in *P. chemeroni* lies below the inferior border of the acetabulum. In KNM-WT 16827 the ischial spine is sharp and the notch is narrow but deep with the spine almost at the level of the inferior border of the acetabulum. Both have a marked, shallow fossa for the *m. gemelli* attachment superior to the ischial spine and positioned in between the dorsal acetabular border and the greater sciatic notch. The dorso-lateral

surface is bordered medially by the lateral border of the obturator foramen, and laterally by the lower half of the greater sciatic notch and ischial spine. Both KNM-WT 16827 and *P. chemeroni* have a cranio-caudally convex surface.

The ischial tuberosities in both are poorly preserved so it is difficult to compare their overall shapes and dimensions. KNM-WT 16827 may have been antero-posteriorly wider than in *P. chemeroni*. Although it is not well-preserved, the ischial tuberosity is relatively short and broad which is more consistent with terrestrial locomotion than the longer ischium typical of arboreal cercopithecines and colobines (Steudal, 1981; Ward, 1991; Gebo and Chapman, 1995; Ting, 2001).

Femur (KNM-WT 16827I Rt.)

The right femur has been reconstructed from five fragments and preserves the head, greater trochanter, lesser trochanter, and about 2/3 of the diaphysis. It is robust with a relatively short femoral neck and thick diaphysis (see Figure 3.18). The proximal articular surfaces are well-preserved with the head, neck, and trochanters present and robust with defined muscle attachments. Although broken, the diaphysis is similarly robust and thick although no functionally relevant features are preserved (Figure 3.18).

Preservation

The femur has been reconstructed from 5 major fragments: the femoral head and neck, greater and lesser trochanter, and three fragments of the cervical neck. The diaphysis is also fragmented, but the pieces are continuous with the most distal portion ending just below the mid-shaft. The proximal end is weathered but retains well-preserved articular surfaces and features. The head, neck, greater trochanter, and lesser

Figure 3.18 Ventral (L) and dorsal (R) view of *Paracolobus mutiwa* specimen WT 16827I.



trochanter are present with only a small piece of the neck missing at the medial junction of head-diaphysis repair. The first two diaphysis fragments are complete, but the most distal fragment has an oblique fracture running from the supero-medial to infero-lateral aspect exposing about half of the mid-shaft medullary cavity. The presence of fossilized matrix within the cavity indicates that distal femur fragmentation likely occurred perimortem. There is a small rounded indentation on the ventral aspect of the most proximal diaphysis fragment that could be carnivore or termite damage (pers. obs.). Except for a fragment that appears to be a heavily weathered partial condyle, no identifiable portion of the distal femur is preserved.

Description

The head is very round and hemispherical and proportionally more similar in size

to terrestrial taxa such as *C. williamsi*, *C. meaveae*, *Papio*, and *Theropithecus* (Figure 3.19). The articular surface extends further laterally on its ventral aspect than *P.*

Figure 3.19 From L-R: Comparative ventral view of femora from ♂ *?Paracolobus mutiwa*, ♂ *Paracolobus chemeroni*, ♂ *Cercopithecoides williamsi*, ♂ *Cercopithecoides meaveae*, and ♂ *Theropithecus darti*. Specimen KNM-BC 3AR has been flipped vertically for ease of comparison as the right femur for KNM-BC 3 does not preserve the greater trochanter. The length for AL 2-70+28 is an estimate.



chemeroni and is more similar in shape to *C. williamsi* than *P. chemeroni*. This may indicate more of an emphasis on flexion and abduction at the hip joint although this extension is not as extreme as in *Theropithecus* or extant *Papio* (Figure 3.19; Gilbert et al., 2011; Guthrie, 2011). When compared to the lower iliac height, the femoral head groups closer with large bodied fossil taxa such as *P. chemeroni* and *T. oswaldi*, but still

falls closer to the colobine trend for this feature (Figure 3.20; Ting, 2001; Hammond, 2013). The fovea capitis is deeply excavated and ovoid with some proximo-distal compression and is located on the posterior aspect of the midline in medial view and is rounder and less excavated than the comparably proximo-distally compressed fovea in *P. chemeroni*. This feature on both KNM-WT 16827 and KNM-BC 3 is positioned more towards the posterior aspect of the articular surface although not as much as in *C. williamsi*, *C. kimeui*, or *R. turkanensis*. The neck is thick and relatively short with no torsion in superior view especially when compared to extant colobines such as *Colobus*, *Nasalis*, *Rhinopithecus*, and *Semnopithecus* although it is longer than in *P. chemeroni* (Figure 3.19). The femoral neck angle is also lower than that seen in extant colobines which combined with the relatively short neck length suggests hip joint dimensions more consistent with terrestrial locomotion (Ward, 1992; Ting, 2001).

The greater trochanter is robust with a thick base and extends more superiorly above the femoral head than in arboreal extant colobines and is relatively large compared to the femoral head diameter and more closely resembles terrestrial taxa such as *C. williamsi*, *C. meaveae*, and *T. oswaldi* (Figure 3.19, 3.21). This is further supported by the prominence of the greater trochanter relative to the femoral head width which, along with *P. chemeroni*, also groups more closely with terrestrial cercopithecines (Figure 3.21).

KNM-WT 16827 has a rugose pit for the attachment of the *m. gluteus minimus* on the anterior face which extends as a blunt crest obliquely from the apex to the lateral border. This feature is not as pronounced in *P. chemeroni* suggesting a greater emphasis on hip rotation in KNM-WT 16827 (Anemone, 1993; Ting, 2001). The rugosity of the superior

and dorsal aspects of the greater trochanter also suggest well-developed *m. gluteus medius*, which combined with the gluteal attachments, point to an emphasis on medial rotation and extension of the hip and an emphasis on leverage/power with reduced abduction; although not to the extent seen in arboreal leapers (Harrison and Harris, 1998; Jablonski et al., 2008; Gebo, 2014). The *m. piriformis* attachment is present as a small, round pit on the superior aspect of the greater trochanter and a thickened area immediately distal to the *m. gluteus minimus* attachment suggests a strong origin for the *m. vastus lateralis* providing strong extension ability. The trochanteric fossa is deep with a well-developed intertrochanteric crest for a strong *m. quadratus femoris* aiding in lateral/external rotation and stability of the hip. This emphasis on rotation at the hip joint is further supported by a deep trochanteric fossa for the *m. obturator internus* and *externus* also associated with thigh adduction and hip rotation (Jablonski et al., 2008).

Although it is larger and more robust, KNM-WT 16827 more closely resembles *C. williamsi* than *P. chemeroni* in its greater trochanter morphology; particularly in the shape of the superior aspects, the sharpness of the *m. gluteus minimus* insertion, and its overall prominence (Figures 3.18-3.22). KNM-WT 16827 has a prominent lesser trochanter similar to *C. williamsi* particularly when compared to extant, but not as prominent as *P. chemeroni*. This feature has a strong posterior extension with an insertion for the *m. psoas major* that is oriented face. This attachment is smaller than in *P. chemeroni*

and less robust. The intertrochanteric crest although strong in its superior aspect, weakens as it moves towards the lesser trochanter base on the superior-medial aspect. It differs

further from *P. chemeroni* by being oriented more medially suggesting more of an emphasis on flexion at the hip joint (Birchette, 1982).

The trochanteric fossa is comparably deep in both KNM-WT 16827 and *P. chemeroni* to accommodate a strong *m. obturator internus* and *externus*. The posterior intertrochanteric line is slightly more prominent in KNM-WT 16827 and remains visible until it merges with the ventral border of the lesser trochanter. Although it does not display the extreme terrestrial morphology present in *C. williamsi* or *Theropithecus*, the orientation of the lesser trochanter combined with the rugosity of muscle attachments in the proximal femur support an emphasis on flexion, rotation and stability consistent with terrestrial locomotion (Strasser, 1992; Anemone, 1993; Harrison and Harris, 1996, MacLatchy, 1998; Jablonski et al., 2002).

The diaphysis has a slight ventral curvature beginning at the most proximal portion that reaches its peak at mid-shaft. What is preserved is straight and robust with a slight ventral curvature that is more pronounced than in extant colobines, but not as extreme as in terrestrial cercopithecines of *Theropithecus*. The location of this curvature suggests it was shorter and more robust than *P. chemeroni*. There is a small tubercle on the lateral portion of the posterior diaphysis near the lesser trochanter for the attachment of the upper slips of *m. gluteus maximus* which is more prominent in KNM-WT 16827 than *P. chemeroni* although the prominence is likely exaggerated by a crack in the diaphysis. The pectineal line and linea aspera are very weak suggesting adductors that are not well-developed. This in conjunction with the morphology of the proximal femur is suggestive of an emphasis on stability of the hip with muscles well-developed for medial rotation/extension. Moderate development of muscles associated with hip adduction

Figure 3.20 Scatter plot of femoral head width and lower iliac height by genus. Individual data points represent genus specific mean values and *P. chemeroni* is represented by KNM-BC 3. See Tables 2.2 and 2.4 for a full list of extant species included in the sample and metric descriptions.

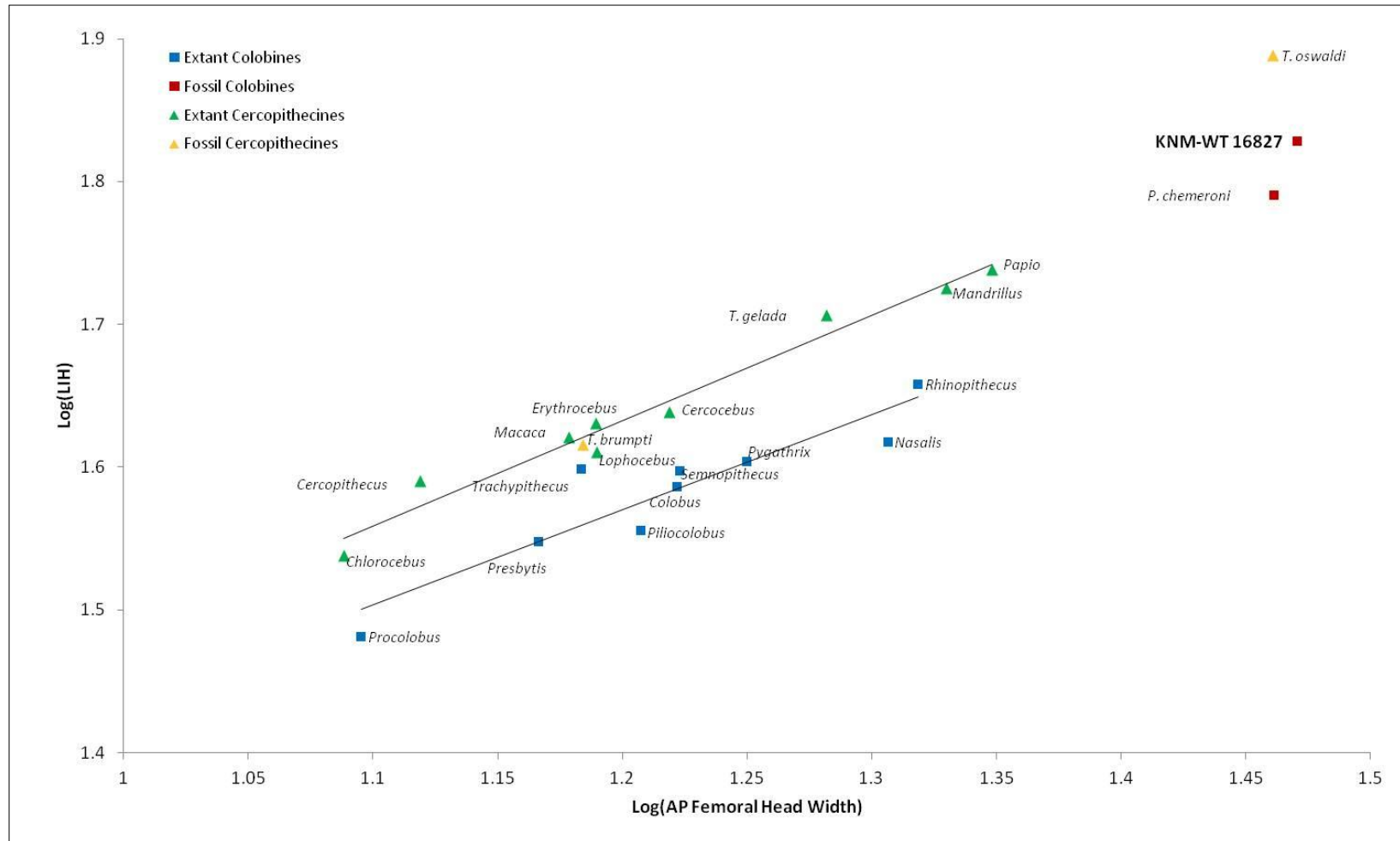


Figure 3.21 Scatter plot of femoral head width and greater trochanter height by genus. Individual data points represent genus specific means and *P. chemeroni* is represented by specimen KNM-BC 3. See Tables 2.2 and 2.4 for a full list of extant species included in the sample and metric descriptions.

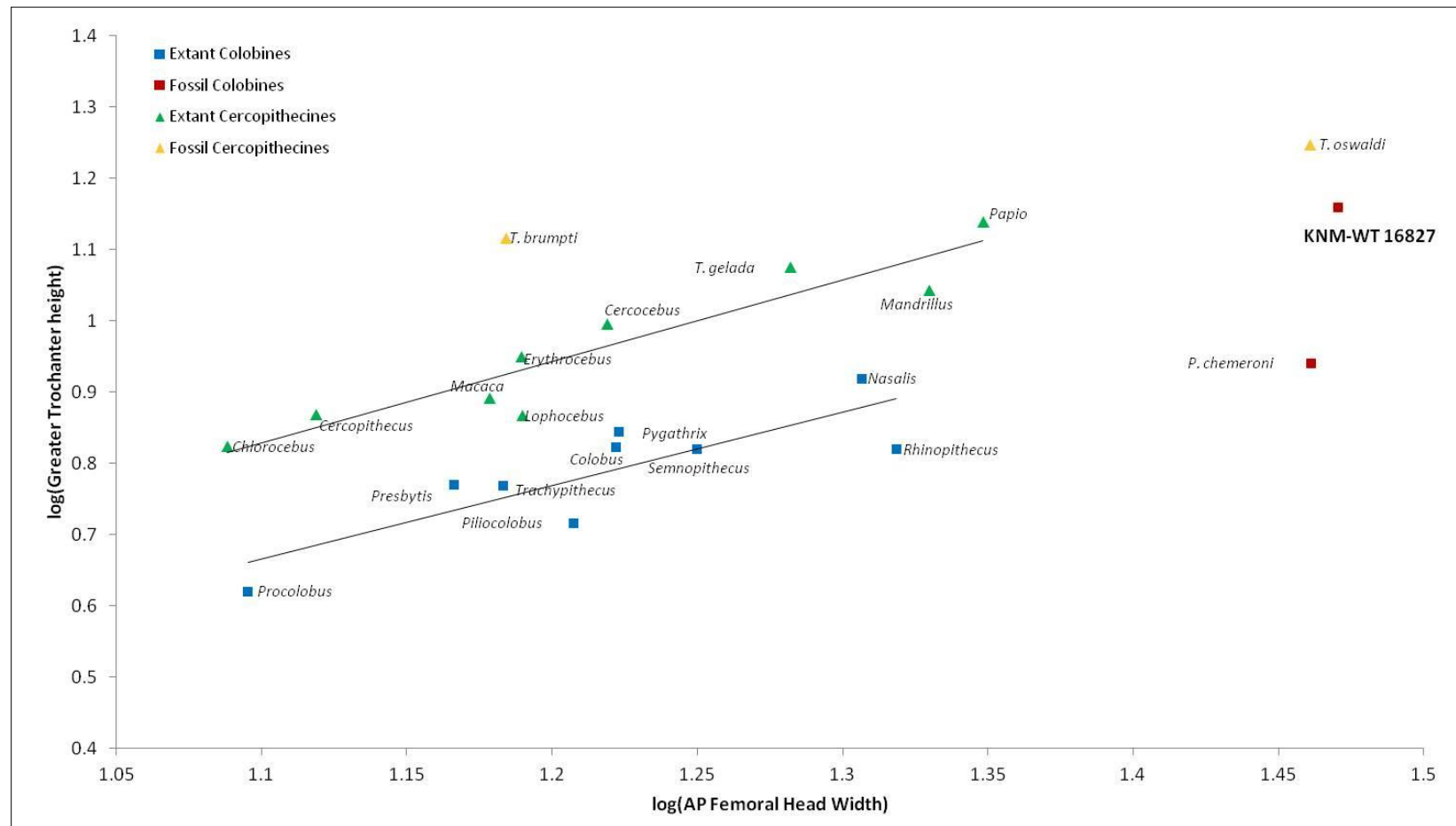
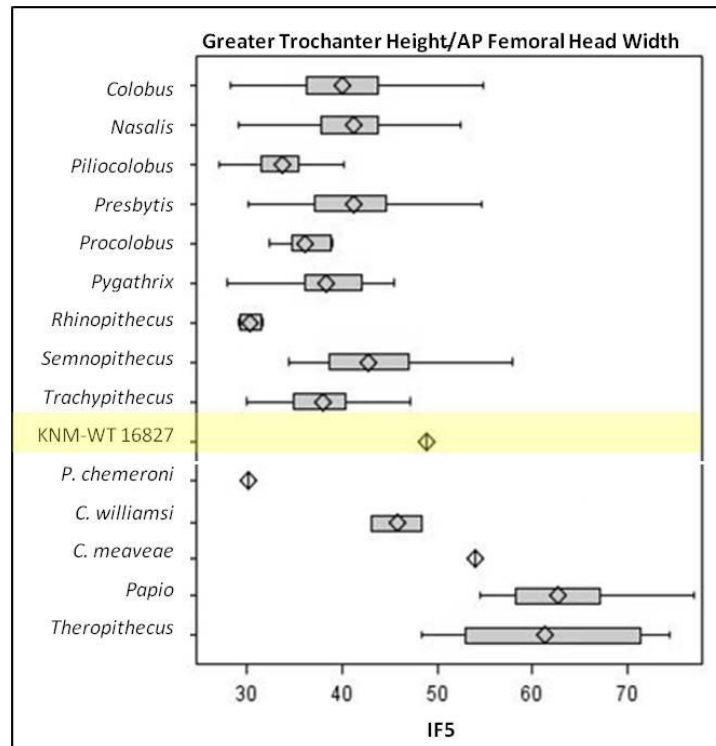


Figure 3.22 Box plot showing index of relative greater trochanter height. Values for the comparative sample are organized by genus. *P. chemeroni* is represented by KNM-BC 3.



suggest some adaptation for efficient walking movements without any of the morphologies associated with leaping seen in some extant colobines and cercopithecines (Strasser, 1992; Ward, 1992; Anemone, 1993; Gebo, 1994; MacLachy, 1998; Ting, 2001; Hammond, 2013).

Astragalus (KNM-WT 16827Q Lt. and 16827R Rt.)

Preservation

Both the right (R) and left (Q) astragali are preserved. The right side has damage to its posterior aspect the lateral trochlea that also extends onto the fibular facet and inferiorly onto the calcaneal facet. The left side is complete with slight weathering on the cortical surface (Figure 3.23).

Description

Figure 3.23 Top: Superior view of left and right astragali from ♂ ?*Paracolobus mutiwa* specimens KNM-WT 16827R and WT 16827Q respectively. Bottom: plantar view of same specimens.



Due to its better state of preservation, the functional description will focus on the left astragalus (KNM-WT 16827Q). The most notable difference between KNM-WT 16827 and *P. chemeroni* is its small size compared to the relative robusticity of its other long bones (Figure 3.24). As is typical for colobines, the trochlea widens distally with a higher lateral margin for stability at the talo-crural joint which is associated with increased abduction in the foot during dorsiflexion in more terrestrial taxa (Strasser, 1988; Turley and Frost, 2013). In this feature KNM-WT 16827 is closer to more terrestrial taxa such as *Theropithecus* and *Papio* while *P. chemeroni* falls within the range of extant colobines (Figure 3.25a). On the proximal aspect of the trochlea is a shallow groove for the *m. flexor hallucis longus* which is narrower than in *P. chemeroni* (Figure 3.24) and distinct from the deeper and more excavated groove seen in extant arboreal colobines such as *Nasalis*, *Semnopithecus*, and *Colobus*. The groove is obliquely oriented but not to the extreme seen in arboreal taxa such as *Colobus* suggesting less of an

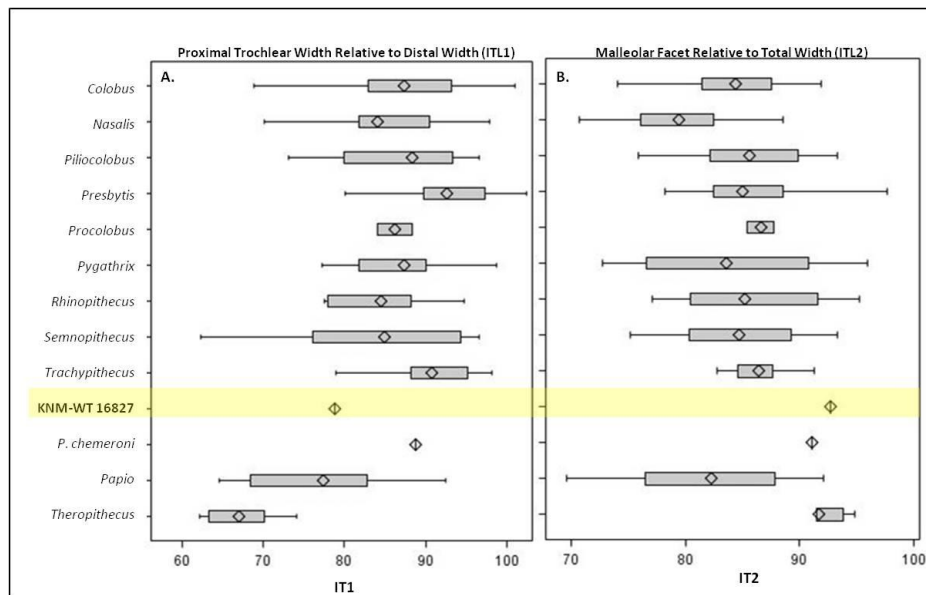
Figure 3.24 From L-R: Superior view comparing left astragali from ♂ *Paracolobus mutiwa* KNM-WT 16827Q, ♂ *Paracolobus chemeroni*, and ♂ *Theropithecus brumpti*.



emphasis on the inversion/eversion found in climbing behaviors and perhaps more on some terrestrial abilities (Latimer et al., 1987; Marquardt, 2008; Gilbert et al., 2010; Guthrie, 2011). The relative width of the malleolar facet for both KNM-WT 16827 and *P. chemeroni* falls within the range of *Theropithecus* and is associated with terrestriality in papionins (Figure 3.25b; Strasser, 1988; Harrison, 1989; Jablonski et al., 2008). The talar neck is similar in length to *P. chemeroni* and thick compared to *Theropithecus* with a relatively wide head displaying superior-inferior flattening (Figure 3.24).

On the inferior surface the talo-calcaneal facet is a wide hourglass shape and is continuous with the articular surface of the talar head and more closely resembles *Theropithecus* in shape than *P. chemeroni* (Figure 3.24). On the plantar surface, the proximal facet widens towards its lateral aspect and is curved, but not as much as *P. chemeroni* or arboreal colobines (Strasser, 1988; Gilbert et al., 2010). This facet is separated from the distal facet by the talar sulchus which is slightly narrower than *P. chemeroni* and continuous with the navicular facet. There is no preserved distal tibia, but the broad articular surface of the trochlea suggests stability at the tibio-talar joint more

Figure 3.25 Box plots of astragalus indices associated with locomotor mode. Values for the comparative genera are organized by genus. *P. chemeroni* is represented by KNM-BC 3.



typical in terrestrial taxa (Turley and Frost, 2013).

Calcaneus (KNM-WT 16827P Lt.)

Like its astragalus, KNM-WT 16827's calcaneus is smaller and less robust than might be expected given the robusticity of the other long bones; particularly in comparison to *P. chemeroni* with a markedly long and narrow calcaneal tuberosity (Figures 3.26, 3.27, 3.28a). It is also distinct from *P. chemeroni* and extant colobines in its talar facet proportions and is proportionally more in the range of terrestrial cercopithecines (Figure 3.28).

Preservation

The left calcaneus is well-preserved with no taphonomic distortion. Damage is minimal and limited to mild abrasions on the lateral and medial edges of the calcaneal tuberosity and rim of the cuboid facet (Figure 3.26).

Figure 3.26 Superior (L) and plantar (R) view of left side calcaneus of *Paracolobus mutiwa* specimen WT 16827P.

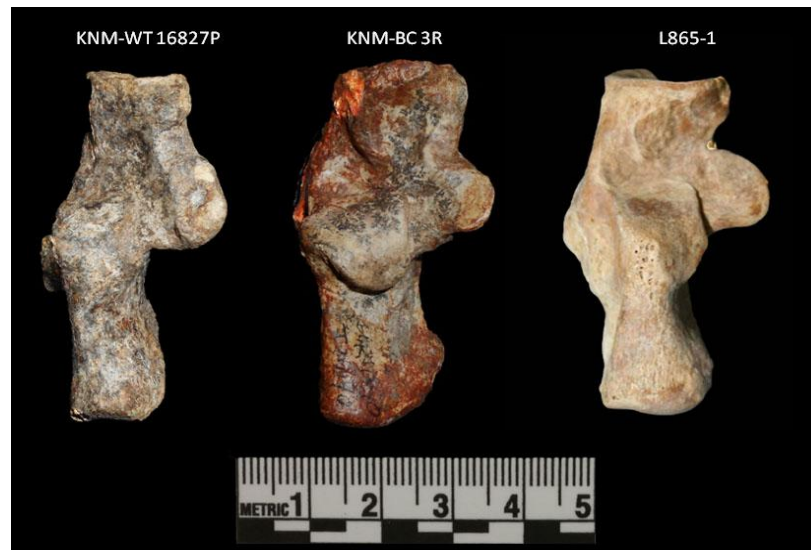


Description

The overall shape of the calcaneus is typically cercopithecoid with a relatively long calcaneal tuberosity and prominent anterior articular facet (Strasser, 1988; Leakey et al., 2003). Although it is larger than extant taxa including *Nasalis*, *Semnopithecus*, and *Trachypithecus*, it is significantly smaller than *P. chemeroni* despite the two specimens having overlapping estimated body mass (Figure 3.36; Delson et al., 2000; Ting, 2001).

In superior view the anterior articular facet is ovoid and significantly smaller than the medial facet from which it is separated by a shallow non-articular groove. On the medial face beneath the medial talar facet is a wide and shallow sustentacular sulcus for the *m. flexor hallucis longus* tendon. This feature is proportionally similar to *P. chemeroni* and neither show the deep and narrow morphology seen in extant colobines. This may indicate less of an emphasis on digit flexion in both specimens which is more consistent with more terrestrial ankle movements (Rose, 1983; Langdon, 1986; Latimer et al., 1987). The posterior facet is large with proximo-distal convexity and is separated

Figure 3.27 From L-R: Superior view comparing left calcanei from ♂ *Paracolobus mutiwa* KNM-WT 16827P, ♂ *Paracolobus chemeroni*, and right side from ♂ *Theropithecus brumpti*. Specimen NME L865-1 has been flipped vertically for ease of comparison.

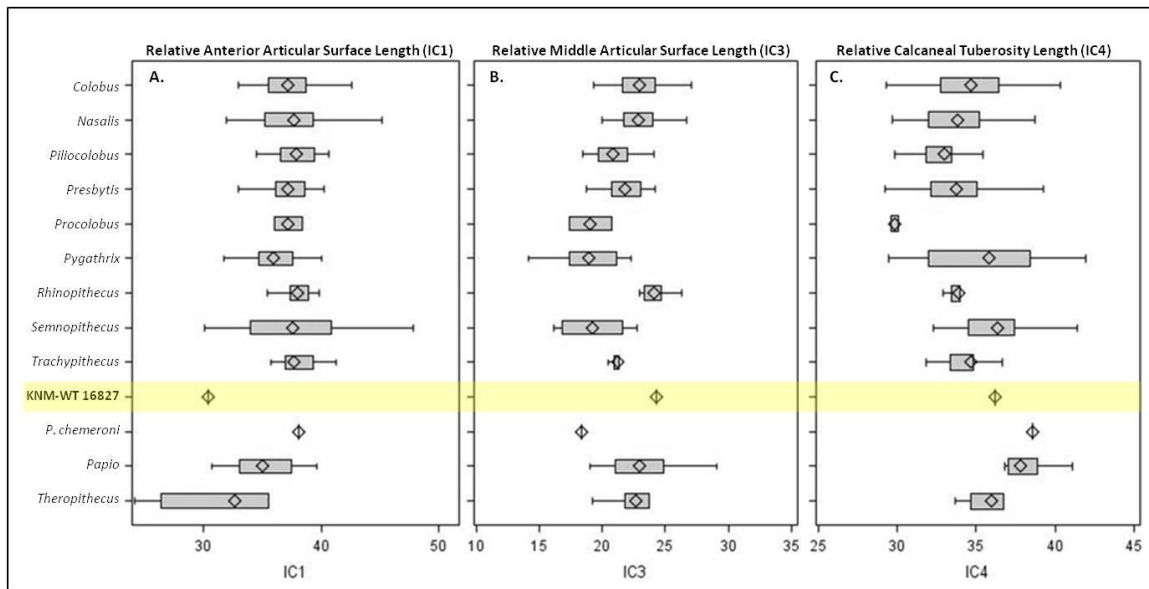


from the middle facet by a wide sulchus calcanei. Its articular surface is similar in size to *P. chemeroni*, but its overall smaller size puts the surface more proportionally similar to terrestrial cercopithecines (Figure 3.28b). In fact, the entire talar articular plane is large relative to the length of the calcaneus and also more in the range of *Papio* and *Theropithecus* than *P. chemeroni* and extant colobines (Figure 3.28a). The lateral margin of the facet is sharper than *P. chemeroni* but quickly tapers as it merges into the calcaneal facet.

Immediately distal to the posterior facet is an ovoid depression for the attachment of the talo-calcaneal ligament smaller and shallower than *P. chemeroni*. The calcaneal tuberosity is also long relative to the total calcaneal length which in contrast to the more cercopithecine proportions of its other features falls more within the range of extant colobines (Figure 3.28c). In cercopithecids, a long calcaneal tuberosity is associated with

increasing the power of the *m. triceps surae* for increased plantarflexion in more leaping locomotor patterns while colobines tend to have longer calcaneal tuberosities relative to body size than cercopithecines (Langdon, 1986; Strasser, 1988). KNM-WT 16827 does fall closer in this index to large-bodied extant taxa such as *Semnopithecus* than to *P. chemeroni*, but species within this extant genus are known to exhibit some semi-terrestrial behaviors (Harrison, 1989; Osterholtz et al., 2008; Ting et al., 2008; Jablonski and Frost, 2010).

Figure 3.28 Box plot showing calcaneal indices of **A.** anterior articular surface relative to length, **B.** relative middle articular surface relative to length, and **C.** relative length of the calcaneal tuberosity.



Immediately distal to the proximal articular surface on the lateral face of the calcaneus is a prominent peroneal tubercle which is exaggerated by a steep border giving it an almost triangular shape distinct from *P. chemeroni* as well as extant taxa including *Colobus*, *Nasalis*, and *Trachypithecus*. The shape and prominence of the tubercle relative to the length of the calcaneus suggests a well-developed *m. peroneus longus* and *brevis*

for strong plantar flexion of the foot necessary for more terrestrial substrates, but not as extreme as those seen in *Theropithecus* (Figure 3.26; Jolly, 1972; Jablonski, 2002; Jablonski et al., 2008). Immediately superior and parallel to the peroneal tubercle is a shallow groove for the calcaneo-fibular facet that fades as it moves distally towards the cuboid facet. The cuboid facet is semi-circular and concave and similar in shape to *P. chemeroni*. On the medial border of the facet is a small round fossa for the attachment of the short plantar ligament. This feature is smaller than in *P. chemeroni*, but more prominent in both fossil specimens than in arboreal extant taxa such as *Colobus*, *Nasalis*, *Semnopithecus* and *Trachypithecus*.

Discussion

KNM-WT is one of only two specimens with associated postcrania attributed to the genus *Paracolobus* and the only one attributed to the species *mutiwa*. This makes it a valuable specimen for exploring locomotor adaptations in the fossil record and as a comparator for as yet isolated and unassigned specimens from primate rich regions such as the Shungura Formation. The preserved elements of KNM-WT 16827 present a large, robust monkey possessing morphology consistent with terrestrial movement in its shoulder, elbow, hip, and ankle distinct from extant colobines, cercopithecines, and other contemporaneous large-bodied taxa such as *C. williamsi*, *R. turkanensis*, *T. oswaldi*, and *T. brumpti*.

The size and concavity of the glenoid fossa on the scapula combined with the roundness of the humeral head suggest scapulo-humeral joint emphasizing rotational flexibility combined with lateral extension of the superior glenoid suggests stability consistent with weight-bearing at the joint (Figure 3.4). This particular feature of the

glenoid more closely resembles *P. chemeroni* than arboreal taxa such as *R. turkanensis*, *Colobus*, and *Nasalis*. This is also seen in terrestrial colobines such as *C. williamsi* and *C. meaveae* although the overall shape of the glenoid in these taxa is distinct from KNM-WT 16827. In cercopithecids, the scapular blade is the origin for several muscles associated with shoulder stability, rotation, flexion, and abduction important for terrestrial movement (Ashton and Oxnard, 1964). Unfortunately, this feature is not preserved on KNM-WT 16827, but the insertion points for muscles including the *teres major*, *subscapularis*, *latissimus dorsi*, *biceps brachii*, *deltoideus*, and *triceps brachii* are partially preserved on the proximal humerus allowing for some functional analysis of the shoulder joint (Figure 2 and 3). Although the greater tubercle is not preserved, the robusticity seen in the deltoid tuberosity and deltoid crest suggest well-developed *m. deltoideus*, *m. triceps brachii*, and *m. subscapularis* for adduction, rotation, and flexion of the elbow. Although these features are not as developed as more extreme terrestrial taxa like *Theropithecus* and *C. williamsi*, they are more prominent than extant arboreal colobines, *R. turkanensis*, and *P. chemeroni* (Figure 3.5, 5).

The elbow also displays several features consistent with a more terrestrial locomotor mode and the better preservation of the relevant elements allows for more confident functional analysis. The deep olecranon fossa on the humerus and projecting coronoid process on the ulna are associated with stability in prolonged flexion of the elbow joint (Jolly, 1972; Delson, 1973; Birchette, 1982; Rose, 1988; Harrison, 1989). This emphasis on stability is further supported by relatively weak *m. brachialis* attachments on the ulna compared to those of arboreal taxa such as *R. turkanensis*, *Nasalis*, *Colobus*, and, *Trachypithecus* which tend to show increased adaptations for

flexibility in the elbow flexors, and the retroflexed medial epicondyle (Figure 3.6, 9; Jolly, 1967, 1972; Conroy, 1976; Harrison, 1989; Schmitt, 1998; Jablonski et al., 2008). Although little of the radius is preserved, the rugosity of the radial tuberosity shows a well-developed *m. biceps brachii* for elbow stability and weight bearing in more terrestrial locomotion compared to the rotational flexibility seen in arboreal taxa (Ashton and Oxnard, 1964; Harrison, 1989; Fleagle and McGraw, 2002; Jablonski et al., 2008). Perhaps the most striking feature of the forelimb is how much shorter it appears compared to the long and relatively gracile humerus of *P. chemeroni* (Figure 3.6) particularly when KNM-WT 16827's larger cranium is taken into consideration. Although it varies in several features, the forearm of KNM-WT 16827 more superficially resembles that of the terrestrial *C. williamsi* in its proportions than it does KNM-BC 3 (Figure 3.8, 8). Overall, the forelimb morphology is consistent with a more terrestrial locomotor preference than *R. turkanensis*, *P. chemeroni*, or any extant colobines, but less so than *C. williamsi*.

Os coxae as well-preserved as those of KNM-WT 16827 and KNMN-BC 3 are rare in the fossil record making it difficult to compare with extinct taxa. Ting (2001) and Hammond (2013) both include functional assessments of the hip congruent with the results of this study. Extant large-bodied colobines such as *Nasalis* and *Semnopithecus* tend to have shorter ilia than cercopithecines for the absorption of force during leaping activities associated with arboreal substrates when compared to the proximal femur (Steudal, 1981; Ward, 1991; McLatchy, 1998). KNM-WT 16827 has a relatively shorter ilium and ischium than *P. chemeroni*, but both specimens more closely resemble the colobine pattern in this metric (Figure 3.20; Ting, 2001; Hammond, 2013). The relatively

tall greater trochanter and its prominent gluteal attachments of the femur are consistent with strong medial rotational abilities at the hip and limited abduction and adduction and is more typical of terrestrial cercopithecines, but is also present in *C. williamsi* and to a lesser extent *C. meaveae* (Figure 3.21; Ward, 1992; Frost and Delson et al., 2002; Tallman et al., 2012). This is further supported by the relatively low femoral neck angle which has been calculated as within the range of extant terrestrial cercopithecines (Ting, 2001). Although KNM-WT 16827 shares some terrestrial features with *P. chemeroni* in its hip, the much greater emphasis on terrestrial movement displayed in the ilium, ischium, and gluteal attachments.

The distal femur and proximal tibia are not preserved in KNM-WT 16827, but both the astragalus and calcaneus are well-preserved allowing for an assessment of the ankle. Perhaps the most striking feature of the ankle is the shape and size disparity between KNM-WT 16827 and *P. chemeroni* (Figure 19 and 20). KNM-WT 16827 has a significantly less robust calcaneus with a much smaller anterior articular surface and calcaneal tuberosity relative to the total length than *P. chemeroni* (Figure 3.26). The astragalus possesses the typical colobine morphology of having a trochlea that is wider at its distal aspect, but the extreme asymmetry shown between the lateral and medial trochlear border is more similar to *Theropithecus* and terrestrial cercopithecines which provides tibio-talar joint stability during abduction of the foot during dorsiflexion (Strasser, 1988; Gebo, 1992; Turley, 2013; Turley and Frost, 2013). The groove for the *m. flexor hallucis longus* tendon is more pronounced on both the astragalus and calcaneus in KNM-WT 16827 than in *P. chemeroni* although neither are as pronounced as in arboreal taxa such as *Nasalis* and *Trachypithecus*. These features suggest an ankle joint

that emphasizes adapted for dorsi/plantarflexion necessary for terrestrial locomotion and lacking in the digit flexion flexibility seen in more arboreal taxa (Strasser, 1988).

Many of the morphological similarities KNM-WT 16827 bears to *P. chemeroni* are either typical for colobines or likely due to both sharing adaptations for terrestrial locomotion relative to extant taxa (Leakey, 1982, 1985, 1987; Harris et al., 1988; Ting, 2001; Jablonski, 2002; Grubb et al., 2003). In addition to their functional morphology, the limb and ankle bones of KNM-WT 16827 are proportionally distinct in being relatively short relative to the specimen's cranial size and when compared to other fossil colobines with similarly large body mass estimates such as *C. williamsi* and *P. chemeroni* (Figure 5, 12, 23, 26; Delson et al., 2000). The relatively short forelimb is not unusual for a more terrestrially adapted cercopithecoid, but the small foot bones contrast with the morphology of terrestrial taxa such as *P. chemeroni* and *Theropithecus* making (Figure 22-27). It is possible that this is a feature unique to the taxon, but until more specimens attributed to *P. mutiwa* are described, the locomotor significance of small ankle bones is difficult to assess.

Paracolobus mutiwa was also sympatric with many of the other Plio-Pleistocene taxa suggesting a greater level of taxonomic diversity than is seen among extant African colobines (Leakey, 1982, 1987; Harris et al., 1988; Jablonski, 2002; Grubb et al., 2003; Ting et al., 2008). The postcranial analyses presented here support previous assertions (Harris et al., 1988; Ting, 2001; Hammond, 2013) that KNM-WT 16827 possesses postcranial proportions and joint morphologies distinct from *Paracolobus chemeroni* and other Plio-Pleistocene cercopithecoids. This adds to the already diverse primate ecology of the Turkana Basin during this time period where there is evidence for the presence of at

least four large-bodied sympatric colobine species: *C. williamsi*, *C. kimeui*, *R. turkanensis*, and *P. mutiwa* as well as papionin taxa such as *T. oswaldi*, *T. brumpti*, and *Soromandrillus quadratirostris* (Jablonski et al., 2008; Gilbert, 2013). This level of sympatry is not seen in among East African cercopithecids today suggesting niche separation in such realms as diet and substrate preference have played an important role in cercopithecoid evolution (Elton, 2006). Although KNM-WT 16827 does appear to be a large terrestrial monkey, its unique ankle morphology suggests it is doing something different from other terrestrial taxa such as *C. williamsi* and *Theropithecus*. If this is the case, it may explain how these environments were able to support such a diversity of large primate taxa. Based on this unique postcranial morphology, KNM-WT 16827 is distinct from the genus type species and all specimens attributed to the species warrant generic reassessment.

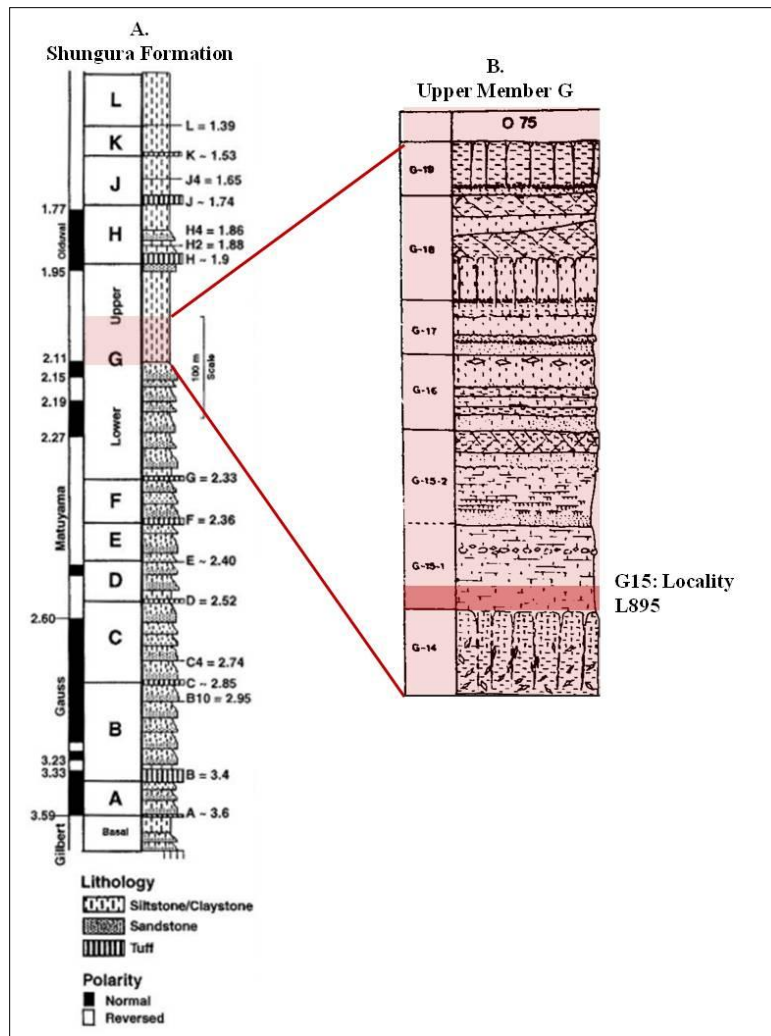
CHAPTER IV

AN ASSESSMENT OF THE POSTCRANIAL SKELETON OF THE LARGE-BODIED COLOBINE SPECIMEN L895-1 FROM SHUNGURA, OMO VALLEY, ETHIOPIA

Background

The Shungura Formation lies in the northern part of the Turkana Basin in the lower Omo Valley of Ethiopia (De Heinzelin, 1983). It has a faunal record spanning 3.6-1.05 Ma, particularly between 3-2 Ma, and has excellent geochronological control based on radiometric dates from $^{40}\text{Ar}/^{39}\text{Ar}$ analysis of volcanic tephra, paleomagnetic correlation, and tephro-correlation to other parts of the Turkana Basin (e.g. Feibel et al., 1989; Bobe and Eck, 2001; Boisserie et al., 2008, 2010; McDougall et al., 2012). The formation is divided into 12 members (Basal, A, B, C, D, E, F, G, H, J, K, and L) which are further broken up into units representing a sedimentary cycle, each except the Basal have eponymous volcanic tuff at their bases (Figure 4.1; de Heinzelin, 1983). Although highly fossiliferous, the fluvial nature of most of the sediments has resulted in a fossil record comprised mostly of isolated teeth, cranial fragments, and unassociated postcrania (de Heinzelin, 1983). In addition to its many archaeological sites and rich Plio-Pleistocene mammalian record, the Shungura Formation has produced many important hominin fossils including specimens of *Australopithecus*, *Paranthropus*, and early *Homo* as well as a diverse assemblage of bovids, suids, perrisodactyls, carnivorans, proboscideans, giraffids, hippopotamids, and cercopithecids (Howell & Petter, 1976; White and Harris, 1978; Vrba, 1980; Harris et al., 1983; Gentry, 1985; Hooijer & Churcher, 1985; Harris, 1991; Suwa et al., 1996; Harris and Cerling, 2002; Alemseged, 2003; Bobe and Behrensmeyer, 2004; Negash et al., 2015; Patterson et al., 2017).

Figure 4.1 Stratigraphic map of L895-1's locality within the Shungura Formation. A. Modified from Alemseged, 2003, Figure 4.1a, pg. 454 B. modified from de Heinzelin, 1983, Figure 4.0, pg. 102.



Although they are not the most prevalent faunal group in the Shungura Formation, cercopithecids are well-represented with over six-thousand specimens attributed to at least 10 species representing both subfamilies (Eck, 1977, 1987; Leakey, 1987; Eck and Jablonski, 1987; Delson and Dean, 1993; Frost, 2001; Martin et al., 2018).

Despite its discovery in 1973, the cercopithecid specimen L895-1 has never been described. It was tentatively classified *Paracolobus mutiwa* based on its large size, but a

lack of associated cranial elements makes this difficult to verify as several large colobines are known from Member G (Figure 4.2; Leakey, 1987; Frost, 2001; Jablonski et al., 2008; Frost, pers. comm.). Based on its position in unit G15 just above the top of the Reunion II (2.08 Ma) and below the base of the Olduvai (1.954 Ma) paleomagnetic subchrons, at the lowermost part of Upper Member G, L895-1's age can be more precisely estimate to between about 2.05 and 2.07 Ma based on stratigraphic scaling (Figure 4.1; DeHeinzelin, 1983; Kidane et al., 2007).

Figure 4.2 All postcranial elements associated with specimen L895-1.



Despite its discovery in 1973, L895-1 has never been described. Lack of associated cranial elements makes it difficult to allocate to species and although L895-1 is the only cercopithecoid from Locality 895, several other large cercopithecoids are known from Member G and temporally overlapping deposits in the Turkana Basin including *Paracolobus mutiwa*, *Cercopithecoides kimeui*, *C. williamsi*, *Rhinocolobus turkanensis*, *Theropithecus oswaldi*, *T. brumpti*, and *Soromandrillus quadratiostris* (Iwamoto, 1982; Eck and Jablonski 1984; 1987; Eck, 1987b; Leakey, 1987; Harris et al., 1988; Delson and Dean, 1993; Frost, 2001; Jablonski et al., 2008; Gilbert, 2013). Many of these taxa, including *C. williamsi* and *P. mutiwa*, have been reconstructed as terrestrial and semiterrestrial while *R. turkanensis* is more arboreal (Birchette, 1982; Leakey, 1987; Frost, 2001; Frost and Delson, 2002; Jablonski et al., 2008; Anderson, 2016, 2019). Smaller bodied taxa including *Colobus* sp. and *Cercopithecus* sp. are known from Members K and L, but the size and geological age of L895-1 make these unlikely (Eck, 1987a; Leakey, 1987).

In addition to colobines, there are many large-bodied cercopithecine taxa known from localities within the Shungura Formation. *T. brumpti* is known from members B-G with some possible elements also known from Member A and the Usno Formation (Eck and Jablonski, 1987). *T. oswaldi darti* is known from Member C and *T. oswaldi oswaldi* has been identified from Members E-G with some elements tentatively attributed from H-L (Eck, 1987b; Frost, 2001). The postcrania of both *T. brumpti* and the *T. oswaldi* lineage are known from multiple associated specimens or unambiguous contexts (Jolly, 1972; Jablonski, 1986; 2002; Krentz, 1993; Jablonski et al., 2008; Guthrie, 2011). *S. quadratiostris* is also known from Members D-G, but no postcrania are directly

associated (Iwamoto, 1982; Eck and Jablonski, 1984; Delson and Dean, 1993; Frost, 2001; Gilbert, 2013).

The description presented here will focus on elements of the fore and hindlimb with an emphasis on functionally relevant features shared with contemporaneous large-bodied colobines. Although the lack of associated cranial elements makes taxonomic assignment difficult, L895-1 does preserve a number of elements with functionally relevant features that can help to eliminate certain taxa (Table 4.1). The limbs show more morphologies more consistent with the colobine morphotype than *Theropithecus* or other papionins such as a weak trochlear flange on the humerus, symmetrical coronoid process on the ulna, medially curved greater trochanter on the femur, calcaneus, and middle cuneiform (Figures 4.4, 4.9, 4.16, 4.25, 4.30; Jablonski, 2002; Guthrie, 2011; Gilbert et al., 2011). It is also distinct from the more arboreal *R. turkanensis* in its distal humerus morphology (Figures 4.5, 4.7) and lacks some of the more extreme terrestrial features seen in *C. williamsi* such as a retroflexed medial epicondyle of the humerus (Figure 4.6). It is also proportionally distinct from *P. chemeroni* with its comparably short and robust long bones; also seen in the *P. mutiwa* specimen *P. mutiwa*.

Based on its geological age, body size, and morphology there are still a few possibilities as to its classification. L895-1 could be *P. mutiwa* so a detailed comparison with the male specimen *P. mutiwa* from West Turkana is made (Harris et al., 1988; Anderson, in review). L895-1 is also consistent in size with *C. kimeui* which is larger than *C. williamsi* and known from this time period. Unfortunately, there are currently few well-preserved elements attributed to *C. kimeui*, but those available, mostly KNM-ER 176, are included in this analysis (Jablonski et al., 2008). The postcranial analyses

Table 4.1 All identifiable elements associated with L895-1. Elements in bold are included in the functional descriptions and analyses. Elements not included are either too fragmentary for functional assessment, or nondiagnostic. a. These fragments were found in two separate bags simply labeled “L895-1.”

Cat. No.	Side	Element	Description
L895-1a	L	Femur	proximal end and shaft fragment.
L895-1a	L	femur	distal end shaft fragment
L895-1b	R	femur	proximal end and shaft/distal fragment
L895-1c	R	tibia	proximal end, shaft fragment, distal end
L895-1d	L	tibia	all but tibial plateau
L895-1e	L	ulna	proximal end and shaft fragment.
L895-1f	R	ulna	prox end, midshaft fragment, and distal shaft
L895-1g	L	radius	head to radial tuberosity, shaft fragment
L895-1h	R?	clavicle	acromial end fragment
L895-1i	L	humerus	proximal fragment, shaft, and distal end
L895-1j	R	fibula	proximal end, midshaft, and distal shaft
L895-1k	R	clavicle	sternal end
L895-1L	L	fibula	distal fragment.
L895-1L		caudal vertebrae	
L895-1m	L	calcaneus	
L895-1m		caudal vertebrae	
L895-1n		caudal vertebrae	
L895-1o		caudal vertebrae	
L895-1p		caudal vertebrae	
L895-1q		tarsal	
L895-1r		tarsal	
L895-1r		axis (C2)	dens process and body fragment
L895-1t	L	MT I	
L895-2a		vertebrae	body fragment.
L895-2b		vertebrae	body fragment.
L895-2c		vertebrae	body fragment
L895-2d		vertebrae	body fragment.
L895-2e		vertebrae	lumbar? body fragment.
L895-2g	L	MT IV	base fragment
L895-2h	L	MT III	base shaft fragment.
L895-2i		P2	
L895-2k		P2	
L895-2L	L	MC IV	base and head fragment
L895-2n	L	cuboid	
L895-2o	R	navicular	
L895-2p	L	navicular	
L895-2s	R	patella	
L895-2s		vertebrae	body fragment

Table 4.1 continued			
Cat. No.	Side	Element	Description
L895-2t	R	middle cuneiform	
L895-2u	L	middle cuneiform	
L895-1	L	MT V	base fragment
L895-1		P1	head and shaft fragment
L895-1		MC	head
L895-1		MC	head and shaft fragment
L895-1	R	astragalus	trochlea and condyle fragments
L895-1	R	astragalus	superior trochlea fragment
L895-1	R	astragalus	head fragment.
L895-1		shaft fragment	
L895-1		shaft fragment	
L895-1		MC I	base fragment
L895-1		lumbar vertebrae	spinous process fragment
L895-1		long bone fragment	maybe Rt. femur?
L895-1	L	scapula?	glenoid fragment.
L895-1		fragments	13 mostly long bone fragments
L895-1		shaft fragments	possible radius
L895-1		rib	fragment
L895-1		bone fragments ^a	
L895-1		bone fragment ^a	vertebrae, tarsals, carpals, fragments
L895-1		ulna	spinous process

presented here will emphasize comparisons with *P. mutiwa* and other large-bodied cercopithecids with which it is contemporaneous as well as extant large bodied colobine taxa such as *Nasalis* and *Semnopithecus*. Whatever the identification of L895-1, it preserves a number of associated elements that, despite the lack of cranial material, make it one of the more complete partial colobine skeletons known from the Plio-Pleistocene. It also possesses elements not seen in other identified specimens making it important for gaining a better understanding of the variation within and among colobine taxa during the Plio-Pleistocene and a valuable comparator for other isolated elements.

Results

Humerus: L895-1 (Lt. Side)

The humerus is robust and more resembles *P. mutiwa* and *C. williamsi* than *P. chemeroni* which is significantly longer and more gracile (Figures 4.3, 4.4). The diaphysis has a well-developed deltoid tuberosity suggesting some emphasis on medial rotation of the shoulder and forelimb (Ashton and Oxnard, 1964; Larson, 1993; Gebo and Sargis, 1994; Jablonski et al., 2008). The distal end has fewer obvious terrestrial features than *C. williamsi* and *Theropithecus* but is distinct from the arboreal *R. turkanensis*.

Figure 4.3 Left humerus L895-1i.



Preservation

The humerus is in 3 pieces that have not been reconstructed: a head fragment, the diaphysis, and a fragment of the distal articular surface (Figure 4.3). The head fragment is about 3 cm. long and preserves the superior aspect of the articular surface, but is missing the ventral, dorsal, and medial sections. The most superior portion of the greater tubercle

is preserved except that the lateral face immediately inferior to the tubercle is broken. The lesser tubercle is not preserved.

The second fragment is a mostly complete diaphysis, which has been reconstructed from three previously broken fragments and is about 19 cm. long. The proximal end retains the medial surgical neck as well as the superior aspect of the deltoid crest and tuberosity. At the most distal aspect of this fragment, where it is reattached to the midshaft, there are several small pieces missing from the lateral border of the deltoid tuberosity, the dorsal face, and the deltoid crest. The midshaft fragment preserves the most distal portion of the deltoid tuberosity and is complete except for a few fragments missing at its proximal aspect and some minor damage to the cortical bone. It fits tightly with the distal fragment which preserves most of the brachioradialis flange. The flange is broken obliquely at its most distal point to just above the medial epicondyle.

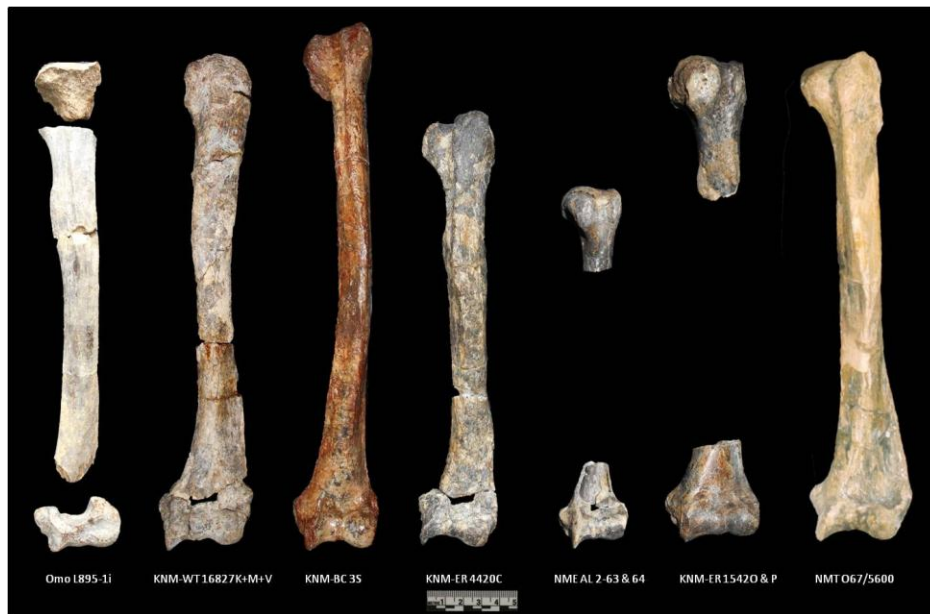
The distal articular surface separate from the shaft and is missing the intervening bone that would have joined them (Figure 4.3). It preserves the medial epicondyle, capitulum, trochlea, and the distal aspect of the lateral epicondyle. The most distal extensions of the margins of the olecranon fossa are preserved along with the inferior border of the fossa. Although the humeral fragments are not continuous, enough features are preserved to allow for a reasonable estimate of the total length of the humerus.

Description

The humeral head is anterior-posteriorly wide with a greater tubercle that is level with the most proximal extension of the head and is similar in prominence to that of *C. meaveae*. A projecting greater tubercle as seen in more terrestrial taxa such as *C. williamsi* and *Theropithecus* provides shoulder stability while more arboreally adapted cercopithecids

like extant colobines and *R. turkanensis* tend to have tubercles that are lower than the humeral head (Figure 4.4; Birchette, 1982; Fleagle and Simons, 1982; Harrison, 1989; Gosselin-Ildari, 2013). The dorsal border of the greater tubercle is thick and rugose with a small portion of the *m. infraspinatus* attachment still preserved.

Figure 4.4 Ventral view comparing humeri from (L-R) L895-1i, ♂ *Paracolobus mutiwa*, ♂ *Paracolobus chemeroni*, ♂ *Cercopithecoides williamsi*, ♂ *Cercopithecoides meaveae*, ♂ *Rhinocolobus turkanensis*, and ?*Theropithecus oswaldi*. *P. mutiwa* and KNM-BC 3 have been flipped vertically for ease of comparison.



Unfortunately, the articular surface of the head is too fragmentary to determine its overall shape.

On the diaphysis, the medial border of the deltoid tuberosity begins about 3 cm. below the surgical neck. It is significantly sharper and more prominent than the lateral border and is similar in prominence, but slightly shorter than in *P. mutiwa* and *P. chemeroni* (Figure 4.7d). The lateral border is a continuation of the lateral border of the bicipital groove, but damage makes its proximal shape impossible to estimate. This

border extends distally and fades out just distal to the midshaft. A longitudinal groove in the tuberosity suggest a strong *m. deltoideus*. This morphology is also seen in *P. chemeroni*, *C. williamsi*, and *Theropithecus*, but not in *P. mutiwa* although its deltoid tuberosity is robust. The prominence of this feature in L895-1 more closely resembles more terrestrial fossil taxa than extant arboreal colobines (Ashton and Oxnard, 1964; Jablonski, 2002).

The proximal shaft has a slight ventral curve and an anterior crest that begins just distal to the deltoid tuberosity and grows more prominent distally before merging with the medial epicondyle. What is preserved of the brachioradialis flange is more prominent than *C. williamsi*, but not as sharp as *C. meaveae* or as long as *P. chemeroni* and *P. mutiwa* (Figure 4.5). This may suggest as less developed *m. brachialis* and less emphasis

Figure 4.5. Ventral view comparing distal humeri from (L-R) L895-1i, ♂ *Paracolobus mutiwa*, ♂ *Paracolobus chemeroni*, ♂ *Cercopithecoides williamsi*, ♂ *Cercopithecoides meaveae*, ♂ *Rhinocolobus turkanensis*, and ?*Theropithecus oswaldi*. *P. mutiwa* and KNM-BC 3 have been flipped vertically for ease of comparison.



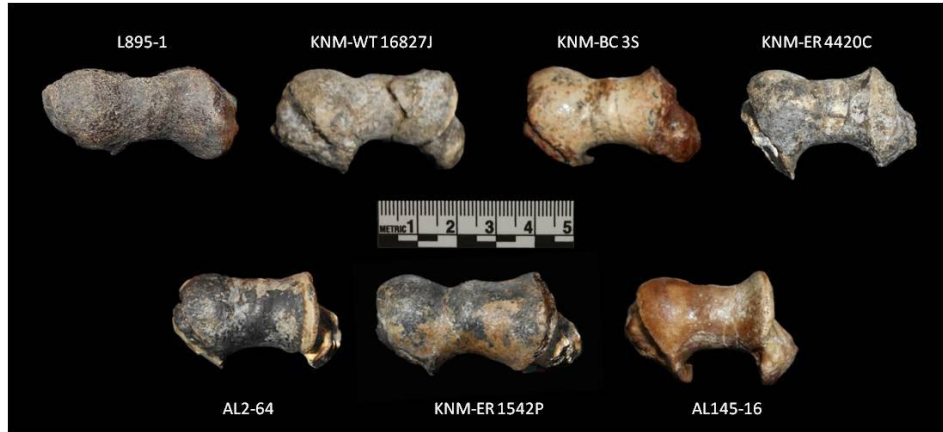
on pro/supination abilities of the elbow compared these taxa, but its prominence compared to the arboreal colobines suggests a more terrestrial pattern (Jolly, 1972; Conroy, 1976; Harrison, 1989; Fleagle and McGraw, 2002; Gilbert et al., 2010). The

most distal portion of the diaphysis is broken, but appears to display the antero-posterior compression seen in extant colobines, *P. chemeroni*, *C. williamsi*, *C. meaveae*, and *R. turkanensis*. Unfortunately preservation does not allow for analysis of the *m. brachioradialis*, or *extensor carpi radialis longus* attachments.

The distal articular surface retains a broad capitulum and trochlea, and a weak trochlear flange. The preserved portion of the lateral epicondyle is more prominent than in *T. oswaldi* specimens known from Omo and positioned in the superior portion of the disto-lateral surface. It is more ventrally oriented than that of *C. meaveae* and is similar in placement to those of *C. williamsi*, *P. chemeroni*, and *Paracolobus mutiwa*, although L895-1 most closely resembles the latter in its lateral projection. It is also more prominent relative to the size of the distal humerus than that of *R. turkanensis* and has a more rugose surface. This suggests well-developed elbow, wrist and hand extensors and supinators compared to the arboreal *R. turkanensis*, but the tubercle for the *m. extensor carpi radialis* is not preserved preventing further comparison (Ciochon, 1993; Rose, 1998; Schmitt, 1998). Immediately distal to the lateral epicondyle is a small, but marked rounded fossa with a prominent dorsal border for the attachment of the radial collateral ligament. It is similar in depth and prominence to that of *P. chemeroni* and slightly more excavated than in *P. mutiwa*. The fossa is shallower than in *R. turkanensis* and more ventrally oriented and larger than those of *C. meaveae* or *C. williamsi*.

The medial epicondyle is wide and rugose with proximo-distal compression and little retroflexion compared to *P. chemeroni*, *P. mutiwa*, *C. williamsi*, and *Theropithecus* (Figure 4.6). It is oriented more ventrally on the medial face than in these taxa and more closely resembles *R. turkanensis* in its medial projection, although that of L895-1 is less

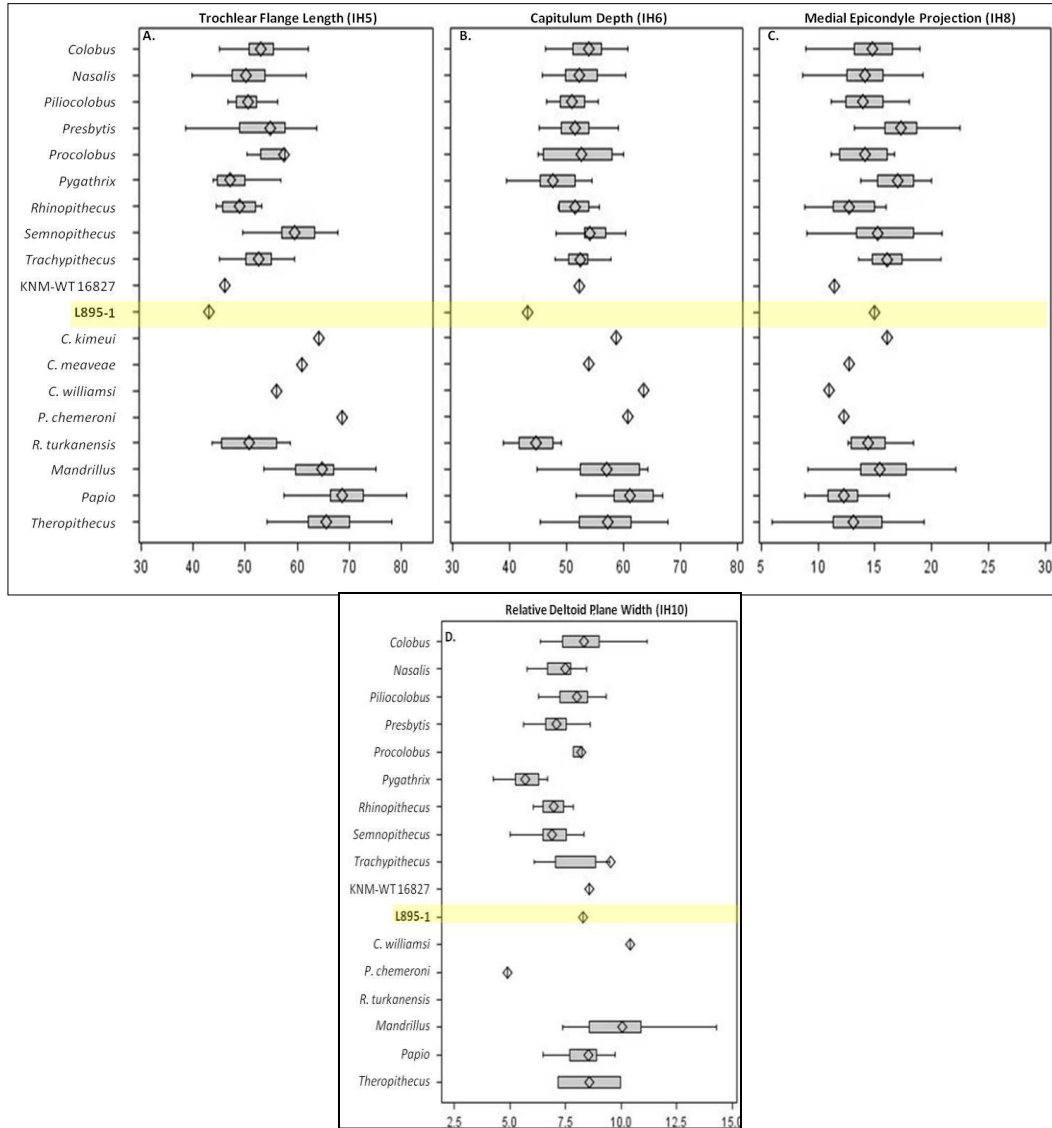
Figure 4.6 Inferior view comparing the distal humeral articular surface from (L-R) L895-1i, ♂ *Paracolobus mutiwa*, ♂ *Paracolobus chemeroni*, ♂ *Cercopithecoides williamsi*, ♂ *Cercopithecoides meaveae*, ♂ *Rhinocolobus turkanensis*, and *Theropithecus oswaldi*. L895-1 has been flipped vertically as all comparative elements had better preserved right sides for the distal humerus.



prominent (Figure 4.6, 6C). It accounts for about 3/4 of the medial face and is rough and pitted suggesting well-developed carpal and digital flexors more common in arboreal cercopithecids (Patel, 2010). In dorsal view, the medial epicondyle is separated from the superior trochlear flange by a shallow ulnar groove that extends superiorly to the inferior border of the olecranon fossa.

The trochlear flange is sharp, but weakly developed with very little distal projection compared to *P. chemeroni*, *C. williamsi*, *C. meaveae*, and *Theropithecus*. Although not as sharply defined, L895-1 most closely resembles *P. mutiwa*, *Semnopithecus*, and *Trachypithecus* in its prominence and is longer than in *R. turkanensis*, *Nasalis*, and *Colobus*. However, relative to the width of the distal humerus, the flange length is proportionally more similar to arboreal extant colobines and *R. turkanensis* than terrestrial forms (Figure 4.7a). This may suggest some emphasis on medial stability in the elbow more consistent with some terrestrial locomotor behavior,

Figure 4.7 Box plots showing ranges of humeral indices **A.** humeral head to total length **B.** capitulum width relative to length **C.** articular surface relative to the medial epicondyle ("Harrison's Breadth") and **D.** width of the deltoid tuberosity relative to humeral length. Indices organized by genus for comparative sample and *P. chemeroni* is represented by KNM-BC-3.



but not to the extreme seen in papionins or more extreme terrestrial colobines (Jolly, 1967; Delson, 1973; Frost and Delson, 2002). The distal border of the flange remains sharply defined as it wraps beneath the distal end before fading into the inferior border of the olecranon fossa. The trochlea is narrower than those of *P. mutiwa*, *P. chemeroni*, and *C. williamsi*, but wider than in *Theropithecus* and has a faint zona conoidea. The zona

conoidea is not as distinct as in *C. meaveae* or *T. oswaldi*, but similar in appearance to *P. mutiwa* and *R. turkanensis*. The capitulum is wide and bulbous with a mostly ventral orientation and more similar in its proportions to *R. turkanensis* than more terrestrial taxa such as *P. chemeroni*, *C. kimeui*, *C. williamsi*, *Theropithecus*, *Papio*, and *Mandrillus* (Figure 4.7b).

Ulna: L895-1f (Rt. Side) and L895-1e (Lt. Side)

The ulnae are short and robust compared to those of *P. chemeroni*, *C. williamsi*, *R. turkanensis*, and *Theropithecus* with marked muscle attachments and an asymmetrical olecranon process. The proximal ulna is more morphologically consistent with terrestrially adapted cercopithecids rather than *R. turkanensis* or arboreal extant colobines. Although the whole diaphysis is not preserved in either specimen, it appears to have been similar in length and robusticity to that of *Paracolobus mutiwa* (Figure 4.8, 4.9).

Preservation

The right side is in four separate but undistorted pieces that are complete enough to include estimates of the total length (Figure 4.8, Table 4.2). The proximal epiphyseal fragment fits onto the proximal diaphyseal fragment and the distal diaphyseal fragment does not but based on comparison with the fragments from the left side, is not missing much of the intervening bone. The distal articular surface preserves only an isolated styloid process which does not fit onto the diaphyseal fragments. The proximal fragment preserves the olecranon process, olecranon fossa, coronoid process, anconeal process, trochlear notch, and radial notch. A small piece is missing from the medial aspect of the olecranon and the radial notch is missing a small fragment from its lateral margin, but the

Figure 4.8 Ventral view of right (L895-1f) and left (L895-1e) ulnae.



proximal articular surface is in otherwise good condition. About 1.8 cm. of the proximal shaft is present with some cortical bone damage on the ventral face immediately proximal to the fragment's end. This damage continues onto the first shaft fragment, which is about 7 cm. long. There are fractures on the lateral aspect that cause minor distortion to the fragment likely caused by postmortem crushing. The distal shaft fragment is about 7 cm. long and has an oblique fracture at its midpoint that has been repaired. The styloid process is well-preserved and most likely from the right side based on its orientation.

The left side is in three pieces that fit together and were once reconstructed, but the glue has since disintegrated. The first fragment preserves the olecranon process, olecranon fossa, coronoid process, anconeal process, trochlear notch, and radial notch as well as about 4 cm. of the diaphysis. The medial edge of the olecranon process is broken

as is the coronoid process and the lateral lip of the radial notch. The dorso-medial surface also shows superficial damage to the cortical bone. The midshaft fragment is about 4 cm. long and is in good condition except for a missing flake of cortical bone on the dorso-lateral aspect. Small pieces missing from the disto-medial surface prevent it from perfectly aligning with the distal fragment, but enough is preserved for the two pieces to fit together. The distal fragment is just over 7 cm. long and is well-preserved except for a small piece missing from the ventral part of the proximo-lateral aspect. The distal articular surface is not preserved.

Description

The functional description will focus on the right side (L895-1f) as it is better preserved. The olecranon process is similar in proportional height to *C. meaveae*, *P. chemeroni*, and *R. turkanensis* although it is obliquely oriented, which is more typical in terrestrial taxa than arboreal forms like *Rhinocolobus* (Figure 4.9). This asymmetry is not as pronounced or as prominent as in *Theropithecus*. A longer olecranon process is associated with increased leverage of the *m. triceps brachii* during elbow flexion needed in arboreal locomotion and the short, but robust process seen in L895-1 is more consistent with prolonged extension seen in more terrestrial (Jolly, 1967; Conroy, 1974; Ashton et al., 1976; Jablonski, 2002). In this feature, L895-1 more closely resembles *C. williamsi* and groups closer to terrestrial cercopithecines such as *Papio* than to the extant colobines (Figure 4.10). The process shows an antero-posterior incline at its apex and the base is anteriorly oriented similar to that of *R. turkanensis*. This contrasts with its more dorsal placement in *C. williamsi* and *P. chemeroni*. The *m. biceps brachii* insertion is a small pit on the superior surface of the process smaller than in *Theropithecus* and similar

in relative size to *P. chemeroni* and *C. meaveae*. A small round pit in between the olecranon and anconeal processes on the medial aspect is the origin for the *m. flexor digitorum profundus* which is less excavated than *Theropithecus*, but similar to *P. chemeroni* and *C. williamsi*. This attachment is also more marked than in arboreal taxa such as *R. turkanensis* and extant colobines. Together these suggest an adaptation for stability in the elbow during prolonged flexion and supination as seen in more terrestrial locomotor patterns (Ashton and Oxnard, 1964; Rose, 1988; Jablonski and Leakey, 2008). The weak digital flexors compared to *Theropithecus* are likely due to the latter's unique adaptations for hand dexterity that are not seen in other cercopithecids (Jolly, 1967, 1972; Jablonski, 2002; Jablonski et al., 2008).

The articular surface of the trochlear notch is deep and wraps around the lateral edge. The anconeal process is symmetrical without the lateral flare seen in more terrestrial cercopithecines and shows less anterior projection than the coronoid process (Figure 4.10, 4.11). The coronoid process extends medially with a less pronounced medial decline than *P. mutiwa*, *P. chemeroni*, or *C. williamsi*, but all are more prominent than *Theropithecus* and extant colobines. The beak of the coronoid process is smooth and blunt in contrast to the sharper form seen in *Nasalis* and *R. turkanensis*. Immediately distal to the trochlear notch on the medial face is a marked crest about 2 cm. long for the *m. brachialis* insertion. This feature is more developed than in *P. mutiwa*, *P. chemeroni*, or *C. meaveae* and is more similar in prominence to *R. turkanensis* and *Colobus*. The radial notch is round with an articular surface that is continuous with the trochlear notch similar to what is seen in *P. mutiwa* and *P. chemeroni*, but is positioned more distally relative to the coronoid process. The radial articular surface is

Figure 4.9 Ventral view comparing ulnae from (L-R) L895-1f, ♂ *Paracolobus mutiwa*, ♂ *Paracolobus chemeroni*, ♂ *Cercopithecoides williamsi*, ♂ *Cercopithecoides meaveae*, ♂ *Rhinocolobus turkanensis*, and *Theropithecus oswaldi*. KNM-BC 3B and AL 2-65+37 have been flipped vertically for ease of comparison.



flat with defined, but not prominent, borders Figure 4.10, 4.11). Immediately below the notch on the lateral face is a long, but weakly defined supinator crest. This feature is not as prominent as *T. oswaldi*, but is more marked than *R. turkanensis*, *Rhinopithecus*, or *Semnopithecus*. This suggests that L895-1 had better developed *mm. abductor pollicis longus*, *extensor pollicis longus*, and *extensor indicis* than these more arboreal taxa, but not to the degree seen in *T. oswaldi* (Jablonski, 2002). On the medial margin of the dorsal surface of the proximal ends is a defined and oblique line for the origin of the *m. flexor carpi ulnaris* with a moderately excavated fossa for the *m. flexor digitorum profundus*. Both are similarly defined as *P. mutiwa*, but less prominent than seen in *Theropithecus* which have unique adaptations for digit flexion (Jablonski, 2002; Guthrie, 2011).

Figure 4.10 Ventral view comparing proximal right ulnae from (L-R) L895-1f, ♂ *Paracolobus mutiwa*, ♂ *Paracolobus chemeroni*, ♂ *Cercopithecoides williamsi*, ♂ *Cercopithecoides meaveae*, ♂ *Rhinocolobus turkanensis*, and *Theropithecus oswaldi*. KNM-BC 3B and AL 2-65+37 have been flipped vertically for ease of comparison.



Figure 4.11 Medial view comparing right ulnae from (L-R) L895-1f, ♂ *Paracolobus mutiwa*, ♂ *Paracolobus chemeroni*, ♂ *Cercopithecoides williamsi*, ♂ *Cercopithecoides meaveae*, ♂ *Rhinocolobus turkanensis*, and *Theropithecus oswaldi*. KNM-BC 3B and AL 2-65+37 have been flipped vertically for ease of comparison.



The diaphysis is straight with slight lateral curvatures at its midpoint and the shaft is relatively short compared to *P. chemeroni*. Based on the similar location of the midshaft curvatures, L895-1 was likely similar in length to *P. mutiwa* (Figure 4.9). There is marked medio-lateral compression of the shaft which lessens distally. The styloid process short and rounded similar to *C. williamsi* and is less prominent than *R. turkanensis*. This may suggest less of an emphasis on stability at the ulnar-carpal joint during dorsiflexion as seen in extant cercopithecids (O'Connor, 1976; Harrison, 1989).

Radius: L895-1g (Lt. Side)

Although total length cannot be determined, the preserved portion of the radius has a wide head and a relatively short neck compared to extant arboreal colobines. The radial tuberosity is not as prominent as *P. chemeroni*, *C. williamsi*, or *T. oswaldi*, but is more pronounced than *C. meaveae*. Although better preserved, L895-1 is not as robust as *P. mutiwa* although the two have similarly shaped radial tuberosities (Figures 4.12, 4.13).

Figure 4.12 Ventral view of left radius fragment L895-1g.



Preservation

The left radius fragment includes two reconstructed pieces that have been reattached to be about 5 cm. in length (Figure 4.12). Four long bone fragments were also recovered from a bag of unlabeled fragments that appear to be radial in shape. Although they are included Figure 4.1, these fragments cannot be reattached to the better preserved proximal end preventing any length estimates. The labeled fragment has been reconstructed just below the radial neck where an oblique fracture running latero-medially originally split the two pieces. The head, neck, and humeral articular surface are

well-preserved except for a small fragment missing from the dorsal rim of the head. The shaft is broken immediately below the distal extension of the radial tuberosity.

One of the long bone fragments labeled "h" was initially included in the assessment, but further examination of its morphology makes its identification as part of the radius less clear. There are no identifiable features on this piece which is about 2 cm. long. Another unlabeled long bone fragment is definitely radial based on its cross-section, but is poorly preserved and does not fit onto fragment "g." Three other possible radial shaft fragments are also present do not preserve any relevant or diagnostic features.

Description

The radial head is large with a thick, blunt border. The articular surface is ovoid with its long medio-lateral axis and a mild indentation at its center for articulation with the capitulum. This ovoid shape is associated with radio-ulnar joint stability and limited supination abilities in terrestrial cercopithecines, but can be variable and may not always be indicative of terrestrial locomotor patterns (Krentz, 1993; Jablonski, 2002; Guthrie, 2011). In an index of radial head shape, terrestrial cercopithecines such as *Mandrillus*, *Papio*, and *Theropithecus* fit this pattern, but also overlap with large-bodied colobines like *Nasalis* and *Semnopithecus*. This more elliptical shape is may be associated with habitual pronograde and limited pronation abilities in terrestrial cercopithecids (Conroy, 1974), but it has also been suggested to be related more to size than function (Jablonski, 2002). In ventral view the head tilts slightly laterally similar to *P. mutiwa*, *C. williamsi*, *C. meaveae*, and extant colobines, but not to the degree as *T. oswaldi* which also possesses an elevated medial border that is not present in the colobines (Figure 4.13).

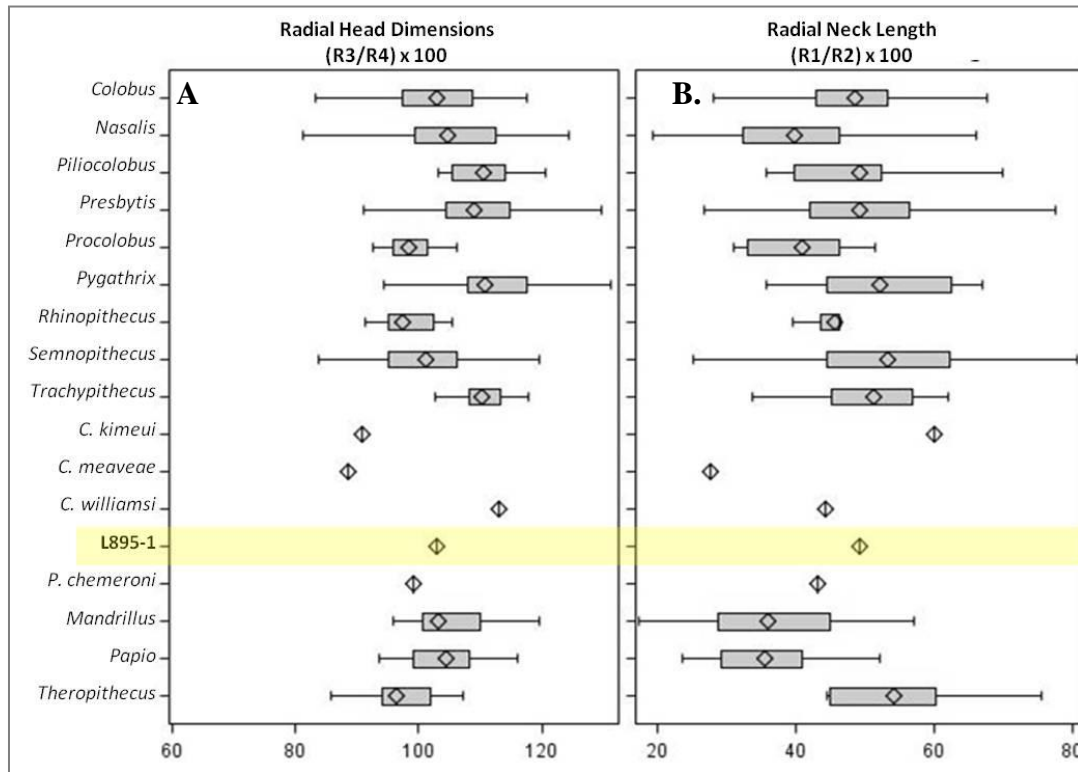
The radial neck is relatively wide and about the same width medio-laterally as the

Figure 4.13 Ventral view comparing radii from (L-R) ♂ *Paracolobus mutiwa*, ♂ *Paracolobus chemeroni*, ♂ *Cercopithecoides williamsi*, ♂ *Cercopithecoides meaveae*, ♂ *Rhinocolobus turkanensis*, and *Theropithecus oswaldi*. KNM-WT 16827AD, KNM-BC 3V, and AL 431-1G are from the right side and have been flipped vertically as they are better preserved than their associated left radii.



proximal shaft. It is also longer than *C. meaveae* and constricted more medio-laterally than *P. chemeroni* and *P. mutiwa* (Figure 4.13). In cercopithecids longer radial necks increase the force of the elbow during flexion of the *m. biceps brachii* during more arboreal locomotor behaviors, but L895-1 is proportionally similar to both arboreal and terrestrial colobines in this metric (Figure 4.14b; Conroy, 1974; Harrison, 1989). L895-1 is similar in length to *P. chemeroni* and *C. williamsi*, but when compared to the size of the radial head, is closer to the proportions seen in extant colobines such as *Trachypithecus*, *Semnopithecus*, and *Pygathrix* suggesting perhaps less or different emphasis on terrestriality (Figure 4.14). The neck has marked antero-posterior compression and the medial lip of the radial head extends further distally on the medial aspect than on the lateral. The radial tuberosity is also wide and longer than *C. williamsi* or *C. meaveae*. The medial border is sharper than the lateral which is quite blunt. A small groove begins at the most proximal portion of the medial face then fades at about the

Figure 4.14 Box plots showing radial indices of **A.** radial head dimensions and **B.** radial neck length relative to the total length. *P. chemeroni* is represented by specimen KNM-BC 3.



midpoint of the tuberosity and is much more pronounced in *P. chemeroni*, *C. meaveae*, and *C. williamsi* suggesting L895-1 has a less developed *m. biceps brachii*. This feature is associated with strong flexion capabilities and flexibility in supination in both arboreal (Ciochon, 1986) and more terrestrial cercopithecids so is difficult to assess on its own (Guthrie, 2011). What is preserved of the interosseous crest on the long bone fragment "h" is not as sharp as *P. chemeroni*, *T. oswaldi*, or extant colobines, but is more prominent than *Rhinopithecus* and *Nasalis*.

The radius displays features associated with both terrestrial and arboreal locomotion. The shape and tilt of the radial head and prominent radial tuberosity are more associated with terrestrial behavior, but the neck length is closer to extant arboreal

colobines. This is consistent with previous analyses which have concluded that it is difficult to distinguish locomotor pattern based on the radial morphology and more variation is present intragenerically than among differing locomotor patterns (Jolly, 1965; Birchette, 1982; Jablonski, 2002).

Femur: L895-1b (Rt. Side) and L895-1a (Lt. Side)

Both femora are undistorted and although only the right side preserves the proximal articular surfaces, the left side preserves the whole diaphysis allowing for a length estimate for the specimen (Figure 4.15). The femora from L895-1 are short and robust compared to *P. chemeroni* and extant colobines such as *Nasalis*, *Colobus*, *Semnopithecus*, and *Trachypithecus*. The right side preserves a greater trochanter that is

Figure 4.15 Femora associated with L895-1. (L-R) Ventral and dorsal view of right femur L895-1b, ventral view of left femur L895-1a, dorsal view of L895-1b, and dorsal view of L895-1a.



larger than extant taxa, but comparable in relative height to terrestrial forms such as *P. mutiwa* and *C. williamsi*, but not as prominent as in terrestrial cercopithecines.

Preservation

The right side (L895-1b) is in two separate and unreconstructed pieces. The proximal fragment preserves the head, neck, greater trochanter, intertrochanteric fossa, and about 2 cm. of the diaphysis (Figure 4.15). The head displays mild abrasion on its ventral margin and a portion of the neck has been sheared off revealing the trabecular bone on the dorsal aspect of the femoral neck and the lesser trochanter is not preserved. The second fragment It is comprised of two separate fragments that have been reattached to be about 13 cm. long and preserves the distal articular surface. A large portion of cortical bone is missing on the medial aspect of the diaphysis and a thin layer of matrix is still present on this specimen, but not to a degree that affects measurements. The distal articular surface has a small piece missing from the most lateral border of the lateral condyle. The medial border of the medial condyle is abraded all the way up to the most proximal extensions of the feature on the dorsal aspect and is missing a thin piece of cortical bone on its lateral face.

The left side is in three separate fragments that have been reattached: the femoral head with partial neck, greater trochanter, and lesser trochanter, about 7 cm. of diaphysis, and the distal articular surface with about 6 cm. of the distal diaphysis (Figure 4.15). About 7 cm. of cortical bone is missing from the ventral diaphysis. Most of the superior greater trochanter along with the medial femoral neck is also broken off distorting the intertrochanteric fossa shape. The lesser trochanter is well-preserved. The distal articular surface is undistorted and the lateral condyle is in good condition. The dorsal aspect of the medial condyle is broken off exposing the trabecular bone. Unless otherwise noted,

the functional description will focus on the right side (L895-1b) due to the better preservation of its articular surfaces.

Description

The femoral head is round and relatively large with an articular surface extending onto the femoral neck on the posterior aspect. This extension of the articular surface is greater than seen in *P. mutiwa*, *P. chemeroni*, *C. williamsi*, and *C. meaveae*. This feature is associated with prolonged flexion, abduction, and rotated hip positions such as those seen in arboreal leapers and climbers, but L895-1 does not display this feature to quite the degree seen in these taxa (Figure 4.16; Napier and Walker, 1967; Harrison, 1982;

Figure 4.16 Ventral comparing femora from (L-R) from L895-1b, ♂ *Paracolobus mutiwa*, ♂ *Paracolobus chemeroni*, ♂ *Cercopithecoides williamsi*, ♂ *Cercopithecoides meaveae*, and ♂ *Theropithecus darti*. The length of AL 2-70+28 is an estimate.



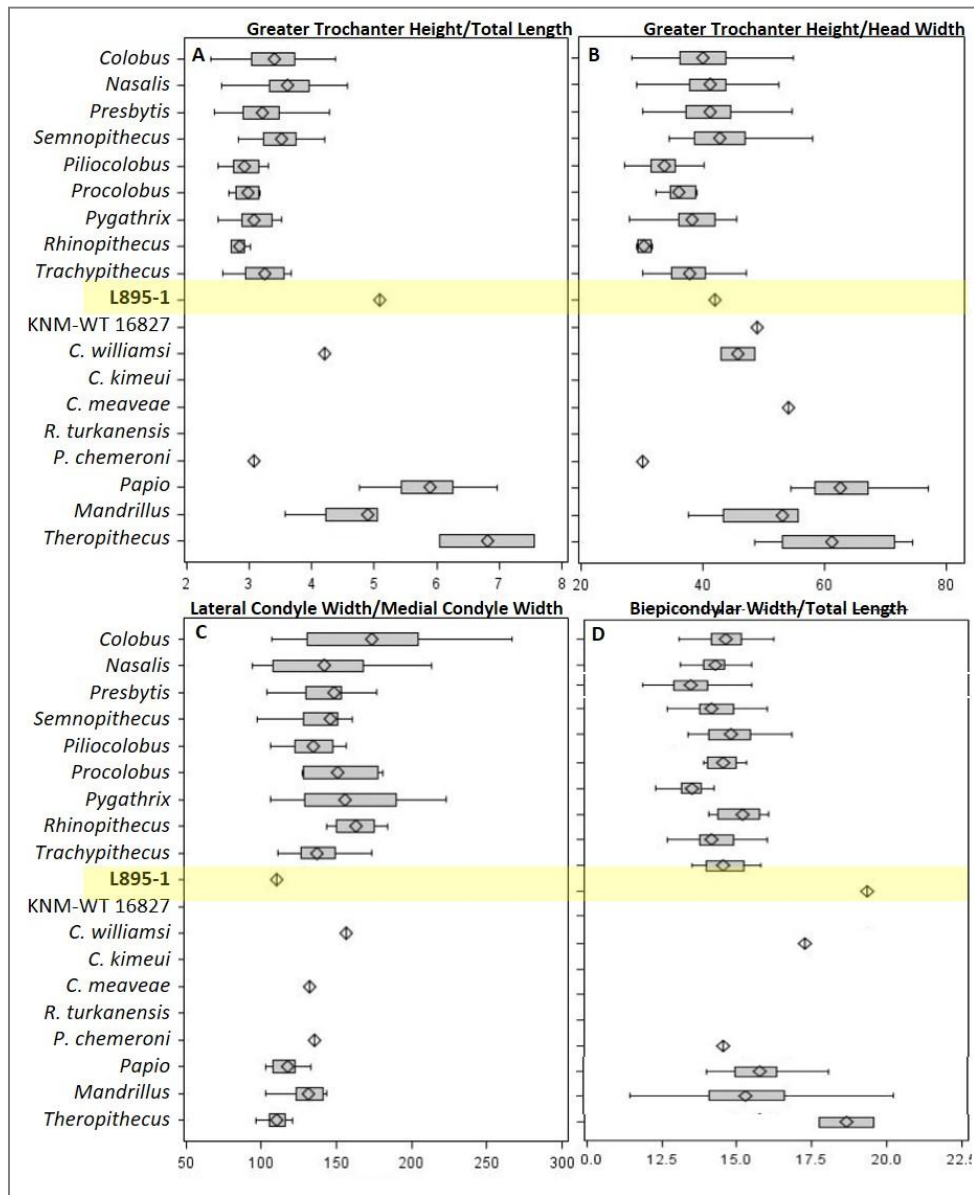
Anemone, 1990; Harrison and Harris, 1996). The fovea capitis is preserved on the left side (L895-1a) and is deep and ovoid in shape. It is widest antero-posteriorly and oriented dorsally on the articular surface with its most ventral margin located at the midpoint of the head. The femoral neck is longer than arboreal extant colobines such as *Colobus* and *Nasalis* and relatively thick with no torsion relative to the diaphysis as seen in more terrestrial taxa such as *Theropithecus*. The neck angle is about 110° which is slightly lower than *C. williamsi*, *C. meaveae*, *P. mutiwa*, and most extant colobines, but similar to *P. chemeroni* (Harrison, 1989; Frost and Delson, 2002). The large articular surface combined with this neck angle suggests an emphasis on abduction, but not to the degree seen in more arboreal cercopithecids and falls within the range seen in more terrestrial and semiterrestrial taxa (Harrison, 1982, 1989; Anemone, 1990; MacClatchy et al., 2000).

The greater trochanter extends above the femoral head but is not as prominent as *C. williamsi*, *Theropithecus*, or *Papio* but is taller relative to the total length of the femur compared to extant colobines (Figure 4.17a). Unfortunately, *P. mutiwa* does not preserve enough of the femur to make such a comparison, but relative to the width of the within the range of extant colobines such as *Colobus*, *Nasalis*, and *Semnopithecus* and is similar to *C. williamsi* (Figure 4.17b). On the most lateral margin of the trochanter in ventral view is a distinctive crest for the *m. gluteus minimus* which is seen in both *C. williamsi* and *P. mutiwa* although weathering in the latter makes it difficult to compare prominence. On the superior aspect of the trochanter is a small but distinctive pit for the *m. piriformis* insertion which is smaller than *C. williamsi* and larger than in *P. mutiwa*, *C. meaveae* and *P. chemeroni*. This combined with the marked rugosity of the *m. gluteus*

minus attachments suggest an emphasis on abduction at the hip (MacLatchy et al., 2000; Guthrie, 2011; Hammond, 2013). On the medial edge is a crest for the *m.*

quadratus femoris similar to what is seen in terrestrial colobines such as *P. mutiwa*, *C.*

Figure 4.17 Box plots showing femoral indices for **A.** relative greater trochanter height **B.** greater trochanter relative to femoral head breadth **C.** lateral condyle width relative to medial condyle and **D.** biepicondylar width relative to total femoral length. *P. chemeroni* is represented by specimen KNM-BC 3.



williamsi, and *C. meaveae*. The intertrochanteric fossa is deep for a well-developed *m. obturator externus* also similar to *P. mutiwa*, *C. williamsi*, and *C. meaveae*. This again suggests strong abduction and lateral rotation at the hip joint similar to what is seen in extant terrestrial taxa such as *Papio* (Stern and Larson, 1993; Jablonski et al., 2008).

The intertrochanteric crest and lesser trochanter are preserved only on the left side (L895-1a). The lesser trochanter has an elliptical base and is more distally oriented relative to the intertrochanteric fossa compared to extant colobines. It is also more distally oriented compared to *C. meaveae*, but similar to fossil colobines that preserve this feature including *C. williamsi*, *P. chemeroni*, and *P. mutiwa*. The intertrochanteric crest is marked weak and fades out completely just before becoming level with the lateral margin of the lesser trochanter. The trochanter is very prominent relative to the length of the femur and positioned primarily in the sagittal plane with marked posterior projection in contrast to *Semnopithecus*, *Rhinopithecus*, and *Procolobus* which all display a more medially oriented projection. This is also seen in terrestrial fossil specimens of *C. meaveae* and *C. williamsi* and is associated with increased efficiency at the hip for the parasagittal movements more typical of terrestrial locomotion than arboreal leaping (Harrison and Harris, 1996; Gilbert et al., 2011). The facet for the *m. psoas major* is weathered, but ovoid in shape and wider than *C. meaveae* but similar in shape and size to *P. chemeroni* and *P. mutiwa* which may indicate similar adaptations for more terrestrial quadrupedalism in these specimens.

On the lateral face of the diaphysis is a marked crest beginning immediately distal to the greater trochanter that continues to just above the midshaft fracture for the origin of the *m. vastus lateralis*. The pectineal line is faint, but detectable by touch and begins

immediately distal to the lesser trochanter in dorsal view. It is relatively short compared to *Semnopithecus* and *Pygathrix* but similar in length and prominence to *C. meaveae*, *P. chemeroni*, *P. mutiwa*, and *C. williamsi* although the latter is particularly weak. This suggests a weak *m. pectineus* and less emphasis on hip flexion and adduction as is seen in more arboreal climbers or leapers (Kimura et al., 1981). There is no visible linea aspera, but taphonomic damage to the dorsal face of the diaphysis may obscure it. The diaphysis has more ventral curvature than *Procolobus*, but is similar to *P. chemeroni*, *P. mutiwa*, and *Nasalis* although none of the fossil forms are as curved as *Theropithecus*.

The distal end is wide relative to the total length of the femur and is proportionally more within the range of *Theropithecus* and *Mandrillus* than extant arboreal colobines (Figure 4.17d). In this index L895-1 and *C. williamsi* are closer to the ranges displayed by terrestrial cercopithecines while the extant colobines have relatively narrow ranges in contrast to *P. chemeroni* which displays a more extant colobine proportion due to its relatively gracile long bones and small greater trochanter. The patellar surface is short and wider than *P. chemeroni* and *C. meaveae* although the actual dimensions may be exaggerated by the abrasions present on the distal diaphysis. The borders are even in height in contrast many extant arboreal colobines which display a taller lateral border.

Although damaged, the medial epicondyle appears to have been larger and taller proximo-distally than the lateral condyle. At its superior aspect is a round fossa for the medial collateral ligament which is not present in *C. meaveae*, but visible in *P. chemeroni* although L891-1's is more superiorly oriented. In posterior view the medial condyle is wider anterior-posteriorly than the lateral condyle similar to *C. williamsi* and overlaps

with both *Colobus* and *Rhinopithecus* in this index (Figure 4.17c). Although some of the extant colobines overlap in this feature with more terrestrial cercopithecines, the latter tend to have wider medial condyles. This trait is associated with more terrestrial locomotor patterns and well-developed *m. quadriceps femoris* for extension at the knee (Elton, 2002; Guthrie, 2011). L895-1 and the more terrestrial fossil colobines are all closer in this metric to the extant taxa which suggests terrestrial adaptations may not be totally analogous across subfamilies. The lateral epicondyle is well-preserved and largely taken up by a deep and round fossa for the origin of the *m. anterior popliteus*. Immediately dorsal to this fossa is a wide groove for the *m. popliteus* which forms most of the dorsal border of the condyle which is deeper than *C. meaveae*, but similarly excavated compared to *P. chemeroni*. This morphology is not unusual among cercopithecids and its functional significance is not fully understood (MacLatchy et al., 2000).

All together the femora of L895-1 are an intriguing mix of morphologies that overlap both with arboreal extant colobines and more terrestrial fossil forms. Proportionally it most closely resembles *P. mutiwa* in being relatively short and robust with a prominent greater trochanter and thick neck. Distally it falls within the range of both terrestrial cercopithecines and semiterrestrial colobines. There are no preserved femora attributed to arboreal fossil taxa such as *R. turkanensis* and other fossil taxa known from the Turkana Basin do not preserve enough for length estimates, but based on what is preserved of L895-1, it is distinct from *P. chemeroni*, *C. williamsi*, *C. meaveae*, *Theropithecus*, and most similar in its shared preserved features to the ?*P. mutiwa* specimen *P. mutiwa*.

Tibia: L895-1c (Rt. Side) and L895-1d (Lt. Side)

L895-1's tibia resembles many extant in having a relatively straight diaphysis, prominent tibial tuberosity, and long medial malleolus (Figure 4.18). However, it is proportionally quite distinct from the extants colobines and *P. chemeroni*, the only identified fossil colobine with a well-preserved diaphysis in the comparative sample, with its relatively wide proximal articular surface and short total length. In size it most closely resembles *T. oswaldi* but is not as robust and lacks the medial shaft curvature seen in *Theropithecus* (Figure 4.19).

Preservation

The right tibia (L895-1c) is the better preserved of the two and is composed of two separate pieces that fit together just below midshaft (Figure 4.18). The two parts were once glued together but the adhesive has since disintegrated. The proximal fragment

Figure 4.18 Ventral view of tibiae associated with L895-1. (L-R) right side L895-1c and left side L895-1d.



is just under 11 cm. long and includes the proximal articular surfaces and 8 cm. of shaft. The lateral preserves only the dorso-lateral portion, but the lateral portion of the fibular facet is preserved. Most of the ventral face of the proximal end just above the tibial tuberosity is missing along with the most proximal portion of the tibial tuberosity and intercondylar tubercle. The medial condyle shows weathering on its ventro-medial border and is missing its lateral margin preventing any measurements of its dimensions. The diaphysis of this fragment is well-preserved except for some superficial wear on the cortical bone and adhered matrix. The distal fragment is complete except for the medial malleolus which is broken off and a small crack on the medial aspect of the distal articular surface.

The left tibia (L895-1d) does not preserve the proximal articular surface but has a nearly complete shaft and distal articular surface (Figure 4.18). Neither condyle is preserved and there is damage to the proximal and lateral aspects of the tibial tuberosity. The diaphysis is in good condition except for damage to the cortical bone on the lateral aspect just below midshaft and for a small piece missing from the most distal portion of the lateral face. The medial malleolus and distal articular surfaces are well-preserved. Because the medial malleolus is not preserved on the right side, the length of the left side's has been added to its total length (T1) so that a total length estimate is available for index calculations (Table 4.2).

Description

Functional description will focus on the right side (L895-1c) as it is more complete except for any mention of the distal articular surface which is better preserved on the left side (L895-1d). The articular surface of the lateral condyle is too damaged for

Figure 4.19 Ventral view comparing tibiae from (L-R) L895-1c, ♂ *Paracolobus chemeroni*, ♂ *Cercopithecoides williamsi*, ♂ *Cercopithecoides meaveae*, and ♂ *Theropithecus darti*. The length for KNM-ER 1542W+U is an estimate.

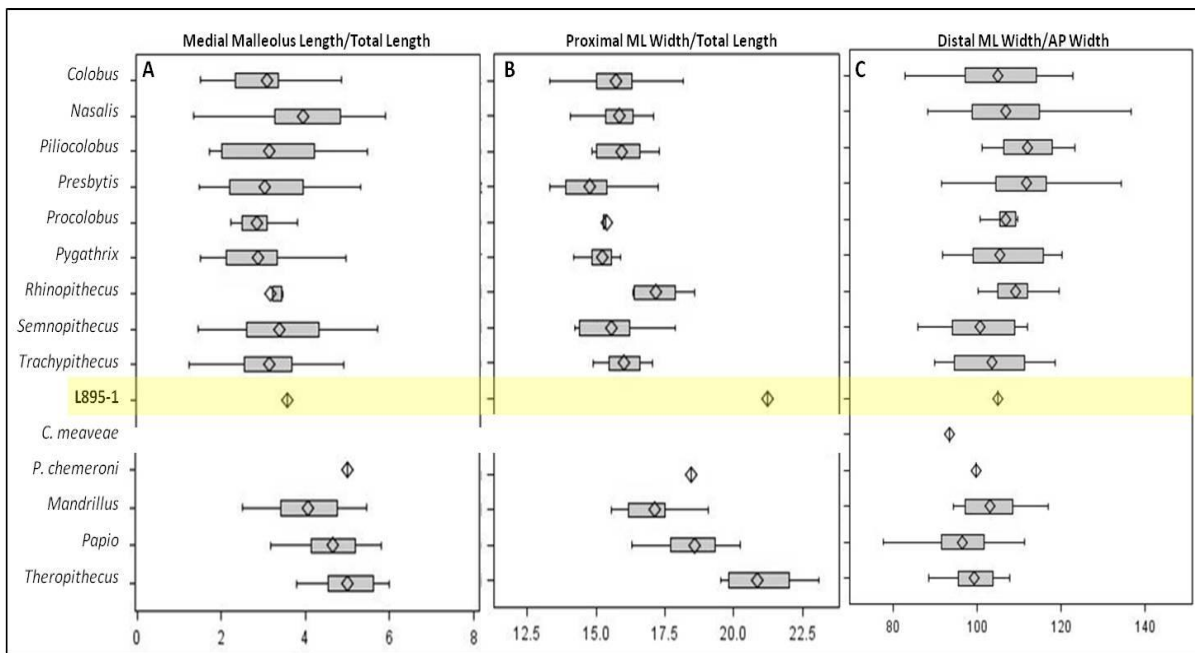


assessment but is slightly elevated relative to the medial condyle. The medial condyle, although damaged, is ovoid and appears to have been the larger of the two which matches the morphology seen on the distal femur. It is mildly concave but damage prevents much comparison. Just below the medial border is a small round depression for the *m. semitendinosus* which is deeper than *C. meaveae* perhaps indicating more of an emphasis on medial rotation, flexion, and extension in the hip and knee joint (MacLatchy et al., 2000). The tibial tuberosity is flatter than *C. meaveae* and similar in prominence to *R. turkanensis* and *P. chemeroni*. The tuberosity is wider at its most proximal extension than *P. chemeroni* and *T. oswaldi* and also shorter in its distal extension. On the dorsal surface just inferior to the lateral condyle is a weakly-defined *m. popliteus* insertion that is

similar in size to *P. chemeroni* and smaller than *Semnopithecus*. The film of matrix that still adheres to the specimen obscures the distal extension of this attachment, but its lack of prominence suggests less of an emphasis on stability in the knee joint as would be advantageous for rotation in vertical climbing (MacLatchy et al., 1988, 2000).

The diaphysis is compressed medio-laterally and has a triangular cross-section proximally becoming more ovoid as it continues distally. The shaft is short relative to the width of the proximal end and *P. chemeroni* (Figure 4.20b) and straight in anterior view

Figure 4.20 Box plots showing tibial indices **A.** medial malleolus length relative to total length **B.** width of the tibial plateau relative to total length and **C.** width of distal end relative to breadth.



although the posteriorly oriented position of the proximal end gives a slight ventral curvature in profile. L895-1 lacks the medial curvature seen in *P. chemeroni*, *T. oswaldi*, and extant cercopithecids such as *Trachypithecus*, *Semnopithecus*, and *Papio* (Figure 4.19).

The distal end and articular surface are better preserved on the left side specimen (L895-1d). The medial malleolus is prominent and its posterior border slopes supero-anteriorly giving the malleolus a markedly triangular shape in medial view. The malleolus is longer than *P. chemeroni*, *R. turkanensis*, and *T. oswaldi* (Figure 4.19). It is relatively straight and lacks the lateral curling seen in extant papionins. Although the malleolus is more prominent than *P. chemeroni*, it is proportionally more similar in prominence to large-bodied extant colobines including *Semnopithecus*, *Trachypithecus*, and *Nasalis* (Figure 4.20a). The malleolar groove is similarly narrow, but deeper compared to *P. chemeroni* and *C. meaveae* for the *m. tibialis posterior* tendon. This combined with the lack of angulation of the malleolus suggests less flexibility for inversion of the ankle as is seen in climbers and *T. gelada* due to its unique foraging behaviors (Maier, 1972; Krentz, 1993; Jablonksi and Leakey., 2008).

The talar facet would be square except for a projection on the ventro-lateral aspect. This is also seen, although less prominent, in *P. chemeroni* and *C. meaveae*, but is lacking in *R. turkanensis* and *T. oswaldi* (Figure 4.21). This is due to the relatively deep

Figure 4.21 Inferior view comparing the talar surface of the left distal tibia from (L-R) ♂ *Paracolobus chemeroni*, ♂ *Rhinocolobus turkanensis*, and ♂ *Theropithecus darti*. KNM-ER 1542U and AL 431-1O are from the right side and have been flipped for ease of comparison.



and distally oriented fibular facet on the lateral surface in L895-1 and *P. chemeroni* which is broader and less distinct in *R. turkanensis* and *T. oswaldi*. The center of the articular surface is mildly concave and is more medio-laterally compressed than *C. meaveae*, *R. turkanensis*, and other colobine tibiae known from the region. The concavity is more similar to the more terrestrial *P. chemeroni*, but the overall dimensions of the talar facet are more similar to *R. turkanensis* and arboreal extant colobines although they do overlap with *Mandrillus* (Figure 4.20c).

Astragalus: No Cat. No. (Rt. Side)

Preservation

The astragalus is too damaged to be fully reconstructed or measured. It is in three pieces which that have not been reconstructed (Figure 4.22). The fragments were located in a bag of unlabelled specimens and lack accession numbers. The largest fragment is the lateral facet which preserves the fibular facet and most of the tibio-talar articular surface. Most of the distal portion is broken off and there is a crack on the tibio-talar surface on the distal aspect. The plantar surface preserves about 3/4 of the posterior articular surface but the rest is damaged. The second fragment is the medial aspect of the trochlea which

Figure 4.22 Superior view of right astragalar fragments from L895-1



fits onto the other trochlear fragment. It preserves a small portion of the malleolar facet but the distal aspect is too damaged for the head/neck fragment to rearticulate. The final fragment preserves part of the neck and head. Damage to the trochlear fragments prevents re-articulation making its actual angle difficult to estimate. The medial aspect of the head has been sheared off and there is a piece missing from the superior aspect of the neck revealing the trabecular bone. What is left of the neck is distorted due to cracking.

Description

The trochlea appears to have been relatively wider than *P. mutiwa*, *P. chemeroni*, and *Theropithecus*, but damage prevents much functional comparison (Figure 4.23). The lateral margin of the articular surface is higher than the medial edge which is also

Figure 4.23 Superior view comparing astragali from (L-R) L895-1, ♂ *Paracolobus mutiwa*, ♂ *Paracolobus chemeroni*, ♂ *Rhinocolobus turkanensis*, and ♂ *Theropithecus brumpti*.



seen the more terrestrial fossil comparators, but the symmetry of the trochlea cannot be determined and the fibular facet is not well-preserved enough for analysis (Strasser, 1988). On the plantar surface the posterior articular facet shows mild concavity antero-posteriorly. The neck is thick, but the length cannot be determined. Due to its poor

preservation, I hesitate to make any functional assessments as it is impossible to tell how the fragments fit together in life.

Calcaneus: L895-2m (Lt. Side)

The calcaneus is large and robust with a thick calcaneal tuberosity, prominent sustentaculum tali, and what is preserved of the cuboid facet is only mildly concave compared to extant colobines such as *Nasalis*, *Pygathrix*, and *Presbytis* and although it is damaged, appears to have been wider than *P. mutiwa* (Figures 4.24-4.26). The anterior

Figure 4.24 Superior view of right calcaneus from L895-1m.



portion of the calcaneus containing the middle and anterior facet is shorter relative to the total length than most extant arboreal colobines. However, although significantly larger, L895-1 more superficially resembles the extant colobines than *Theropithecus* or extant cercopithecines primarily due to the prominent sustentaculum tali and the orientation of the posterior and middle talar facets (Figure 4.25).

Preservation

The left calcaneus preserves all of the talar facets and the plantar surface. There is a small depression fracture in the center of the most proximal portion of the calcaneal

tuberosity, but it is well-preserved enough to calculate total length. There are thin cracks on the lateral face and one on the most distal aspect of the posterior talar facet but both are superficial and do not distort the element's shape. The cuboid facet is missing its medial border and part of the medial articular surface making it impossible to estimate its original shape or width.

Description

L895-1 is slightly shorter than both *P. mutiwa* and *P. chemeroni* and overall more similar in robusticity to *P. chemeroni* although the latter has a much less prominent sustentaculum tali (Figure 4.25). The posterior facet is ovoid and fairly uniform in width proximo-distally without the distal widening seen in *P. chemeroni*, *Nasalis*, *Semnopithecus*, *Papio*, and *Mandrillus*. It is oriented laterally with its medio-lateral

Figure 4.25 Superior and plantar view comparing calcanei from (L-R) L895-1m, ♂ *Paracolobus mutiwa*, ♂ *Paracolobus chemeroni*, and ♀ *Theropithecus oswaldi*. Bottom: plantar view of same specimens.



midline at the same level as the root of the sustentaculum tali. The most posterior border blends into the superior surface of the calcaneal tuberosity which is a feature also seen in *P. mutiwa* whereas *P. chemeroni*, extant colobines, and cercopithecines tend to have a distinct lip. The medial margin is slightly raised but smooth and blunt at the lateral edge. Proportionally the posterior facet is typically cercopithecoid in being short relative to the total length of the calcaneus, but groups closer to *P. mutiwa* and *Theropithecus* when plotted against body mass (Figure 4.27; Szalay, 1975; Langdon, 1986; Strasser, 1988).

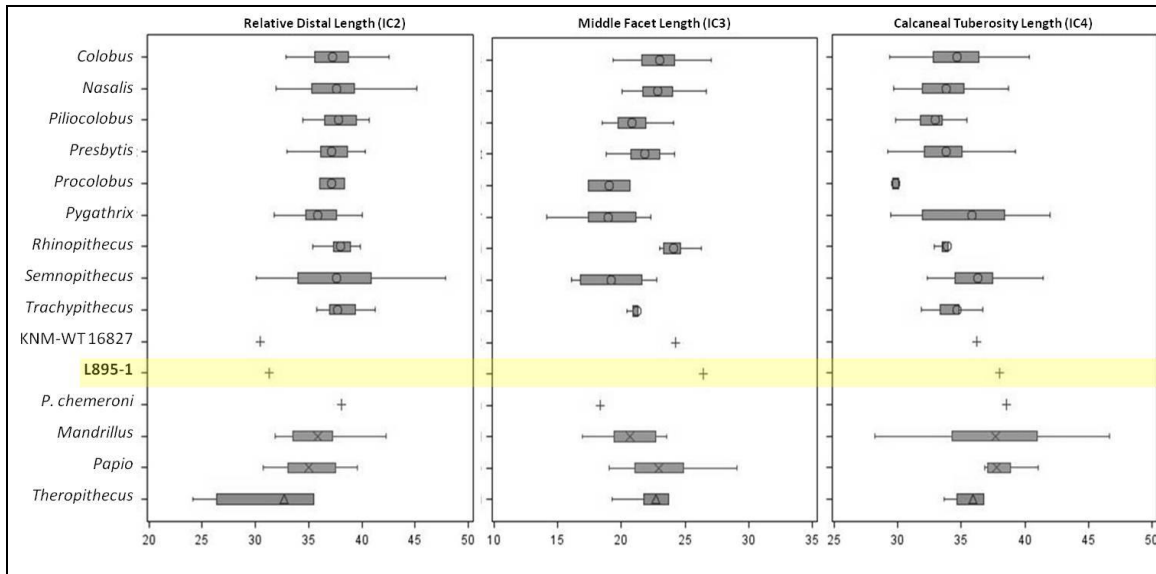
The middle facet is relatively long and ovoid contributing the medial projection of the sustentaculum tali (Figure 4.24). It is separated from the posterior facet by a wide groove which is larger than *P. mutiwa*, *P. chemeroni*, *T. brumpti*, and all extant colobines in the comparative sample except for *Semnopithecus*, but the latter has a much less prominent sustentaculum than L895-1 (Figure 4.25). The anterior facet is broken off but based on what is preserved of the distal portion, appears to have been separated from the middle facet. The depression for the anterior talocalcaneal ligament is very shallow. Immediately inferior to the posterior facet in lateral view is a blunt peroneal tubercle. This feature is not as prominent as *P. mutiwa*, but similar to *P. chemeroni*

Inferior to the posterior talar facet is the peroneal tubercle. In superior view it is in line with the lateral border; a morphology also seen in *P. mutiwa* and *P. chemeroni*, but not in *T. brumpti* where the peroneal tubercle is more laterally projecting (Figure 4.25). Despite its similar orientation, L895-1 is more prominent than *P. chemeroni* but less than *P. mutiwa*, *Colobus*, *Procolobus*, and *Nasalis* which have a very sharp and triangular shape. L895-1 by contrast is proximo-distally wide and the lack of development of the peroneal tubercle point to L895-1 having a less-developed *m peroneus longus* and *brevis*

suggesting less emphasis on plantar flexion in the foot as seen in more terrestrial or arboreal quadrupeds (Jolly, 1972; Jablonski, 2002; Jablonski et al., 2008). Posterior to the tubercle is a shallow groove for the calcaneo-fibular ligament which is shorter than either *P. mutiwa* or *P. chemeroni*. The groove fades as it moves toward the cuboid facet which is smooth and mildly concave, but damage to its medial aspect prevents a full shape analysis.

The calcaneal tuberosity is shorter and thicker than *P. mutiwa* but comparable to *P. chemeroni* although the latter has a wider proximal face (Figure 4.25). The sides of the tuberosity are asymmetrical with the medial side much more gradually sloping than the lateral which is steeper. The groove for the *m. flexor hallucis longus* tendon is barely discernible due to damage to the most proximal face. Relative to extant colobines L895-1 has a shorter calcaneal tuberosity putting it proportionally more in the range of *P. mutiwa*, *P. chemeroni* and cercopithecines such as *Mandrillus*, *Papio*, and *Theropithecus* (Figure 4.26c). In cercopithecids a long tuberosity is associated with strong *m. triceps surae* needed for increased leverage in plantarflexion movements found in leaping locomotor patterns and the shorter tuberosity seen in L895-1 is more similar to dimensions seen in terrestrial *P. chemeroni* and extant cercopithecines although it is close to *P. mutiwa*. (Figure 4.26c; Langdon, 1986; Strasser, 1988). The cuboid facet is mildly concave and the preserved portion is similar in depth to *P. mutiwa* and *P. chemeroni* although the medial articular surface is broken off making the original shape difficult to estimate. Although L895-1 had been suggested to be *P. mutiwa*, it is in the calcaneus that it most differs from the *P. mutiwa* specimen KNM-WT 1627. Although the two specimens do overlap in proportions more consistent with terrestriality, L895-1 more

Figure 4.26 Box plots showing calcaneal indices **A.** relative length of anterior articular surfaces **B.** Middle articular surface relative to total length and **C.** relative length of calcaneal tuberosity. *P. chemeroni* is represented by specimen KNM-BC 3.



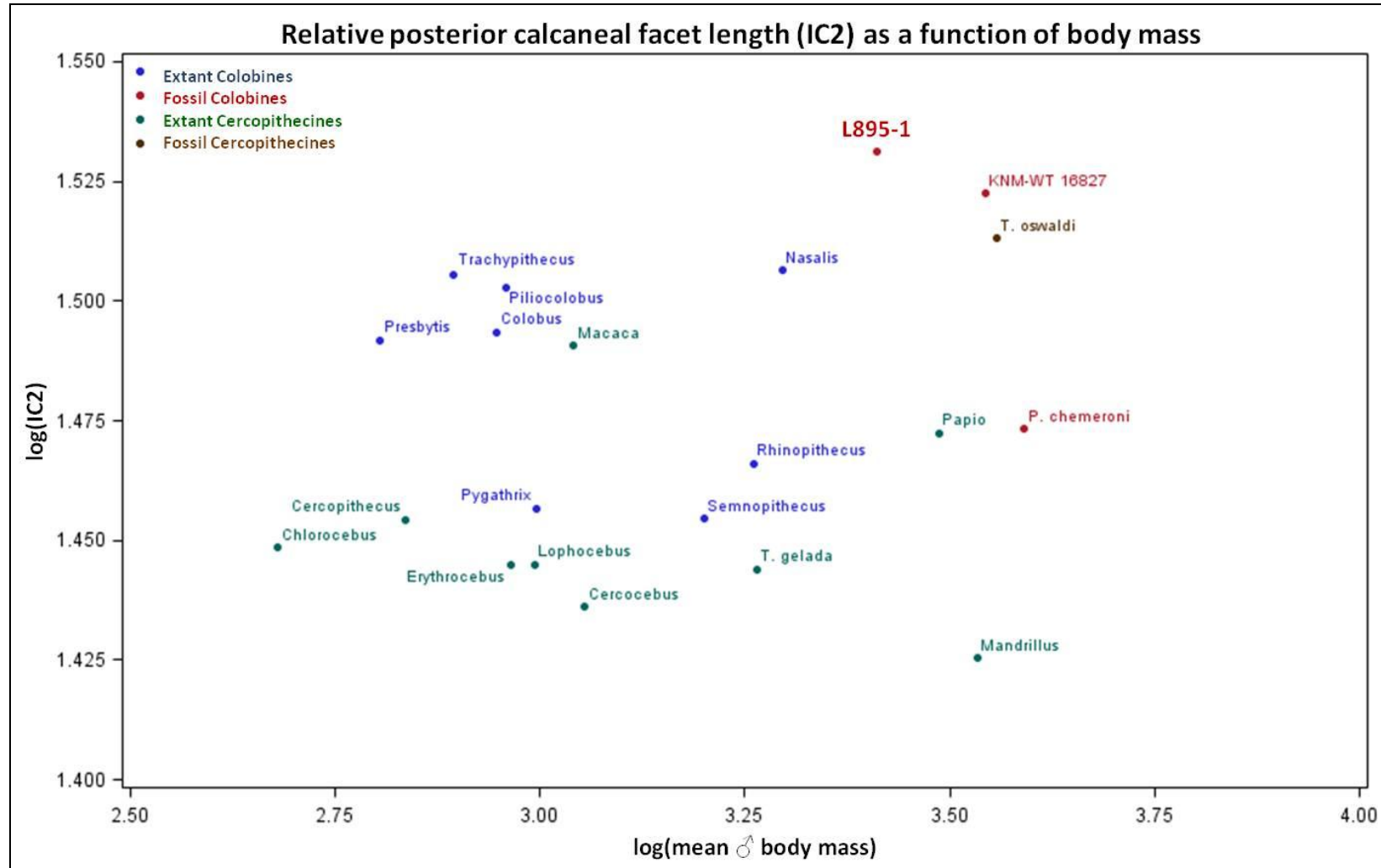
closely resembles *P. chemeroni* in qualitative shape as both share a wide calcaneal tuberosity, prominent sustentaculum tali, and wide cuboid facet (Figure 4.25). On the plantar surface L895-1 also lacks the distinctive “zig-zag” shape caused by a prominent peroneal tubercle as seen in *P. mutiwa*. Unfortunately, there are no calcanei identified from *C. williamsi* or *R. turkanensis* to compare it to, but based on its overall morphology, the calcaneus appears to be more terrestrial than any extant colobines.

Cuboid: L895-2n (Lt. Side)

Preservation

Only the left cuboid is preserved and like many of the smaller elements attributed to L895-1 has been given the ascension number of “L895-2.” It articulates perfectly with the calcaneus except for on its medial aspect as this corresponding region is broken on the calcaneus (Figure 4.28). The cuboid is complete except for a small piece that is

Figure 4.27 Scatter plot of relative posterior calcaneal facet length (IC2) and body mass. IC2 values are genus means and body mass values are genus means as reported in Table 4.3.



broken off from the antero-medial aspect and mild abrasions on the antero-lateral margin. There are also several light scratches on the facets for the MTIV and MTV that appear to be from preparation.

Figure 4.28 Superior and distal view of the left cuboid of L895-1n.



Description

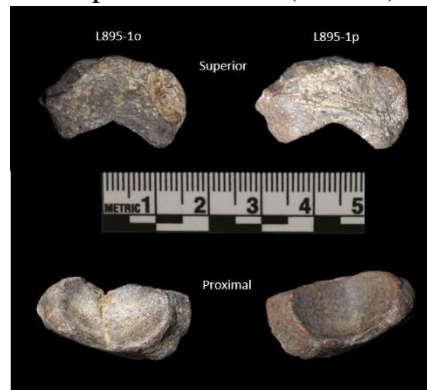
The calcaneal facet is shaped like a kidney bean and convex at its medial aspect corresponding to the concavity seen on the cuboid facet of the calcaneus (Figure 4.28). The lateral face is partially obscured by mild weathering, but most of the proximal aspect is taken up by the lateral lip of the groove for the peroneus longus tendon. The groove is ovoid with a sharp proximal border composed of the lateral aspect of the calcaneal facet. The medial surface is mildly convex with a slight proximal projection also seen in *P. chemeroni*. There is a small elliptical facet for the navicular articulation, but the distal aspect of the medial edge is too abraded to discern the articular surface for the middle cuneiform. The distal end has a weak vertical crest separating the articular facets for the MT IV and MT V. On the plantar surface is a mildly excavated fossa for the short plantar ligament attachment which begins just proximal to the peroneal groove. This contrasts with *P. chemeroni* which Birchette (1982) describes as deeply excavated.

Navicular: L895-2o (Rt. Side) and L895-1p (Lt. Side)

Preservation

The right navicular is cracked proximo-distally but has been repaired. There is a small piece missing from the inferior border of the talar facet that wraps around onto the plantar facet preventing the two halves from realigning perfectly. The left side is better preserved and complete except for mild abrasions on the superior surface and a small wedged-shaped piece missing from the distal portion of the lateral border (Figure 4.29).

Figure 4.29 Navicular bones L895-1o (Rt. side) and L895-1p (Lt. side). Superior (top) and proximal view (bottom).



Description

Description will focus on the left side (L895-2p) as it is better preserved. The proximal surface is convex for articulation with the talar head. The articular surface is ovoid with its longest axis running medio-laterally and takes up most of the proximal surface except for the most lateral aspect. On the distal end both of the facets for the cuneiforms are preserved. The lateral facet is the larger of the two and convex with a rounded articular surface for the lateral cuneiform and is weakly separated from the medial facet is smaller and similarly convex for articulation with the intermediate

cuneiform (Figure 4.29). The medial face has a small concave facet for the medial cuneiform at its distal aspect.

On the plantar surface the groove for the *m. flexor hallucis longus* is moderately excavated and similar in relative depth to extant colobines. On the medial aspect of the plantar surface is a small rectangular facet for the cuboid articulation. The antero-medial aspect of the distal face has a small tuberosity that is visible in superior view for the *m. tibialis posterior* and *dorsal cuneonavicular* ligaments. Unfortunately, it is damaged on both sides making comparison difficult. The navicular is much wider medio-laterally than proximo-distally which is a trait associated with more climbing behaviors in cercopithecines but is overall more similar in shape to the extant colobines (Gebo and Sargis, 1994; Nakatsukasa et al., 2010).

Middle cuneiform: L895-2t (Rt. side) and L895-2u (Lt. side)

Preservation

The right side (L895-2t) is complete and preserves all articular surfaces on its medial, lateral, proximal, and distal faces. The left side (L895-2u) is mostly complete except for a small piece missing from the lateral edge of its distal articular surface (Figure 4.30).

Description

The middle cuneiform has a smooth superior surface and two small facets on its medial face for articulation with the medial cuneiform. The larger facet is located on the superior aspect of the distal portion of the medial face while the second is significantly smaller and restricted to the most proximal corner on the inferior aspect (Figure 4.30). This contrasts with the morphology seen in extant cercopithecines where this second

Figure 4.30 Middle cuneiforms of L895-1 in superior (top) and medial view (bottom). Note the relatively small anterior facet in the medial view. This size discrepancy between the two medial facets is more typical of extant colobines than cercopithecines



articular surface takes up the whole proximal edge of the medial face.

MT I: L895-2f (Lt. Side)

Preservation

The left MT1 is well-preserved with only slight abrasion on the lateral aspect of the distal articular surface (Figure 4.31).

Description

Figure 4.31 Left side MT1 of L895-1t.



In anatomical position the plantar surface is slightly rotated infero-medially with the medial border inferiorly oriented similar to *P. chemeroni*. The diaphysis is compressed medio-laterally with sharply defined axial edges. The base is ovoid and weakly concave for articulation with the medial cuneiform. On the medial aspect of the base is a small tubercle for the insertion of the *m. abductor hallucis longus* and on the lateral border is a small tubercle for the dorsal tarso-metatarsal ligament. In plantar view the inferior border of the base extends to a point that is slightly laterally oriented. The head is robust with a round articular surface that extends onto the dorsal face. Except for its much larger size, the L895-2f resembles extant colobines in its overall shape.

Body Mass Estimates

The estimated mean body mass values (Est. Mean) reported in Table 4.3 are the mean values from all humeral and femoral indices preserved in L895-1 that were used to estimate body mass based on the regression parameters in Delson et al. (2000). All body mass estimates are based on the regression parameters in Delson et al. (2000). The fossil colobine and cercopithecine mean body masses, with the exception of the values for L895-1, are based on mean values based on dental and mass means (Mean) for male and female extant taxa in Table 4.3 were calculated from individual body weights of all representative specimens for each genus as reported in postcranial body estimates of relevant specimens. Delson et al. (2000) separates some taxa with wide geographic distribution, such as *C. williamsi*, by region. For fossil taxa where such estimates were reported, the values from specimens from East Africa or the Turkana Basin were used rather than values based off of specimens from South Africa. For *T. oswaldi* Delson et al. (2000) reports a Turkana Basin mean which is the value shown in Table 4.3. The estimated body mass values (Est. Mean) reported in this table

Table 4.3 Body mass estimates of comparative extant and fossil specimens. Known extant body mass means, published fossil body mass estimates. See Chapter II for metric descriptions. Tibia estimates are not sex specific so are reported separately from the other postcranial estimates.

Extant Colobines	Mean	♂ Mean	♀ Mean	Est. Mean	Est. ♂ Mean	Est. ♀ Mean	Tibia Mean
<i>Colobus</i>	8.5	8.8	8.2	9.8	10.5	7.5	11.4
<i>Nasalis</i>	14.7	19.8	9.6	15	18.6	9.7	16.6
<i>Ptilocolobus</i>	8	9.1	6.8	13.9	25.1	6.9	9.7
<i>Presbytis</i>	6.3	6.4	6.2	7.6	8.4	6.9	7.5
<i>Procolobus</i>	4.4	4.6	4.2	6.3	7.7	5.4	5.9
<i>Pygathrix</i>	9.7	9.9	9.5	8.1	4.1	8.2	12
<i>Rhinopithecus</i>	15.3	18.2	12.3	12.4	11.7	10	15.6
<i>Semnopithecus</i>	13.6	15.9	11.4	11.7	14.6	8.8	11.8
<i>Simias</i>	8	9.1	6.9
<i>Trachypithecus</i>	7.3	7.8	6.8	7.4	7.7	6.7	7.8
Fossil Colobines							
<i>Cercopithecoides kimeui</i>	38	51	25
<i>C. meaveae</i>	21	21	.	22.6	.	.	22.6
<i>C. williamsi</i>	21.5	27	16	19.7	19.7	.	.
<i>Paracolobus mutiwa</i>	31	35	27	33.8	33.8	.	.
L895-1	25.1	25.8	.	25.1	25.8	.	24.3
<i>P. chemeroni</i>	39	39	.	39.9	37.9	.	41.8
<i>Rhinocolobus</i>	24	31	17	27.9	.	.	27.9
Extant Cercopithecines							
<i>Cercocebus</i>	10.1	11.3	8.9	10	13	7	.
<i>Cercopithecus</i>	5.6	6.9	4.4	5.8	7.4	4.3	.
<i>Chlorocebus</i>	4.5	4.8	4.3	4.6	5.5	3.6	.
<i>Erythrocebus</i>	9	9.2	8.7	10.5	15.3	5.6	.
<i>Lophocebus</i>	8.2	9.8	6.6	8.5	10.5	6.5	.
<i>Macaca</i>	8.2	11	5.3	8.3	11.2	5.4	.
<i>Mandrillus</i>	23.3	34.2	12.3	24.2	34.8	13.5	.
<i>Miopithecus</i>	2.5	2.5	.	1.9	1.9	.	.
<i>Papio</i>	22.7	30.7	14.8	25.9	40.8	15	22.1
<i>T. gelada</i>	15.1	18.4	11.9	12.8	15.2	10.3	.
Fossil Cercopithecines							
<i>T. brumpti</i>	30	36	24	19.4	13	.	25.8
<i>T. oswaldi</i>	31	36	26	53.2	84.3	41	34.1

are the values resulting from using the postcranial metrics reported in Chapter II. These values are reported so that they can be compared to the values based on the known

weights of the extant taxa and the fossil estimates derived from more complete skeletal assemblages.

Humerus

Two humeral metrics were used to estimate body mass: humeral length excluding the capitulum (H2) and the medio-lateral width of the diaphysis at midshaft (H11). The estimates based on these metrics yielded body masses of 26 kg and 29 kg respectively with a mean estimate of 28 kg. This is slightly smaller than the body mass estimate for *P. mutiwa* of 35 kg although the latter also includes estimates made using craniodental parameters. This estimate is also within the range of humeral estimates for *C. kimeui*, larger than *C. williamsi*, and smaller than *P. chemeroni* (Table 4.3; Delson et al., 2000).

Femur

Body mass estimates were made based on three femoral metrics: the length from head to medial condyle (F2), the antero-posterior diameter at midshaft (F8), and the medio-lateral diameter at midshaft (F9). The body mass estimates from these metrics were 15 kg., 36 kg., and 23 kg. respectively for a mean femoral mass estimate of 24 kg. All of these are lower than *P. mutiwa* although the latter lacks a distal end so only metrics F8 and F9 were able to be used. Based on its femoral estimates, L895-1 is also larger than *C. williamsi* and smaller than *P. chemeroni*. *P. chemeroni*, *C. meaveae*, and *R. turkanensis* have associated tibiae with the preserved features for this estimate and came out as 42 kg, 23kg, and 28 kg respectively (Table 4.3). It is worth noting that *P. chemeroni* has a much larger distal end than L895-1 despite the latter being more robust in its proximal tibial morphology (Figure 4.19) which likely explains the relatively large estimate based on this metric. The estimate generated for the extant taxa were fairly close

to measured genus means although the extant cercopithecine specimens with body mass estimates larger than L895-1, the mean estimate of 24 kg is larger than any extant colobine genera (Table 4.3).

Tibia

Unlike the other postcranial estimates, the regression parameters for tibial estimation do not distinguish between male and female or colobine and cercopithecine taxa so are reported separate from the humeral and femoral based estimates (Ruff et al., 2002, 2003). The body mass estimates for L895-1 based on the proximal tibia width and distal area were nearly identical at about 24.4 kg each. This is slightly smaller than the estimates from the humerus and within the range of those based on the femur. Only *P. chemeroni* shows a tibial body mass estimate greater than that based on more complete parameters. This could be due to the representative specimen having relatively long and gracile long bones compared to the other fossil taxa.

Discussion

Sex Estimation

Despite its lack of associated cranial remains, L895-1 is one of the most complete partial cercopithecoid skeletons known from the Plio-Pleistocene. The preserved elements indicate it is a large, robust monkey possessing some morphology more consistent with terrestrial locomotion than extant colobines, and most probably *R. turkanaensis*; particularly in its ulna, radius, femur, tibia, and calcaneus and from both *T. oswaldi* and *T. brumpti*. Many of the fossil specimens well-preserved enough for comparison are from males based on canine morphology and the lack of associated dentition for L895-1 makes a sex estimation difficult as the level of sexual dimorphism in the postcrania can vary

intragenerically and across individuals of the same species. The tentative classification of this specimen as *P. mutiwa* allows for some comparison with the known male specimen KNM-WT 16827, to which it is similar in size. Furthermore, body mass estimates derived from dentition suggest females of *P. mutiwa* were smaller than L895-1, suggesting L895-1 was most probably male.

Functional Morphology

Although the humeral head is fragmentary, the size of the greater tubercle is more consistent with terrestriality and more similar in prominence to *C. meaveae* than *R. turkanensis* or extant arboreal colobines. Most of the insertions for the shoulder girdle are not preserved, but the strong deltoid tuberosity is also distinct from extant colobines and suggests well-developed *m. deltoideus*, *m. triceps brachii*, and *m. subscapularis* for adduction, rotation, and flexion at the shoulder (Ashton and Oxnard, 1964; Larson, 1993; Gebo and Sargis, 1994; Jablonski et al., 2008). The deltoid tuberosity is also longer than is typical for terrestrial cercopithecids, and although it is slightly shorter than *P. mutiwa*, the presence of the longitudinal groove shared with *P. chemeroni*, *C. williamsi*, and *Theropithecus* also suggests a strong *m. deltoideus*, but a lack of preserved features prevents further shoulder analysis.

Although the distal humerus preserves only the articular surface, the presence of both the proximal ulna and radius on the right side allows for a better functional assessment. The elbow displays several features more consistent with terrestrial locomotion but is still distinct in morphology from the cercopithecines. Despite the olecranon fossa not being preserved, the deep trochlear notch and projecting coronoid process on the proximal ulna are associated with stability during prolonged flexion in the

elbow joint and is similar to the terrestrial morphology seen in *P. mutiwa*, *P. chemeroni*, and *C. williamsi* (Figure 4.6; Jolly, 1972; Delson, 1973; Birchette, 1982; Rose, 1988; Harrison, 1989). Interestingly the *m. brachialis* insertion on the proximal ulna is more defined than its relatively weak origin on the humerus might suggest, although this could in part be due to the better preservation of this feature in L895-1 compared to *P. mutiwa*, *P. chemeroni*, and *C. meaveae*. In contrast to this, the supinator crest is weak on the ulna and although its humeral insertion is not preserved and is not as defined as in more arboreal taxa (Figure 4.11). L895-1 has a radial tuberosity similar in size to *P. mutiwa* suggesting well-developed *m. biceps brachii* as does the insertion for this muscle on the olecranon process of the ulna which is more similar to terrestrial taxa. For many features of the elbow L895-1 overlaps in its functionally relevant humeral and radial indices with large-bodied extant colobines known to display occasional semi-terrestrial behavior such as *Semnopithecus* (Figures 4.6C, 4.13; Harrison, 1989; Osterholtz et al., 2008; Ting et al., 2008; Jablonski and Frost, 2010). However, proportionally L895-1 has forelimbs that are more similar to the terrestrial *P. mutiwa* and *C. williamsi* in being short and robust compared to the longer limbs typical of extant arboreal taxa and *P. chemeroni* (Figures 4.5, 4.9). Although it varies in several features, the forearm more resembles that of the terrestrial species *P. mutiwa* and *C. williamsi* in its proportions than it does *P. chemeroni*, arboreal colobines, or terrestrial cercopithecines. It is also not particularly similar to *C. kimeui* in any shared elbow joint features and the difference between L895-1 and the admittedly small *C. kimeui* sample, is greater than seen intragenerically for most taxa in the comparative sample (Figures 4.7, 4.14).

Like the forearm, the hindlimb displays an intriguing mix of traits associated with terrestrial and arboreal locomotion. Although there are no associated pelvic bones, the proximal femur is well-preserved allowing for comparative analysis of at least part of the hips joint. The long femoral neck, low femoral neck-shaft angle, and prominent greater trochanter are more consistent with terrestrial modes of locomotion and more similar to terrestrial colobines such as *C. williamsi* and *P. mutiwa* than to the extant arboreal climbers or leapers (Figure 16A, 16B). The morphology of the greater trochanter is also more similar to that seen in the large-bodied terrestrial colobines than it is to that of terrestrial cercopithecines (Figure 15). Other features more similar to terrestrial taxa include the rugose *m gluteus minimus*, *quadratus femoris*, and *obturator externus* attachments which are associated with abduction and lateral rotation of the hip (Stern and Larson, 1993; Jablonski et al., 2008). Features in which L895-1 is more similar to arboreal colobines are mostly limited to the femoral head which has a laterally extended articular surface on its superior aspect and is relatively wide compared to the height of the greater trochanter. However, although this latter feature is more extreme in the arboreal extant colobines, some more terrestrial taxa including *C. williamsi*, *P. chemeroni*, and *Mandrillus* also fall in the upper range of this index so could be more indicative of a smaller sample size than a strong functional signal (Figure 16B). Overall, L895-1 has a proximal femur that is most qualitatively similar to that of *P. mutiwa* and falls within the range of terrestrial and semiterrestrial taxa for its quantitative features.

Although the diaphysis of the femur is damaged, the distal end and proximal tibia are preserved enough for an analysis of the knee joint. Unfortunately, *P. mutiwa* does not preserve its knee, but fossil comparators from *P. chemeroni*, *C. meaveae*, *R. turkanensis*,

and *Theropithecus* are available. As with the forelimb, the hindlimbs are shorter and more robust than that of *P. chemeroni* and extant colobines (Figure 18). The femoral condylar index is closer to terrestrial cercopithecines such as *Papio* and *Mandrillus* but does fall in the lower range for *Nasalis* although the latter has a wider range of variation than the papionins (Figure 16C). Although the functional significance of the *m. popliteus* attachment on the femur is not well understood, its size when considered with its weak insertion on the tibial tuberosity may suggest less of an emphasis on stability of the knee joint as is seen in vertical climbers (MacLatchy et al., 1988, 2000). The condyles of the femur, although differing in height, lack the asymmetry seen in arboreal taxa. A larger relative medial condyle is associated with increased medial load bearing in some hominoids, but a larger lateral condyle is the more typical pattern seen in both terrestrial colobines such as *P. chemeroni*, *C. williamsi*, and *C. meaveae* and arboreal extant taxa (Figure 16C; Jungers, 1988). The depth of the patellar fossae are also more consistent with stability, but not to the extreme seen in extant colobines with leaping locomotor patterns. Based on the knee joint, L895-1 is distinct from extant and fossil cercopithecines, *R. turkanensis*, *P. chemeroni*, and *C. williamsi*.

Unfortunately, there are not many preserved colobine tibiae in the fossil record for comparison other than *P. chemeroni* and the astragalus from L895-1 is highly fragmentary. The distal tibia is distinct in its articular surface proportions from *P. chemeroni* and *C. meaveae* (Figure 4.20c) although it does fall within the range of extant colobines in its medial malleolus length (Figure 4.20a). Although longer, the shape of the malleolus is however more similar to colobines and lacks the lateral curling at its apex seen in papionins. When combined with the higher lateral margin of the trochlear surface

on the astragalus, this suggests more of an emphasis on stability at the ankle joint than is seen in arboreal climbers (Maier, 1972; Krentz, 1993; Jablonksi and Leakey, 2008).

The calcaneus also plots separate from semi-terrestrial colobines like *Semnopithecus* and is distinct from extant arboreal cercopithecines (Figure 4.26). Interestingly, *P. chemeroni* plots closer to the extant colobines in the index and is separated by its larger size. This is also reflected in its long bones which, although showing morphologies consistent with semi-terrestriality, are proportionally still more similar to the extant colobines than the Plio-Pleistocene fossil taxa. L895-1 is most similar to *P. mutiwa* in this metric although the two do differ in their estimated body masses. In the index comparing the posterior articular facet to length, L895-1 and *P. mutiwa* are both distinct from the extant colobines even when their body mass is taken into consideration (Figure 4.26). In cercopithecids, a longer posterior facet is associated with more mobility at the lower ankle in arboreal climbers while a shorter facet is more associated with more terrestriality. This longer posterior facet is more typically seen in the extant colobines and separates them from the extant cercopithecines when body mass is taken into consideration (Langdon, 1986; Strasser, 1988). This combined with the relatively shorter calcaneal tuberosity (Figure 4.25a) and square distal tibial shape are more consistent with terrestrial locomotion and the colobine morphology. It is interesting to note, however, that both L895-1 and *P. mutiwa* are distinct from *P. chemeroni* as well as from the extant colobines. In calcaneal shape, despite their superficial differences, these two specimens appear more similar to one another than either is to *P. chemeroni* (Figures 4.25-26). The cuboid, navicular, and middle cuneiform are typically cercopithecoid in shape, but the navicular and middle cuneiform more closely resemble

extant colobines (Strasser, 1988; Gebo and Sargin, 1994; Nakatsukasa et al., 2010). The MT1, although large compared to extant colobines, is also similar in shape to the extant colobine taxa in the comparative sample. There are also unfortunately few well-preserved metatarsals attributed to any of the fossil colobines to compare it to.

Body Mass Estimates

The body mass estimates of L895-1 show it to be slightly smaller than *P. mutiwa* as well both *C. kimeui* and *P. chemeroni* (Figures 4.31, Table 4.3.6). The humerus, femur, and tibia are all complete enough to be used in the postcranial body mass estimates as described by Delson et al. (2000) and Ruff et al. (2002, 2003). The mean body mass for L895-1 estimated based on these parameters about 25 kg. (Table 4.3.3). Craniodental estimates of body mass are available for *P. mutiwa*, *P. chemeroni*, and *C. willamsi* so the estimates reported here may not perfectly match published estimates based on more complete metrics with more included specimens. For example, KNM-WT 16827 is estimated to be about 34 kg. based on its humeral and femoral estimates which is close to the 35 kg estimate resulting from all available elements (Ward, 1991; Ting, 2001). The estimate of 40 kg for *P. chemeroni* is very close to that derived from more complete metrics; perhaps due to this species having relatively long and gracile limbs more similar to the extant colobines than L895-1 and *P. mutiwa* which are shorter and more robust (Table 4.3; Birchette, 1982; Ward, 1991; Delson et al., 2000). As the regressions for body estimation are derived from extant taxa of known weight, the fact that *P. chemeroni* is more similarly proportioned to the extant colobines may have an effect. It is therefore entirely possible that L895-1 was larger than these postcranial estimates show. However precise this estimate is, it is clear that L895-1 is a large monkey

well outside the ranges of extant large-bodied colobines such as *Nasalis*, *Rhinopithecus*, and *Semnopithecus* and larger than most extant cercopithecines with the exceptions of male *Mandrillus* and *Papio* (Table 4.3). The mass estimate difference between L895-1 and *P. mutiwa* falls within the range seen in some extant male colobines so could represent individual variation rather than taxonomic differences between the two.

Taxonomic Status

L895-1 is distinct in its postcranial morphology from most of the other Plio-Pleistocene colobines known from the Turkana Basin including *C. kimeui*, *C. williamsi*, and *R. turkanensis* (Jablonski et al., 2008; Gilbert, 2013). It is also distinct from *Theropithecus* and although no postcrania attributed to *Soromandrillus* have yet been described, the morphology of the long bones and tarsals is more similar to other colobines and the morphology of the proximal ulnae, femur, and middle cuneiform show features more typical of colobines than cercopithecines. Although L895-1 does differ from *P. mutiwa* in some features of the distal humerus (Figure 4.6b, c) and proximal femur (Figure 4.16b), they are consistently more similar to each other than to the other fossil colobines in the comparative sample. Unfortunately, many of the elements in which L895-1 shows differences from other colobine and cercopithecine taxa cannot be compared to *P. mutiwa* due the latter having fewer associated elements and fewer long bones complete enough for any indices requiring lengths. L895-1 is more qualitatively and quantitatively similar to *P. mutiwa*, attributed to the species *P. mutiwa*, than it is to the other large Plio-Pleistocene cercopithecids. Unfortunately, a secure taxonomic designation is difficult without craniodental remains. If L895-1 is the same species as *P.*

mutiwa, the two specimens are separated in age by about 500ka so their morphological differences could be explained by temporal variation.

Whatever its taxonomic affiliation, L895-1 is a large-bodied, semi-terrestrial/terrestrial, colobine monkey. Not only is it the most complete colobine specimen known from the Plio-Pleistocene, but it reinforces the level of locomotor diversity seen in these fossil colobines as being very different than their extant counterparts. The level of sympatry seen among these fossil cercopithecids is unique from the environments their descendents inhabit today suggesting further supporting how niche separation in such realms as diet and substrate preference have played an important role in cercopithecoid evolution (Elton, 2006). Although L895-1 does appear to be a large at least semi-terrestrial monkey, its unique ankle morphology (Figure 4.20b, 4.26, 4.27) suggests it is doing something different from other terrestrial taxa like *C. williamsi* and *Theropithecus*. Based on its postcranial morphology, L895-1 is distinct from contemporaneous colobine and cercopithecine taxa and, whether or not the two are the same species, most closely resembles *P. mutiwa*.

CHAPTER V

NICHE SEPARATION AMONG THE LARGE-BODIED COLOBINAE OF THE TURKANA BASIN

Background

Sympatry of multiple large-bodied primates, including hominins, in the fossil record suggests that niche-partitioning has played an important role in both cercopithecoid and human evolution (Elton, 2006). This idea is used to explain the shared occupation of similar ecological zones by multiple, sometimes closely related, taxa that exploit different food sources and/or substrates. The more closely-related these sympatric species, the more competition for resources predicted. In many sympatric primates, niches can overlap not only among species, but also among higher taxa such as the subfamilies colobinae and cercopithecinae (Reed and Bidner, 2004). However, ecological overlap alone is not necessarily evidence for competition. Richer habitats like the tropical forests inhabited by many primates, have more ecological niches and therefore increased species diversity (Ganzhorn, 1989; Fleagle and Reed, 1996; Reed and Bidner, 2004). This idea has also been applied to examine the apparent greater degree of ecological overlap between fossil species compared to extant forms (Cerling et al., 2015). One example of this approach in extant Platyrrhines proposed that changes to the rainforest micro-habitats and river courses over time led to much of the extant species differentiation (Rosenberger, 1992). An example of this in extant colobines is seen with *Piliocolobus* and *Colobus*, which overlap in their ecological zones with multiple mammalian and avian predators including humans (Reed and Bidner, 2004). Niche-partitioning has also driven the evolution of interspecific variation particularly in body size among guenons (Cardini and Elton, 2008).

It is also important to consider factors competitive pressures of other mammalian species and how they may be affecting the exploitation of certain environments and dietary preferences by primates (Feibel et al., 1991; Behrensmeyer et al., 1997; Hakala, 2012; Cerling et al., 2015; Martin et al., 2018). This niche differentiation is thought to have played a role in the decrease in colobine diversity that occurred in the Plio-Pleistocene. Many terrestrial habitats previously exploited by large-bodied colobines became dominated by other mammals such as alcelaphine bovids (Jablonski, 2002). Some hypothesize that colobines were limited in range expansion by their morphology leading to the extinction of terrestrial colobines in Africa seen today (Jablonski and Leakey, 2008).

The specimens described in Chapters III and IV add to the known diversity of fossil colobines by adding *Paracolobus mutiwa* to the known sample of colobine postcranial elements. Chapter II describes the large-bodied colobine specimen KNM-WT 16827, which is attributed to the species *Paracolobus mutiwa* (even if *P. mutiwa* may warrant generic distinction). *P. mutiwa* is known from cranial and dental specimens at many sites in Turkana Basin including West Turkana, Koobi Fora, and Omo between approximately 2.6 and 1.9 Ma (Leakey, 1982; 1987; Jablonski et al., 2008; MacDougal et al., 2012; Kidane et al., 2014). KNM-Wt 16827 itself is dated to between 2.58 and 2.53 Ma (Harris et al., 1988; MacDougal et al., 2012). The specimen described in Chapter IV, L895-1, lacks associated cranial material making taxonomic allocation difficult, but is most similar to *P. mutiwa* among contemporary cercopithecids. Based on its position within Upper Member G of the Shungura Formation this specimen is fairly securely dated to approximately 2.05 – 2.07 Ma (DeHeinzelin, 1983; Kidane et al., 2007), within

the known range of *Paracolobus mutiwa* although it is younger than the KNM-WT 16827.

The diversity of primates seen in the Turkana Basin during the Plio-Pleistocene includes at least four large-bodied fossil colobine taxa: *Cercopithecoides kimeui*, *C. williamsi*, *Paracolobus mutiwa*, and *Rhinocolobus turkanensis*; three large-bodied cercopithecines: *Theropithecus brumpti*, *T. oswaldi*, and *Soromandrillus quadratiostris*; and up to four hominin species which may be evidence of niche partitioning at this site (Iwamoto, 1982; Eck and Jablonski, 1984; Leakey, 1987; Frost, 2001 diss; Elton, 2006; Jablonski and Leakey, 2008; Leakey et al., 2012; Gilbert, 2013; Anderson, 2018, 2019). All of these cercopithecoid taxa except for *Soromandrillus quadratiostris* are represented by specimens with associated postcrania which show a greater diversity of locomotor adaptations than is seen in East Africa today.

The primary objective of this chapter is to incorporate the functional morphology, taxonomic diversity, and body mass estimates from Chapters IV and V to explore areas in which these large-bodied Cercopithecidae may overlap in such niche categories as body mass, time spent on the ground, and diet. This is difficult to do with extinct species as proxies are limited by sample size, preservation, and sites sampled. Many of the species in this study are known from multiple sites within the Turkana Basin, for example, but not all specimens with available postcranial elements come from the same localities or from localities of the same age. Dietary proxies such as carbon isotopes from dental enamel and molar microwear in particular can be difficult as they may only capture the dietary information of a very restricted period of time (months or even days) for a particular population while proxies such as molar morphology may reflect the results of

longer term adaptation (Benefit, 1987, 1989; Ungar et al., 2011; Cerling et al., 2013; Levin et al., 2013, 2015). Many of the colobine taxa highlighted here have no modern analogs complicating estimates of substrate preference. Many of the taxa known from the Turkana Basin including *C. kimeui*, *C. williamsi*, and *P. mutiwa* show functional morphology consistent with a greater degree of terrestriality than is seen in the modern colobines. Although there are qualitative and quantitative metrics that are useful for estimating such adaptations, the reliance of comparison with contemporary and extant terrestrial taxa, many of which are cercopithecines, is limiting and no doubt important functional information is missed due to this lack of modern analogs.

This chapter, therefore, will not examine the niche separation present at each relevant site, but instead will examine the broader region in which these large-bodied monkeys may have been exploiting. By necessity, many of the specimens with associated postcranial elements discussed here come from different sites within the Turkana Basin, but are nonetheless used as exemplars for their species. Thus, the results presented are with full understanding that there is likely a great deal of ecological nuance that is not being captured. These three variables, size, diet, and locomotion/substrate preference are among the most important in primate ecology, at least of those available for fossils. Therefore, they should provide the most complete picture of broad patterns of niche separation among these taxa available, and perhaps help to clarify the conditions that allowed for the extreme degree of overlap within the Turkana Basin.

Materials and Methods

Estimates of Terrestriality for Extant Cercopithecidae

Here the functional morphological analyses will be used to estimate substrate

preferences and synthesized with body mass and dietary estimates based on molar morphology to examine ecological overlap among the fossil colobines and sympatric cercopithecine species. This will be done by incorporating my body size estimates as well as those from published sources (Delson, 2000; Ruff et al., 2003), dietary data based dental morphology (Benefit, 1987, 1999), and observational data about substrate preference among extant (Dunbar and Dunbar, 1974; Rodman, 1979; Rose, 1979; Norris, 1988; Nakagawa, 1989; Thomas, 1991; McGraw, 1998; Moermond, 2000; Ren et al., 2001; Li, 2007; Janmaat and Chancellor, 2010; Cooke, 2012; Gosselin-Ildari, 2013; Rowe and Myers, 2013). Many of the taxa included in the comparative extant dataset have been studied behaviorally in the wild and have estimates for substrate preference and percentage of time spent on the ground. Of the extant taxa included in the comparative sample, 17 had published data available including 11 cercopithecine and 6 colobine taxa. Where possible, the minimum, maximum, and mean observed time spent on the ground were recorded (Table 5.1). As demonstrated in Chapters 3 and 4, sixteen postcranial indices can be used to distinguish more arboreal from more terrestrial taxa at least on average. These indices are used here to quantify the substrate preferences of the fossil taxa (Table 2.2). The mean of each index was calculated for each taxon represented in the extant data set and transformed by its natural logarithm. To determine the indices most correlated with terrestriality, logged taxon means indices were regressed on the observed percent time on the ground. Indices with $p < .05$ were used in the relative terrestriality estimates for the fossil taxa (Table 5.2). It is important to note that although the observed ground use data is weighted more heavily towards arboreal cercopithecids, and most of the terrestrial species are cercopithecines, semi-terrestrial colobines such as

Table 5.1 Data on observed terrestriality of extant Cercopithecidae used in the regression for estimating relationships with relevant postcranial indices.

Taxon	Ground Min	Ground Max	Ground Mean	Citation
<i>Cercocebus torquatus</i>	.	.	39.4	Cooke, 2012
<i>Cercopithecus mitis</i>	2	5	3.5	Thomas, 1991; Kaplan and Moermond, 2000
<i>Cercopithecus neglectus</i>	15	20	17.5	Rowe and Myers, 2013
<i>Chlorocebus aethiops</i>	19.4	43.4	31.4	Dunbar and Dunbar, 1974
<i>Colobus guereza</i>	.	.	4.4	Rose, 1979
<i>Erythrocebus patas</i>	59.6	90.5	75.05	Nakagawa, 1989
<i>Lophocebus albigena</i>	1	8	4.5	Janmaat and Chancellor, 2010
<i>Macaca fascicularis</i>	2	10	6	Rodman, 1979
<i>Macaca thibetana</i>	.	.	0.47	Gosselin-Ildari, 2013
<i>Mandrillus sphinx</i>	.	.	80	Norris, 1988
<i>Papio anubis</i>	.	.	72.1	Gosselin-Ildari, 2013
<i>Ptilocolobus badius</i>	.	.	1	McGraw, 1998
<i>Ptilocolobus kirkii</i>	.	.	2	Rowe and Myers, 2013
<i>Pygathrix nemaeus</i>	.	.	0	Rowe and Myers, 2013
<i>Rhinopithecus roxellana</i>	2.9	15.3	9.1	Ren et al., 2001; Li, 2007
<i>Semnopithecus entellus</i>	15.7	34	24.85	Gosselin-Ildari, 2013
<i>Theropithecus gelada</i>	.	.	98.4	Dunbar and Dunbar, 1974

Rhinopithecus roxellana and *Semnopithecus entellus* are included allowing for some variability within colobines (Ren et al., 2001; Li, 2007; Gosselin-Ildari, 2013).

Estimates of Terrestriality for Fossil Cercopithecidae

Of the 16 indices found to differentiate arboreal from terrestrial forms in Chapters III and IV, 6 were determined to be significantly correlated with the observed behavioral data and had a $R^2 < 0.3$ when regressed against known male body mass (Figures 5.1, 5.2; Table 5.4). The y-intercept and slope resulting from each of these regressions was used to estimate the percentage of time on the ground for each fossil taxon. Due to variability in preservation, not all indices were able to be used for each fossil taxon (Appendix B). The minimum and maximum estimates and their midpoint were used in the bivariate plots to

Table 5.2 Male body mass range estimates used in the niche separation plots. KNM-WT 16827 estimates are being used to represent *P. mutiwa* as it is the only specimen of this taxon to be included in the postcranial estimates of ground use.

Taxon	♂ Body Mass Min	♂ Body Mass Max	♂ Body Mass Midpoint
<i>Cercopithecoides kimeui</i>	41	61	51
<i>C. williamsi</i>	20	34	27
<i>Paracolobus mutiwa</i>	29	42	35
L895-1	24	28	26
<i>Rhinocolobus turkanensis</i>	23	39	31
<i>Theropithecus brumpti</i>	39	60	45.5
<i>T. oswaldi</i>	36	49	42.5

capture the ranges of the various estimates for each taxon. Male body mass estimates from Delson et al., (2000), Ruff et al. (2003), and Chapter IV (Table 4.5) were used in the niche separation analyses as most of the postcranial specimens included are from male individuals. The midpoints of these estimates were calculated for use in the visualization plots (Table 5.6).

Dietary Estimates

Diet is difficult to estimate in fossil taxa, requiring the use of proxies such as enamel carbonate isotopic ratios, dental microwear analysis, and relative cusp height in assessing the diets of extinct species. Carbon and oxygen isotopic data from fossil dentition has been used as a dietary proxy to examine broad patterns of site-specific diet (e.g. Cerling et al., 2015; Levin et al., 2015). However, neither carbon isotopic nor microwear data are available for all, or even most, of the species included here. The dietary estimates used here are taken from Benefit (1987, 1999) and based on regressions of molar morphology including relative cusp height, relatively cusp width, and shear-

Table 5.3 Minimum, maximum, and range midpoints for leaf consumption in the relevant Turkana Basin taxa. These are the values used in the bivariate plots to visualize the degrees of niche separation (Benefit, 1989, 1999).

Taxon	Leaf Min	Leaf Max	Midpoint
<i>Cercopithecoides. kimeui</i>	48	51	49.5
<i>C. williamsi</i>	52	69	60.5
<i>Paracolobus. mutiwa</i>	49	55	52
L895-1	.	.	.
<i>Rhinocolobus turkanensis</i>	44	50	47
<i>Theropithecus brumpti</i>	.	.	.
<i>T. oswaldi</i>	33	42	37.5

crest length. These have the advantage of being available for all included taxa, often from the specific populations being studied here. These data are biased in revealing more about reliance on leaves over fruit sources, but do provide some general patterns of dietary preference. The minimum, maximum, and midpoint values for each relevant taxon are given in Table 5.3. As with the estimates for percentage time on the ground, the midpoint of the minimum and maximum values are used.

Results

Estimates of Terrestriality for Extant Cercopithecidae

Six of the functional indices were correlated ($p < 0.05$) with percent time spent on the ground in extant taxa. Estimates of relative terrestriality for the fossil taxa and are presented in Table 5.6. Although many of the indices are qualitatively useful for separating terrestrial from arboreal taxa in the box and whisker plots in Chapters III and IV, only some showed significant correlations.

Despite the relatively crude nature of this regression, the functional indices showing a relationship with observed ground time are known to be qualitatively useful in distinguishing more terrestrial from more arboreal taxa such as the relative length of the

Figure 5.1 Regression plots of relevant functional indices from the forelimb and observed time spent on the ground in extant Cercopithecoidea. See Table 5.1 for list of taxa included in analyses. For a description of the linear indices see Table 2.2.

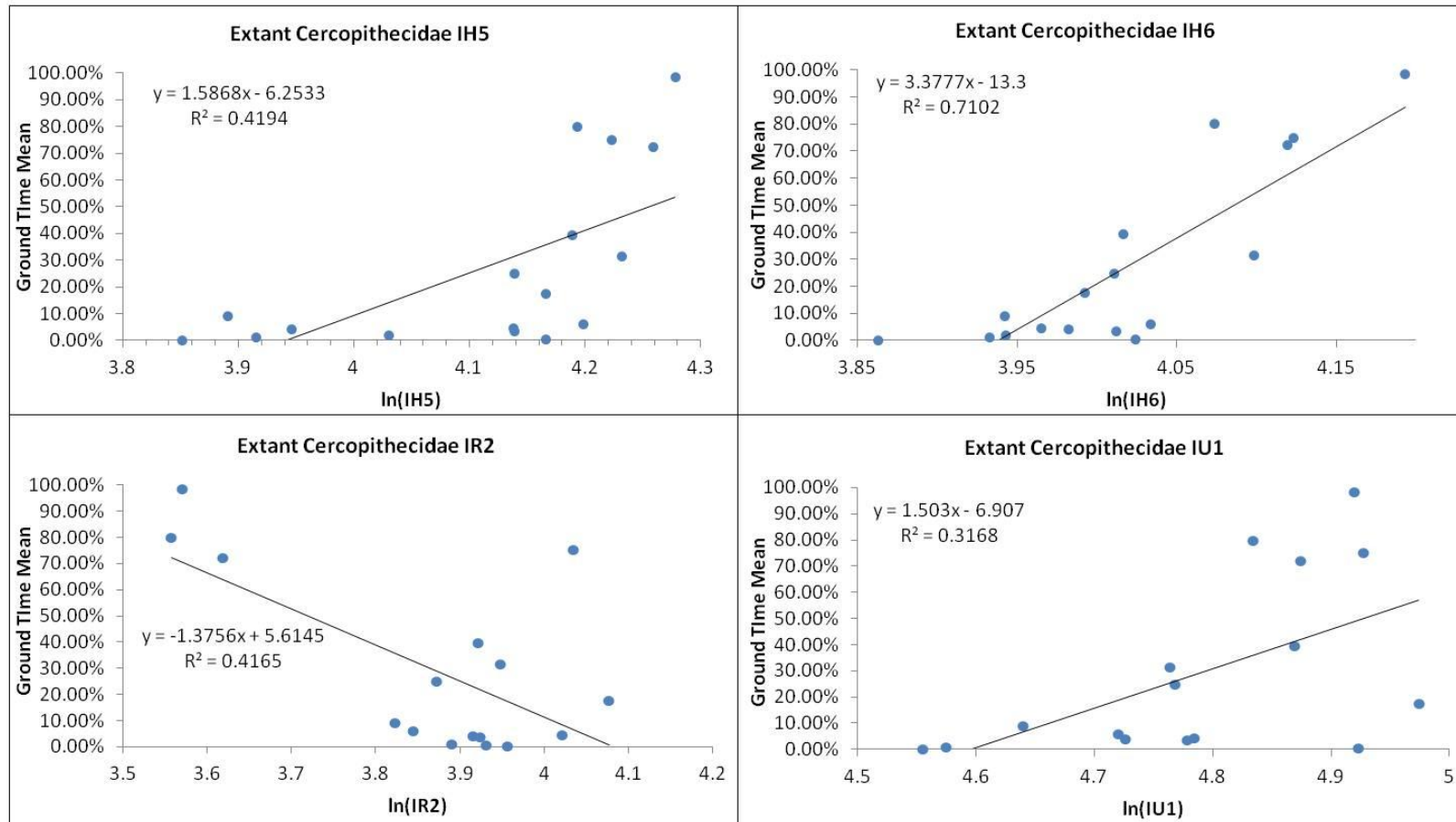
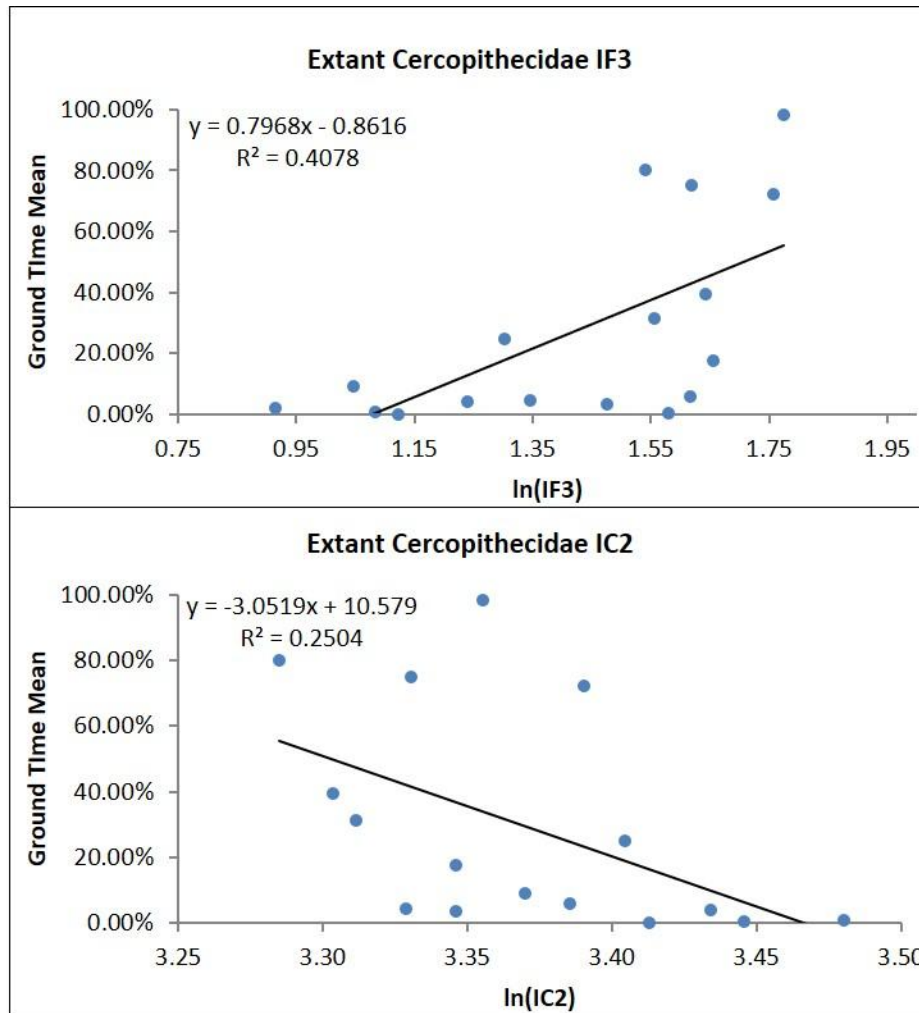


Figure 5.2 Regression plots of functional indices from the hindlimb and observed time spent on the ground in extant Cercopithecidae. See Table 5.1 for list of taxa included in analyses. For a description of the linear indices see Table 2.2.



trochlear flange on the humerus (IH5), radial neck length (IR2), olecranon process height on the ulna (IU1), greater trochanter height on the femur (IF3), and relative length of the posterior calcaneal facet (IC2) (Figures 5.1, 5.2). It is important to note that most of the terrestrial taxa with available locomotor behavior data available are cercopithecines and features like a rounder capitulum, more prominent, greater trochanter, and shorter calcaneal tuberosity are associated with terrestriality and seen in some of the fossil colobines.

Table 5.4 Results of the regression of functional indices on observed terrestriality for the extant Cercopithecidae with available data. Only indices with resulting p-values < 0.05 are shown here.

Index	r^2	CI (95%)	y-Intercept	Slope
IH5	0.42	0.65	1.5868	-6.2533
IH6	0.71	0.84	3.3777	-13.2998
IR2	0.42	0.64	-1.3756	5.6145
IU1	0.31	0.55	1.5030	-6.9070
IF3	0.41	0.64	0.7968	-0.8616
IC2	0.25	0.5	-3.0519	10.5791

Table 5.5 Results of the terrestriality estimate regressions on the extant taxa compared to the observed (Obs.) behavioral ranges for the indices shown in Figures 5.5 and 5.6.

Taxon	Obs. Min	Obs. Max	Obs. Mean	Est. Mean	IH5	IH6	IR2	IU1	IF3	IC2
<i>Colobus guereza</i>	.	.	0.04	0.14	0.01	0.15	0.23	0.21	0.13	0.10
<i>Ptilocolobus badius</i>	.	.	0.01	0.02	0.04	0.02	0.26	0.02	0.00	0.04
<i>Ptilocolobus kirkii</i>	.	.	0.02	0.10	0.14	0.02	.	.	0.13	.
<i>Pygathrix nemaeus</i>	.	.	0.00	0.01	0.14	0.25	0.17	0.05	0.03	0.16
<i>Rhinopithecus roxellana</i>	2.9	15.3	0.09	0.12	0.08	0.02	0.36	0.08	0.03	0.29
<i>Semnopithecus entellus</i>	15.7	34	0.25	0.25	0.31	0.25	0.29	0.27	0.18	0.19
<i>Cercocebus torquatus</i>	.	.	0.39	0.37	0.39	0.27	0.22	0.42	0.45	0.50
<i>Cercopithecus mitis</i>	2	5	0.04	0.29	0.32	0.25	0.22	0.29	0.31	0.37
<i>Cercopithecus neglectus</i>	15	20	0.18	0.33	0.36	0.19	0.01	0.58	0.46	0.37
<i>Chlorocebus aethiops</i>	19.4	43.4	0.31	0.38	0.46	0.55	0.18	0.26	0.38	0.47
<i>Erythrocebus patas</i>	59.6	90.5	0.75	0.42	0.45	0.63	0.06	0.51	0.43	0.41
<i>Lophocebus albigena</i>	1	8	0.05	0.24	0.31	0.09	0.08	0.29	0.21	0.42
<i>Macaca fascicularis</i>	2	10	0.06	0.32	0.41	0.33	0.33	0.20	0.43	0.25
<i>Macaca thibetana</i>	.	.	0.00	0.20	0.36	0.29	0.21	0.50	0.40	0.06
<i>Mandrillus sphinx</i>	.	.	0.80	0.48	0.40	0.46	0.72	0.37	0.37	0.55
<i>Papio anubis</i>	.	.	0.72	0.48	0.51	0.62	0.64	0.43	0.54	0.23
<i>Theropithecus gelada</i>	.	.	0.98	0.58	0.54	0.87	0.70	0.50	0.55	0.34

Many useful indices used to assess locomotor adaptations in extant taxa like the brachial and intermembral indices cannot be compared as the fossil taxa lack long bones well-preserved enough for full length measurements to be taken. However, despite the

relatively crude nature of this estimation, it is still useful to know which functional features in extant taxa can be quantitatively linked to behavioral data. This is particularly relevant in paleontology which has a fossil record skewed towards epiphyseal fragments and being able to quantify feature with qualitative functional significance can strengthen arguments for functional significance and allow for more fragmentary specimen to be included in such analyses.

Estimates of Terrestriality for Fossil Cercopithecidae

Each index regression was run on the fossil specimens to quantify their ground preferences. Of the Cercopithecidae known from the Turkana Basin, 5 have at least some postcranial adaptations consistent with terrestriality: *C. kimeui*, *C. williamsi*, *P. mutiwa* (represented by KNM-WT 16827), L895-1, and *T. oswaldi*. Taxa with some arboreal adaptations include *R. turkanensis* and *T. brumpti*, although the terrestriality of the latter is likely be driven down by its low radial index estimate (Table 5.8). The values resulting from the regressions are very likely affected by the nonconcordant and small sample sizes of shared elements among the taxa but are intended as a proxy measure rather than an actual estimate of percentage of time spent on the ground. For example, the estimate for *R. turkanensis* seems relatively high given its functional morphology being more consistent with arboreal adaptations but is within the range of some extant taxa such as *Semnopithecus entellus* which has been observed as being semi-terrestrial (Table 5.1; Gosselin-Ildari, 2013). The low level of terrestriality estimated for *T. brumpti* also contrasts functional description based on more complete skeletal analyses and the low radial estimate in particular may be due to unique adaptations in this taxon for elbow mobility during foraging behaviors similar to those seen in its wrist and hand morphology

Table 5.6 Estimates of terrestriality for the fossil taxa as calculated using the parameters from Table 5.4. *C. kimeui* has too few attributed postcranial elements so is not included in the niche separation plots concerning time on the ground.

Taxon	IH5	IH6	IR2	IU1	IF3	IC2	Mean
<i>C. williamsi</i>	0.13	0.72	0.40	0.83	0.28	.	0.48
KNM-WT 16827	0.17	0.07	.	0.66	.	0.12	0.25
L895-1	0.28	0.58	0.26	0.50	0.44	0.18	0.37
<i>R. turkanensis</i>	0.02	0.46	0.40	0.49	.	.	0.34
<i>T. brumpti</i>	0.39	0.42	0.03	0.49	0.57	0.11	0.33
<i>T. oswaldi</i>	0.37	0.31	0.22	0.45	0.71	0.24	0.38

(Jolly, 1967, 1972; Jablonski, 2002; Jablonski et al., 2008; Guthrie, 2011). Another interesting result is that KNM-WT 16827 is estimated as spending less time on the ground than L895-1 despite the former displaying more qualitative features consistent with terrestriality (Chapter III). This may in part be explained by the fact that KNM-WT 16827 lacks a complete radius and femur from which to calculate the radial neck length (IR2) and greater trochanter height (IF3) which are very strongly correlated with substrate preference (Figures 5.1, 5.2). The small estimates based on the relative size of the calcaneal posterior facet (IC2) for both of these specimens are also notable as it is in the calcaneal morphology that KNM-WT 16827 most contrasts with *P. chemeroni* and contemporaneous cercopithecines such as *T. oswaldi*. If these two specimens are indeed both *P. mutiwa*, this may indicate a unique ankle morphology characteristic to the taxon. Even if they are shown not to be the same species, this suggests that both may present morphologies unique to terrestrial colobines.

Niche Separation: Body mass and substrate use

Perhaps the most striking characteristic of the fossil colobinins is their large body mass relative to their extant counterparts. Body mass estimates for the females of the

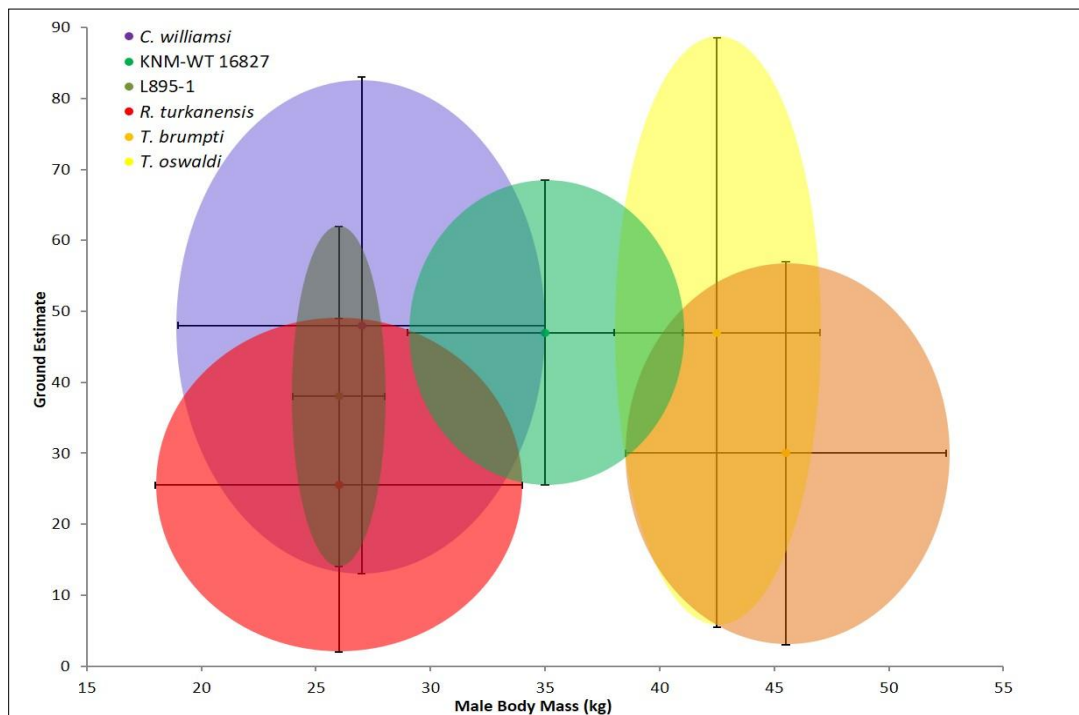
fossil species are larger than all except for a couple of the largest extant males and estimated mean body mass for males is larger than all but some of the largest extant cercopithecines (Table 4.5). Not only are they significantly larger, as demonstrated in Chapters III and IV, but many of the fossil colobines display postcranial morphologies consistent with some degree of terrestrial locomotion which is further supported by the results of the regression on the postcranial indices for these taxa (Table 5.6). Although the parameters used to estimate relative terrestriality are based on observed behavioral data, the results presented here are not intended to provide actual percentage estimates for the fossil taxa, but rather a number that can be applied to rank by potential degree of terrestriality. As mentioned above, the fact that the observational ground preference data is based primarily on estimates derived from cercopithecine behavior, there are limitations to how accurately it represents the reality of substrate preference for the fossil colobines.

However, the indices shown to have a significant correlation with this preference are based on those that separate out the more terrestrially adapted fossil taxa from their more arboreal extant counterparts. The qualitative descriptions presented in Chapters III and IV demonstrate that although there are some features in the terrestrial colobines that overlap with terrestrial cercopithecines, the lack of extant colobine analogs makes it likely that some important functional signals are not easily observed. In KNM-WT 16827 for example, the calcaneal indices are more consistent with terrestrial cercopithecines, but the qualitative morphology is distinct enough from cercopithecines such as *T. oswaldi* to suggest that these taxa were not exploiting their environments in the exact same way (Figures 3.26, 3.27). A lack of calcanei attributed to large colobines makes it difficult at

this point to parse out exactly which features are unique to terrestrial colobines, but further analysis may provide some answers.

Despite these limitations, the results of the relative terrestriality estimates for the fossil colobines show that although there is overlap among them in body mass, they do separate out based on substrate use. *C. williamsi* is the largest and most terrestrial of the fossil taxa and *T. oswaldi* plots as more terrestrial than any of the colobines (Figure 5.3).

Figure 5.3 Plot showing the range overlap in male body mass and relative terrestriality as estimated based on the regressions of the postcranial indices. Axes are uneven to more easily distinguish separation among the taxa.



R. turkanensis overlaps with body mass ranges of *C. williamsi*, L895-1, and KNM-WT 16827, but separates out based on substrate preference. It is the most arboreal of the known fossil colobines and falls closer to the extant arboreal colobines in its postcranial

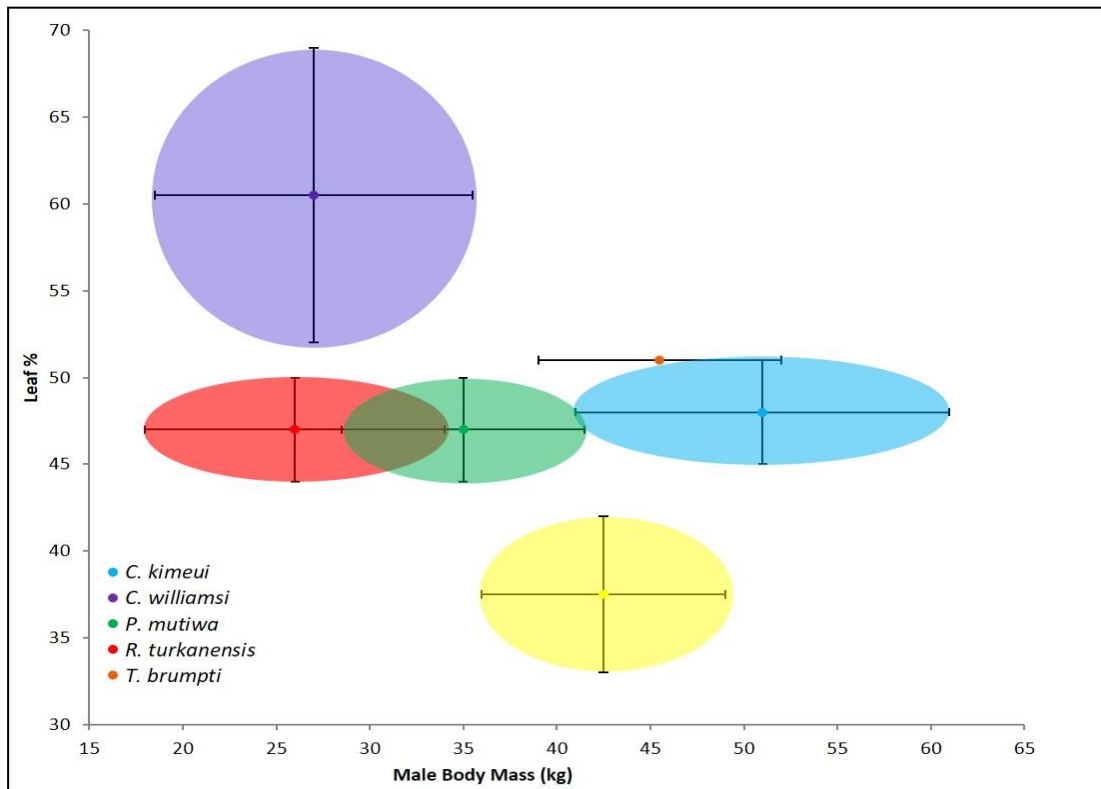
indices (Figures 3.10b, 4.6). It does however separate out from *T. brumpti* which although both share some arboreal adaptations, do not overlap in body mass. This is also likely further proof that while colobine and cercopithecines may share broad adaptive traits, the ways in which the two subfamilies are exploiting their environments may still be different. *P. mutiwa* (KNM-WT 16827) and L895-1 overlap in their estimated amount of time on the ground, but the latter is smaller but because *P. mutiwa*'s mass estimates are based on more specimens and skeletal elements, they may have overlapped more in body mass than the postcranial estimates show.

Niche Separation: Body mass and diet

Despite a number of techniques showing some success, reconstructing the dietary preferences of fossil taxa is difficult. In extant primates, diet can vary with the season, population, between sexes, and within the lifetime of an individual. Still, site specific studies on large mammals and hominins have been able to illustrate to some degree the niche separation of species within paleoenvironments using carbon and oxygen isotopes (e.g. Cerling et al., 2015; Levin et al., 2015). Although they are not a perfect proxy, shear crest morphology, cuspal height, and crown flare of the molar teeth are the only dietary proxies available for all of the taxa in this study and like the ground estimates, are presented as a tentative range to visualize patterns among the species (Benefit, 1999).

In the plot of estimated male body mass against diet, *C. williamsi* overlaps in size with *P. mutiwa* and *R. turkanensis* but is reconstructed as eating more leaves (Figure 5.4). *P. mutiwa* overlaps with *R. turkanensis* in estimated size and diet, but difference in functional morphology between the two may explain the sympatry of the two taxa. It is also worth noting that the dietary and body mass estimates are not necessarily from the same

Figure 5.4 Plot showing the range in overlap in male body mass and diet as estimated based on dental metrics shown to correlate with leaf consumption (Benefit, 1987, 1999). L895-1 has no associated dentition so is excluded from this plot.

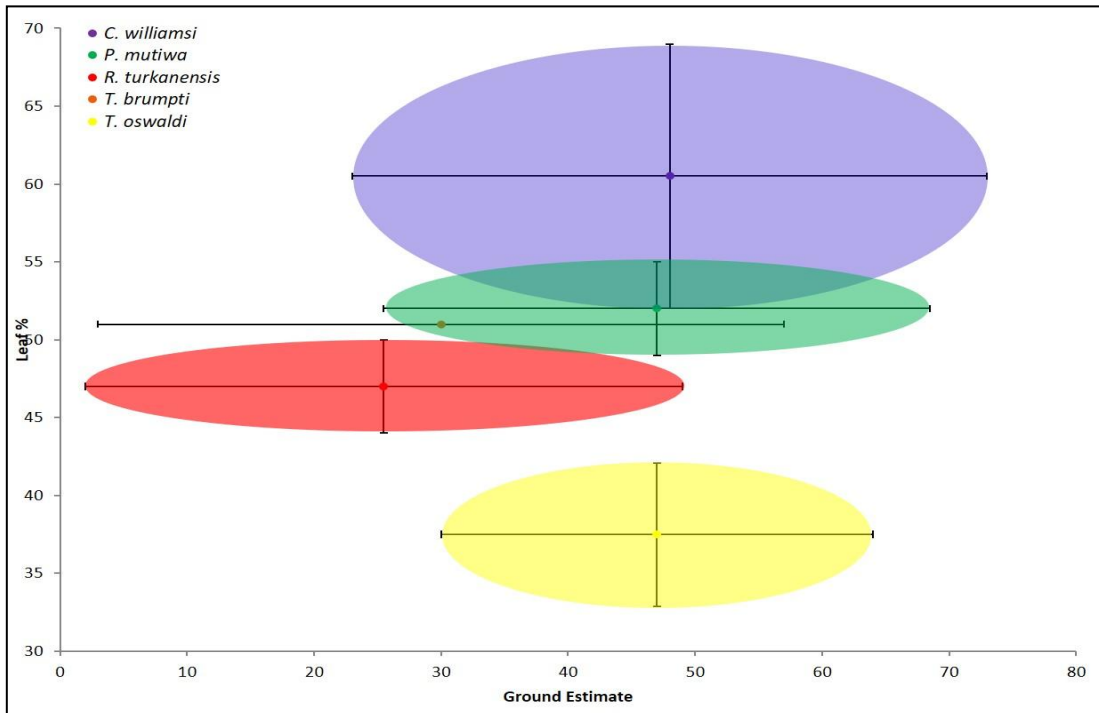


individuals and that some of the true variability among the data is being lost. However, despite this limitation, this does illustrate some separation in body size and dietary preferences among the cercopithecids of the Turkana Basin.

Niche Separation: Substrate use and diet

Some interesting patterns also occur when estimated ground time is plotted against diet estimates (Figure 5.5). Although not all of the relevant taxa are available for this plot there are still some notable differences among the terrestrial colobines. *C. williamsi* and *P. mutiwa* overlap in ground time, but *C. kimeui* appears to have more of an emphasis on leaves in its diet. This may suggest that these two taxa are exploiting similar substrates, but exploitation of different dietary resources may allow them to overlap

Figure 5.5 Plot showing the range in overlap in relative terrestriality and diet L895-1 has no associated dentition so is excluded from this plot and *T. brumpti* has only a mean value for diet so has no bars indicating estimate ranges.



ecologically. *R. turkanensis* and *T. brumpti* are the least terrestrial in this model and although the latter lacks a diet range, its estimated value of 51% is slightly higher than *R. turkanensis*. *T. oswaldi* is the most terrestrial of the Turkana Basin taxa and the least reliant on leaves which is consistent with some reconstructions of this taxon as more reliant on seeds and grasses although seasonal and geographic variation is still visible (Leakey, 1993; Cerling et al., 2013; Levin et al., 2015). Another factor likely driving such sympatry that is not accounted for here is the diversity of plant resources being exploited.

Discussion

All of the colobine taxa included in analyses here are known to overlap in time and range, but not all of the specimens available for postcranial analysis come from the same localities. Sites such as Koobi Fora illustrate a level of sympatry among these taxa,

but a lack of postcranial specimens makes it difficult to assess the level of overlap in substrate preference. Incorporating results from specimens at other localities, however, can help reconstruct some patterns of niche separation among these taxa. There are many limitations to this approach which ignores interspecies variability in such areas as diet, substrate use, and even body mass, but given the limited sample available some broader patterns may still be estimated and assessed.

Although the extant colobines are primarily arboreal this substrate preference encompasses a wide range of actual locomotor adaptations all of which may leave unique patterns in the skeletal morphology. The functional morphological reconstructions for fossil taxa are limited by a number of factors such as sample size, preservation, the ability to taxonomically assign postcranial elements, and interpreting morphology with few modern analogs. Even for the relatively well-preserved specimens described and included in the analyses from Chapters 3 and 4, qualitative and quantitative assessment are limited by which parts of the various elements are preserved. The estimates of percent time on the ground here are limited by metrics that are commonly preserved in fossil taxa, which very often do not include proportional metrics like intermembral and brachial indices that are most useful in extant taxa. Of the indices shown to have some potential morphological signal linked to function in the terrestrial colobines several did not strongly correlate to terrestriality in the regression.

The observational data on extant taxa is skewed toward cercopithecines with only two colobine taxa with significant semi-terrestrial behavior. For the extant taxa, although many of the estimated values were different from the observed, the general ranking of more to less terrestrial were similar between the estimates and observed values (Table

5.5). Even for taxa where the regression underestimated actual terrestriality, their resulting estimates still have them as ranking more terrestrial than any of the others. For both the colobine and cercopithecine groups, the estimates give a reasonable rank of more versus less terrestrial even when the estimated values are different than the observed.

For the fossil colobines some interesting patterns also emerge. All of the taxa with enough postcranial elements available for a reasonable index estimate, all map, based on the estimated mean values alone at least, as more terrestrial than most extant colobines. When viewed as values for ranking most to least terrestrial, the estimated values coincide with qualitative functional estimates with *C. williamsi* as most terrestrial and *R. turkanensis* as least. For *C. williamsi*, a minimum estimate based on the humeral trochlear flange length bring down the mean. In *P. mutiwa*, as represented by KNM-WT 16827, the relative capitulum depth is the value that brings down its mean. Both of these specimens show relatively short and robust humeri which despite showing proportions more similar to terrestrial cercopithecines (Figures 3.6, 4.4), likely display morphologies distinct to terrestrial colobines that are not accurately captured by the indices alone. *Rhinocolobus turkanensis*, although the least terrestrial based on its values, plots as more similar to the extant arboreal colobines in its index values as well as in its qualitative functional morphology (Figures 3.11, 4.7). Despite these indices not being significantly affected by body mass for the extants, there could be an allometric signal present in the fossils that is obscured by small sample sizes. *R. turkanensis* is also only represented in these estimates by forelimb elements, which is also likely contributing to these relatively large values.

Nevertheless, the overall rankings of more versus less terrestrial for the fossil colobines allows for some broad pattern assessment. It is also striking to note how

different the fossil colobines are relative to their extant counterparts in these estimates which further emphasizes how different they are. With larger samples it may someday be possible to more precisely quantify features that are unique to terrestrial colobines, but until then such analyses are limited by what is identifiable in the fossil record.

The substrate use and dietary proxies used here are crude and do not account for intraspecific, intersexual, geographical, seasonal variability, or any of the other biotic and abiotic factors that can affect behavior. Furthermore, the dietary focus on leaves does not give a full picture of the actual diets which likely included such items as fruits, nuts, or even meat. Were such data available, much more separation would likely be detectable even with the broad generalizations of this analysis. *C. kimeui* also lacks a postcranial sample size large enough for any meaningful quantitative estimates of substrate use. Given that it is the largest of the colobines at this time, its inclusion would not doubt provide interesting results. Nevertheless, this does show that there is niche separation among the colobines of the Turkana Basin in both substrate use and diet which likely accounts for the ability of these environments to support so many large-bodied taxa.

CHAPTER VI

CONCLUSIONS

This dissertation is an assessment of the functional morphology of the large-bodied colobine monkeys of the Plio-Pleistocene and implications this may have for the paleoecological conditions of the Turkana Basin during this time. The specimen descriptions in Chapters III and IV provide a detailed overview of two previously undescribed and relatively complete specimens with associated postcrania. The analyses described indicate that not only is the *P. mutiwa* specimen KNM-WT 16827 terrestrial, but that is morphologically distinct enough from *P. chemeroni* to warrant generic reassignment. The specimen discussed in Chapter IV lacks craniodental elements necessary for a secure taxonomic assignment but is more similar to *P. mutiwa* than to other contemporaneous large-bodied cercopithecids including *C. williamsi*, *R. turkanensis*, *T. oswaldi*, and *T. brumpti*. The functional morphology of these and other fossil specimens included in the comparative sample adds to the already diverse primate ecology of the Turkana Basin during this time period where there is evidence for the presence of at least four large-bodied sympatric colobine species: *C. williamsi*, *C. kimeui*, *R. turkanensis*, and *P. mutiwa* as well as papionin taxa such as *T. oswaldi*, *T. brumpti*, and *Soromandrillus quadratiostris* (Jablonski et al., 2008; Gilbert, 2013). This level of sympatry is not seen in among African large-bodied primates today suggesting niche separation in such realms as diet and substrate preference have played an important role in cercopithecoid evolution (Elton, 2006).

Specimen KNM-WT 16827 (Chapter III) displays several postcranial features

unique from *P. chemeroni* including relatively short and robust long bones, relatively small tarsals, and a suite of morphologies consistent with terrestrial locomotion including features of the distal humerus, proximal ulna, and hip joint. Many of the morphological similarities KNM-WT 16827 bears to *P. chemeroni* are either typical for colobines or likely due to both sharing adaptations for terrestrial locomotion relative to extant taxa (Leakey, 1982, 1985, 1987; Harris et al., 1988; Ting, 2001; Jablonski, 2002; Grubb et al., 2003). The significance of the small tarsals is also striking contrasts with the morphology of terrestrial taxa such as *P. chemeroni* and *Theropithecus* perhaps suggesting that this feature is unique to the taxon.

Specimen L895-1 (Chapter IV) shows some similarities to KNM-WT 16827 in having relatively short and robust long bones. It too is displays distinct morphology and shares more postcranial similarities with *P. mutiwa* and *C. williamsi* than to extant colobines. It is also distinct from *T. oswaldi* and although no postcrania attributed to *Soromandrillus*, have yet been described, the morphology of the long bones and tarsals is more similar to other colobines. The prominent coronoid process and symmetrical anconeal process on the ulna, the shape of the greater trochanter on the femur, and size of the medial articular surfaces on the middle cuneiform are features more typical of colobines than cercopithecines. Body mass estimates for this specimen show that it is larger than any known extant colobine or female fossil colobine taxon. It is estimated as being slightly smaller than *P. mutiwa*, but as the latter's estimates are based on many more elements, it may have been even larger.

All of the fossil colobine taxa included in the analyses of functional morphology are known to overlap in time and space. Sites such as Koobi Fora illustrate a level of

sympatry among these taxa, and integrating these data with published data on diet, substrate use, and body mass help to reconstruct broad patterns of niche separation among the taxa (Chapter V). Interestingly, several indices shown to have some potential morphological signal linked to function in the terrestrial colobines did not strongly correlate to terrestriality in ground use regression based on observed ground time in extant cercopithecids. However, the indices that were chosen enabled a relative ranking of terrestriality among the fossil taxa mostly consistent with qualitative results. It is also striking to note how different the fossil colobines are relative to their extant counterparts in these estimates further emphasizing how different the primate ecology of the Turkana Basin used to be.

This project provides functionally relevant information about two previously unpublished specimens which adds to the known cercopithecoid diversity of the time and will help in the assessment of unassociated postcranial specimens. In addition to the two specimens described in this dissertation, two more unpublished postcranial specimens were described, but not included here. The functional analyses presented here along with the comparative dataset may help to identify these individuals. The comparative dataset of both extant and fossil taxa will also prove useful for improving methods of postcranial assessment. Hundreds of isolated and unassociated elements of unknown taxon were measured for this project but not included in the analyses and may include specimens that can be functionally assessed or even tentatively attributed to colobines.

Finally, what fossil primates can tell us about the environments and paleoecological conditions of early humans is of intrinsic interest to paleoanthropology. The presence of terrestriality in colobines during the Plio-Pleistocene emphasizes the

importance of not relying too heavily on the behavior of modern taxa to interpret the fossil record. Although early hominins are morphologically distinct from cercopithecidae in their locomotor patterns, semi-terrestriality seen in some fossil taxa provides a unique opportunity for exploring adaptations for intermediate locomotor patterns. Colobines may not offer a direct parallel with hominins in diet or substrate use, but their sympatry suggests a much more diverse and dynamic environment than seen in East Africa today.

APPENDIX A

A.1 Extant colobine taxa included in the comparative sample. a. Specimens measured by E. Guthrie and used with permission.

Museum	Cat. No.	Genus	Species	Subspecies	Sex	Museum	Cat. No.	Genus	Species	Subspecies	Sex
MNHN	1897-133	<i>Colobus</i>	<i>angolensis</i>	<i>palliates</i>	F	LNMH	72.148	<i>Colobus</i> ^a	<i>guereza</i>	<i>matschei</i>	M
MNHN	1897-139	<i>Colobus</i>	<i>angolensis</i>	<i>palliates</i>	F	LNMH	72.139	<i>Colobus</i> ^a	<i>guereza</i>	<i>matschei</i>	M
MNHN	A12833	<i>Colobus</i>	<i>angolensis</i>	<i>palliates</i>	U	NMNH	163262	<i>Colobus</i>	<i>guereza</i>	<i>matschei</i>	M
MNHN	A12834	<i>Colobus</i>	<i>angolensis</i>	<i>palliates</i>	M	NMNH	163264	<i>Colobus</i>	<i>guereza</i>	<i>matschei</i>	F
NHMUK	1972.158	<i>Colobus</i>	<i>angolensis</i>	<i>palliatus</i>	F	NMNH	163265	<i>Colobus</i>	<i>guereza</i>	<i>matched</i>	F
NHMUK	1930.8.1.13	<i>Colobus</i>	<i>angolensis</i>	<i>palliatus</i>	M	NMNH	452622	<i>Colobus</i>	<i>guereza</i>	<i>matschei</i>	M
NHMUK	1937.8.18.1	<i>Colobus</i>	<i>angolensis</i>	<i>palliatus</i>	M	NMNH	452624	<i>Colobus</i>	<i>guereza</i>	<i>matschei</i>	F
NHMUK	1937.8.18.2	<i>Colobus</i>	<i>angolensis</i>	<i>palliatus</i>	F	NMNH	452625	<i>Colobus</i>	<i>guereza</i>	<i>matschei</i>	M
NHMUK	1938.4.21.2	<i>Colobus</i>	<i>angolensis</i>	<i>palliatus</i>	F	NMNH	452627	<i>Colobus</i>	<i>guereza</i>	<i>matschei</i>	F
NMNH	452615	<i>Colobus</i>	<i>angolensis</i>	<i>palliatus</i>	M	NMNH	452628	<i>Colobus</i>	<i>guereza</i>	<i>matschei</i>	M
NMNH	452616	<i>Colobus</i>	<i>angolensis</i>	<i>palliatus</i>	M	NMNH	452629	<i>Colobus</i>	<i>guereza</i>	<i>matschei</i>	M
NMNH	452617	<i>Colobus</i>	<i>angolensis</i>	<i>palliatus</i>	F	NMNH	452630	<i>Colobus</i>	<i>guereza</i>	<i>matschei</i>	F
NMNH	268946	<i>Colobus</i>	<i>angolensis</i>	<i>ruwenzorii</i>	F	NMNH	452631	<i>Colobus</i>	<i>guereza</i>	<i>matschei</i>	F
NMNH	268947	<i>Colobus</i>	<i>angolensis</i>	<i>ruwenzorii</i>	F	NMNH	452632	<i>Colobus</i>	<i>guereza</i>	<i>matschei</i>	F
KNM	KNM OM 3073	<i>Colobus</i> ^a	<i>guereza</i>		F	NMNH	452634	<i>Colobus</i>	<i>guereza</i>	<i>matschei</i>	F
MNHN	A3842	<i>Colobus</i>	<i>guereza</i>		M	NMNH	452635	<i>Colobus</i>	<i>guereza</i>	<i>matschei</i>	M
NMNH	464983	<i>Colobus</i>	<i>guereza</i>		F	NMNH	452636	<i>Colobus</i>	<i>guereza</i>	<i>matschei</i>	F
NMNH	588480	<i>Colobus</i>	<i>guereza</i>			NMNH	452642	<i>Colobus</i>	<i>guereza</i>	<i>matschei</i>	F
NMNH	163122	<i>Colobus</i>	<i>guereza</i>	<i>kikuyuensis</i>	F	NMNH	452643	<i>Colobus</i>	<i>guereza</i>	<i>matschei</i>	M
NMNH	164522	<i>Colobus</i>	<i>guereza</i>	<i>kikuyuensis</i>	F	MNHN	1976-326	<i>Colobus</i>	<i>guereza</i>	<i>occidentalis</i>	M
NMNH	164524	<i>Colobus</i>	<i>guereza</i>	<i>kikuyuensis</i>	F	MNHN	CG 1904-1963	<i>Colobus</i>	<i>guereza</i>	<i>occidentalis</i>	M
NMNH	164525	<i>Colobus</i>	<i>guereza</i>	<i>kikuyuensis</i>	M	NMNH	268509	<i>Colobus</i>	<i>guereza</i>	<i>occidentalis</i>	M
NMNH	164526	<i>Colobus</i>	<i>guereza</i>	<i>kikuyuensis</i>	M	NMNH	452633	<i>Colobus</i>	<i>guereza</i>	<i>occidentalis</i>	F
NMNH	164631	<i>Colobus</i>	<i>guereza</i>	<i>kikuyuensis</i>	M	NMNH	452619	<i>Colobus</i>	<i>guereza</i>	<i>kikuyuensis</i>	M
NMNH	164749	<i>Colobus</i>	<i>guereza</i>	<i>kikuyuensis</i>	M	NMNH	452620	<i>Colobus</i>	<i>guereza</i>	<i>kikuyuensis</i>	M
NMNH	164844	<i>Colobus</i>	<i>guereza</i>	<i>kikuyuensis</i>	F	MCZ	21147	<i>Colobus</i>	<i>polykomos</i>	<i>caudatus</i>	F
NMNH	452621	<i>Colobus</i>	<i>guereza</i>	<i>kikuyuensis</i>	M	MCZ	21148	<i>Colobus</i>	<i>polykomos</i>	<i>caudatus</i>	M
NMNH	452641	<i>Colobus</i>	<i>guereza</i>	<i>kikuyuensis</i>	F	MCZ	21151	<i>Colobus</i>	<i>polykomos</i>	<i>caudatus</i>	F
LNMH	72.134	<i>Colobus</i> ^a	<i>guereza</i>	<i>kikuyuensis</i>	F	MCZ	21152	<i>Colobus</i>	<i>polykomos</i>	<i>caudatus</i>	M
LNMH	72.138	<i>Colobus</i> ^a	<i>guereza</i>	<i>matschei</i>	F	MCZ	21149	<i>Colobus</i>	<i>polykomos</i>	<i>caudatus</i>	M
LNMH	72.15	<i>Colobus</i> ^a	<i>guereza</i>	<i>matschei</i>	F	MCZ	21150	<i>Colobus</i>	<i>polykomos</i>	<i>caudatus</i>	M

Museum	Cat. No.	Genus	Species	Subspecies	Sex	Museum	Cat. No.	Genus	Species	Subspecies	Sex
MCZ	21153	<i>Colobus</i>	<i>polykomos</i>	<i>caudatus</i>	F	MCZ	7099	<i>Nasalis</i>	<i>larvatus</i>		M
MCZ	25541	<i>Colobus</i>	<i>polykomos</i>	<i>caudatus</i>	F	MCZ	37327	<i>Nasalis</i>	<i>larvatus</i>		M
MCZ	37941	<i>Colobus</i>	<i>polykomos</i>	<i>cottoni</i>	M	MCZ	37328	<i>Nasalis</i>	<i>larvatus</i>		M
MCZ	24776	<i>Colobus</i>	<i>polykomos</i>	<i>polykomos</i>	U	MCZ	37329	<i>Nasalis</i>	<i>larvatus</i>		M
MCZ	47977	<i>Colobus</i>	<i>polykomos</i>	<i>satanas</i>	M	MCZ	37330	<i>Nasalis</i>	<i>larvatus</i>		M
LNMH	72.151	<i>Colobus</i> ^a	<i>polykomos</i>	<i>uellensis</i>	F	MCZ	37331	<i>Nasalis</i>	<i>larvatus</i>		F
LNMH	72.152	<i>Colobus</i> ^a	<i>polykomos</i>	<i>uellensis</i>		MCZ	37337	<i>Nasalis</i>	<i>larvatus</i>		F
LNMH	72.153	<i>Colobus</i> ^a	<i>polykomos</i>	<i>uellensis</i>		MCZ	37339	<i>Nasalis</i>	<i>larvatus</i>		F
LNMH	1930.8.1.11	<i>Colobus</i> ^a	<i>polykomos</i>	<i>uellensis</i>		MCZ	37340	<i>Nasalis</i>	<i>larvatus</i>		F
MCZ	37938	<i>Colobus</i>	<i>polykomos</i>	<i>uellensis</i>	M	MCZ	37341	<i>Nasalis</i>	<i>larvatus</i>		F
MNHN	CG 1958-710	<i>Colobus</i>	<i>polykomos</i>		M	MCZ	37342	<i>Nasalis</i>	<i>larvatus</i>		F
MNHN	CG 1961-1017	<i>Colobus</i>	<i>polykomos</i>		F	MCZ	37343	<i>Nasalis</i>	<i>larvatus</i>		F
NMNH	164584	<i>Colobus</i>	<i>polykomos</i>		M	MCZ	37344	<i>Nasalis</i>	<i>larvatus</i>		F
NMNH	164603	<i>Colobus</i>	<i>polykomos</i>		M	MCZ	41554	<i>Nasalis</i>	<i>larvatus</i>		F
NMNH	477321	<i>Colobus</i>	<i>polykomos</i>		M	MCZ	41555	<i>Nasalis</i>	<i>larvatus</i>		F
NMNH	598560	<i>Colobus</i>	<i>satanas</i>		F	MCZ	41557	<i>Nasalis</i>	<i>larvatus</i>		M
NMNH	598561	<i>Colobus</i>	<i>satanas</i>		F	MCZ	41559	<i>Nasalis</i>	<i>larvatus</i>		F
NMNH	498706	<i>Colobus</i>	<i>sp.</i>		M	MCZ	41560	<i>Nasalis</i>	<i>larvatus</i>		F
NHMUK	1856.12.29.1	<i>Colobus</i>	<i>satanas</i>		F	MCZ	41561	<i>Nasalis</i>	<i>larvatus</i>		M
NHMUK	30.12.15.1	<i>Colobus</i>	<i>satanas</i>		F	MCZ	45163	<i>Nasalis</i>	<i>larvatus</i>		M
NMNH	598558	<i>Colobus</i>	<i>satanas</i>		F	MNHN	1897.1302	<i>Nasalis</i>	<i>larvatus</i>		F
NMNH	598559	<i>Colobus</i>	<i>satanas</i>		U	MNHN	A3838	<i>Nasalis</i>	<i>larvatus</i>		F
NMNH	429488	<i>Colobus</i>	<i>vellerosus</i>		F	NHMUK	1939.1152	<i>Nasalis</i>	<i>larvatus</i>		M
NMNH	477322	<i>Colobus</i>	<i>vellerosus</i>		M	NHMUK	1855.12.26.242	<i>Nasalis</i>	<i>larvatus</i>		F
AIM	A.S. 1537	<i>Nasalis</i>	<i>larvatus</i>		M	NMNH	142215	<i>Nasalis</i>	<i>larvatus</i>		M
AIM	A.S. 1556	<i>Nasalis</i>	<i>larvatus</i>		F	NMNH	142220	<i>Nasalis</i>	<i>larvatus</i>		M
AIM	A.S. 1557	<i>Nasalis</i>	<i>larvatus</i>		M	NMNH	151817	<i>Nasalis</i>	<i>larvatus</i>		F
AIM	A.S. 1640	<i>Nasalis</i>	<i>larvatus</i>		F	NMNH	151817	<i>Nasalis</i>	<i>larvatus</i>		F
AMNH	10674	<i>Nasalis</i> ^a	<i>larvatus</i>		M	NMNH	153802	<i>Nasalis</i>	<i>larvatus</i>		M
AMNH	28255	<i>Nasalis</i> ^a	<i>larvatus</i>		U	NMNH	198276	<i>Nasalis</i>	<i>larvatus</i>		M
AMNH	103670	<i>Nasalis</i> ^a	<i>larvatus</i>		M	NMNH	399070	<i>Nasalis</i>	<i>larvatus</i>		M
AMNH	103671	<i>Nasalis</i> ^a	<i>larvatus</i>		M	NMNH	536050	<i>Nasalis</i>	<i>larvatus</i>		F
AMNH	103689	<i>Nasalis</i> ^a	<i>larvatus</i>		F	AMNH	106273	<i>Nasalis</i> ^a	<i>larvatus</i>		M
AMNH	106272	<i>Nasalis</i> ^a	<i>larvatus</i>		M	AMNH	106275	<i>Nasalis</i> ^a	<i>larvatus</i>		M

Museum	Cat. No.	Genus	Species	Subspecies	Sex	Museum	Cat. No.	Genus	Species	Subspecies	Sex
FMNH	68684	<i>Nasalis</i> ^d	<i>larvatus</i>		M	MCZ	35607	<i>Presbytis</i>	<i>cristata</i>	<i>ultima</i>	F
NMNH	A 22954	<i>Nasalis</i>	<i>larvatus</i>		M	MCZ	35669	<i>Presbytis</i>	<i>cristata</i>	<i>ultima</i>	F
MNHN	1961-1018	<i>Ptilocolobus</i>	<i>badius</i>		F	MCZ	35671	<i>Presbytis</i>	<i>cristata</i>	<i>ultima</i>	M
NMNH	477323	<i>Ptilocolobus</i>	<i>badius</i>	<i>badius</i>	M	MCZ	35672	<i>Presbytis</i>	<i>cristata</i>	<i>ultima</i>	M
MNHN	1962-299	<i>Ptilocolobus</i>	<i>badius</i>		F	NMNH	151820	<i>Presbytis</i>	<i>frontata</i>		F
MCZ	37932	<i>Ptilocolobus</i>	<i>badius</i>	<i>langi</i>	F	NMNH	151823	<i>Presbytis</i>	<i>frontata</i>		F
MCZ	37933	<i>Ptilocolobus</i>	<i>badius</i>	<i>langi</i>	F	NMNH	151824	<i>Presbytis</i>	<i>frontata</i>		F
MCZ	37935	<i>Ptilocolobus</i>	<i>badius</i>	<i>langi</i>	F	NMNH	151825	<i>Presbytis</i>	<i>frontata</i>		M
MCZ	37936	<i>Ptilocolobus</i>	<i>badius</i>	<i>langi</i>		NMNH	154362	<i>Presbytis</i>	<i>frontata</i>		F
MCZ	37943	<i>Ptilocolobus</i>	<i>badius</i>	<i>nigrimanus</i>	M	NMNH	198831	<i>Presbytis</i>	<i>frontata</i>		M
NHMUK	40.109	<i>Ptilocolobus</i>	<i>badius</i>	<i>preussi</i>	F	NMNH	198832	<i>Presbytis</i>	<i>frontata</i>		F
NHMUK	1940.108	<i>Ptilocolobus</i>	<i>badius</i>	<i>preussi</i>	M	NMNH	198833	<i>Presbytis</i>	<i>frontata</i>		F
NHMUK	72.133	<i>Ptilocolobus</i>	<i>badius</i>	<i>tephrosceles</i>	M	MNHN	1897-1310	<i>Presbytis</i>	<i>hosei</i>	<i>everetti</i>	F
NHMUK	1030.3.1.6	<i>Ptilocolobus</i>	<i>badius</i>	<i>tephrosceles</i>	F	MCZ	37370	<i>Presbytis</i>	<i>hosei</i>	<i>hosei</i>	F
NHMUK	1901.8.9.46	<i>Ptilocolobus</i>	<i>badius</i>	<i>tephrosceles</i>	M	MCZ	37371	<i>Presbytis</i>	<i>hosei</i>	<i>hosei</i>	M
NHMUK	1930.8.1.1	<i>Ptilocolobus</i>	<i>badius</i>	<i>tephrosceles</i>	M	MCZ	35621	<i>Presbytis</i>	<i>hosei</i>	<i>sabana</i>	F
NHMUK	1930.8.1.2	<i>Ptilocolobus</i>	<i>badius</i>	<i>tephrosceles</i>	M	AMNH	106599	<i>Presbytis</i> ^d	<i>melalophos</i>		M
NHMUK	1968.7.25.1	<i>Ptilocolobus</i>	<i>badius</i>	<i>tephrosceles</i>	M	AMNH	106606	<i>Presbytis</i> ^d	<i>melalophos</i>		F
NMNH	452644	<i>Ptilocolobus</i>	<i>badius</i>	<i>tephrosceles</i>	M	AMNH	1879.8.30.6	<i>Presbytis</i> ^d	<i>melalophos</i>		M
MNHN	1967-1000	<i>Ptilocolobus</i>	<i>foai</i>	<i>oustaleti</i>	M	LNMH	1879.8.30.7	<i>Presbytis</i> ^d	<i>melalophos</i>		F
MNHN	1967-966	<i>Ptilocolobus</i>	<i>foai</i>	<i>oustaleti</i>	M	NMNH	49749	<i>Presbytis</i>	<i>melalophos</i>	<i>melalophos</i>	M
NMNH	452646	<i>Ptilocolobus</i>	<i>kirkii</i>		F	NHMUK	71.708	<i>Presbytis</i>	<i>obscurus</i>		F
NMNH	452646	<i>Ptilocolobus</i>	<i>kirkii</i>		F	NHMUK	71.709	<i>Presbytis</i>	<i>obscurus</i>		M
MNHN	1897-1305	<i>Presbytis</i>	<i>chrysomelas</i>		M	NHMUK	71.718	<i>Presbytis</i>	<i>obscurus</i>		M
NMNH	156299	<i>Presbytis</i>	<i>comata</i>		M	NHMUK	71.719	<i>Presbytis</i>	<i>obscurus</i>		F
MCZ	12728	<i>Presbytis</i>	<i>cristata</i>	<i>sondaica</i>	F	NHMUK	71.72	<i>Presbytis</i>	<i>obscurus</i>		F
MCZ	12732	<i>Presbytis</i>	<i>cristata</i>	<i>sondaica</i>	U	NMNH	151826	<i>Presbytis</i>	<i>rubicunda</i>		M
MCZ	35567	<i>Presbytis</i>	<i>cristata</i>	<i>ultima</i>	F	NMNH	292561	<i>Presbytis</i>	<i>rubicunda</i>		F
MCZ	35584	<i>Presbytis</i>	<i>cristata</i>	<i>ultima</i>	F	NMNH	252757	<i>Presbytis</i>	<i>thomasi</i>		F
MCZ	35586	<i>Presbytis</i>	<i>cristata</i>	<i>ultima</i>	F	NHMUK	71.721	<i>Presbytis</i>	<i>obscurus</i>		F
MCZ	35597	<i>Presbytis</i>	<i>cristata</i>	<i>ultima</i>	F	NHMUK	71.722	<i>Presbytis</i>	<i>obscurus</i>		M
MCZ	35603	<i>Presbytis</i>	<i>cristata</i>	<i>ultima</i>	F	NHMUK	71.733	<i>Presbytis</i>	<i>obscurus</i>		M
MCZ	35604	<i>Presbytis</i>	<i>cristata</i>	<i>ultima</i>	F	MCZ	35610	<i>Presbytis</i>	<i>cristata</i>	<i>ultima</i>	F
MCZ	35605	<i>Presbytis</i>	<i>cristata</i>	<i>ultima</i>	F	MCZ	35618	<i>Presbytis</i>	<i>cristata</i>	<i>ultima</i>	F

Museum	Cat. No.	Genus	Species	Subspecies	Sex	Museum	Cat. No.	Genus	Species	Subspecies	Sex
MCZ	35636	<i>Presbytis</i>	<i>cristata</i>	<i>ultima</i>	F	AIM	7974	<i>Pygathrix</i>	<i>nemaeus</i>		F
MCZ	35640	<i>Presbytis</i>	<i>cristata</i>	<i>ultima</i>	F	AIM	8407	<i>Pygathrix</i>	<i>nemaeus.</i>		F
NHMUK	71.735	<i>Presbytis</i>	<i>obscurus</i>		M	AIM	10753	<i>Pygathrix</i>	<i>nemaeus</i>		F
NHMUK	71.737	<i>Presbytis</i>	<i>obscurus</i>		F	AIM	10772	<i>Pygathrix</i>	<i>nemaeus</i>		F
NMNH	121673	<i>Presbytis</i>	<i>potenziani</i>		M	AIM	11036	<i>Pygathrix</i>	<i>nemaeus</i>		M
MCZ	35564	<i>Presbytis</i>	<i>rubicunda</i>		M	AIM	12100	<i>Pygathrix</i>	<i>nemaeus</i>		M
MCZ	35566	<i>Presbytis</i>	<i>rubicunda</i>		M	MNHN	1880.1152	<i>Pygathrix</i>	<i>nemaeus</i>		M
MCZ	35570	<i>Presbytis</i>	<i>rubicunda</i>			MNHN	A3845	<i>Pygathrix</i>	<i>nemaeus</i>		F
MCZ	35577	<i>Presbytis</i>	<i>rubicunda</i>		F	NMNH	256917	<i>Pygathrix</i>	<i>nemaeus</i>		M
MCZ	35596	<i>Presbytis</i>	<i>rubicunda</i>		M	NMNH	356576	<i>Pygathrix</i>	<i>nemaeus</i>		F
MCZ	35599	<i>Presbytis</i>	<i>rubicunda</i>		F	NMNH	356577	<i>Pygathrix</i>	<i>nemaeus</i>		M
MCZ	35609	<i>Presbytis</i>	<i>rubicunda</i>		F	MNHN	1929.447	<i>Rhinopithecus</i>	<i>avunculus</i>		M
MCZ	35616	<i>Presbytis</i>	<i>rubicunda</i>		M	NMNH	258986	<i>Rhinopithecus</i>	<i>roxellana</i>	<i>roxellana</i>	M
MCZ	35617	<i>Presbytis</i>	<i>rubicunda</i>		F	NMNH	268886	<i>Rhinopithecus</i>	<i>roxellana</i>	<i>roxellana</i>	F
MCZ	35624	<i>Presbytis</i>	<i>rubicunda</i>		F	NMNH	268887	<i>Rhinopithecus</i>	<i>roxellana</i>	<i>roxellana</i>	M
MCZ	35630	<i>Presbytis</i>	<i>rubicunda</i>		M	NMNH	268888	<i>Rhinopithecus</i>	<i>roxellana</i>	<i>roxellana</i>	M
MCZ	35630	<i>Presbytis</i>	<i>rubicunda</i>		M	NMNH	268889	<i>Rhinopithecus</i>	<i>roxellana</i>	<i>roxellana</i>	F
MCZ	35632	<i>Presbytis</i>	<i>rubicunda</i>		F	NMNH	268890	<i>Rhinopithecus</i>	<i>roxellana</i>	<i>roxellana</i>	U
MCZ	35632	<i>Presbytis</i>	<i>rubicunda</i>		F	NMNH	268891	<i>Rhinopithecus</i>	<i>roxellana</i>	<i>roxellana</i>	U
MCZ	35637	<i>Presbytis</i>	<i>rubicunda</i>		M	NMNH	268892	<i>Rhinopithecus</i>	<i>roxellana</i>	<i>roxellana</i>	F
MCZ	356601	<i>Presbytis</i>	<i>rubicunda</i>		M	NMNH	268893	<i>Rhinopithecus</i>	<i>roxellana</i>	<i>roxellana</i>	F
MNHN	1897-1312	<i>Presbytis</i>	<i>rubicunda</i>		F	NMNH	268894	<i>Rhinopithecus</i>	<i>roxellana</i>	<i>roxellana</i>	U
NMNH	153794	<i>Presbytis</i>	<i>rubicunda</i>	<i>carinatae</i>	M	NMNH	268895	<i>Rhinopithecus</i>	<i>roxellana</i>	<i>roxellana</i>	F
NMNH	151827	<i>Presbytis</i>	<i>rubicunda</i>	<i>rubida</i>	M	NMNH	268896	<i>Rhinopithecus</i>	<i>roxellana</i>	<i>roxellana</i>	M
NMNH	153789	<i>Presbytis</i>	<i>rubicunda</i>	<i>rubida</i>	M	NMNH	268897	<i>Rhinopithecus</i>	<i>roxellana</i>	<i>roxellana</i>	F
AIM	A.S. 1654	<i>Presbytis</i>	<i>rubicunda</i>		M	NHMUK	1908.10.9.1	<i>Rhinopithecus</i>	<i>roxellana</i>		M
AIM	6155	<i>Procolobus</i>	<i>verus</i>		M	NMNH	520675	<i>Semnopithecus</i>	<i>johnii</i>		U
MNHN	1962.178	<i>Procolobus</i>	<i>verus</i>		F	NMNH	357628	<i>Pygathrix</i>	<i>nemaeus</i>		M
MNHN	1963.1375	<i>Procolobus</i>	<i>verus</i>		F	NMNH	358107	<i>Pygathrix</i>	<i>nemaeus</i>		M
NMNH	477327	<i>Procolobus</i>	<i>verus</i>		F	NMNH	536409	<i>Pygathrix</i>	<i>nemaeus</i>		M
NMNH	477330	<i>Procolobus</i>	<i>verus</i>		M	AIM	A.S. 1823	<i>Semnopithecus</i>	<i>entellus</i>		F
MCZ	36224	<i>Pygathrix</i>	<i>nemaeus</i>	<i>nigripes</i>	F	AIM	PAL-75	<i>Semnopithecus</i>	<i>entellus</i>		M
MCZ	36259	<i>Pygathrix</i>	<i>nemaeus</i>	<i>nigripes</i>	M	LNMH	1845.1.12.453	<i>Semnopithecus</i> ^a	<i>entellus</i>		
NMNH	256916	<i>Pygathrix</i>	<i>nemaeus</i>	<i>nigripes</i>	F	LNMH	1850.8.15.5	<i>Semnopithecus</i> ^a	<i>entellus</i>		F

Museum	Cat. No.	Genus	Species	Subspecies	Sex	Museum	Cat. No.	Genus	Species	Subspecies	Sex
MNHN	1880.1154	<i>Semnopithecus</i>	<i>entellus</i>		U	MNHN	1880.1146	<i>Trachypithecus</i>	<i>auratus</i>		F
MNHN	1970.246	<i>Semnopithecus</i>	<i>entellus</i>		M	MNHN	1880-1151	<i>Trachypithecus</i>	<i>auratus</i>		U
NMNH	21843	<i>Semnopithecus</i>	<i>entellus</i>		F	MNHN	A12529	<i>Trachypithecus</i>	<i>cristatus</i>	<i>pyrrhus</i>	M
NMNH	22461	<i>Semnopithecus</i>	<i>entellus</i>		U	MNHN	1925.197	<i>Trachypithecus</i>	<i>cristatus</i>		U
NMNH	49701	<i>Semnopithecus</i>	<i>entellus</i>		M	AIM	10720	<i>Trachypithecus</i>	<i>germaini</i>		U
NMNH	A 49779	<i>Semnopithecus</i>	<i>entellus</i>		U	MNHN	1878-83	<i>Trachypithecus</i>	<i>germaini</i>		F
NMNH	A 49881	<i>Semnopithecus</i>	<i>entellus</i>		F	AIM	8070	<i>Trachypithecus</i>	<i>obscurus</i>		F
NMNH	174083	<i>Semnopithecus</i>	<i>entellus</i>		M	MCZ	35921	<i>Trachypithecus</i>	<i>obscurus</i>		U
MNHN	1925-6	<i>Semnopithecus</i>	<i>johnii</i>		F	MNHN	A10935	<i>Trachypithecus</i>	<i>obscurus</i>		M
MNHN	A3859	<i>Semnopithecus</i>	<i>johnii</i>		M	MNHN	1934-546	<i>Trachypithecus</i>	<i>phayrei</i>		M
NMNH	257005	<i>Semnopithecus</i>	<i>johnii</i>		U	MNHN	1957-103	<i>Trachypithecus</i>	<i>phayrei</i>		F
NMNH	520675	<i>Semnopithecus</i>	<i>johnii</i>		F	NMNH	49659	<i>Trachypithecus</i>	<i>phayrei</i>		F
MCZ	59278	<i>Semnopithecus</i>	<i>vetulus</i>	<i>nestor</i>	F	MCZ	35922	<i>Trachypithecus</i>	<i>phayrei</i>	<i>crepuscula</i>	F
NMNH	240702	<i>Semnopithecus</i>	<i>vetulus</i>	<i>nestor</i>	M	MCZ	37714	<i>Trachypithecus</i>	<i>phayrei</i>	<i>crepuscula</i>	F
NMNH	241547	<i>Semnopithecus</i>	<i>vetulus</i>	<i>nestor</i>	M	MCZ	37716	<i>Trachypithecus</i>	<i>phayrei</i>	<i>crepuscula</i>	M
NMNH	241549	<i>Semnopithecus</i>	<i>vetulus</i>	<i>nestor</i>	M	MCZ	37717	<i>Trachypithecus</i>	<i>phayrei</i>	<i>crepuscula</i>	F
NMNH	397723	<i>Semnopithecus</i>	<i>vetulus</i>	<i>vetulus</i>	M	MCZ	37718	<i>Trachypithecus</i>	<i>phayrei</i>	<i>crepuscula</i>	M
NMNH	399282	<i>Semnopithecus</i>	<i>vetulus</i>	<i>vetulus</i>	F	MCZ	37720	<i>Trachypithecus</i>	<i>phayrei</i>	<i>crepuscula</i>	M
NMNH	521424	<i>Semnopithecus</i>	<i>vetulus</i>	<i>vetulus</i>	F	MCZ	37722	<i>Trachypithecus</i>	<i>phayrei</i>	<i>crepuscula</i>	F
AIM	A.S. 1661	<i>Simias</i>	<i>concolor</i>		F	MCZ	37725	<i>Trachypithecus</i>	<i>phayrei</i>	<i>crepuscula</i>	F
AIM	A.S. 1558	<i>Trachypithecus</i>	<i>auratus</i>		U	MNHN	1934-238	<i>Trachypithecus</i>	<i>phayrei</i>	<i>crepuscula</i>	M

A.2 Extant cercopithecine taxa included in the comparative sample. a. Specimens measured by E. Guthrie and used with permission.

Museum	Cat. No.	Genus	Species	Subspecies	Sex	Museum	Cat. No.	Genus	Species	Subspecies	Sex
AMNH	52634	<i>Cercocebus</i> ^a	<i>agilis</i>		M	NMNH	452523	<i>Cercopithecus</i> ^a	<i>neglectus</i>		M
AMNH	52641	<i>Cercocebus</i> ^a	<i>agilis</i>		M	NMNH	452524	<i>Cercopithecus</i> ^a	<i>neglectus</i>		M
AMNH	81250	<i>Cercocebus</i> ^a	<i>agilis</i>		M	NMNH	452525	<i>Cercopithecus</i> ^a	<i>neglectus</i>		F
RMCA	5999	<i>Cercocebus</i> ^a	<i>agilis</i>		M	RMCA	RG 11526	<i>Cercopithecus</i> ^a	<i>neglectus</i>		F
RMCA	23495	<i>Cercocebus</i> ^a	<i>agilis</i>		M	RMCA	RG 1287	<i>Cercopithecus</i> ^a	<i>neglectus</i>		M
RMCA	23497	<i>Cercocebus</i> ^a	<i>agilis</i>		M	LNMH	72.25	<i>Chlorocebus</i> ^a	<i>aethiops</i>		M
RMCA	36971	<i>Cercocebus</i> ^a	<i>agilis</i>		M	LNMH	72.27	<i>Chlorocebus</i> ^a	<i>aethiops</i>		F
RMCA	23496A	<i>Cercocebus</i> ^a	<i>agilis</i>		F	LNMH	72.28	<i>Chlorocebus</i> ^a	<i>aethiops</i>		M
FMNH	51812	<i>Cercocebus</i> ^a	<i>torquatus</i>		U	LNMH	72.29	<i>Chlorocebus</i> ^a	<i>aethiops</i>		M
FMNH	73806	<i>Cercocebus</i> ^a	<i>torquatus</i>		M	LNMH	72.3	<i>Chlorocebus</i> ^a	<i>aethiops</i>		F
FMNH	73807	<i>Cercocebus</i> ^a	<i>torquatus</i>		M	LNMH	72.31	<i>Chlorocebus</i> ^a	<i>aethiops</i>		M
FMNH	73809	<i>Cercocebus</i> ^a	<i>torquatus</i>		F	LNMH	72.32	<i>Chlorocebus</i> ^a	<i>aethiops</i>		F
LNMH	1948.45	<i>Cercocebus</i> ^a	<i>torquatus</i>		M	LNMH	72.36	<i>Chlorocebus</i> ^a	<i>aethiops</i>		F
LNMH	1938.12.6.1	<i>Cercocebus</i> ^a	<i>torquatus</i>		F	LNMH	1977.3148	<i>Chlorocebus</i> ^a	<i>aethiops</i>		M
LNMH	1938.7.7.2	<i>Cercocebus</i> ^a	<i>torquatus</i>		M	LNMH	1977.3149	<i>Chlorocebus</i> ^a	<i>aethiops</i>		F
LNMH	1938.7.7.3	<i>Cercocebus</i> ^a	<i>torquatus</i>		M	UMT	UMT 137	<i>Chlorocebus</i> ^a	<i>aethiops</i>		M
LNMH	1938.7.7.4	<i>Cercocebus</i> ^a	<i>torquatus</i>		F	UMT	UMT 223	<i>Chlorocebus</i> ^a	<i>aethiops</i>		M
LNMH	1938.7.7.5	<i>Cercocebus</i> ^a	<i>torquatus</i>		F	UMT	UMT 245	<i>Chlorocebus</i> ^a	<i>aethiops</i>		M
NMNH	452551	<i>Cercopithecus</i> ^a	<i>mitis</i>	<i>stuhlmani</i>	M	UMT	UMT 246	<i>Chlorocebus</i> ^a	<i>aethiops</i>		F
AMNH	52368	<i>Cercopithecus</i> ^a	<i>mitis</i>	<i>stuhlmani</i>	M	UMT	UMT 265	<i>Chlorocebus</i> ^a	<i>aethiops</i>		F
AMNH	52420	<i>Cercopithecus</i> ^a	<i>mitis</i>	<i>stuhlmani</i>	M	NMNH	164684	<i>Erythrocebus</i>	<i>patas</i>	<i>pyrrhanotus</i>	M
NMNH	452550	<i>Cercopithecus</i> ^a	<i>mitis</i>	<i>stuhlmani</i>	F	NMNH	238072	<i>Erythrocebus</i>	<i>patas</i>		M
NMNH	452557	<i>Cercopithecus</i> ^a	<i>mitis</i>	<i>stuhlmani</i>	F	NMNH	257013	<i>Erythrocebus</i>	<i>patas</i>		F
LNMH	72.65	<i>Cercopithecus</i> ^a	<i>mitis</i>		M	NMNH	399317	<i>Erythrocebus</i>	<i>patas</i>		M
LNMH	72.66	<i>Cercopithecus</i> ^a	<i>mitis</i>		F	AMNH	34714	<i>Erythrocebus</i> ^a	<i>patas</i>	<i>pyechanatus</i>	M
RMCA	RG 11329	<i>Cercopithecus</i> ^a	<i>mitis</i>		F	AMNH	34713	<i>Erythrocebus</i> ^a	<i>patas</i>	<i>pyrrhanotus</i>	M
RMCA	RG 27963	<i>Cercopithecus</i> ^a	<i>mitis</i>		M	AMNH	38738	<i>Erythrocebus</i> ^a	<i>patas</i>	<i>pyrrhanotus</i>	M
RMCA	RG 5994	<i>Cercopithecus</i> ^a	<i>mitis</i>		F	LNMH	1968.5.11	<i>Erythrocebus</i> ^a	<i>patas</i>		F
AMNH	52421	<i>Cercopithecus</i> ^a	<i>neglectus</i>		M	RMCA	569	<i>Erythrocebus</i> ^a	<i>patas</i>		U
AMNH	52429	<i>Cercopithecus</i> ^a	<i>neglectus</i>		M	AMNH	52596	<i>Lophocebus</i> ^a	<i>albigena</i>	<i>johnstoni</i>	F
LNMH	72.48	<i>Cercopithecus</i> ^a	<i>neglectus</i>		F	AMNH	52603	<i>Lophocebus</i> ^a	<i>albigena</i>	<i>johnstoni</i>	M
NMNH	452520	<i>Cercopithecus</i> ^a	<i>neglectus</i>		F	AMNH	52598	<i>Lophocebus</i> ^a	<i>albigena</i>	<i>johnstoni</i>	M

Museum	Cat. No.	Genus	Species	Subspecies	Sex	Museum	Cat. No.	Genus	Species	Subspecies	Sex
NMNH	452522	<i>Cercopithecus</i> ^a	<i>neglectus</i>		F	AMNH	52627	<i>Lophocebus</i> ^a	<i>albigena</i>	<i>johnstoni</i>	M
KNM	452499	<i>Lophocebus</i> ^a	<i>albigena</i>	<i>johnstoni</i>	M	NMNH	49691	<i>Macaca</i> ^a	<i>nemistrina</i>		M
NMNH	164578	<i>Lophocebus</i> ^a	<i>albigena</i>	<i>johnstoni</i>	F	NMNH	49696	<i>Macaca</i> ^a	<i>nemistrina</i>		M
KNM	452499	<i>Lophocebus</i> ^a	<i>albigena</i>	<i>johnstoni</i>	M	NMNH	49874	<i>Macaca</i> ^a	<i>nemistrina</i>		M
NMNH	164578	<i>Lophocebus</i> ^a	<i>albigena</i>	<i>johnstoni</i>	F	NMNH	258230	<i>Macaca</i> ^a	<i>nemistrina</i>		F
NMNH	164579	<i>Lophocebus</i> ^a	<i>albigena</i>	<i>johnstoni</i>	M	NMNH	305069	<i>Macaca</i> ^a	<i>nemistrina</i>		F
NMNH	164580	<i>Lophocebus</i> ^a	<i>albigena</i>	<i>johnstoni</i>	F	AMNH	60160	<i>Macaca</i> ^a	<i>thibetana</i>		M
NMNH	452498	<i>Lophocebus</i> ^a	<i>albigena</i>	<i>johnstoni</i>	F	FMNH	39499	<i>Macaca</i> ^a	<i>thibetana</i>		M
NMNH	452500	<i>Lophocebus</i> ^a	<i>albigena</i>	<i>johnstoni</i>	M	FMNH	39500	<i>Macaca</i> ^a	<i>thibetana</i>		F
NMNH	452501	<i>Lophocebus</i> ^a	<i>albigena</i>	<i>johnstoni</i>	F	NMNH	241162	<i>Macaca</i> ^a	<i>thibetana</i>		U
NMNH	452503	<i>Lophocebus</i> ^a	<i>albigena</i>	<i>johnstoni</i>	M	NMNH	241163	<i>Macaca</i> ^a	<i>thibetana</i>		M
NMNH	452502	<i>Lophocebus</i> ^a	<i>albigena</i>		M	NMNH	254800	<i>Macaca</i> ^a	<i>thibetana</i>		M
RMCA	1282	<i>Lophocebus</i> ^a	<i>albigena</i>		F	NMNH	258649	<i>Macaca</i> ^a	<i>thibetana</i>		M
RMCA	1782	<i>Lophocebus</i> ^a	<i>albigena</i>		M	NMNH	258650	<i>Macaca</i> ^a	<i>thibetana</i>		F
RMCA	5969	<i>Lophocebus</i> ^a	<i>albigena</i>		M	NMNH	258651	<i>Macaca</i> ^a	<i>thibetana</i>		M
RMCA	5998	<i>Lophocebus</i> ^a	<i>albigena</i>		M	NMNH	258686	<i>Macaca</i> ^a	<i>thibetana</i>		M
RMCA	12250	<i>Lophocebus</i> ^a	<i>albigena</i>		M	MNHN	1880-1306	<i>Mandrillus</i>	<i>leucophaeus</i>		F
RMCA	27746	<i>Lophocebus</i> ^a	<i>albigena</i>		M	MNHN	1917-17	<i>Mandrillus</i>	<i>leucophaeus</i>		M
RMCA	29107	<i>Lophocebus</i> ^a	<i>albigena</i>		M	MNHN	1940-1195	<i>Mandrillus</i>	<i>leucophaeus</i>		M
RMCA	37572	<i>Lophocebus</i> ^a	<i>albigena</i>		M	MNHN	1940-712	<i>Mandrillus</i>	<i>leucophaeus</i>		F
RMCA	RG 6002	<i>Lophocebus</i> ^a	<i>albigena</i>		M	AIM	PAL 109	<i>Mandrillus</i>	<i>sphinx</i>		M
AMNH	30622	<i>Macaca</i> ^a	<i>fascicularis</i>		F	MNHN	1934-1418	<i>Mandrillus</i>	<i>sphinx</i>		M
AMNH	103659	<i>Macaca</i> ^a	<i>fascicularis</i>		M	MNHN	1985-1995	<i>Mandrillus</i>	<i>sphinx</i>		F
AMNH	175460	<i>Macaca</i> ^a	<i>fascicularis</i>		M	MNHN	1995-238	<i>Mandrillus</i>	<i>sphinx</i>		F
AMNH	193654	<i>Macaca</i> ^a	<i>fascicularis</i>		F	MNHN	CG 1916-77	<i>Mandrillus</i>	<i>sphinx</i>		F
FMNH	65451	<i>Macaca</i> ^a	<i>fascicularis</i>		F	MNHN	CG 1962-4123	<i>Mandrillus</i>	<i>sphinx</i>		F
NMH	1910.12.24.1	<i>Macaca</i> ^a	<i>fascicularis</i>		F	LNMH	49.82	<i>Mandrillus</i> ^a	<i>leucophaeus</i>		M
NMNH	308723	<i>Macaca</i> ^a	<i>fascicularis</i>		U	LNMH	49.83	<i>Mandrillus</i> ^a	<i>leucophaeus</i>		F
NMNH	308725	<i>Macaca</i> ^a	<i>fascicularis</i>		U	LNMH	82.492	<i>Mandrillus</i> ^a	<i>leucophaeus</i>		M
NMNH	458727	<i>Macaca</i> ^a	<i>fascicularis</i>		U	LNMH	1949.86	<i>Mandrillus</i> ^a	<i>leucophaeus</i>		F
NMNH	573504	<i>Macaca</i> ^a	<i>fascicularis</i>		M	LNMH	1944.85a	<i>Mandrillus</i> ^a	<i>leucophaeus</i>		F
NMNH	1847.121.11.5	<i>Macaca</i> ^a	<i>fascicularis</i>		M	AMNH	89358	<i>Mandrillus</i> ^a	<i>sphinx</i>		F
AMNH	106563	<i>Macaca</i> ^a	<i>nemistrina</i>		M	AMNH	89364	<i>Mandrillus</i> ^a	<i>sphinx</i>		M
AMNH	106564	<i>Macaca</i> ^a	<i>nemistrina</i>		M	AMNH	89367	<i>Mandrillus</i> ^a	<i>sphinx</i>		F

Museum	Cat. No.	Genus	Species	Subspecies	Sex	Museum	Cat. No.	Genus	Species	Subspecies	Sex
AMNH	282256	<i>Macaca</i> ^a	<i>nemistrina</i>		M	AMNH	170364	<i>Mandrillus</i> ^a	<i>sphinx</i>		M
FMNH	99688	<i>Macaca</i> ^a	<i>nemistrina</i>		F	AMNH	170366	<i>Mandrillus</i> ^a	<i>sphinx</i>		U
AMNH		<i>Mandrillus</i> ^a	<i>sphinx</i>		F	AMNH	52668	<i>Papio</i> ^a	<i>anubis</i>	<i>anubis</i>	F
FMNH	105658	<i>Macaca</i> ^a	<i>nemistrina</i>		F	LNMH	1948.8.3.2	<i>Papio</i> ^a	<i>anubis</i>	<i>tessellatus</i>	M
LNMH	1948.7.6.2	<i>Mandrillus</i> ^a	<i>sphinx</i>		M	LNMH	35.2.14.1	<i>Papio</i> ^a	<i>anubis</i>	<i>tessellatus</i>	M
NMNH	30.12.15.9	<i>Mandrillus</i> ^a	<i>sphinx</i>		M	FMNH	18868	<i>Papio</i> ^a	<i>anubis</i>		M
MCZ	23197	<i>Miopithecus</i>	<i>talapoin</i>		M	KNM	KNM OM 3141	<i>Papio</i> ^a	<i>anubis</i>		F
MCZ	60963	<i>Miopithecus</i>	<i>talapoin</i>		M	KNM	KNM OM 5061	<i>Papio</i> ^a	<i>anubis</i>		M
MCZ	60983	<i>Miopithecus</i>	<i>talapoin</i>		M	KNM	KNM OM 5068	<i>Papio</i> ^a	<i>anubis</i>		M
MCZ	60984	<i>Miopithecus</i>	<i>talapoin</i>		M	KNM	KNM OM 6264	<i>Papio</i> ^a	<i>anubis</i>		F
MCZ	61323	<i>Miopithecus</i>	<i>talapoin</i>		F	KNM	KNM OM 6271	<i>Papio</i> ^a	<i>anubis</i>		F
MCZ	21160	<i>Papio</i>	<i>anubis</i>		M	LNMH	72.127	<i>Papio</i> ^a	<i>anubis</i>		M
MCZ	21161	<i>Papio</i>	<i>anubis</i>		M	LNMH	1901.8.9.23	<i>Papio</i> ^a	<i>anubis</i>		F
NMNH	236976	<i>Papio</i>	<i>anubis</i>		M	LNMH	1940.1.20.21	<i>Papio</i> ^a	<i>anubis</i>		M
NMNH	239743	<i>Papio</i>	<i>anubis</i>		U	LNMH	1962.12.14.6	<i>Papio</i> ^a	<i>anubis</i>		F
NMNH	384228	<i>Papio</i>	<i>anubis</i>		M	RMCA	RG 1285	<i>Papio</i> ^a	<i>anubis</i>		M
NMNH	384234	<i>Papio</i>	<i>anubis</i>		M	RMCA	RG 2230	<i>Papio</i> ^a	<i>anubis</i>		M
AIM	677	<i>Papio</i>	<i>hamadryas</i>		F	RMCA	RG 6149	<i>Papio</i> ^a	<i>anubis</i>		M
AIM	6781	<i>Papio</i>	<i>hamadryas</i>		M	AMNH	201008	<i>Theropithecus</i> ^a	<i>gelada</i>		M
AIM	6785	<i>Papio</i>	<i>hamadryas</i>		M	FMNH	27040	<i>Theropithecus</i> ^a	<i>gelada</i>		M
AIM	6819	<i>Papio</i>	<i>hamadryas</i>		F	HERC	HKNM-ERC 108	<i>Theropithecus</i> ^a	<i>gelada</i>		M
AIM	6935	<i>Papio</i>	<i>hamadryas</i>		M	HERC	HKNM-ERC 109	<i>Theropithecus</i> ^a	<i>gelada</i>		M
AIM	6936	<i>Papio</i>	<i>hamadryas</i>		M	HERC	HKNM-ERC 110	<i>Theropithecus</i> ^a	<i>gelada</i>		F
AIM	PL 102	<i>Papio</i>	<i>ursinus</i>		F	HERC	HKNM-ERC 113	<i>Theropithecus</i> ^a	<i>gelada</i>		F

APPENDIX B

B.1 All humeral indices calculated for fossil Cercopithecidae specimens. a. Specimen measurements made by E. Guthrie and used with permission.

HUMERUS												
Taxon	Museum	Cat. No.	Sex	IH1	IH2	IH3	IH4	IH5	IH6	IH7	IH8	IH9
<i>Cercopithecoides kimeui</i>	KNM	KNM-ER 176	M	.	115.49
	NME	AL577-1	Unk	.	.	.	-19.18	64.19	58.74	.	16.09	74.93
<i>Cercopithecoides meaveae</i>	NME	AL2	M	.	108.51	.	-14.53	60.77	53.90	.	12.68	74.00
<i>Cercopithecoides williamsi</i>	KNM	KNM-ER 4420	M	100.93	90.24	12.47	-12.29	55.92	63.54	20.22	10.95	63.49
<i>Cf. Cercopithecoides</i>	KNM	KNM-ER 39261	Unk	87.36
<i>Paracolobus chemeroni</i>	KNM	BC 3	M	99.42	92.00	9.76	-14.02	68.63	60.73	16.96	12.30	90.26
<i>Paracolobus mutiwa</i>	KNM	WT 16827	M	.	.	12.27	-12.89	46.09	52.31	20.32	11.42	78.10
	NME	L895-1	M	100.88	.	.	-17.63	43.00	43.13	19.73	14.98	.
<i>Rhinocolobus turkanensis</i>	NME	AL300-1	Unk	.	.	.	-15.41	43.60	49.14	.	13.36	86.44
	KNM	KNM-ER 1542	M	.	109.98	.	-15.21	53.29	46.28	.	13.20	65.48
	KNM	KNM-ER 16	Unk	.	.	.	-22.53	58.67	44.48	.	18.39	70.82
	KNM	KNM-ER 40076	Unk	.	95.15
	KNM	KNM-ER 45611	Unk	.	.	.	-14.48	47.30	38.86	.	12.65	.
<i>Cf. Rhinocolobus sp. indet.</i>	KNM	KNM-ER 12	Unk	.	.	.	-18.48	55.67	44.28	.	15.60	55.59
<i>Theropithecus brumpti</i>	KNM	KNM-ER 3013 ^a	Unk	.	.	.	-18.48	62.51	50.79	.	15.60	77.59
	KNM	KNM-ER 3013 ^a	Unk	.	.	.	-15.42	60.53	58.58	.	13.36	93.97
	KNM	KNM-ER 3084 ^a	Unk	.	102.41
	KNM	KNM-WT 38669 ^a	Unk	.	.	.	-13.98	67.23	61.26	.	12.26	52.75
	KNM	KNM-WT 38736 ^a	Unk	.	.	.	-12.33	70.87	53.20	.	10.98	66.01
	KNM	KNM-WT 38738 ^a	Unk	99.85	105.03	.	-13.75	62.64	58.35	18.97	12.09	56.92
	KNM	KNM-WT 38738 ^a	Unk	.	99.95
	KNM	KNM-WT 39368 ^a	M	99.86	120.02	14.00	-12.82	.	65.73	20.81	11.37	88.59
	HERC	L 865 ^a	Unk	.	.	.	-17.44	71.20	.	.	14.85	72.79
<i>Theropithecus oswaldi darti</i>	HERC	AL 163-10 ^a	Unk	.	.	.	-19.83	67.79	55.17	.	16.55	79.68
	HERC	AL 285-11a ^a	Unk	.	.	.	-15.21	78.07	64.34	.	13.20	87.30

HUMERUS												
Taxon	Museum	Cat. No.	Sex	IH1	IH2	IH3	IH4	IH5	IH6	IH7	IH8	IH9
	HERC	AL 322-10 ^a	Unk	.	.	.	-13.15	66.39	67.72	.	11.63	93.29
	UO	AI 196-3C ^a	Unk	.	.	.	-20.48	66.77	64.12	.	17.00	98.21
	UO	AL 285-11a ^a	Unk	.	.	.	-15.16	64.65	62.93	.	13.16	77.21
	UO	AL100-264 ^a	Unk	.	.	.	-21.20	67.75	56.41	.	17.49	84.47
	UO	AL100-265 ^a	Unk	.	.	.	-14.74	62.14	51.26	.	12.84	.
	UO	AL1450-16 ^a	Unk	.	.	.	-23.34	71.56	66.91	.	18.93	80.91
<i>Theropithecus oswaldi</i>	NME	AL116-2A	Unk	.	114.74
	NME	AL126-108	Unk	.	.	.	-11.96	54.17	49.03	.	10.68	79.81
	NME	AL304-2	Unk	.	117.43
	NME	AL431-1	Unk
	NME	L16-59p	Unk	.	.	.	-19.15	69.92	52.23	.	16.07	83.46
	NME	L879-1	Unk	.	.	.	-17.68	56.35	48.66	.	15.03	87.32
	NME	Omo No Label A	Unk	.	.	.	-10.02	45.07	53.02	.	9.11	55.15
	HERC	AL 285-11b ^a	Unk	.	98.50
	KNM	KNM-ER 13 ^a	Unk	.	.	.	-9.97	64.02	57.48	.	9.06	80.67
	KNM	KNM-ER 13 ^a	Unk	.	97.29
	KNM	KNM-ER 18917 ^a	Unk	101.10	99.40	12.38	-17.07	70.93	58.48	18.71	14.58	77.44
	KNM	KNM-ER 40064 ^a	F	.	.	.	-18.73	65.69	59.67	.	15.78	92.89
	KNM	KNM-ER 45657 ^a	Unk	.	.	.	-23.94	61.87	51.34	.	19.32	79.80
	KNM	KNM-ER 5491 ^a	Unk	.	95.69	.	-13.10	61.83	61.30	.	11.58	57.16
	KNM	KNM-ER 567 ^a	Unk	.	96.61
	KNM	KNM-ER 601 ^a	Unk	.	88.88
	KNM	KNM-ER 7331 ^a	Unk	.	.	.	-14.20	62.84	47.98	.	12.44	.
	KNM	KNM-ER 866 ^a	Unk	.	94.21
	KNM	KNM-OG 1056 ^a	Unk	.	.	.	-12.86	69.92	45.41	.	11.40	76.06
	KNM	KNM-OG 1062 ^a	Unk	77.58	.	.	.	78.31
	KNM	KNM-OG 1064 ^a	Unk	58.24
	KNM	KNM-OG 1318 ^a	Unk	63.29

HUMERUS												
Taxon	Museum	Cat. No.	Sex	IH1	IH2	IH3	IH4	IH5	IH6	IH7	IH8	IH9
	KNM	KNM-OG 1461 ^a	Unk	92.31
	KNM	OLD 067 ^a	M	100.94	91.18	14.33	-15.76	72.92	57.00	22.33	13.61	67.78
	LNMH	M11542 ^a	M	66.53	.	.	.	79.18
	LNMH	M11543 ^a	F	.	.	.	-6.34	58.74	56.68	.	5.96	68.85
	LNMH	M18721 ^a	Unk	.	.	.	-8.15	70.99	66.77	.	7.54	67.99
	LNMH	M18789 ^a	Unk	.	.	.	-10.74	68.87	58.50	.	9.70	87.69
<i>?Theropithecus oswaldi</i>	NME	AL116-24	Unk	.	110.37
	NME	AL126-106	Unk	.	111.45
	NME	AL133-1	Unk	.	98.30
	NME	AL137-49	Unk	.	.	.	-13.54	62.20	60.12	.	11.93	99.51
	NME	AL145-16	Unk	.	.	.	-17.65	71.05	59.39	.	15.00	92.01
	NME	AL154-92	Unk	.	.	.	-18.91	62.71	51.03	.	15.91	73.00
	NME	AL158-125	Unk	.	.	.	-13.98	61.27	62.29	.	12.27	66.65
	NME	AL163-10	Unk	.	.	.	-18.32	54.86	55.52	.	15.49	80.37
	NME	AL201-2	Unk	.	108.83
	NME	AL204-3	Unk	.	.	.	-14.37	70.72	58.56	.	12.56	82.08
	NME	AL213-2	Unk	.	116.04
	NME	AL223-24	Unk	.	100.95
	NME	AL244-2	Unk	.	.	.	-11.54	64.88	57.34	.	10.34	78.66
	NME	AL259-1	Unk	.	.	.	-14.04	74.21	63.47	.	12.31	66.62
	NME	AL285-11	Unk	.	97.67	.	-19.09	64.05	57.75	.	16.03	95.30
	NME	AL286-2	Unk	.	.	.	-12.89	50.59	64.54	.	11.42	93.37
	NME	AL322-10	Unk	.	.	.	-10.87	63.33	61.20	.	9.81	94.63
	NME	AL402-1	Unk	.	105.67
	NME	AL693-1	Unk	.	98.81	.	-20.25	49.78	59.02	.	16.84	92.90
	NME	AL700-5	Unk	.	97.61

B.2 All radial indices calculated for fossil Cercopithecidae specimens. a. Specimen measurements made by E. Guthrie and used with permission.

RADIUS						
Taxon	Museum	Cat No.	Sex	Side	IR1	IR2
<i>Cercopithecoides kimeui</i>	KNM	ER 176	M	R	90.79	60.02
<i>Cercopithecoides meaveae</i>	NME	AL2	M	L	88.53	27.60
<i>Cercopithecoides williamsi</i>	KNM	ER 4420	M	L	113.10	44.33
<i>Microcolobus tugenensis</i>	KNM	NA 47915	Unk	R	91.94	34.57
<i>Paracolobus chemeroni</i>	KNM	KNM-BC 3	M	L	99.22	43.16
<i>Paracolobus mutiwa</i>	NME	L895-1	M	L	102.90	49.20
<i>Theropithecus brumpti</i>	KNM	KNM-WT 17554 ^a	Unk	L	93.12	.
	KNM	KNM-WT 39368 ^a	M	R	88.03	60.48
<i>Theropithecus oswaldi</i>	KNM	KNM-ER 18917 ^a	Unk	L	97.64	56.99
	KNM	KNM-ER 28 ^a	Unk	L	85.79	75.63
	KNM	KNM-ER 3876 ^a	Unk	L	101.87	60.34
	KNM	KNM-ER 866 ^a	Unk	L	102.24	54.62
	KNM	OLD 067 ^a	M	R	95.39	50.27
	LNMH	M11544 ^a	F	R	94.04	45.07
	LNMH	M18801 ^a	Unk	R	107.36	44.63
	LNMH	M18802 ^a	Unk	L	97.20	50.24
<i>?Theropithecus oswaldi</i>	NME	AL431-1	Unk	L	94.07	44.45
	NME	AL133-3	Unk	R	103.45	34.85
<i>cf. Rhinocolobus sp. indet.</i>	NME	AL411-9	Unk	R	97.22	37.75
	KNM	ER 40081	Unk	R	98.07	44.37

B.3 All ulnar indices calculated for fossil Cercopithecidae specimens. a. Specimen measurements made by E. Guthrie and used with permission.

ULNA									
Taxon	Museum	Cat No.	Sex	Side	IU1	IU2	IU3	IU4	IU5
<i>Cercopithecoides kimeui</i>	KNM	ER 176	M	L	202.95
<i>Cercopithecoides meaveae</i>	NME	AL2	M	L	92.14	111.71	203.96	107.84	189.14
<i>Cercopithecoides williamsi</i>	KNM	ER 4420	M	L	.	.	171.66	98.94	173.51
<i>cf. Cercopithecoides</i>	KNM	ER 39355	Unk	R	71.38	103.08	204.55	104.55	195.64
<i>Paracolobus chemeroni</i>	KNM	BC 3	M	L	103.27	96.21	137.87	80.58	171.09
<i>Paracolobus mutiwa</i>	NME	L895-1&2	M	R	112.77	118.02	137.87	80.62	171.00
	KNM	WT 16827	M	R	.	.	153.27	87.17	175.83
<i>Rhinocolobus turkanensis</i>	KNM	ER 1542	M	L	103.96	98.79	134.16	94.31	142.26
	KNM	ER 5488	Unk	R	117.09	100.27	139.94	80.08	174.74
<i>Theropithecus brumpti</i>	KNM	KNM-ER 3013 ^a	Unk	Unk	98.50	85.47	122.73	85.76	143.12
	KNM	KNM-ER 30316 ^a	Unk	R	217.18	118.36	50.05	.	.
	KNM	KNM-ER 3084 ^a	Unk	R	126.62	106.76	133.83	77.40	172.91
	KNM	KNM-WT 17560 ^a	Unk	R	106.67	106.48	117.93	86.98	135.59
	KNM	KNM-WT 38669 ^a	Unk	R	.	119.22	.	.	.
	KNM	KNM-WT 39368 ^a	M	L	135.65	114.03	.	.	.
<i>Theropithecus oswaldi</i>	KNM	KNM-ER 13 ^a	Unk	L	.	.	83.84	61.11	137.19
	KNM	KNM-ER 18917 ^a	Unk	L	84.77	99.18	194.29	91.86	211.51
	KNM	KNM-ER 28 ^a	Unk	L	.	118.74	.	.	.
	KNM	KNM-ER 3876 ^a	Unk	R	.	.	138.76	71.50	194.07
	KNM	KNM-ER 3877 ^a	Unk	R	.	110.02	.	.	191.04
	KNM	KNM-ER 40423 ^a	Unk	L	119.59	121.81	198.92	85.82	231.80
	KNM	KNM-ER 46 ^a	Unk	R	286.62	266.88	169.52	86.08	196.93
	KNM	KNM-ER 5491 ^a	Unk	L	126.50	123.74	138.91	85.58	162.31
	KNM	KNM-ER 567 ^a	Unk	L	96.24	134.01	195.09	97.06	201.00
	KNM	KNM-ER 866 ^a	Unk	L	108.04	108.30	149.94	84.55	177.34
KNM	OLD 067 ^a	M	R	140.99	125.22	134.25	76.22	176.14	

ULNA									
Taxon	Museum	Cat No.	Sex	Side	IU1	IU2	IU3	IU4	IU5
	LNMH	M11546 ^a	M	L	148.02	124.28	126.49	72.90	173.51
	LNMH	M18723 ^a	Unk	L	147.51	130.62	133.47	73.46	181.70
	LNMH	M18724 ^a	Unk	L	121.47	111.62	162.06	88.13	183.89
	LNMH	M18726 ^a	Unk	R	140.11	129.15	143.66	74.63	192.49
	LNMH	M18803 ^a	Unk	L	.	.	141.29	88.66	159.36
	NME	AL431-1	Unk	R	143.01	113.43	160.43	83.18	192.87
	NME	L193-42	Unk	R	130.45	110.47	180.93	88.16	205.22
	NME	Omo Ulna No Label	Unk	L	114.27	126.08	163.43	99.83	163.71
<i>?Theropithecus oswaldi</i>	NME	AL126-32	Unk	L	138.17	136.43	165.60	89.36	185.32
	NME	AL133-1	Unk	R	111.15	111.81	187.50	97.13	193.03
<i>Theropithecus oswaldi darti</i>	HERC	AL 309-4 ^a	Unk	R	109.88	.	126.45	.	.
	HERC	AL 332-29 ^a	Unk	L	130.87	126.87	109.20	73.45	148.67
	UO	AL100 397 ^a	Unk	R	117.61	104.82	122.79	86.19	142.47
	UO	AL100-271 ^a	Unk	L	.	111.10	.	.	.

B.4 All os coxae indices calculated for fossil Cercopithecidae specimens. a. Specimen measurements made by E. Guthrie and used with permission.

OS COXAE					
Taxon	Museum	Cat No.	Sex	Side	IL7
<i>Paracolobus chemeroni</i>	KNM	KNM-BC 3Z	M		5.99
<i>Paracolobus mutiwa</i>	KNM	KNM-WT 16827	M		6.22
<i>Theropithecus brumpti</i>	KNM	KNM-TH 46700 ^a	F		5.53
<i>Theropithecus oswaldi</i>	KNM	KNM-ER 866 ^a	Unk		6.49
	KNM	KNM-OLD 067 ^a	M		6.74

B.5 All femoral indices calculated for fossil Cercopithecidae specimens. a. Specimen measurements made by E. Guthrie and used with permission.

FEMUR															
Taxon	Museum	Cat No.	Sex	Side	IF1	IF2	IF3	IF4	IF5	IF6	IF7	IF8	IF9	IF10	IF11
<i>Cercopithecoides meaveae</i>	NME	AL2	M	L	54.0	127.1	.	78.6	100.1	131.7	93.4
<i>Cercopithecoides williamsi</i>	KNM	ER 4420	M	R	48.4
<i>Cercopithecoides cf. williamsi</i>	KNM	ER 974	Unk	L	9.2	20.7	4.2	3.8	43.0	138.9	5.6	72.9	105.3	156.2	101.1
<i>cf. Cercopithecoides</i>	KNM	ER 37117	Unk	L	54.6
<i>Paracolobus chemeroni</i>	KNM	BC 3	M	R	9.4	19.1	3.1	3.1	30.1	110.6	6.9	76.4	78.1	135.0	84.5
<i>Paracolobus mutiwa</i>	KNM	KNM-WT 16827	M	R	48.9
	NME	L895-1	M	R	10.2	22.8	5.1	.	42.0	121.4	8.6	71.1	111.1	110.3	94.7
<i>cf. Rhinocolobus sp. indet</i>	KNM	ER 40078	Unk	R	54.8
	KNM	ER 551	Unk	L	37.0
<i>Theropithecus brumpti</i>	KNM	KNM-ER 3013 ^a	Unk	R	49.2
	KNM	KNM-ER 2022 ^a	Unk	L	59.2
	KNM	KNM-TH 46700 ^a	F	R	9.1	21.6	6.1	4.7	53.0	119.8	10.3	92.4	93.8	110.3	90.3
<i>Theropithecus oswaldi</i>	KNM	KNM-ER 13 ^a	Unk	L	48.4
	KNM	KNM-ER 866 ^a	Unk	R	73.1
	KNM	KNM-WT 19636 ^a	Unk	R	121.4	.	94.3	87.6	100.9	90.5
	KNM	KNM-OG 1075 ^a	Unk	L	71.4
	KNM	KNM-ER 978 ^a	Unk	R	113.6	.	97.9	97.0	120.4	79.5
	KNM	KNM-WT 14663	Unk	R	119.4	.	89.5	85.3	115.0	84.3
	KNM	KNM-ER 3877 ^a	Unk	L	136.3	.	101.4	90.1	117.4	88.1
	NME	L345-21a	Unk	L	61.8
	KNM	KNM-WT 14656 ^a	Unk	L	124.2	.	82.1	88.1	114.1	72.2
	KNM	KNM-OG 1088 ^a	Unk	R	.	24.5	7.6
	KNM	KNM-WT 19676 ^a	Unk	L	60.2
	KNM	KNM-ER 28 ^a	Unk	R	9.1	21.7	6.8	4.4	74.4	121.1	8.8	91.5	86.2	96.4	83.7
	KNM	OLD 067 ^a	M	L	114.7	.	89.9	86.0	110.3	81.5

B.6 All tibial indices calculated for fossil Cercopithecidae specimens. a. Specimen measurements made by E. Guthrie and used with permission.

TIBIA											
Taxon	Museum	Cat No.	Sex	Side	IT1	IT2	IT3	IT4	IT5	IT6	TTSA
<i>Paracolobus mutiwa</i>	NME	L895-1	Unk	R	81.6	.	.	3.6	.	104.9	257.3
<i>Cercopithecoides meaveae</i>	NME	AL2	M	L	78.1	106.3	92.9	.	.	93.4	265.2
<i>Rhinocolobus cf. turkanensis</i>	KNM	ER 40058	Unk	R	101.4	230.9
<i>Paracolobus chemeroni</i>	KNM	KNM BC 3	Unk	L	82.8	105.3	86.0	5.0	4.0	99.7	447.3
<i>Rhinocolobus turkanensis</i>	KNM	ER 1542	M	R	75.6	89.8	100.3	.	.	96.5	346.2
	KNM	ER 40074	Unk	L	75.2	94.1	87.6
	KNM	ER 45613	Unk	R	77.5	93.1	89.2	1.6	4.9	94.5	339.2
<i>Rhinocolobus cf. turkanensis</i>	KNM	ER 5481	Unk	R	85.7	106.9	84.2
<i>cf. Rhinocolobus sp. Indet.</i>	KNM	ER 40077	Unk	R	88.2	266.6
<i>Theropithecus brumpti</i>	KNM	KNM-ER2022 ^a	Unk	L	.	120.1	82.5
	KNM	KNM-WT39368 ^a	M	R	.	.	.	3.8	4.6	.	.
	KNM	KNM-WT38732 ^a	Unk	R	80.1	105.5	74.6
	KNM	KNM-TH46700 ^a	F	R	73.6	110.2	74.1	5.6	4.1	100.0	299.3
<i>Theropithecus oswaldi</i>	LNMH	M18718 ^a	Unk	R	89.2	313.3
	KNM	KNM-ER 13 ^a	Unk	L	105.7	320.0
	KNM	KNM-ER 28 ^a	Unk	L	74.4	97.0	82.3	5.0	4.4	116.3	248.2
	KNM	KNM-ER 3877 ^a	Unk	R	77.7	.	83.0	.	.	101.9	233.6
	KNM	KNM-ER 3823 ^a	Unk	R	101.5	300.7
	KNM	KNM-ER 45661 ^a	Unk	R	79.7	96.2	82.1
	KNM	KNM-ER 5272 ^a	Unk	L	95.5	505.1
	KNM	KNM-ER 5491 ^a	Unk	L	81.5	108.9	79.3	4.5	4.3	99.6	353.3
	KNM	KNM-ER 597 ^a	Unk	L	83.4	111.9	83.9	.	.	88.4	293.0
	KNM	KNM-ER 866 ^a	Unk	R	85.6	.	.	4.6	5.1	107.7	558.5
	KNM	KNM-ER 866 ^a	Unk	L	71.0	108.4	82.4
	KNM	KNM-ER 978 ^a	Unk	R	79.1	103.2	84.3
	KNM	KNM-ER 978 ^a	Unk	L	95.6	275.8
	KNM	KNM-OG1109 ^a	Unk	L	95.6	341.5
KNM	OLD 067 ^a	M	R	81.1	104.8	71.3	5.5	5.0	88.5	457.5	
NME	AL 431-1	Unk	R	78.4	70.5	67.9	6.0	3.9	103.6	248.6	

B.7 All astragalar and calcaneal indices calculated for fossil Cercopithecidae specimens. a. Specimen measurements made by E. Guthrie and used with permission. b. Specimen measurements made by S. Frost and used with permission.

ASTRAGALUS								
Taxon	Museum	Cat No.	Sex	Side	IT1	IT2	IT3	
<i>Paracolobus mutiwa</i>	KNM	KNM-WT 16827	M	2	78.8	92.7	74.0	
<i>cf. Cercopithecoides</i>	KNM	KNM-ER 30320	Unk	1	87.8	86.3	77.0	
<i>Paracolobus chemeroni</i>	KNM	BC 3	M	2	88.7	91.1	73.1	
<i>Theropithecus brumpti</i>	KNM	KNM-WT 17554 ^a	Unk	1	70.1	94.8	78.6	
<i>Theropithecus oswaldi</i>	LNMH	M11549 ^a	Unk	2	65.4	93.8	71.3	
	KNM	KNM-OG 948 ^a	Unk	1	63.3	86.0	87.8	
	KNM	KNM-OG 1195 ^a	Unk	1	74.1	91.4	85.7	
	KNM	KNM-ER 3876 ^a	Unk	1	62.1	92.1	74.6	
CALCANEUS								
Taxon	Museum	Cat No.	Sex	Side	IC1	IC2	IC3	IC4
<i>Paracolobus mutiwa</i>	NME	L895-1&2	M	L	31.3	34.0	26.4	38.0
	KNM	WT 16827	M	L	30.4	33.3	24.3	36.2
<i>Paracolobus chemeroni</i>	KNM	BC 3	M	L	38.0	29.7	18.3	38.6
<i>Theropithecus brumpti</i>	KNM	KNM-WT 38724	Unk	L	51.2	27.8	27.0	34.7
	HERC	L 865 ^b	Unk	L	26.3	34.0	21.9	36.7
<i>Theropithecus oswaldi</i>	KNM	NMZ OLD 067 ^a	M	L	24.1	32.6	19.3	40.7
	LNMH	M11549 ^a	Unk	L	35.5	33.9	22.4	34.7
	KNM	KNM-ER 44378 ^a	Unk	R	28.6	34.7	21.8	33.6
	KNM	KNM-OG 1192 ^a	Unk	R	30.2	37.2	23.7	35.1

REFERENCES CITED

- Alemseged Z. 2003. An integrated approach to taphonomy and faunal change in Shungura Formation (Ethiopia) and its implication for hominid evolution. *Journal of Human Evolution* 44, 461–478.
- Alemseged Z, Bobe R, Geraads D. 2007. Comparability of fossil data and its significance for the interpretation of hominin environments. In *Hominin environments in the East African Pliocene: An assessment of the faunal evidence*. Dordrecht: Springer. pp. 159-181.
- Anderson, M., 2019. An assessment of the postcranial skeleton of the *Paracolobus mutiwa* (Primates: Colobinae) specimen KNM-WT 16827 from Lomekwi, West Turkana, Kenya. *Journal of Human Evolution* (In Review).
- Anderson, M., Frost, S.R., 2016. Pedal Functional Morphology of *Paracolobus chemeroni*. *American Journal of Physical Anthropology*. 159, 80.
- Anemone, R., 1993. The functional anatomy of the hip and thigh in primates. In: Gebo, D.L. (Ed.), *Postcranial Adaptation in Nonhuman Primates*. Northern Illinois University Press, Dekalb, pp. 150-175.
- Bailey, K.E., Lad, S.E., Pampush, J.D., 2017. Functional morphology of the douc langur (*Pygathrix spp.*) scapula. *American Journal of Primatology* 79, 1-9.
- Behrensmeyer, A.K., Todd, N.E., Potts, R., McBrinn, G.E., 1997. Late Pliocene faunal turnover in the Turkana Basin, Kenya and Ethiopia. *Science* 278, 1589–1594.
- Benefit, B.R., 1987. The Molar Morphology, Natural History, and Phylogenetic Position of the Middle Miocene Monkey *Victoriapithecus*. PhD Diss. 1033p.
- Benefit, B.R., 1999. Biogeography, Dietary Specialization, and the Diversification of African Plio-Pleistocene Monkeys. In: Bromage T.G., Schrenk, F. (Eds.) *African biogeography, climate change, and human evolution*. Oxford University Press, New York, pp. 172-188.
- Benefit, B. R., McCrossin, M. L., Boaz, N. T., Pavlakis, P., 2008. New Fossil Cercopithecoids from the Late Miocene of As Sahabi, Libya. *Garyounis Scientific Bulletin*. 5, 267-283.
- Birchette, M., 1982. The Postcranial Skeleton of *Paracolobus chemeroni*. Ph.D. Dissertation, Harvard University.
- Boaz, N.T., 1977. Paleocology of early Hominidae in Africa. *Kroeber Anthropological Society Papers* 50, 37-62.

- Bobe, R., 2011. Fossil Mammals and Paleoenvironments in the Omo-Turkana Basin. *Evolutionary Anthropology* 6, 254-263.
- Bobe, R., Behrensmeyer, A.K., 2004. The expansion of grassland ecosystems in Africa in relation to mammalian evolution and the origin of the genus *Homo*. *Palaeogeography Palaeoclimatology and Palaeoecology* 207, 399–420.
- Bobe R, Eck GG. 2001. Responses of African bovids to Pliocene climatic change. *Paleobiology* 27(suppl), 30.
- Bobe, R., Behrensmeyer, A.K., Chapman, R.E., 2002. Faunal change, environmental variability and late Pliocene hominin evolution. *Journal of Human Evolution* 42, 475-497.
- Boisserie J.R., Guy F., Delagnes A., Hlukso L.J., Bibi F., Beyene Y., Guillemot C., 2008. New palaeoanthropological research in the Plio-Pleistocene Omo Group, Lower Omo Valley, SNNPR (Southern Nations, Nationalities and People Regions), Ethiopia. *Comptes Rendus Palevol* 7, 429-439.
- Boisserie, J.-R., Delagnes, A., Beyene, Y., Schuster, M., 2010. Reconstructing the African background to human expansions in Eurasia: New research in the Shungura Formation, Ethiopia. *Quaternary International* 223-224, 426-428.
- Brown, Francis H., and R. T. Shuey., 1976. Magnetostratigraphy of the Shungura and Usno formations, lower Omo valley, Ethiopia. In: Coppens, Y., Howell, F.C., Isaac, G.L., Leakey, R.E.F. (Eds.), *Earliest man and environments in the Lake Rudolf Basin*. University of Chicago Press, Chicago, pp. 64-78.
- Cerling, T.E., Chritz, K.L., Jablonski, N.G., Leakey, M.G. and Manthi, F.K., 2013. Diet of *Theropithecus* from 4 to 1 Ma in Kenya. *Proceedings of the National Academy of Sciences* 110, pp.10507-10512.
- Cerling, T., Andanje, S.A., Blumenthal, S.A., Brown, F.H., Chritz, K.L., Harris, J.M., Hart, J., Kirera, F.M., Kaleme, P., Leakey, L.N., Leakey, M.G., Levin, N.E., Manthi, F.K., Passey, B.H., Uno, K.T., 2015. Dietary changes of large herbivores in the Turkana Basin, Kenya from 4 to 1 Ma. *Proceedings of the National Academy of Sciences* 112, 11467- 11472.
- Ciochon, R.L., 1993. *Evolution of the Cercopithecoid Forelimb*. University of California Press, Berkeley.
- Cooke, H.B.S., 1976. Suidae from Plio-Pleistocene strata of the Rudolf basin. In: Coppens, Y., Howell, F.C., Isaac, G.L., Leakey, R.E.F. (Eds.), *Earliest Man and Environments in the Lake Rudolf Basin*. University of Chicago Press, Chicago, pp.251-263.

Cooke, C., 2012. The feeding, ranging, and positional behaviors of *C. torquatus*, the red-capped mangabey, from Sette Cama, Gabon: A phylogenetic perspective. Ph.D. Dissertation, The Ohio State University.

Conroy, G.C., 1976. Primate postcranial remains from the Oligocene of Egypt. *Contributions to Primatology* 8, 1-134.

de Heinzelin, J. (Ed.), 1983. The Omo Group: Archives of the International Omo Research Expedition Vol. 1. Musée Royal de L'Afrique Centrale, Tervuren.

Deino, A.L., Hill, A., 2002. $^{40}\text{Ar}/^{39}\text{Ar}$ dating of Chemeron Formation strata encompassing the site of hominid KNM-BC 1, Tugen Hills, Kenya. *Journal of Human Evolution* 42:1-2, 141-151.

Delson, E., 1973. Fossil colobine monkeys of the circum-Mediterranean region and the evolutionary history of the Cercopithecidae (Primates, Mammalia). Ph.D. dissertation, Columbia University.

Delson, E. 1975., Evolutionary history of the Cercopithecidae. In: Szalay, F.S. (Ed.). *Approaches to Primate Paleobiology, Contributions in Primatology, Vol. 5.* Karger, Basel, pp. 167-217.

Delson, E. 1994., Evolutionary history of the colobine monkeys in paleoenvironmental perspective. In: Davies, A.G., Oates, J.F., (Eds.). *Colobine Monkeys: their ecology, behavior and evolution.* Cambridge University Press, Cambridge, pp. 11-43.

Delson, E., Terranova, C.J., Jungers, W.L., Sargis, E.J., Jablonski, N.G., Dechow, P.C., 2000. Body Mass in Cercopithecidae (Primates, Mammalia): Estimation and scaling in Extinct and Extant Taxa. *Anthropological Papers of the American Museum of Natural History* 83, 1-159.

Dunbar, R., Dunbar, E., 1974. Ecological relations and niche separation between sympatric terrestrial primates in Ethiopia. *Folia Primatologica* 21, 36-60.

Dunham, N.T., Kane, E.E., McGraw, W. S., 2015. Scapular Morphology and Forelimb Use during Foraging in Four Sympatric Cercopithecids. *Folia Primatologica* 86, 474-489.

Eck, G., 1977. Diversity and frequency distribution of Omo Group Cercopithecoidea. *Journal of Human Evolution* 6, 55-63.

Eck, G.G., 1987. Plio-Pleistocene specimens of *Cercopithecus* from the Shungura Formation, Southwestern Ethiopia. In: Coppens, Y., Howell, F.C., (Eds.). *Les faunes Plio-Pleistocenes de la Basse Vallee de l'Omo (Ethiopie).* Tome 3, Cercopithecidae de la Formation de Shungura. *Cahiers de Paleontologie, Travaux de Paleontologie Est-Africaine.* Editions du CNRS, Paris, pp. 143-146.

Eck, G., Jablonski, N., 1987. The skull of *Theropithecus brumpti* compared with those of other species of the genus *Theropithecus*. In: Coppens, Y., Howell, C., (Eds.). Cahiers de Paleontologie Travaux de Paleontologie Est-Africaine Les Faunes Plio-Pleistocenes de la Basse Vallee de l'Omo (Ethiopie). Editions du Centre National de la Recherche Scientifique, Paris, pp.11-122.

Elton, S., 2002. A reappraisal of the locomotion and habitat preference of *Theropithecus oswaldi*. *Folia Primatologica* 73, 252-280.

Elton, S., 2006. Forty Years on and Still Going Strong: The Use of Hominin-Cercopithecoid Comparisons in Palaeoanthropology. *The Journal of the Royal Anthropological Institute* 12, 19-38.

Feibel, C.S., Brown, F.H., Mcdougall, I., 1989. Stratigraphic context of fossil hominids from the Omo group deposits: Northern Turkana Basin, Kenya and Ethiopia. *American Journal of Physical Anthropology* 78, 595-622.

Feibel, C. S., Harris, J. M., Brown, F. H., 1991. Palaeoenvironmental context for the late Neogene of the Turkana Basin. In: Harris, J.M. (Ed.), Koobi Fora Research Project. Volume 3. The Fossil Ungulates, Geology, Fossil Artiodactyls and Palaeoenvironments. Oxford University Press, Oxford, pp. 321–370.

Fleagle, J., 1978. Locomotion, posture, and habitat utilization in two sympatric Malaysian leaf-monkeys (*Presbytis obscura* and *Presbytis melalophus*). In: G. G. Montgomery (Ed.), *Ecology of Arboreal Folivores*. Smithsonian Institution Press, Washington D.C., pp. 243-251.

Fleagle, J.G., McGraw, W.S., 2002. Skeletal and dental morphology of African papionins: unmasking a cryptic clade. *Journal of Human Evolution* 42, 267-292

Fleagle, J. G. & Simons, E. L., 1982. The humerus of *Aegyptopithecus zeuxis*, a primitive anthropoid. *American Journal of Physical Anthropology* 59, 175–193

Fleagle, J.G., McGraw, W.S., 2002. Skeletal and dental morphology of African papionins: unmasking a cryptic clade. *Journal of Human Evolution* 42, 267-292.

Frost, S.R., 2001. Fossil Cercopithecidae from the Afar Depression, Ethiopia: Species systematics and comparison to the Turkana Basin. Ph.D. Dissertation, City University of New York.

Frost, S.R., Delson, E., 2002. Fossil Cercopithecidae from the Hadar Formation and surrounding areas of the Afar Depression, Ethiopia. *Journal of Human Evolution* 43, 687-748.

Frost, S.R., Alemseged, Z., 2007. Middle Pleistocene fossil Cercopithecidae from Asbole, Afar Region, Ethiopia. *Journal of Human Evolution* 53, 227-259.

- Gebo, D. L., Chapman, C.A., 1995. Positional behavior in five sympatric Old-World Monkeys. *American Journal of Physical Anthropology* 97, 49-76.
- Gebo, D., Sargis, E., 1994. Terrestrial adaptations in the postcranial skeletons of guenons. *American Journal of Physical Anthropology* 93, 341-371.
- Gentry, A.W., 1985. The Bovidae of the Omo Group deposits, Ethiopia. In: Coppens, Y., Howell, F.C (Eds.), *Les Faunes Plio-Pléistocènes de la Basse Vallée de l'Omo (Ethiophe)*, I: Périssodactyles, Artiodactyles (Bovidae). CNRS, Paris., pp. 119–191.
- Gilbert, C.C., 2013. Cladistic analysis of extant and fossil African papionins using craniodental data. *Journal of Human Evolution* 64, 399-433.
- Gilbert, C.C., Goble, E.D., Hill, A., 2010. Miocene cercopithecoidea from the Tugen Hills, Kenya. *Journal of Human Evolution* 59, 465-483.
- Gilbert, C. C., Goble, E. D., Kingston, J. D., Hill, A., 2011. Partial skeleton of *Theropithecus brumpti* (Primates, Cercopithecidae) from the Chemeron Formation of the Tugen Hills, Kenya. *Journal of Human Evolution* 61, 347-362.
- Grubb, P., Butynski, T.M., Oates, J.F., Bearder, S.K., Disotell, T.R., Groves, C.P., Struhsaker, T.T., 2003. Assessment of the Diversity of African Primates. *International Journal of Primatology* 24, 1301-1357.
- Guthrie, E., 2011. Functional Morphology of the postcranium of *Theropithecus brumpti* (Primates: Cercopithecidae). Ph.D. Dissertation, University of Oregon.
- Hakala, S., 2012. Distribution of Mammalian Fauna During the Early Pleistocene of the Koobi Fora Formation, East Turkana, Kenya. Master's Thesis, University of Georgia.
- Hammond, A., 2013. 3D Analysis of Hip Joint Mobility and the Evolution of Locomotor Abilities in Miocene Hominoids. Ph.D. Dissertation, University of Missouri.
- Harmand, S., Lewis, J.E., Feibel, C.S., Lepre, C.J., Prat, S., Lenoble, A., Boës, X., Quinn, R.L., Brenet, M., Arroyo, A. and Taylor, N., 2015. 3.3-million-year-old stone tools from Lomekwi 3, West Turkana, Kenya. *Nature* 521, p.310-315.
- Harris, J.W.K., 1983. Cultural beginnings: Plio-Pleistocene archaeological occurrences from the Afar, Ethiopia. *African Archaeological Review* 1, 3–31.
- Harris, J.M., 1991. Koobi Fora Research Project, Vol. 3. The Fossil Ungulates: Geology, Fossil Artiodactyls, and Paleoenvironments. Clarendon, Oxford.
- Harris, J.M., Brown, F.H., Leakey, M.G., 1988. Stratigraphy and paleontology of Pliocene and Pleistocene localities west of Lake Turkana, Kenya. *Contributions in Science. Natural History Museum of Los Angeles County* 399, 1-128.

- Harris, J.M. Cerling, T.E., 2002. Dietary adaptations of extant and Neogene African suids. *Journal of Zoology* 256, 45-54.
- Harrison, T., 1989. New Postcranial Remains of *Victoriapithecus* from the Miocene of Kenya. *Journal of Human Evolution* 18, 3-54.
- Harrison, T., 2011. Cercopithecids (Cercopithecidae, Primates). In: Harrison, T. (Ed.), *Paleontology and Geology of Laetoli: Human Evolution in Context*. Netherlands, Springer, pp. 83-139
- Harrison, T., Harris, E. 1996. Plio-Pleistocene cercopithecids from Kanam East, western Kenya. *Journal of Human Evolution* 30, 539-561.
- Hlusko, L., 2006. A new large Pliocene colobine species (Mammalia: Primates) from Asa Issie, Ethiopia. *Geobios* 39, 57-69.
- Hlusko, L.J., 2007. A new late Miocene species of *Paracolobus* and other Cercopithecoidea (Mammalia: Primates) fossils from Lemudong'o, Kenya. *Kirtlandia*. 56, 72-85.
- Hooijer, D. A., and C. S. Churcher. 1985. Perissodactyla of the Omo group deposits (American collections). In: Coppens, Y., Howell, F.C. (Eds.). *Les Faunes Plio-Pléistocènes de la Basse Vallée de l'Omo (Éthiopie)*. CNRS, Paris, pp. 97-117.
- Howell, F.C., 1978. Hominidae. In: Maglio, V.J., Cooke, H.B.S. (Eds.), *Evolution of African mammals*. Harvard University Press, pp. 154-248.
- Howell, F.C., Petter, G., 1976. Carnivora from Omo group formations, southern Ethiopia. In: Coppens, Y. (Ed.). *Earliest Man and Environments in the Lake Rudolf Basin*. University of Chicago Press, Chicago, pp.314-331.
- Jablonski, N.G., 2002. Fossil Old World monkeys: the late Neogene radiation. In: Hartwig, W.C. (Ed.), *The Primate Fossil Record*. Cambridge University Press, Cambridge, pp. 255-299.
- Jablonski, N.G., Frost, S.R., 2010. Cercopithecoidea. In: Werdelin, L., Sanders, W.J. (Eds.), *The Cenozoic Mammals of Africa*. University of California Press, Oakland, pp. 393-428.
- Jablonski, N.G., Leakey, M.G., Kiarie, C., Anton, M., 2002. A new skeleton of *Theropithecus brumpti* (Primates: Cercopithecidae) from Lomekwi, West Turkana, Kenya). *Journal of Human Evolution* 43, 887-923.
- Jablonski, N., Leakey, M., 2008. *Koobi Fora Research Project: The Fossil Monkeys*. California Academy of Sciences, San Francisco.

- Janmaat, K., Chancellor, R., 2010. Exploring new areas: how important is long-term spatial memory for mangabey (*Lophocebus albigena johnstonii*) foraging efficiency? *International Journal of Primatology* 31, 863-886.
- Jolly, C., 1967. The evolution of the baboons. In: Vartog, H. (Ed.). *The Baboon in Medical Research*, Vol. II. University of Texas Press, Austin, pp. 323-338.
- Jolly, C.J., 1972. The classification and natural history of *Theropithecus* (*Simopithecus*) (Andrews, 1916, baboons of the African Plio-Pleistocene. *Bulletin of the British Museum of Natural History, Geology* 22, 1-122.
- Kalb, J., Jolly, C.J., Tebedge, S., Mebrate, A., Smart, C., Oswald, E.B., Whitehead, P.F., Woods, C.B., Adefris, T., Rawn-Schatzinger, V., 1982. Vertebrate Faunas from the Awash Group, Middle Awash Valley, Afar, Ethiopia. *Journal of Vertebrate Palaeontology* 2, 237-258.
- Kaplin, B., Moermond, T., 2000. Foraging ecology of the mountain monkey (*Cercopithecus lhoesti*): Implications for its evolutionary history and use of disturbed forest. *American Journal of Primatology* 50, 227-246
- Kidane, T., Brown, F.H. and Kidney, C., 2014. Magnetostratigraphy of the fossil-rich Shungura Formation, southwest Ethiopia. *Journal of African Earth Sciences*. 97, 207-223.
- Kimura, K., Takahashi, Y., Konishi, M., & Iwamoto, S., 1981. Adductor muscles of the thigh of crab-eating monkeys (*Macaca fascicularis*). *Primates* 22, 119-130.
- Krentz, H., 1993. Postcranial anatomy of extant and extinct species of *Theropithecus*. In: Jablonski, N.G. (Ed.) *Theropithecus: The Rise and Fall of a Primate Genus*. Cambridge University Press, Cambridge, pp. 383-422.
- Langdon, L.H., 1986. Functional Morphology of the Miocene Hominoid Foot. *Contributions to Primatology* 22, 1-255.
- Larson, S.G., 1993. Functional Morphology of the Shoulder in Primates. In: Gebo, D.L. (Ed.). *Postcranial Adaptation in Nonhuman Primates*. Northern Illinois University Press, DeKalb, pp. 45-69.
- Latimer, B., Ohman, J.C., Lovejoy, C.D., 1987. Talocrural joint in African hominoids: implications for *Australopithecus afarensis*. *American Journal of Physical Anthropology* 74, 155-175.
- Leakey, M.G., 1982. Extinct large colobines from the Plio-Pleistocene of Africa. *American Journal of Physical Anthropology* 58, 153-172.
- Leakey, M.G., 1987. Colobinae (Mammalia, Primates) from the Omo Valley, Ethiopia. In: Coppens, Y., Howell, F.C (Eds.), *Les faunes Plio-Pleistocenes de la Basse Vallee de*

l'Omo (Ethiopie). Tome 3, Cercopithecidae de la Formation de Shungura, Cahiers de Paleontologie, Travaux de Paleontologie Est-Africaine. CNRS, Paris, pp.148–169.

Leakey, M.G., Evolution of *Theropithecus* in the Turkana Basin. In: Jablonski, N.G. (Ed.). *Theropithecus: The Rise and Fall of a Primate Genus*. Cambridge University Press, Cambridge, pp. 85-124.

Leakey, M.G., Delson, E., 1987. Fossil Cercopithecidae from the Laetoli Beds. In: Leakey, M.D., Harris, J.M. (Eds.). *Laetoli, A Pliocene Site in Northern Tanzania*. Clarendon Press, Oxford, pp. 91-107.

Leakey, M.G. and Leakey, R.E.F., 1973. New large Pleistocene Colobinae (Mammalia, Primates) from East Africa. In: Leakey, L.S.B., Savage, R.J.G. (Eds.). *Fossil Vertebrates of Africa*. Academic Press, London and New York City, pp. 121-38.

Leakey, M.G., Teaford, M.F., Ward, C.V., 2003. Cercopithecidae from Lothagam. In: Leakey, M.G., Harris, J.M. (Eds.), *Lothagam: The Dawn of Humanity in Eastern Africa*. Columbia University Press, New York, pp. 201-248.

Leakey, R.E.F., 1969 New Cercopithecoidea from the Chemeron Beds, Lake Baringo, Kenya. In Leakey, L.S.B. (Ed.) *Fossil Vertebrates of Africa*. Vol. I. Academic Press, London and New York City, pp. 53-73.

Levin, N.E., Haile-Selassie, Y., Frost, S.R., Saylor, B.Z., 2015. Dietary change among hominins and cercopithecids in Ethiopia during the early Pliocene. *Proceedings of the National Academy of Sciences* 112 12304-12309.

Levin, N.E., Quade, J., Simpson, S.W., Semaw, S., Rogers, M., 2004. Isotopic evidence for Plio-Pleistocene environmental change. *Earth and Planetary Science Letters* 219, 93-110.

Li, Y., 2007. Terrestriality and tree status use in a group of Sichuan snub-nosed monkeys. *Primates* 48, 197-207

MacLachy, L., 1998. Reconstruction of Hip Joint Function in Extant and Fossil Primates. In: Strasser, E., Fleagle, J., Rosenberger, A., McHenry, H. (Eds.). *Primate Locomotion: Recent Advances*. Plenum Press, New York City, pp. 111-130.

Maier, W., 1972. Anpassungstyp und systematische Stellung von *Theropithecus gelada* Ruppell, 1835. *Zeitschrift für Morphologie und Anthropologie* 63, 370-384.

Marquardt, M., 2008. Functional Morphology of the Anthropoid Talocrural Joint. Master's Thesis, University of Missouri.

McCrossin, M.L., Benefit, B.R., Gitau, S.N., Palmer, A.K., Blue, K.T., 1998. Fossil Evidence for the Origins of Terrestriality among Old World Monkeys. In: Strasser, E.,

- Fleagle, J., Rosenberger, A., McHenry, H. (Eds.). Primate Locomotion: Recent Advances. Plenum Press, New York City, pp. 353-396.
- McDougall, I., Brown, F.H., Vasconcelos, P.M., Cohen, B.E., Thiede, D.S., Buchanan, M., 2012. New single crystal $^{40}\text{Ar}/^{39}\text{Ar}$ ages improve time scale for deposition of the Omo Group, Omo-Turkana Basin, East Africa Normal faults. *Journal of the Geological Society* 169, 213-226.
- McGraw, W., 1998. Comparative locomotion and habitat use of six monkeys in the Tai Forest, Ivory Coast. *American Journal of Physical Anthropology* 105, 493-510.
- Morbeck, M.E., 1979. Forelimb use and positional adaptation in *Colobus guereza*: Integration of behavior ecological, and anatomical data. *Environment, behavior and morphology: Dynamic interactions in primates*, 95-118.
- Nakagawa, N., 1989. Activity budget and diet of patas monkeys in Kala Maloue National Park: Cameroon: a preliminary report. *Primates* 30, 27-34
- Nakatsukasa, M., Mbua, E., Sawada, Y., Sakai, T., Nakaya, H., Yano, W., Kunitatsu, Y. 2010. Earliest colobine skeletons from Nakali, Kenya. *American Journal of Physical Anthropology* 143, 365-382.
- Negash, E.W., Alemseged, Z., Wynn, J., Bedaso, Z.K., 2015. Paleodietary reconstruction using stable isotopes and abundance analysis of bovids from the Shungura Formation of South Omo, Ethiopia. *Journal of Human Evolution*, 88: 127-136.
- Norris, J., 1988. Diet and feeding behavior of semi-free ranging mandrills in an enclosed Gabonais forest. *Primates* 29, 449-463.
- Osterholz, M., Walter, L., Roos, C., 2008. Phylogenetic position of the langur genera *Semnopithecus* and *Trachypithecus* among Asian colobines, and genus affiliations of their species groups. *BMC Evolutionary Biology* 8, 58.
- Patel, B., 2010. Functional morphology of cercopithecoid primate metacarpals. *Journal of Human Evolution*. 58, 320-337.
- Patterson, D.B., Braun, D.R., Behrensmeyer, A.K., Merritt, S., Zliobaite, I., Reeves, J.S., Wood, B.A., Fortelius, M., Bobe, R., 2017. Ecosystem evolution and hominin paleobiology at East Turkana, northern Kenya between 2.0 and 1.4 Ma. *Palaeogeography, Palaeoclimatology, Palaeoecology* 481, 1-13.
- Prat, S., Brugal, J.P., Tiercelin, J.J., Barrat, J.A., Bohn, M., Delagnes, A., Harmand, S., Kimeu, K., Kibunjia, M., Texier, P.J., Roche, H., 2005. First occurrence of early *Homo* in the Nachukui Formation (West Turkana, Kenya) at 2.3-2.4 Myr. *Journal of Human Evolution* 49, 230-240.

Raaum, R., Sterner, K.N., Noviello, C.N., Stewart, C.B., Disotell, T.R., 2005. Catarrhine primate divergence dates estimated from complete mitochondrial genomes: concordance with fossil and nuclear DNA evidence. *Journal of Human Evolution*. 48, 237-257.

Ren, B., Zhang, S., Wang, L., Liang, B., Li, B., 2001. Vertical distribution of different age-sex classes in a foraging group of Sichuan golden monkeys (*Rhinopithecus roxellana*). *Folia Primatologica* 72, 96-99.

Roberts D., 1974. Structure and function of the primate scapula. In: Jenkins, F. (Ed.), *Primate Locomotion*. Academic Press, New York, pp. 171-200.

Rodman, P., 1979. Skeletal differentiation of *Macaca fascicularis* and *Macaca nemestrina* in relation to arboreal and terrestrial quadrupedalism. *American Journal of Physical Anthropology* 51, 51-62

Rose, M., 1979. Positional behavior of natural populations: some quantitative results of a field study of *Colobus guereza* and *Cercopithecus atheiops*. *Environment, behavior, and morphology: dynamic interactions in primates*. 75-94.

Rose, M., 1983. Miocene hominoid postcranial morphology: Monkey-like, ape-like, neither, or both? In: Ciochon, R.L., Corruccini, R.S. (Eds.). *New Interpretations of Ape and Human Ancestry*. Plenum Press, New York, pp. 405-417.

Rose, M.D., 1988. Another look at the anthropoid elbow. *Journal of Human Evolution* 17, 193-224.

Rowe, N., and Myers, M., 2013. *All the World's Primates*. Charlestown: Primate Conservation Inc.

Ruff, C.B., 2002. Long bone articular and diaphyseal structure in Old World monkeys and apes. I: Locomotor effects. *American Journal of Physical Anthropology* 119, 305-342.

Ruff, C.B., 2003. Long bone articular and diaphyseal structure in Old World monkeys and apes. II: estimation of bodymass. *American Journal of Physical Anthropology* 120, 16-37.

Schmitt, D., 1998. Forelimb Mechanics during Arboreal and Terrestrial Quadrupedalism in Old World Monkeys. In: Strasser, E., Fleagle, J., Rosenberger, A., McHenry, H. (Eds.). *Primate Locomotion: Recent Advances*. Plenum Press, New York City, pp. 175-200.

Steiper, M., Seiffert, E., 2012. Evidence for a convergent slowdown in primate molecular rates and its implications for the timing of early primate evolution. *PNAS* 10916, 6006-6011.

Stuedel, K., 1981. Functional aspects of primate pelvic structure: a multivariate approach. *American Journal of Physical Anthropology* 59, 399-410.

Strasser, E., 1988. Pedal evidence for the origin and diversification of cercopithecoid clades. *Journal of Human Evolution* 17, 225-245

Strasser, E., 1992. Hindlimb proportions, allometry, and biomechanics in Old World monkeys (Primates, Cercopithecidae). *American Journal of Physical Anthropology* 87, 187-213.

Strasser E, Delson E., 1987. Cladistic analysis of cercopithecoid relationships. *Journal of Human Evolution* 16: 81- 99.

Suwa, G., White, T.D. Howell, F.C., 1996. Mandibular postcanine dentition from the Shungura Formation, Ethiopia: crown morphology, taxonomic allocations, and Plio-Pleistocene hominid evolution. *American Journal of Physical Anthropology* 101, 247-282.

Szalay, F.S., 1975. Haplorhine relationships and the status of the Anthropoidea. In: Tuttle, R.H. (Ed.). *Primate Functional Morphology and Evolution*. Mouton, The Hague, pp. 3-22.

Szalay, F.S., Delson, E., 1979. *Evolutionary History of the Primates*. Academic Press, New York.

Tallman, M., Kegley, A.D., Adams, J.W., 2016. Using geometric shape for subfamily level taxonomic attribution in mixed, unassociated fossil cercopithecoid postcranial samples. *American Journal of Physical Anthropology* 159, 310.

Thomas, S., 1991. Population densities of habitat use among anthropoid primates of the Ituri Forest, Zaire. *Biotropica* 23, 68-83.

Ting, N.T., 2001. A Functional Analysis of the Hip and Thigh of *Paracolobus chemeroni* and *Paracolobus mutiwa*. Master's Thesis, University of Missouri.

Ting, N.T., 2008. Mitochondrial relationships and divergence dates of the African colobines: evidence of Miocene origins for the living colobus monkeys. *Journal of Human Evolution* 55, 312-325.

Turley, K., Frost, S.R., 2013. The shape and presentation of the catarrhine talus: a geometric morphometric analysis. *The Anatomical Record* 296, 877-890.

Vrba, E.S., 1980. The significance of bovid remains as indicators of environment and predation patterns. In: Behrensmeyer AK, Hill A, editors. *Fossils in the making: vertebrate taphonomy and paleoecology*. Chicago: University of Chicago Press, pp. 247–271.

Wang, X., Zhang, Y., Yu, L., 2013. Summary of phylogeny in subfamily Colobinae (Primate: Cercopithecidae). Chinese Scientific Bulletin 5818, 2097-2103.

Ward, C., 1991. Functional anatomy of the lower back and pelvis of the Miocene hominoid *Proconsul nyanzae* from Mfangano Island, Kenya. Ph.D. Dissertation, The Johns Hopkins University.

White, T.D., Harris, J.M., 1978. Stratigraphic interpretation of the Omo, Shungura, and Lake Turkana fossil suid record. Science, 202, 1309-1309.